Hydrology and Geochemistry of Aquifer and Stream Contamination Related to Acidic Water in Pinal Creek Basin Near Globe, Arizona

United States Geological Survey Water-Supply Paper 2466

AVAILABILITY OF BOOKS AND MAPS OF THE U.S. GEOLOGICAL SURVEY

Instructions on ordering publications of the U.S. Geological Survey, along with prices of the last offerings, are given in the current-year issues of the monthly catalog "New Publications of the U.S. Geological Survey." Prices of available U.S. Geological Survey publications released prior to the current year are listed in the most recent annual "Price and Availability List." Publications that may be listed in various U.S. Geological Survey catalogs (**see back inside cover**) but not listed in the most recent annual "Price and Availability List" may be no longer available.

Order U.S. Geological Survey publications **by mail** or **over the counter** from the offices given below.

BY MAIL

Books

Professional Papers, Bulletins, Water-Supply Papers, Techniques of Water-Resources Investigations, Circulars, publications of general interest (such as leaflets, pamphlets, booklets), single copies of Earthquakes & Volcanoes, Preliminary Determination of Epicenters, and some miscellaneous reports, including some of the foregoing series that have gone out of print at the Superintendent of Documents, are obtainable by mail from

U.S. Geological Survey, Information Services
Box 25286, Federal Center, Denver, CO 80225

Subscriptions to periodicals (Earthquakes & Volcanoes and Preliminary Determination of Epicenters) can be obtained ONLY from the

Superintendent of Documents
Government Printing Office
Washington, DC 20402

(Check or money order must be payable to Superintendent of Documents.)

Maps

For maps, address mail orders to

U.S. Geological Survey, Information Services
Box 25286, Federal Center, Denver, CO 80225

OVER THE COUNTER

Books and Maps

Books and maps of the U.S. Geological Survey are available over the counter at the following U.S. Geological Survey Earth Science Information Centers (ESIC), all of which are authorized agents of the Superintendent of Documents:

- **ANCHORAGE, Alaska**—Rm. 101, 4230 University Dr.
- **LAKEWOOD, Colorado**—Federal Center, Bldg. 810
- **MENLO PARK, California**—Bldg. 3, Rm. 3128, 345 Middlefield Rd.
- **RESTON, Virginia**—USGS National Center, Rm. 1C402, 12201 Sunrise Valley Dr.
- **SALT LAKE CITY, Utah**—Federal Bldg., Rm. 8105, 125 South State St.
- **SPOKANE, Washington**—U.S. Post Office Bldg., Rm. 135, West 904 Riverside Ave.
- **WASHINGTON, D.C.**—Main Interior Bldg., Rm. 2650, 18th and C Sts., NW.

Maps Only

Maps may be purchased over the counter at the following U.S. Geological Survey offices:

- **ROLLA, Missouri**—1400 Independence Rd.
- **STENNIS SPACE CENTER, Mississippi**—Bldg. 3101

Hydrology and Geochemistry of Aquifer and Stream Contamination Related to Acidic Water in Pinal Creek Basin Near Globe, Arizona

Edited by JAMES G. BROWN and BARBARA FAVOR

U.S. GEOLOGICAL SURVEY WATER-SUPPLY PAPER 2466

U.S. DEPARTMENT OF THE INTERIOR
BRUCE BABBITT, Secretary

U.S. GEOLOGICAL SURVEY
Gordon P. Eaton, Director

UNITED STATES GOVERNMENT PRINTING OFFICE, WASHINGTON : 1996

For sale by the
U.S. Geological Survey
Information Services
Box 25286, Federal Center
Denver, CO 80225

Library of Congress Cataloging in Publication Data

Hydrology and geochemistry of aquifer and stream contamination related to acidic water in Pinal Creek Basin near Globe, Arizona / by James G. Brown and Barbara Favor, editors.
p. cm.—(U.S. Geological Survey water-supply paper ; 2466)
Includes bibliographical references.
Supt. of Docs. no. : I 19. 13:2466
1. Acid mine drainage—Environmental aspects—Arizona—Pinal Creek Watershed. 2. Groundwater—Pollution—Arizona—Pinal Creek Watershed. 3. Water—Pollution—Arizona—Pinal Creek Watershed. 4. Copper mines and mining—Environmental aspects—Arizona—Pinal Creek Watershed. 5. Acid mine drainage—Environmental aspects—Arizona—Globe Region. 6. Groundwater—Pollution—Arizona—Globe Region. 7. Water—Pollution—Arizona—Globe Region. 8. Copper mines and mining—Environmental aspects—Arizona—Globe Region.
I. Brown, James G. (James Gary), 1956– II. Favor, Barbara O.
III. Series
TD427.A28H93 1996
363.73'942'0979175—dc20 96–24416
CIP

CONTENTS

Chapter A.

Research of Acidic Contamination of Ground Water and Surface Water, Pinal Creek Basin, Arizona, *by James G. Brown and James H. Eychaner*

Chapter B.

Simulation of Reactions Affecting Transport of Constituents in the Acidic Plume, Pinal Creek Basin, Arizona, *by Kenneth G. Stollenwerk*

Chapter C.

Assessment of Colloidal Transport in Ground Water, Pinal Creek Basin, Arizona, *by Robert W. Puls, Robert M. Powell, and Donald A. Clark*

Chapter C.

Distribution of Chemical Constituents in Surface Water, Pinal Creek Basin, Arizona, *by James G. Brown and James H. Eychaner*

Chapter E.

Manganese and Iron Oxide Deposits and Trace-Metal Associations in Stream Sediments, Pinal Creek Basin, Arizona, *by Carol J. Lind and John D. Hem*

FIGURES

TABLES

CONVERSION FACTORS, VERTICAL DATUM, AND ABBREVIATED WATER-QUALITY UNITS

Multiply	By	To obtain
centimeter (cm)	0.3937	inch
meter (m)	3.281	foot
kilometer (km)	0.6214	mile
square kilometer (km^2)	0.3861	square mile
cubic meter per second (m^3/s)	35.3107	cubic foot per second
liter per minute (L/min)	0.2642	gallon per minute
gram (g)	0.03527	ounce

In this report, temperature is reported in degrees Celsius (°C), which can be converted to degrees Fahrenheit (°F) by using the following equation:

$$°F = 1.8\ (°C) + 32$$

VERTICAL DATUM

Sea level: In this report, "sea level" refers to the National Geodetic Vertical Datum of 1929—a geodetic datum derived from a general adjustment of the first-order level nets of the United States and Canada, formerly called Sea Level Datum of 1929.

ABBREVIATED WATER-QUALITY UNITS

Chemical concentration and water temperature are given only in metric units. Chemical concentrations in water is given in milligrams per liter (mg/L), micrograms per liter (µg/L), or moles per liter (mol/L). Milligrams per liter is a unit expressing the solute concentration (milligrams) per unit volume of solution. Millimoles per liter (mmol/L) is a unit expressing the solute concentration per unit volume of solution. One thousand millimoles per liter is equivalent to 1 mol/L. One thousand micrograms per liter is equivalent to 1 mol. For concentrations less than 7,000 mg/L, the numerical value is about the same as for concentrations in parts per million (ppm). Specific conductance is given in microsiemens per centimeter (µS/cm) at 25°C. Chemical concentration in solid-phase material from core samples and stream sediments is given in millimoles per kilogram (mmol/kg), milligrams per kilogram (mg/kg), and micrograms per gram (µg/g). Micrograms per gram is equivalent to parts per million.

Chapter A

Research of Acidic Contamination of Ground Water and Surface Water, Pinal Creek Basin, Arizona

By James G. Brown *and* James H. Eychaner

Abstract

The Pinal Creek Basin in central Arizona has been an area of large-scale copper mining for more than 100 years. Contamination sources, mainly impoundments of water related to mining, generally were acidic. A manmade lake formed in 1941 and drained in 1988 probably was the single largest source of contamination. Concentrations of dissolved iron and sulfate in the lake were greater than 2,000 and 13,000 milligrams per liter, respectively. Acidic water from this lake and other mining-related sources has generated a 15-kilometer-long plume of acidic ground water in the alluvial aquifer. Contaminated ground water is neutralized mainly by calcite dissolution as it moves through the alluvium and the shallow basin fill. Acid-base, oxidation-reduction, and sorption reactions accompany the neutralization of acidic ground water. Oxidation-reduction reactions involve principally iron and manganese. Sorption of oxidized precipitates controls the distribution of cobalt, copper, and nickel. These metals and other trace metals are near detection limits in neutralized ground water.

Neutralized ground water, which had a pH of 6.1 in 1990, discharges to the land surface to form a reach of perennial flow in Pinal Creek. Carbon dioxide decreases and dissolved oxygen increases in the surface water as it flows downstream. As a result, pH rises to about 8, and dissolved-solids concentrations decrease slightly. The rise in pH along the perennial reach causes manganese and iron-oxide minerals to precipitate on the streambed. Although trace metals, such as copper, nickel, zinc, and lead, are more concentrated on iron oxides than manganese oxides, trace-metal sorption to manganese oxides is more important because manganese oxides are much more abundant than iron oxides in the streambed.

Research at the Pinal Creek toxic site was funded mainly by the U.S. Geological Survey's Toxic Substances Hydrology Program and has been ongoing since 1984. Focus of the study included the acidic plume and areas affected by neutralized water. A combination of column and other laboratory experiments and computer simulations characterized oxidation-reduction, neutralization, and sorption reactions that evidently occur in the core of the plume. Solid-phase associations of copper, manganese, zinc, calcium, aluminum, and sulfate in the subsurface were determined through the use of sequential extractions. Field sampling and laboratory work identified oxide precipitates, associated trace metals, and trends in water chemistry in the area of perennial flow.

INTRODUCTION

The Pinal Creek drainage basin is in central Arizona about 100 km east of Phoenix (fig. 1). Globe and Miami are the principal communities in the basin, which had a population of about 18,000 in 1990 (U.S. Bureau of the Census, 1991). The boundary of the basin forms the boundary of the study area (fig. 1),

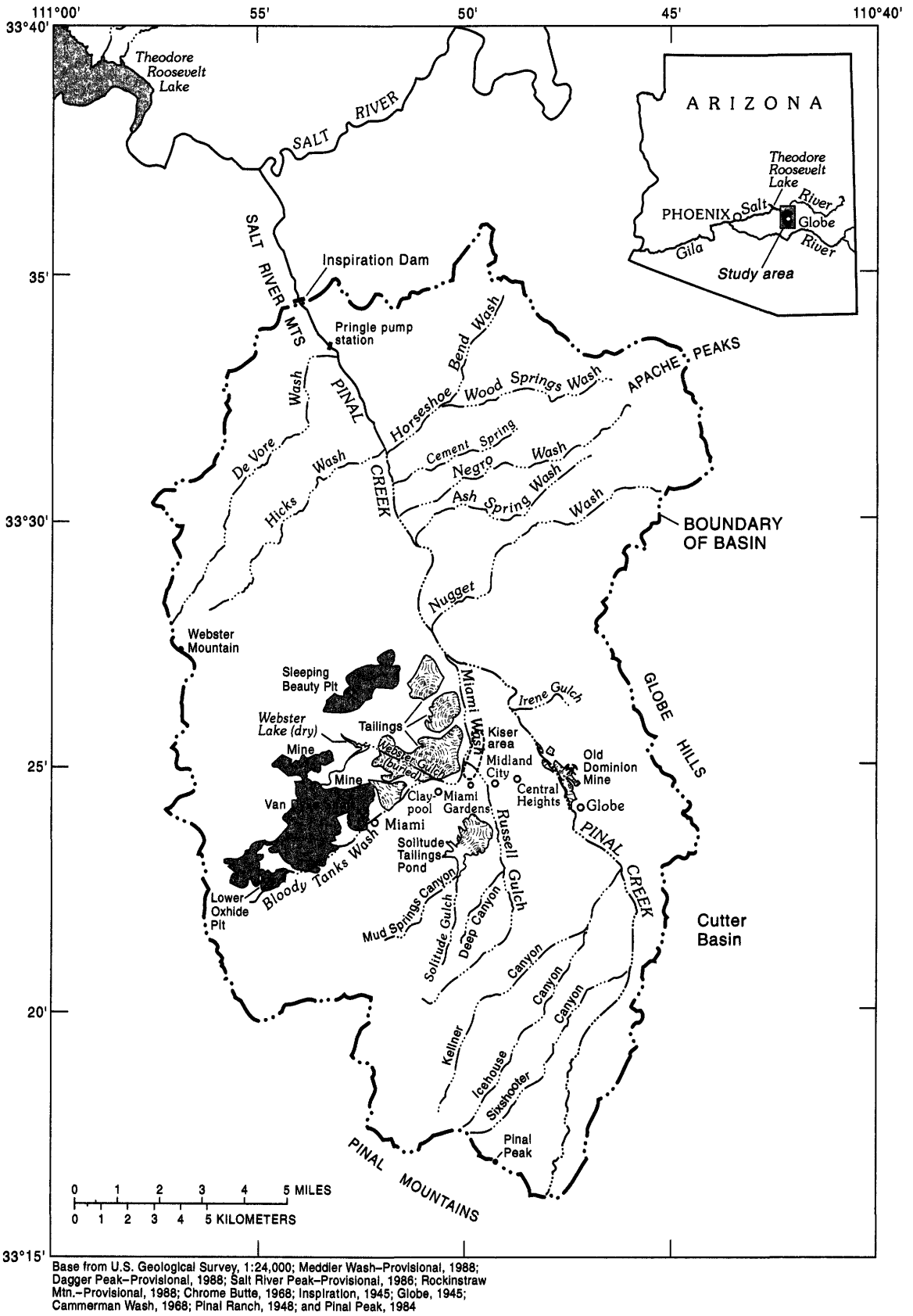

Base from U.S. Geological Survey, 1:24,000; Meddler Wash–Provisional, 1988; Dagger Peak–Provisional, 1988; Salt River Peak–Provisional, 1988; Rockinstraw Mtn.–Provisional, 1988; Chrome Butte, 1968; Inspiration, 1945; Globe, 1945; Cammerman Wash, 1968; Pinal Ranch, 1948; and Pinal Peak, 1984

Figure 1. Location of study area, Pinal Creek Basin, Arizona.

which lies entirely within Gila County. Streams flow generally northward and ultimately flow into Pinal Creek, which empties into the Salt River just above Roosevelt Lake.

Mining began in the area in the late 1870's with the production of silver ore from several underground mines (Ransome, 1903, p. 115). Copper has been mined in the basin since 1882, first in underground mines and in open-pit mines beginning in 1948. Acid-mine drainage resulted from oxidation of sulfide minerals, from ore processing, and from other mining activities in the basin. Contaminated acidic ground water was first recognized in the area in the 1930's, and perennial streamflow in Pinal Creek is known to have been affected by contamination since 1963 (Envirologic Systems, Inc., 1983, p. 6) and possibly earlier. The contamination has generated a 15-km-long plume of acidic ground water in the alluvium of Miami Wash and lower Pinal Creek.

A study began in 1984 that focused on the acidic contaminant plume beneath Miami Wash and Pinal Creek and the contaminated water in the perennial reach of Pinal Creek. The work and research summarized in this report was done primarily by the U.S. Geological Survey (USGS), the U.S. Environmental Protection Agency (USEPA), the University of Arizona, and the Arizona State University. Principal funding was from the USGS Toxics Substances Hydrology Program.

The investigations in the Pinal Creek Basin have had local and national objectives. On the local level, the study objective was to describe the extent of contamination in populated areas, monitor the evolution of the contaminants through time, and evaluate the potential for breakthrough of acidic contamination to the perennial reach of Pinal Creek, which flows into the Salt River about 10 km upstream from Roosevelt Lake. Roosevelt Lake is a principal source of water for the Phoenix metropolitan area, which had a population of 2,100,000 in 1990 (U.S. Bureau of the Census, 1991). On the national level, the objective was to identify and quantify the reactions that alter the chemistry of the contaminated water, provide data to test simulation models that link advective transport with geochemical reactions, and verify laboratory experiments on the transport and reactions of contaminants.

Purpose and Scope

The purpose of this report is to present the results of research at the site through 1992. The report summarizes the sampling and data-collection program and describes the geohydrology of the system, the chemical characteristics and extent of the principal contaminant plume, and the physical and chemical processes that alter aqueous and solid phases. This report also presents the results of geochemical-computer model simulations that were done to increase understanding of these physical and chemical processes.

Physical Setting and Climate

The Pinal Creek Basin is an area of block-faulted mountains and valleys that range in altitude from 670 to 2,400 m above sea level. The surface-drainage area of the basin is 516 km^2. Inspiration Dam, which is about 6 km upstream from the Salt River and mouth of Pinal Creek, is an abandoned, concrete diversion dam about 3 m high and 22 m long. The dam was built in 1912 but was never used and it has been filled to the crest with sediment since at least 1979. Most studies have been done upstream from Inspiration Dam because access is difficult in the 6.2-km reach between the dam and the mouth of the creek (fig. 1).

Land-surface altitudes in the basin generally increase to the south. The altitude of Inspiration Dam is 835 m above sea level. The highest altitude is 2,392 m above sea level on Pinal Peak in the Pinal Mountains, which form the south boundary of the basin. The basin is bounded on the east by Apache Peaks and the Globe Hills, which reach a maximum altitude of 1,000 m. The basin is bounded on the west by the Salt River Mountains and Webster Mountain, which has an altitude of 1,700 m.

Mining operations in the basin range in altitude from 1,000 to 1,300 m above sea level. The largest open-pit mines in the basin are adjacent to and north of Miami, where mines and tailings dominate the local landscape. Tailings cover about 27 km^2 of hills and drainages around Miami (fig. 1). By 1989, mine pits and dumps had prevented surface runoff from an area of about 85 km^2 from contributing to flow in Pinal Creek.

Average precipitation increases with altitude and ranges from about 340 to about 780 mm/yr and is about 450 mm/yr near the mines (University of Arizona, 1965). From 1914 to 1991, precipitation at Miami

ranged from 167 to 578 mm/yr and averaged 493 mm/yr (Longsworth and Taylor, 1992). Precipitation occurs as brief, often intense summer thunderstorms or as winter storms that may last several days. Snow accumulates in the Pinal Mountains during most years. Average monthly temperatures near the mines range from 6 to 29°C, with extremes of -15 and 45°C (Sellers and others, 1985).

Previous Investigations

The geology of the area has been described in detail by Ransome (1903, 1919), Peterson (1962), and Kiven and Ivey (1981). The general geology of Arizona copper deposits and a general history of copper mining in Arizona were described by Arizona Bureau of Mines (1969, p. 117–156), and Titley and Hicks (1966). Manganese deposits were described by Farnham and others (1961). Gilkey and Beckman (1963) described water-use practices at several mines in the area, and Sheffer and Evans (1968) described methods of copper leaching and precipitation. Central Arizona Association of Governments (1983) reviewed the mining history of the basin.

Studies funded primarily by the USEPA from 1979 through 1983 first quantified the severity and extent of ground-water contamination (Envirologic Systems, Inc., 1983). During this time, the Mineral Extraction Task Force (METF) of the Central Arizona Association of Governments studied potential areas of ground-water contamination near Globe (Rouse, 1981, 1983; Central Arizona Association of Governments, 1983; Envirologic Systems, Inc., 1983). Their work included chemical analyses of water samples from possible contaminant sources, from streams and existing wells, and from 52 wells drilled for the study. Progress in the investigations by the USGS since 1984 has been summarized by Eychaner and Stollenwerk (1985, 1987) and Eychaner (1988, 1989, 1990, 1991a).

The USEPA (1986) found Inspiration Consolidated Copper Company (ICCCo) in violation of the Clean Water Act and ordered a series of actions to eliminate contaminant sources, remove contaminated water from the aquifer, and monitor remediation progress. The administrative record leading to the order and its successive revisions (USEPA, 1978–89) includes information on the history of contaminant sources. Arthur (1987b) summarized the evidence supporting the order and included two subsequent modifications of the required actions. The company's initial response to the order (Timmers, 1986) contains a large number of data. Studies related to the design of remediation work were described by Hydro Geo Chem, Inc. (1989).

Acknowledgments

Cyprus Miami Mining Corporation, Pinto Valley Division of Magma Copper Company, and their predecessor corporations provided access to their records and properties. The late Noel B. Gillespie, a long-time resident of the Globe area and a senior employee of both companies, was especially helpful. Greg V. Arthur of the USEPA provided access to data from that agency. Nellie A. and Eva M. Setka generously provided access to sampling sites.

This report includes significant contributions by researchers other than the principal authors. Robert W. Wallin, Ronald S. Reese, and Dr. Randy L. Bassett, University of Arizona, investigated organic contamination of the aquifer. Judith Haschenburger, Arizona State University, described manganese oxide and copper distribution and quantity in sediments in the perennial reach of Pinal Creek. The late Walter H. Ficklin, Geologic Division, USGS, conducted sequential extractions.

Well-Numbering and Naming System

Each project well is identified by a two- or three-digit number that denotes well number and group. For example, well 103 is the third well drilled in group 100. Project well numbers that include the characters, EX, represent exploration holes that were abandoned after water samples and cuttings were collected. The exploration holes were sealed with concrete to their total depths. Mining companies and other well owners use different systems, which are identified and located individually.

DATA COLLECTION AND ANALYSIS

Data collection began in 1984 with the drilling of wells adjacent to Miami Wash into the acid core of the plume. Initially, the focus of data collection and study was on the acidic ground-water plume but quickly expanded to include areas affected by neutralized contamination especially the perennial reach of Pinal Creek above Inspiration Dam.

Well-Drilling Program and Data-Collection Network

From 1984 through 1990, 32 observation wells and 6 exploration holes were drilled at 9 sites in the area (fig. 2). The wells were constructed with 10-cm-diameter, solvent-welded PVC casing and factory-slotted pipe; most well screens were 1 m in length (table 1). Aquifer materials were collected at each site during drilling. Wells were used for collection of water samples along the length of the plume and at various depths. Two wells were completed in uncontaminated basin fill beneath the plume; well 10 was drilled upgradient from all known mining activities.

Since 1984, ground-water samples were obtained for chemical analysis from selected project wells at least twice yearly and at most wells once a year. A streamflow-gaging station was established on Pinal Creek at Inspiration Dam (station number 09498400) in July 1980; water-quality data have been collected from the site on a regular basis (usually six times per year) since November 1979. Water-quality samples have been collected from Pinal Creek at Setka Ranch (09498380) since July 1987 (fig. 2). Water samples were collected on an intermittent basis from 1984 to 1987 at 12 nonproject wells and 11 surface-water sites along Miami Wash, lower Pinal Creek, and tributaries. Data collected by or related to this project were presented by Eychaner and others (1989), Brown (1990), and Longsworth and Taylor (1992). The reports include well-construction data, water levels in wells, streamflow discharge, and chemical analyses of ground water and surface water.

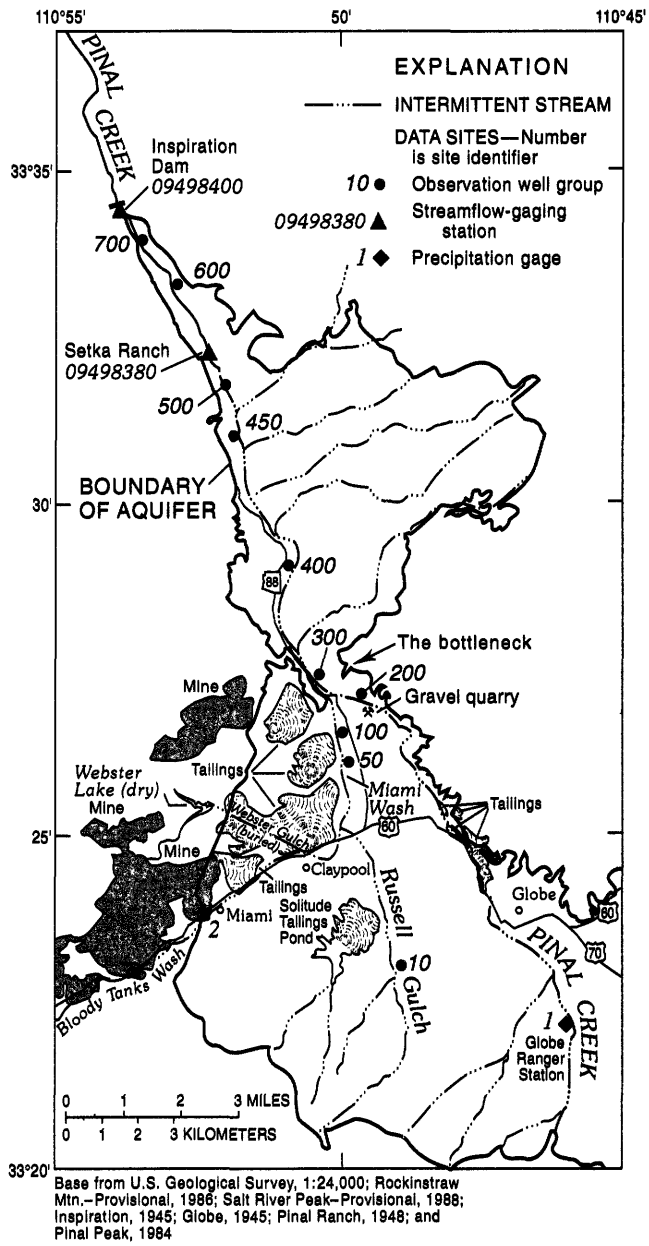

Figure 2. Ground-water, surface-water, and precipitation data-collection sites, Pinal Creek Basin, Arizona.

Data-Collection Methodology

Most ground-water samples were collected using either a 4.4- or 9.5-cm-diameter stainless-steel submersible pump, which was placed in the well just before sampling and removed immediately after sampling. The 4.4-cm-diameter pump produced about 4 L/min. The 9.5-cm-diameter pump produced 20 to 100 L/min. A few samples were collected using a bladder pump or bailer. In most instances, samples were obtained only after three casing volumes of water were evacuated and after temperature, pH, and specific conductance stabilized. These measures helped ensure that the sample collected represented water in the aquifer. In a few instances, one or more of the field measurements was not stable but the number of casing volumes exceeded three. Occasionally, samples were taken after field measurements had stabilized but before three casing volumes were pumped if evacuating the three volumes would have lowered water levels excessively. During many sample sets, dissolved-oxygen concentration, oxidation-reduction potential, and water-level drawdown also were monitored for stability.

Decontamination of the 9.5-cm-diameter pump between wells was accomplished by pumping more

Table 1. Observation well construction data, Pinal Creek Basin, Arizona

[C, caliper, D, drillers; E, electric; G, geologist; J, gamma; P, particle-size; U, gamma-gamma. ---, no data]

Well number	Date completed	Drilling method	Depth of hole, in meters	Depth of well, in meters	Interval of screen, in meters		Geologic unit	Bottom of seal, in meters	Logs available
					From	To			
10	01–09–89	Air hammer	27.9	27.1	18.0	27.1	Basin fill	2.4	D, G. P
51	10–11–84	Rotary, bentonite	33.5	33.4	32.4	33.3	Basin fill	3	C, E, G,P
52	10–12–84	Rotary, bentonite	20.1	19.8	18.8	19.7	Alluvium	3	---
53	10–12–84	Rotary, bentonite	28.0	27.8	26.8	27.7	Basin fill	3	---
54	10–12–84	Rotary, bentonite	11.3	11.0	10.0	10.9	Alluvium	3	---
101	10–10–84	Rotary, bentonite	36.3	36.1	35.1	36.0	Basin fill	3	C, E, G, P, U
102	10–11–84	Rotary, bentonite	25.3	25.2	24.2	25.1	Alluvium	3	---
103	10–11–84	Rotary, bentonite	19.2	25.3	18.1	19.0	Alluvium	3	---
104	10–11–84	Rotary, bentonite	11.3	11.2	10.2	11.1	Alluvium	3	---
1EX	12–11–85	Dual-wall air rotary	77.7	---	---	---	---	---	D, G, P
105	05–22–86	Rotary, bentonite	49.1	48.8	47.2	48.1	Basin fill	38.1	D
106	05–20–86	Rotary, bentonite	62.5	---	---	---	---	---	---
107	12–14–88	Hollow-stem auger	22.6	19.2	14.9	19.3	Alluvium	1.5	D,G, P
201	10–05–84	Rotary, bentonite	18.6	18.6	17.6	18.5	Basin fill	3	C, E, G, J, P, U
202	10–06–84	Rotary, bentonite	12.5	12.3	11.3	12.2	Alluvium	3	---
301	10–07–84	Rotary, bentonite	59.4	59.1	58.1	59.0	Basin fill	3	C, E, G, P, U
302	10–08–84	Rotary, bentonite	36.0	35.8	34.8	35.7	Alluvium	3	---
303	10–08–84	Rotary, bentonite	14.6	14.4	13.4	14.3	Alluvium	3	D
3EX	12–17–85	Dual-wall air rotary	54.9	---	---	---	---	---	D, G, P
3EX2	12–19–85	Dual-wall air rotary	36.6	---	---	---	---	---	---
3EX3	01–09–86	Dual-wall air rotary	102.1	---	---	---	---	---	G, P
304	05–24–86	Rotary, bentonite	48.8	30.3	28.7	29.6	Alluvium	27.4	D
401	10–09–84	Rotary, bentonite	34.4	34.2	33.2	34.1	Basin fill	3	C, E, G, P
402	10–10–84	Rotary, bentonite	21.0	20.9	19.8	20.7	Alluvium	3	---
403	10–10–84	Rotary, bentonite	13.1	13.0	12.0	12.9	Alluvium	3	---
4EX	01–07–86	Dual-wall air rotary	73.2	---	---	---	---	---	D, G, P
404	09–04–86	Cable tool	55.5	55.3	53.7	54.6	Basin fill	48.5	D
451	12–21–88	Hollow-stem auger	24.7	24.4	21.5	24.4	Alluvium	3.0	D, G
452	12–17–88	Hollow-stem auger	8.5	8.2	5.2	8.2	Alluvium	1.8	G, P
453	05–08–90	Hollow-stem auger	24.4	6.3	3.3	6.3	Alluvium	2.3	D, G, P
5EX	12–13–86	Dual-wall air rotary	89.9	---	---	---	---	---	D, G, P
501	05–22–86	Rotary, bentonite	17.1	17.0	15.4	16.3	Alluvium	15.2	D
502	05–22–86	Rotary, bentonite	38.1	38.0	36.5	37.4	Basin fill	32.6	D
503	05–22–86	Rotary, bentonite	73.2	25.3	23.4	24.1	Alluvium	19.8	D
504	07–24–86	Cable tool	69.5	69.2	67.6	68.6	Basin fill	64.0	D
505	12–17–88	Hollow-stem auger	22.2	21.6	15.5	21.6	Alluvium	1.5	D, G, P
506	12–15–88	Hollow-stem auger	7.3	6.7	5.2	6.7	Alluvium	1.5	D, G, P
507	05–10–90	Hollow-stem auger	22.2	---	---	---	---	---	D, G, P
701	05–11–90	Hollow-stem auger	8.5	4.7	3.8	4.7	Alluvium	1.1	D
702	05–11–90	Hollow-stem auger	8.1	7.3	6.4	7.3	Alluvium	1.1	D, G, P

than 500 L of water from the next well before sampling. Pump and column pipe were thoroughly drained between wells. The 9.5-cm-diameter pump generally was flushed with more than 75 L of water before sampling. The 4.4-cm-diameter pump was drained between wells and flushed with local tap water.

Surface-water samples were obtained using standard USGS sampling practices (Wood, 1976; and Guy and Norman, 1970). Ground-water and surface-water samples were processed, filtered, acidified, and preserved when appropriate at the site immediately after sampling.

Analytical Methods and Quality Assurance

Most ground-water samples were analyzed at the USGS National Water-Quality Laboratory (NWQL) or by Kenneth G. Stollenwerk, USGS National Research Program (NRP). Robert W. Puls of the USEPA analyzed samples in June 1988 and March 1989 to study the effect of filter pore size, discharge, and atmosphere on concentrations of selected constituents (Puls and others, 1990). Stollenwerk, Puls, and NWQL analyzed most metals using inductively coupled plasma atomic-emission spectrometry. Methods are described by Fishman and Friedman (1989). Linda Faires (USGS) analyzed selected surface-water and ground-water samples collected in 1989 using inductively coupled plasma-mass spectrometry. Data quality was assessed by submitting duplicate samples (about 25 percent of all samples were sent to at least two laboratories), by comparison with previous analyses for the same or similar sites, by computation of ionic balance, and by evaluation of blind samples submitted to each laboratory.

GEOHYDROLOGY

The geohydrologic characteristics of the Pinal Creek Basin are the result of past geologic events, past and present climates, and human activities over the last 100 years. The movement, storage, and chemical nature of ground water are controlled mainly by rock lithology and basin configuration. Climate, especially the amount and distribution of rainfall, determines the quantity and frequency of large surface-water flows and subsequent ground-water recharge. Because the area is semiarid, most of the drainages in the basin are dry but may convey large amounts of storm runoff during and after severe storms. Streams in the foothills of the Pinal Mountains also flow during and following snowmelt in late winter and early spring. Infiltration through permeable stream alluvium (fig. 3) is a major pathway for recharge to the regional aquifer, which occupies about 170 km^2 within Pinal Creek Basin.

In the northern part of the basin, the aquifer becomes constricted by impermeable rocks and Pinal Creek flows perennially from near Horseshoe Bend Wash to Inspiration Dam and beyond to the Salt River

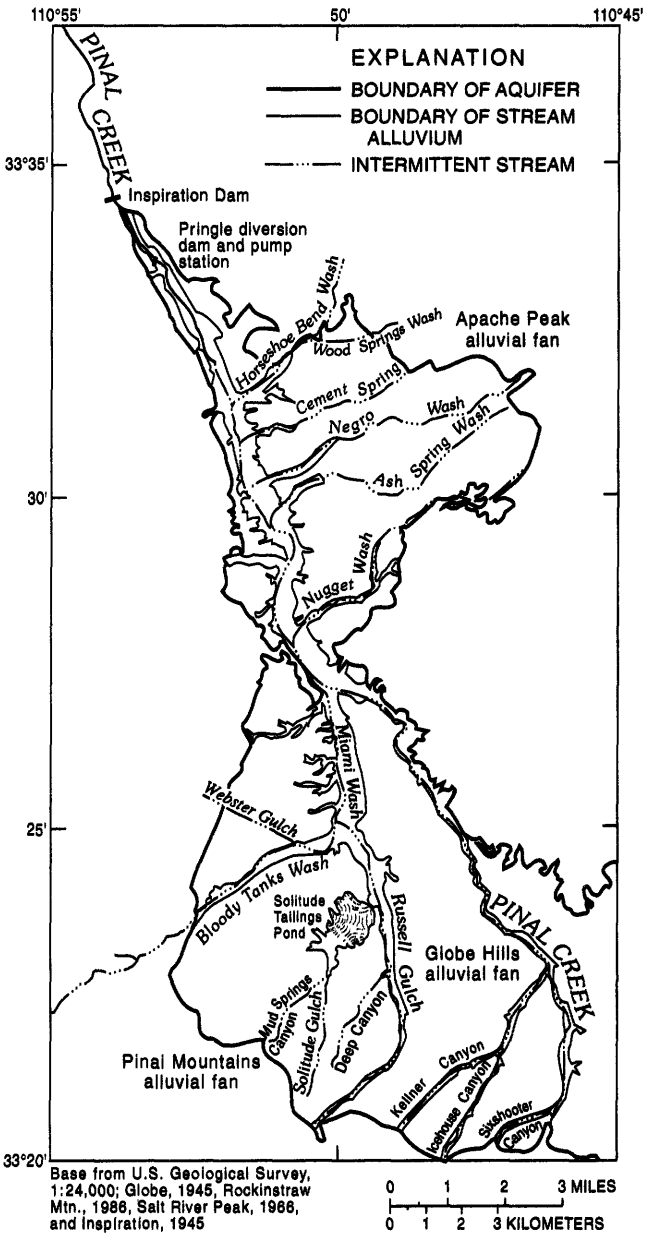

Figure 3. Aquifer area, alluvial fans, and tributary streams, Pinal Creek Basin, Arizona

(fig. 3). The exact point at which perennial flow appears varies in response to changes in climate, particularly rainfall. From 1988 to 1989, the head of flow migrated 600 m downstream. By November 1991, the head of flow was about 4.5 km south of Inspiration Dam. Ground water and surface water provide physical pathways for contaminant movement in the study area.

Rocks in Pinal Creek Basin range in age from Precambrian to Holocene. The regional aquifer is bounded laterally and at depth by impermeable rocks that range in age from Precambrian to Tertiary. Block faulting in the Tertiary and Quaternary Systems created the graben into which basin fill and stream deposits accumulated. Basin-fill sediments, which are Tertiary to Quaternary in age, and stream alluvium, which is Quaternary to Holocene in age, compose the regional aquifer. Basin-fill deposits are known locally as the Gila Conglomerate. Heindl (1958), however, showed that basin fill in the Globe area includes sediments not equivalent to sediments in the type section of the Gila Conglomerate (Gilbert, 1875), which is east of the study area.

The present basin configuration was created by crustal expansion that began 19 to 15 million years (m.y.) ago and continued until about 8 m.y. ago. This event was characterized by high-angle block faulting associated with basin subsidence, and the deposition of basin fill. Subsequent downcutting of the basin fill has created the present topography.

Deposits of Precambrian to Tertiary Age

The following discussion is summarized from Peterson (1962, pl. 1, 7), who described in detail the geology and mineral deposits of the area. Rocks of Precambrian age include schist, diorite, granite, conglomerate, quartzite, limestone, and basalt. These deposits are widely exposed in the hills and mountains throughout the study area. Rocks of Paleozoic age include quartzite, limestone, and shale. Rocks of Mesozoic and Cenozoic age are mainly intrusive and include granite, granodiorite, diabase, and monzonite, all of which are Cretaceous or Tertiary in age. Rocks of Mesozoic and Cenozoic age are exposed in the hills and mountains north of Globe and Miami. Although impermeable in most areas, locally these rocks yield water to wells. Nine wells produced water from the limestone unit(s) of Paleozoic age that underlie basin-fill deposits north of Central Heights between Miami Wash and Pinal Creek (fig. 1, this report; Rouse, 1983, p. A–29 through A–31).

Permeability was measured in "crystalline bedrock" in the Lower Oxhide pit west of Miami through the use of pressure tests. Hydraulic conductivity in one set of holes was estimated to range from 0.008 to 0.014 m/d (Rouse, 1981, p. 46) but was negligible in "a number" of other holes. Earl (1973, p. 89) estimated the hydraulic conductivity of fractured rock in the Copper Cities (now called the Sleeping Beauty) pit area to be 0.15 m/d on the basis of flow-net analysis of a seepage area in the pit. He estimated the maximum storage coefficient to be 0.06 in fractured material at the open-pit face.

The igneous and metamorphic rocks include a major body of copper porphyry ore that was formed by downward percolation of ground water, which leached metals from sulfides in the capping material and redeposited the metals into the host rocks, which are composed mainly of granite and schist (Peterson, 1962, p. 83). Ore minerals, which were originally deposited as sulfides, are disseminated in the granite mass and are enriched locally in abundant small quartz-filled veins. Chalcocite, chalcopyrite, and pyrite predominate in the deeper parts of the ore body. Chrysocolla, malachite, and azurite predominate in the upper, oxidized zone of the ore body.

Deposits of Tertiary and Quaternary Age

Sediments and rocks of Tertiary and Quaternary age include Whitetail conglomerate, basalt, granite, dacite, stream alluvium, and basin fill. The dacite, basalt, and Whitetail conglomerate are Tertiary in age and are older than the basin fill and alluvium (Peterson, 1962, p. 36, 38). The dacite and basalt are exposed in the hills and mountains north of Globe and Miami. Granite of Tertiary age is exposed southwest of Miami. Whitetail conglomerate is exposed about 2 km northwest of Webster.

Basin-Fill Deposits

Basin-fill deposits are widespread in the Pinal Creek Basin and overlie older rocks from the valley floor to the fronts of the mountains and hills. In most places, the boundary of the aquifer coincides with the boundary of basin fill with older rocks. Locally, for example along Pinal Creek south of the mouth of Miami Wash, the boundary of the aquifer is the contact

between stream alluvium and older rocks. In the southeastern part of the study area, basin fill extends eastward into Cutter basin.

Basin fill is underlain by the rock types exposed in the hills and mountains that bound the basin. In much of the basin, especially where the aquifer generally is thick, the rock type at a particular location is unknown. Just west of the Globe Hills, basin fill is underlain by diorite that is Precambrian in age. Beneath Bloody Tanks Wash, the basin fill is underlain by schist that is Precambrian in age.

Basin fill generally is thinnest along the margins and thickens to more than 1,000 m in the central part of the basin. Basin fill is about 600 m thick beneath Bloody Tanks Wash (Peterson, 1962, pl. 2) and thickens to more than 1,220 m about 0.5 km south of Bloody Tanks Wash (Peterson, 1962, p. 41). Basin fill overlies a shallow ridge of crystalline rocks about 1 km south of the mouth of Miami Wash. Basin fill at this location decreases in thickness from 260 m to about 120 m over a horizontal distance of 580 m (D.L. Igou, Cities Service Oil Company, written commun., 1967). At the mouth of Miami Wash, basin fill is less than 100 m thick and about 1 km wide. Between the mouth of Miami Wash and Horseshoe Bend Wash, the unit reaches a maximum width of 8 km. North of Horseshoe Bend Wash (fig. 3), the aquifer is constricted laterally and at depth by impermeable rocks; and at Inspiration Dam, the aquifer is truncated by volcanic rocks.

Basin fill, which is derived from rocks of the surrounding mountains, ranges "from completely unsorted and unconsolidated rubble of angular blocks as much as 4.5 m in diameter, to well-stratified deposits of firmly cemented sand, silt, and gravel containing well-rounded pebbles and cobbles" (Peterson, 1962, p. 41). The character of the deposits at a given spot reflect the distance traveled and mode of deposition. The contact between basin fill and older material is unconformable.

On the flanks of the Pinal Mountains, basin fill includes alluvial-fan deposits composed mainly of diorite and schist. North of Globe, basin fill includes fragments of basalt, limestone, quartzite, and conglomerate of Precambrian age and dacite and diabase of Paleozoic age (Peterson, 1962, p. 41). The relative amounts of each type of fragment varies from place to place. Carbonate content of the basin fill is about 1.5 percent (Eychaner, 1989, p. 570). Along Miami Wash and Pinal Creek, samples of shallow basin-fill material obtained during observation-well drilling typically contained more than 80-percent sand and gravel by weight.

Hydraulic conductivity of basin fill is estimated to range from 0.03 to 0.05 m/d on the basis of aquifer tests done by Envirologic Systems, Inc. (1983), and depends on whether confined or unconfined conditions are assumed, and on the estimated aquifer thickness (Hydro Geo Chem, Inc., 1989, p. 45). Two aquifer tests done by Cities Services Company south of the mouth of Miami Wash yielded estimates of hydraulic conductivity between 0.1 and 0.2 m/d (C.G. Taylor, Environmental Engineer, Magma Copper Corporation., written commun., 1987).

The storage properties of basin fill have not been measured. Freethey and others (1986), however, studied similar deposits in nearby basins and provided information that was used to characterize aquifer-storage properties at Pinal Creek. Basin-fill deposits studied by Freethey and others (1986) were deposited at about the same time and under similar tectonic conditions as deposits in Pinal Creek Basin. Freethey and others (1986, sheet 1) found that the storage properties of basin fill were controlled mainly by average particle size. Freethey and others (1986) designated basin fill as being either coarse, intermediate, or fine grained and estimated the range in specific yield of each type of deposit. Basin fill in Pinal Creek Basin ranges in size from boulder to clay but is composed predominately of fine sand to silt-sized material. This size distribution would place these deposits into the intermediate grain-sized facies, in which specific yield ranges from 5 to 25 percent (Freethey and others, 1986, sheet 1).

Stream Alluvium

Unconsolidated stream alluvium overlies the basin fill along Miami Wash, Pinal Creek, and other major drainages (fig. 3). The alluvium is from 300 to 800 m wide and is less than 50 m thick. A thin veneer of alluvium covers much of the basin fill but generally is not shown on published geologic maps.

The alluvium contains poorly sorted, subangular to subrounded cobble- to clay-sized material (Hydro Geo Chem, Inc., 1989, p. 22) although sand- to gravel-sized material is most abundant. Drill cuttings from observation wells (fig. 3) typically contained greater than 90-percent sand and gravel by weight; auger samples indicated the presence of silt or clay beds several inches thick. Uncontaminated alluvium contains about 0.3 percent calcite (Eychaner, 1989, p. 567).

Where the plume is acidic, all the calcite in the alluvium has been completely dissolved through reaction with acidic ground water. Drill cuttings of alluvium along Russell Gulch typically contained 75- to 98-percent sand and gravel. Sand-sized particles contained mainly quartz, feldspar, and lesser amounts of mica and a variety of rock fragments. Gravel-sized material consisted mainly of rock fragments of granite, volcanic rocks, and schist. Alluvium contains interbedded clays and lenticular clay layers that were as much as 12 m thick at Nugget Wash, 0.5 km north of the mouth of Negro Wash, and in the southwestern part of the Kiser area. Particle-size analyses of drill cuttings indicate that these lenticular clay layers thin toward the center of the basin (Hydro Geo Chem, Inc., 1989, p. 27) and extend an indeterminate distance in length parallel to the axis of the basin.

The effective hydraulic conductivity of the alluvium between well groups 400 and 500 was estimated to be 260 m/d by applying Darcy's law to observed outflow, water-level gradients, and the cross-sectional area of the alluvium perpendicular to the direction of flow (Neaville, 1991). Hydro Geo Chem, Inc. (1989, p. 47) obtained hydraulic-conductivity values for the alluvium that ranged from 150 to 220 m/d from aquifer tests done in the Kiser area and along Pinal Creek north of the mouth of Miami Wash. These tests yielded estimates of specific yield that ranged from 0.20 to 0.22.

Estimates of specific yield of the alluvium also were obtained using the temporal-gravity technique (Pool and Eychaner, 1995). Gravity surveys in the basin were done on four occasions between February 1991 and March 1993, during which time ground-water levels were gradually rising. During each survey, gravity was measured at USGS observation wells and at two bedrock stations, and water levels were measured at the observation wells. On the basis of observed gravity changes and water-level rises, average specific yield was estimated to range from 0.16 to 0.21. Variations in specific yield were related mainly to variations in lithology. Smaller values of specific yield generally were associated with sandy, silty, or low-porosity intervals (Pool and Eychaner, 1995, p. 431).

Occurrence and Movement of Ground Water

Anderson and others (1992, p. 39) described the hydrologic setting of alluvial basins in Arizona in terms of annual unit downvalley-flow rates. Under this scheme, Pinal Creek Basin is classified as a multiple source-sink group, in which the basin response to ground-water pumping depends on the location and magnitude of recharge, natural discharge, and pumping. Rainfall and snowmelt provide uncontaminated water to Pinal Creek Basin; no surface streams or adjacent ground-water bodies deliver water into the study area.

Ground water in rocks of Precambrian to Tertiary age generally is restricted to intensely fractured and (or) faulted areas. Elsewhere, these rocks are impermeable. In the Globe Hills, precipitation enters the subsurface through faults and joints mainly in shale and quartzite formations associated with the Old Dominion vein fault (Peterson, 1962, p. 44, Beckett, 1917, p. 41). This water was intercepted by mining operations in the eastern part of the Old Dominion Mine. Beckett (1917) noted that the mining of successively lower levels of the mine drained this water from the overlying level. Because this water was encountered only as mining proceeded to the east, it is doubtful that before mining these fracture zones were hydraulically connected to basin fill or stream alluvium to the west. Limestone units of Paleozoic age underlie basin fill between Miami Wash and Pinal Creek northwest of Globe and yield usable quantities of water to wells. The degree of hydraulic interconnection between these units and basin fill is unknown.

Ground water in basin fill flows generally northward from the flanks of the Pinal Mountains and westward from the Apache Peak alluvial fan (fig. 3). On the basis of measured tritium concentrations, water in shallow alluvium near recharge areas (well 10) was recharged less than 40 years ago; however, uncontaminated water in basin fill (well 404) underlying the contaminant plume probably is more than 40 years old. Most ground water in basin fill that is not withdrawn by wells eventually moves upward into the stream alluvium, discharges to the perennial reach that originates north of Horseshoe Bend Wash (fig. 3), and exits the basin as surface flow at Inspiration Dam. Evapotranspiration is estimated to account for between 20 and 25 percent of ground-water outflow (Neaville, 1991, p. 58). Most rainfall or snowmelt that does not evaporate or run off recharges the aquifer through stream alluvium in main channels and tributaries. In addition to basin-scale movement of water between alluvium and basin fill, pumping-induced gradients can cause the local-scale movement of ground water either

upward or downward. A ground-water divide extends from Globe southward to the Pinal Mountains. East of the divide, which may be caused by a fault along Pinal Creek (Hazen and Turner, 1946, p. 24), ground water flows generally eastward into the Cutter basin.

From about 1942 through May 1988, seepage from Webster Lake (fig. 1) contributed flow to the regional aquifer. Lake water leaked through coarse leach-plant discard material and the alluvium of Webster Gulch, moved downgradient, and entered the regional aquifer near the confluence of Russell Gulch and Bloody Tanks Wash. Flow from Webster Gulch for 1987–88 was estimated to be between 0.04 and 0.08 m^3/s (Hydro Geo Chem Inc., 1989, p. 50).

Water levels have been monitored in observation wells that were drilled along Miami Wash and Pinal Creek between 1984 and 1992 (fig. 2). Seasonal and other variations in recharge caused rapid water-level changes even in wells that are more than 50 m deep. Water levels along Miami Wash and lower Pinal Creek rose 1 m or less from 1984 to 1985 but dropped steadily from 1986 to 1990 in response to (1) less-than-average rainfall in the basin; (2) the draining of Webster Lake by May 1988, which was a significant source of water to the regional aquifer; and (3) increased pumping in the Kiser area for the purpose of remediation. The water-level decline generally decreased downstream. Water-level declines from 1986 to 1990 were 17, 10, and 1 m at sites 100, 400, and 500, respectively. During early 1991, water levels rose in all observation wells in response to larger-than-average amounts of precipitation that fell during winter and spring. The greatest water-level increase was 9 m in 3 months at well 10. Beckett (1917, p. 41) reported a similar rise of 12 m in 3 months near Globe in 1915.

At each site, the lowest head generally is near the contact between the basin fill and alluvium; higher heads were measured in both deeper and shallower wells. Such a head distribution probably is caused by preferential flow of water into coarse, highly permeable material near the base of the alluvium. At sites 100, 400, and 500, the highest head is in the deepest well. Differences in head between wells at a site were less than 0.5 m. The horizontal hydraulic gradient along Miami Wash and Pinal Creek is about 0.008. Using the estimated hydraulic conductivity of 260 m/d, the observed slope of 0.008, and an estimated porosity of 25 percent, the average linear ground-water velocity is estimated to be about 8 m/d.

Occurrence and Movement of Surface Water

Streams in most of the basin are dry except following periods of intense or prolonged rainfall. The direction of flow in tributaries is mostly northward and eastward to Pinal Creek, which flows in a north- to northwest-trending direction to the Salt River. Pinal Creek is perennial for about 6 km upstream from Inspiration Dam to the mouth at the Salt River. In most years during late winter and spring, snowmelt produces flow in streams on the flanks of the Pinal Mountains. During years of greater-than-average snowfall in the Pinal Mountains, flow may be uninterrupted from the Pinal Mountains to Inspiration Dam for a period of weeks. Hazen and Turner (1946, p. 25) measured a net flux of flow from streams to the aquifer on the flanks of the Pinal Mountains. In the spring of 1989, following a dry winter, Neaville (1991) measured a total of 0.03 m^3/s of streamflow in six tributaries underlain by granitic rock. The entire flow infiltrated stream alluvium just north of the fault contact between the basin fill and crystalline rocks.

Webster Lake

Webster Lake was at the confluence of Webster Gulch and Lost Gulch about 3 km north of Miami (fig. 1). After 1926, leach-plant discard material was dumped from rail cars along the south edge of Webster Gulch and formed a slope at the angle of repose. The material had been crushed to less than 1 cm in diameter but was not as fine as concentrator tailings. One or more landslides blocked the channel at a point where the drainage area was about 36 km^2. These deposits later were extended across the whole valley. The lake was formed in 1941 (Timmers, 1986, p. 3) and was present in aerial photographs taken January 23, 1942 (T.A. Conto, Senior Project Engineer, Cyprus Miami Mining Corporation, oral commun., October 6, 1988). Lake stage was controlled by a tunnel that later was blocked. The lake was drained by order of the USEPA in 1986, and by May 1988, the lake was completely dry.

The capacity of Webster Lake was estimated from topographic maps made after the lake was drained (Cooper Aerial Survey Co., 1989). USGS topographic maps from 1947 show the lake area to be 104,000 m^2 in December 1945, which corresponds to a calculated volume (using the 1989 maps) of 480,000 m^3. In this study, the maximum area and

volume of the lake was calculated to be 462,000 m^2, and 7.15 million m^3, respectively. Gilkey and Beckman (1963), however, reported an area of 526,000 m^2 at an unknown elevation.

Spills of acidic lake water occurred when intense or prolonged rainfall caused the lake to overflow. Records of spills are nonexistent for the 1940's through the 1960's, but during the late 1970's and 1980's, the lake overflowed on more than eight occasions. Perhaps the most prolonged spill of lake water occurred from January 16 to January 30, 1978, when the lake flowed at a maximum discharge of 0.69 m^3/s and had a pH as low as 2.57.

Webster Lake was used in the production of copper (Cu) to store water from many sources until it was needed again. These waters generally were acidic with large concentrations of metals (Timmers, 1986, p. 17–22). The largest volumes of water came from the dewatering of underground or open-pit mines, and from iron launders, in which Cu was recovered by precipitation in a solution containing scrap iron. The solution also contained about 2,000 and 7,000 mg/L of dissolved sulfuric acid (H_2SO_4) and iron (Fe), respectively (Hardwick, 1963, p. 59). Launder solutions were first produced by ICCCo in 1941 from water that drained into their underground mine and became acidic during unforced leaching (Central Arizona Association of Governments, 1983, p. 27). In 1944, the electrolytic precipitation plant was destroyed by fire, and iron launders were used exclusively for about 1 year. In 1950, intentional leaching of caved areas was begun above the mine (Honeyman, 1954). The leach water came from Webster Lake, which had a pH of 2.5 and contained at least 10 mg/L of ferrous iron (Fe). Inspiration's vat and in-situ leaching iron-launder facilities were closed in 1974 and 1981, respectively (Timmers, 1986, p. 18–22). The iron launders were replaced by a solvent-extraction plant that began operating in 1979 (Central Arizona Association of Governments, 1983, p. 52).

Analyses of lake water, which were collected from the mid-1970's until the lake was drained, indicate that the pH of lake water was between 2 and 3. Concentrations of dissolved Fe and sulfate (SO_4) were greater than 2,000 and 19,000 mg/L, respectively (see chapter D, this report).

Perennial Streamflow

The aquifer is constricted laterally and at depth near site 500 (fig. 2) north to Inspiration Dam. In 1992, ground-water discharge to the surface sustained perennial flow from about 1 km below site 500 to Inspiration Dam at the basin boundary and beyond to the mouth of Pinal Creek. Streamflow measurements made during a period of base flow in March 1990 indicate that about 40 percent of base flow surfaces in the first 600 m of the perennial reach (Faires and Eychaner, 1991). Ground-water levels and the point at which perennial flow begins are controlled by variations in precipitation, ground-water withdrawals, and the removal of contamination sources. From 1987 through 1990, rainfall in the basin was 80 percent of normal and the head of flow migrated about 700 m downstream. Following record streamflows in the winter of 1992–93, the head of flow moved about 1 km upstream.

Discharge and water quality have been monitored since 1979 on Pinal Creek at the streamflow-gaging station at Inspiration Dam (figs. 3 and 4). During 1981–91, average discharge at Inspiration Dam was 0.31 m^3/s and includes ground-water discharge and direct runoff. Ground-water discharge to the perennial reach varied from 0.21 to 0.28 m^3/s from 1980 to 1989. Streamflow diversions and ground-water withdrawals from stream alluvium at Pringle pump station, about 2 km upstream from Inspiration Dam, averaged 0.09 m^3/s during 1979–85 and 1988–89. Dissolved-solids concentration in streamflow gradually increased from 1979 through 1988 but decreased slightly from 1989 through 1991.

Discharge measurements made concurrently with water-chemistry samples at Pinal Creek at Setka Ranch provided limited information on the nature of base flow near the head of perennial flow. All discharges and water samples were measured and collected when no ephemeral flow was contributing to the creek. Superimposed on the long-term trend of decreasing discharge was a yearly cycle in which minimum discharges occurred generally during the summer, and maximum discharges occurred during the winter. The minimum discharge measured in 1988 was 29 percent below the average of the maximum discharges measured during the preceding and following winters. The long-term decrease is accompanied by downstream movement of head of flow and declining ground-water levels, all of which are controlled by variations in fluxes in the upper part of the basin. Chloride (Cl), a conservative constituent in the flow system at Pinal Creek, changed little during 1988, indicating that the yearly variation in flow probably is not related to increased evapotranspiration during summer

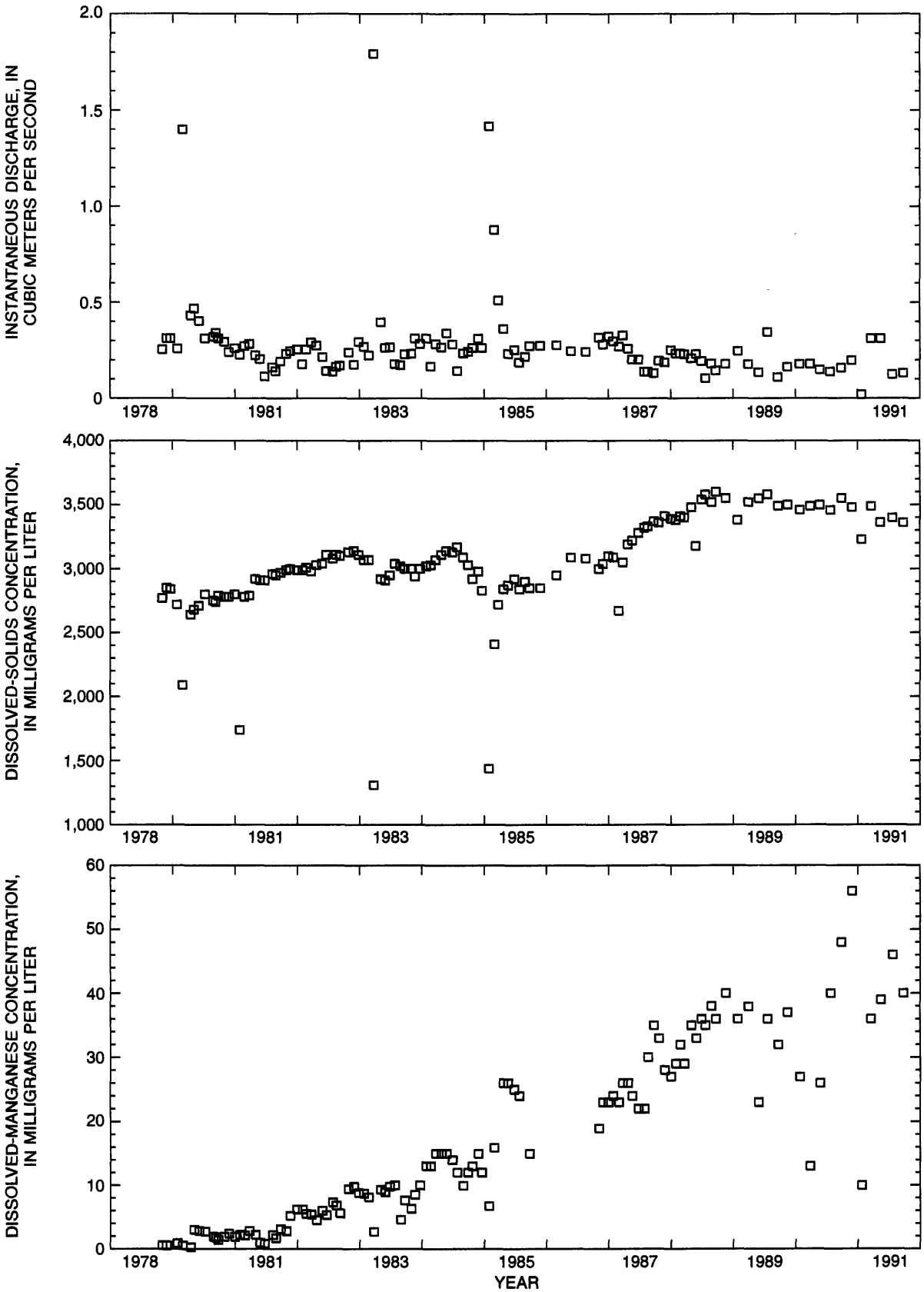

Figure 4. Instantaneous discharge and concentrations of dissolved solids and dissolved manganese, Pinal Creek at Inspiration Dam, 1979–91.

months. The decrease may be caused by increased withdrawals for stock and domestic use in the area or may reflect seasonal variations in local recharge.

Water Chemistry

Although uncontaminated water was present throughout Pinal Creek Basin before development, quantitative evidence is limited to describe that water. Ground water in recharge areas of alluvial basins in Arizona typically is a calcium bicarbonate type, has a pH from 6.9 to 7.4, and is nearly saturated with dissolved oxygen (Robertson, 1991, p. 22–23). The average composition of such water in seven basins totaled about 500 mg/L dissolved solids, and included 21 mg/L of SO_4 and 44 mg/L of silica (SiO_2). Before major mining operations began in the Miami-Inspiration ore body, wells 1 km south of the mouth of Miami Wash yielded "large quantities" of potable water (Daily Silver Belt, September 8, 1912, p. 5).

Precipitation about 100 km southeast of the basin had a mean dissolved-solids concentration of less than 3 mg/L and a mean pH of 5.5 in 1989 (National Atmospheric Deposition Program, 1990, p. 72). Uncontaminated water in the basin has a near-neutral pH and contains less than 300 mg/L dissolved solids (table 2). Hazen and Turner (1946) sampled streamflow on the northern slopes of the Pinal Mountains in April 1945. Median dissolved-solids concentration of five samples was 105 mg/L (table 2). Ground water from uncontaminated parts of the aquifer along the central parts of the basin contained no more than 300 mg/L dissolved solids from 1986–87 (Eychaner and others, 1989).

Locally, water from fractures in mineralized areas may naturally contain more than 2,000 mg/L dissolved solids. Beckett (1917) recognized two distinct waters in the Old Dominion Mine, which was plagued by water problems throughout most of its active life. Water that Beckett called "Westside" water was low in dissolved solids and was similar to water found today in uncontaminated basin fill and alluvium. This water entered the mine from basin fill to the west where mine adits intercepted fractures in underlying dacite. "Eastside" water was intercepted by workings in the mine as drifts were extended eastward into the Globe Hills. This water came from fractures and faults in shale and quartzite formations (Beckett, 1917). The temperature of the water was 32°C (Beckett, 1917, p. 41) and contained about 2,300 mg/L dissolved solids (Peterson, 1962, p. 44).

Contamination sources in the basin generally were acidic and contained large concentrations of metals such as Fe and Cu. Webster Lake, a major source of contamination, was a mixture of water from the mining process, wastewater, and natural water. Samples of lake water taken sporadically during the 1970's and 1980's indicate that the lake was consistently acidic and contained large concentrations of metals and SO_4, although concentrations varied horizontally, vertically, and temporally. From 1981 through 1988, pH at and near the lake surface varied from 2.4 to 2.8 (Arthur, 1987a). From 1976 to 1988, concentrations of measured SO_4 ranged from 13,000 to 39,000 mg/L. Concentrations of dissolved Fe were larger than 2,000 mg/L (Arthur, 1987a), and concentrations of other metals generally were greater than 100 mg/L.

Wells drilled into Webster Gulch alluvium downgradient from Webster Lake yield water similar in chemical composition to water in the lake (table 3). In May 1989, water from Webster Wash Dewatering Well 3 (WWDW3) had a pH of 3.4, a specific conductance of 13,100 μS/cm, and concentrations of SO_4 and Fe of 13,200 and 4,270 mg/L, respectively. Although still acidic, water from well 51 contained smaller concentrations of many constituents than did water from WWDW3. The major process retarding acidic water movement is dissolution of calcite from the aquifer, which raises solution pH and causes most metals to precipitate. Bicarbonate that occurs naturally in ground water also provides some neutralization capacity. All available calcite has been consumed for at least 15 km along a ground-water flow path below the lake. At a point 6 km from the lake, water at the base of the alluvium has a pH of 3.6 and elevated concentrations of dissolved metals and SO_4 (fig. 5 and table 2). Silicate minerals also neutralize ground water but at a slower rate than calcite and bicarbonate (Stollenwerk, 1988).

The distribution of Fe in the aquifer is closely related to pH, which controls Fe solubility. Stollenwerk (1991) showed that attenuation of Cu, cobalt (Co), and nickel (Ni) in column experiments was a function of pH and could be quantitatively modeled by the diffuse-layer surface-complexation model in MINTEQA2 (Allison and others, 1991). In addition, attenuation of Cu, Co, and Ni along a flow path in the aquifer was simulated reasonably well using the same model and equilibrium constants as for the column data.

Table 2. Chemical analyses of native water, Pinal Creek Basin, Arizona

[---, no data]

Site name	Date of sample	Temperature, in degrees Celsius	pH	Dissolved solids, in milligrams per liter	Calcium, in milligrams per liter (Ca^{2+})	Magnesium, in milligrams per liter (Mg^{2+})	Sodium and potassium, in milligrams per liter ($Na^{+}+K^{+}$)	Alkalinity, in milligrams per liter ($CaCO_3$)	Sulfate, in milligrams per liter (SO_4^{2-})	Chloride, in milligrams per liter (Cl^{-})	Silica, in milligrams per liter (SiO_2)	Copper, in micrograms per liter (Cu)	Iron, in micrograms per liter (Fe)
Well 10[1]	5-20-91	18.0	6.7	251	38	12	27	116	69	9.2	0.50	<0.010	0.017
Well 404[1]	5-24-90	19.3	7.6	232	44	14	26	181	8.3	5.1	.40	<.010	0.013
Streamflow from the Pinal Mountains[2].	4-45	---	---	105	19	7.8	9.0	65	14	3	.3	---	---

[1]Longsworth and Taylor, 1992.

[2]Median of between five and eight streamflow samples from the Pinal Mountains. Data from Hazen and Turner (1946).

Table 3. Chemical analyses of contaminated water, Pinal Creek Basin, Arizona

[---, no data. Water filtered through 0.45-micrometer filter before analysis except where indicated. Data from Longsworth and Taylor (1992) except where indicated]

Site name	Date of sample	Temperature, in degrees Celsius	Specific conductance, in microsiemens per centimeter	pH	Calcium, in milligrams per liter (Ca^{2+})	Magnesium, in milligrams per liter (Mg^{2+})	Sodium, in milligrams per liter (Na^{+})	Alkalinity, in milligrams per liter ($CaCO_3$)	Sulfate, in milligrams per liter (SO_4^{2-})	Chloride, in milligrams per liter (Cl^{-})	Aluminum, in micrograms per liter (Al^{3+})	Copper, in micrograms per liter (Cu)	Iron, in micrograms per liter (Fe)	Manganese, in micrograms per liter (Mn)
Webster Lake[1]	2-1-88	11.0	---	2.7	510	730	240	0	19,000	350	850	210	6,000	730
Webster Wash Dewatering Well 3[2].	5-5-89	21.5	13,100	3.4	460	689	210	0	13,200	396	670	194	4,270	689
Well 51	11-6-90	18.0	8,200	3.6	460	280	160	0	5,800	250	150	100	1,700	280
Well 451	11-7-90	18.0	3,980	4.3	480	160	110	0	2,600	160	7.3	16	240	160
Well 501	8-25-90	19.0	3,370	6.1	670	150	91	96	2,400	110	<1	<.020	<.040	150
Pinal Creek at Inspiration Dam near Globe, Arizona (09498400).	9-27-90	30.5	3,450	7.8	600	150	92	114	2,100	100	---	.008	.03	150

[1]Samples at lake edge. Data from Brown (1990).

[2]Water unfiltered. Data from Hydro Geo Chem, Inc. (1989).

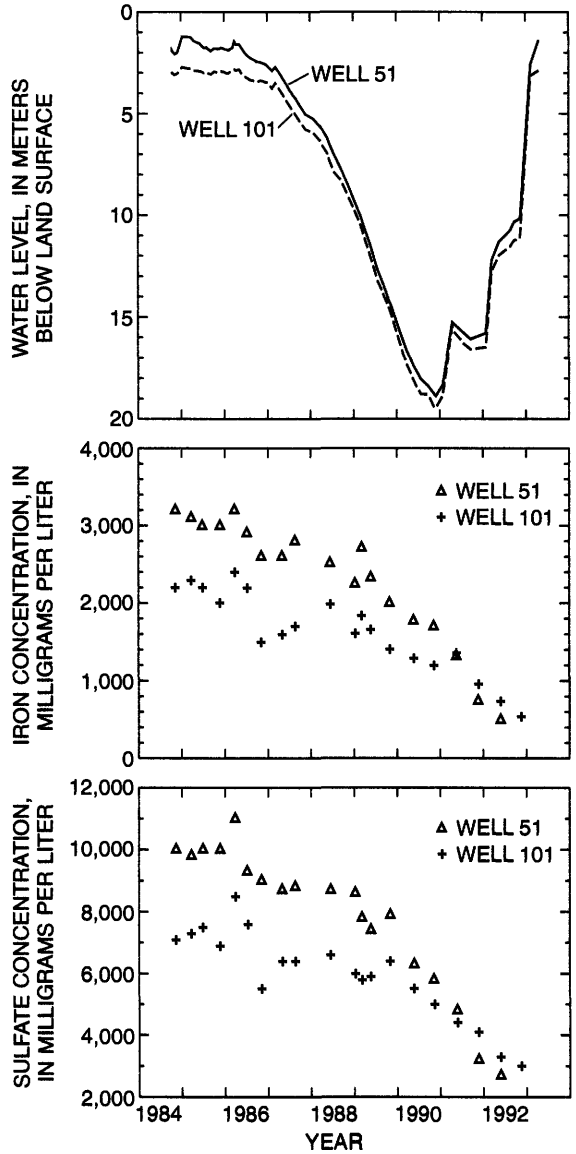

Figure 5. Ground-water levels and concentrations of iron and sulfate adjacent to Miami Wash.

Stollenwerk (chapter B, this report) provides details of the significant reactions.

In the lower alluvium, pH increases gradually to 4.5 at a point 15 km from the lake, then increases more abruptly within 2 km to 6.1 km at site 500. Neutralized water from well 501 (table 3) had a pH of 6.1 in 1990 and contained concentrations of dissolved metals near detection limits. Neutralized water is present at the lateral fringes and below the acidic core of the plume. Uncontaminated water is present in basin fill beneath and adjacent to stream alluvium.

Neutralized water discharges along the entire perennial reach. As carbon dioxide (CO_2) degases and pH increases downstream, black manganese (Mn) oxide precipitates. From March 6 to March 8, 1990, samples of streamflow and shallow ground water collected at 11 sites showed that through the reach pH increased 1.5 units, Mn decreased 80 percent, and dissolved inorganic carbon decreased 45 percent. A reaction-path model using the computer program PHREEQE (Parkhurst and others, 1985) specified CO_2 degassing, Mn precipitation, and calcium (Ca) dissolution to represent pH, Mn, and inorganic-carbon trends (Eychaner, 1991b). Water at the lower end of the reach had a pH of nearly 8 and contained slightly less dissolved solids than water from well 501.

MINING IN PINAL CREEK BASIN

Over the past century, the Globe-Miami Mining District has been one of most productive mining areas in the Nation. The total value of extracted minerals since 1878 exceeds $1 billion mainly from Cu, although other minerals have been mined in the district. The settlement and development of the area in large part was due to mining and related activities.

History of Mining

The history of mining in Pinal Creek Basin in some ways also is the history of evolving technologies to extract Cu from rock most efficiently. The technologies described below were used independently or in combination at various times and in different mines in the area. An awareness of the various technologies or methods is important because of the different effects each could have had on water chemistry in the basin.

Mining began in Pinal Creek Basin in 1878 with the extraction of silver from the hills adjacent to Globe. Silver ore from mines in the northern Globe Hills was processed in a mill in the perennial reach of Pinal Creek until 1882 (Ransome, 1903, p. 115). Cu production began in 1881 and was followed by gold in 1896 and molybdenum in 1938 (Peterson, 1962, p. 81). As of 1993, only Cu is mined, although the other metals are recovered as byproducts (Greeley and Kissinger, 1990). Lead (Pb) was produced mainly from 1911 to 1953, and zinc (Zn) was produced intermittently (Peterson, 1962). Mn has been mined intermittently during periods of unusually high prices (Arizona Bureau of Mines, 1969, p. 211–225).

After an initial period when many companies were active, three principal mining corporations extracted ore in Pinal Creek Basin (Peterson, 1962). The Old Dominion Copper Company produced Cu from 1882 until 1931 from a mine at the northwest edge of Globe (fig. 1). The Miami Copper Company was organized in 1907 and began production in 1911. ICCCo was formed in 1912 and began production in 1915. The Miami and Inspiration properties are adjacent properties just north of Miami (fig. 1). Miami Copper Company purchased the Old Dominion property in 1940. Throughout the life of the district, many smaller companies have operated for short periods and generally were absorbed into the major firms. In July 1988, the Inspiration property was sold to Cyprus Miami Mining Corporation, which is the owner as of 1993. The Miami property has had several owners since 1960 and as of 1993, is operated by the Pinto Valley Division of Magma Copper Company. This report will refer to properties and companies by name as needed for clarity.

Beginning in 1882, cuprite, malachite, chrysocolla, and native Cu were mined from vein deposits on the Old Dominion property (Ransome, 1903, p. 122–124). Nearly all the ore produced until 1901 was from oxidized minerals (Ransome, 1903, p. 120).

During 1912–14, Inspiration experimented with ore concentration using froth flotation, and a large concentrator went into operation in 1915 (Burch, 1916). Other companies also began using flotation. Crushed ore was agitated in a water bath containing reagents that selectively aggregated SO_4 minerals such as chalcocite, which is the principal mineral in the ore body (Peterson, 1962, p. 69). Air bubbled through the bath and carried the mineral to a froth at the surface, where it could be skimmed off.

Leaching of mixed oxide and SO_4 ores in tanks of an acid ferric SO_4 solution began in 1926 at Inspiration (Peterson, 1962, p. 84); Cu metal was produced by electrolytic precipitation. Tank leaching produced solutions containing 25 to 30 g/L of Cu, of which about 5 g/L could be recovered by direct electrolysis (Sheffer and Evans, 1968, p. 44; Hardwick, 1963, p. 58). Inspiration chose to recycle solutions repeatedly between leaching and electrolysis mainly because the alternative, "precipitation with iron... means difficulties in the disposal of large amounts of waste liquor" (Van Arsdale, 1926, p. 59).

The Old Dominion mine closed in October 1931, and Miami and Inspiration closed in May 1932 as prices dropped in the early 1930's. Miami Copper remained closed for about 2 years, and Inspiration was closed for about 4 years; however, Old Dominion never reopened.

In 1941, Miami Copper began leaching residual Cu from the caved-in areas of earlier underground works, and Inspiration began a similar process in 1950 (Peterson, 1962, p. 85). Dilute H_2SO_4 was sprayed over the land surface and later collected from mine tunnels below. The resulting solutions generally contained 1 to 2 g/L of Cu (Sheffer and Evans, 1968, p. 11) and were too dilute to precipitate Cu metal electrolytically (Hardwick, 1963, p. 56). At Inspiration, similar solutions containing an average of 3.2 g/L of Cu resulted from washing tank-leached ores before discarding the solid residue (Hardwick, 1963, p. 59).

Cu was recovered from these weak solutions using Fe launders (Sheffer and Evans, 1968, p. 32–44). The Cu solution was passed over shredded scrap Fe, which caused the Fe to dissolve and the Cu to precipitate as a sludge containing 60- to 90-percent Cu (Central Arizona Association of Governments, 1983, p. 39).

As the remaining ore grade decreased, Inspiration began open-pit mining in 1948 in order to reduce costs (Peterson, 1962, p. 85). In 1954, Miami Copper began production by open-pit mining from an ore body that averaged 0.5-percent Cu (Peterson, 1962, p. 85). Since 1954, open-pit mining has supplied all the ore from the Inspiration property (Central Arizona Association of Governments, 1983, p. 50).

In 1964, Ranchers Exploration and Development Corporation began mining and heap leaching from an ore body about 2 km west of Miami that was bordered on three sides by Inspiration property. In 1968, Ranchers became the first company to operate a commercial solvent-extraction plant to increase concentrations of Cu in solution after leaching (Larson and Henkes, 1970, p. 101).

In the solvent-extraction process, leach solutions containing 1 to 5 g/L of Cu are mixed with an organic solvent (Biswas and Davenport, 1980, p. 279). Cu ions bind to the organic molecules and leave Fe, SO_4, and other constituents behind. The organic liquid containing Cu is then mixed with a second aqueous solution at lower pH, which removes the Cu from the organic molecules, resulting in a solution that contains from 40 to 50 g/L of Cu that can be precipitated electrolytically. Miami Copper opened a solvent-extraction plant in 1976, and Inspiration opened a solvent-extraction plant in 1979 (Central Arizona Association of Governments,

1983). Ranchers ceased operations in 1982 and was purchased by Inspiration in 1984 (Burgin, 1986, p. 73). Although solvent extraction generally has replaced iron launders for treatment of leach solutions, one small company began operating an iron launder near Miami in 1988 (Greeley and Kissinger, 1990, p. 72).

Sources of Contamination

Ground-water and surface-water contamination at Pinal Creek is the cumulative result of decades of large-scale mining on a number of properties. Because of its size, length of existence, and hydrogeologic setting, Webster Lake probably was the single biggest source of contamination in the basin. Significant contamination of water in the basin, however, was noted before the existence of Webster Lake. A well field in the Kiser area became acidic in the late 1930's. A well field 1 km south of the mouth of Miami Wash similarly became unusable in 1947, only 5 years after Webster lake was known to exist. In the mid-1980's, USEPA inspectors documented 47 wastewater, process-water, and drainage impoundments associated with one mine. Most of these impoundments were unlined, and some drained into nearby washes (Arthur, 1986, p. 6). The quantity of infiltration and intermittent spills from impoundments at this and other mines is unknown.

Some mining methods have a greater potential to affect water resources than others. During solution mining, which began in the area in the 1940's, H_2SO_4 was distributed over waste dumps and abandoned underground mining areas (Hardwick, 1963, p. 46). At another mine, water was pumped on mine dumps. Following percolation, the solution was collected by dams in natural drainage channels. In both instances, some of the processed water probably percolated into underlying materials and into the regional aquifer.

Runoff from tailings also is a probable source of contamination. When crushed and placed in tailings piles, sulfide minerals, of which pyrite is the most abundant, react with water in the presence of air to produce SO_4 and acidity, which often drains into natural channels and ultimately to the regional aquifer.

Remedial Action

Remedial action began in the basin in the late 1970's as mining companies placed more emphasis on control of surface impoundments. Inspiration began a wastewater management program in 1979 (Timmers, 1986, p. 3) that was directed at reducing the volume of wastewater in storage. Later actions were initiated with the goal of removing contaminants already in the aquifer.

The surface-drainage area contributing to Webster Lake was decreased by a series of impoundments beginning in 1979. After 1983, the original surface-drainage area was reduced from 36 to 15 km^2. After 1984, surface-drainage area was reduced to 6.4 km^2, and after 1986, it was reduced to 3.2 km^2 (R.A. Prescott, ICCCo, written commun., 1987). As a result of these impoundments, Webster Lake was less susceptible to overflow in response to runoff from intense or prolonged rainfall.

From March to December 1986, acidic ground water discharged into low-lying areas in the Kiser area. The USEPA determined that the major source of this contamination was Webster Lake water that had entered the regional aquifer through the alluvium of Webster Gulch. The USEPA considered these flows to be discharges of pollutants from a point source to the waters of the United States, and in 1986 issued an order under the Clean Water Act to ICCCo to eliminate the sources of contamination, remove contamination already in the aquifer, and monitor water chemistry (Arthur, 1986). The administrative record leading to the order and its successive revisions includes information on the history of contamination sources. Arthur (1987b) summarized the evidence supporting the order and included two subsequent modifications of the required actions. Studies on which remediation work was based were described by Hydro Geo Chem, Inc. (1989).

Webster Lake was drained beginning in late 1986 and was completely dry by June 1988 (Hydro Geo Chem, Inc., 1989, p. 8). When remediation began, lake volume was about 4.4 million m^3 (table 4). Most of the water was spread on 1.8 km^2 of inactive tailings piles to evaporate, and some water was used for dust control or process-makeup water. As the lake was being drained, five wells were drilled through overlying tailings into the alluvium in Webster Gulch to prevent additional contamination to the regional aquifer. Water from the wells was spread on tailings to evaporate.

Wells also were completed in the plume along Miami Wash and Lower Pinal Creek to remove contaminated water from the aquifer. In May 1987, the first of nine production wells was drilled in the Kiser area for this purpose. Contaminated water also was

Table 4. Elevation and volume of Webster Lake, Arizona,1966–88

[Prior to August 1986, dates of measurements are unknown]

Date	Elevation, in meters	Volume, in cubic meters times 1,000	Date	Elevation, in meters	Volume, in cubic meters times 1,000	Date	Elevation, in meters	Volume, in cubic meters times 1,000
– –66	1,122.6	5,160	– –86	1,122.0	4,180	10–31–87	1,107.1	930
– –67	1,121.1	4,600	08–18–86	1,120.6	4,410	11–24–87	1,106.0	776
– –68	1,122.9	5,320	09–22–86	1,120.6	4,410	12–01–87	1,105.6	722
– –69	1,122.0	4,960	10–13–86	1,120.5	4,370	01–04–88	1,103.8	499
– –70	1,120.1	4,220	11–17–86	1,119.8	4,110	01–11–88	1,103.4	454
– –71	1,119.5	4,000	12–31–86	1,118.9	3,780	01–19–88	1,103.0	416
– –75	1,115.0	2,550	01–31–87	1,118.32	3,580	02–23–88	1,101.5	285
– –80	1,125.3	6,360	02–28–87	1,117.82	3,410	02–29–88	1,101.0	246
– –81	1121.1	4,600	02–30–87	1,116.2	2,890	03–07–88	1,100.4	202
– –82	1,119.8	4,110	06–01–87	1,115.0	2,550	03–15–88	1,099.3	129
– –83	1,120.7	4,450	06–30–87	1,113.6	2,200	04–01–88	1,098.0	59
– –84	1,123.2	5,450	07–31–87	1,112.0	1,820	04–29–88	1,095.6	6.2
– –85	1,122.6	5,200	08–31–87	1,110.4	1,480	06–13–88	1,094.7	0

pumped from a drift that extends into basin fill beneath Miami Wash about 1 km south of Pinal Creek. This water was neutralized with ammonia and pumped out of the basin to the Pinto Valley Division of Magma Copper Company. In addition, wells were installed along the alluvium between well sites 400 and 450 in order to remove contaminated water near the acidic front of the plume.

This remediation, combined with variations in rainfall, had significant effects on both water levels and contaminant concentrations in the Kiser area (fig. 1) and along lower Pinal Creek. The saturated thickness of the alluvium in the Kiser area decreased by much as 50 percent between 1986 and 1991. From 1991 to 1993, recharge from rainfall and melting snow raised water levels as much as 18 m (fig. 5). Concentrations of dissolved Fe at sites 50 and 100 decreased by more than two-thirds and one-third, respectively, from 1986 to 1992 (fig. 5). The chemical changes observed in water in resaturated sediment provide a more complete model of short-term cleanup effects. Samples were collected in May 1991 from six wells that had been completely dewatered. In resaturated alluvium at site 400, pH remained at about 4 following rewetting, but concentrations of dissolved metals decreased. Fe decreased from 36 mg/L before drying to 0.07 mg/L following resaturation. Over the same time, SO_4 decreased from 2,000 to 100 mg/L. Most other constituents exhibited similar declines.

SYNOPSIS OF RESEARCH ELEMENTS

Research at the Pinal Creek toxics site has been ongoing since 1984 and has involved hydrologists and other scientists from the USGS, the USEPA, and several universities. The following chapters of this volume summarize the results of research on plume geochemistry, the role of colloids in contaminant transport in the plume, surface-water chemistry, and oxide precipitation on streambed material in the perennial reach.

Stollenwerk (chapter B, this report) presents a detailed analysis of ground-water geochemistry. Stollenwerk characterized the major reactions and processes that accompany the neutralization of acidic ground water including acid-base and oxidation-reduction reactions and sorption phenomena through the results of column experiments and computer geochemical models. Fe is oxidized and precipitated as Mn is reduced. The distribution of Co, Cu, and Ni in the aquifer are controlled by sorption to Fe hydroxide precipitates. Ficklin and others (1991a) determined solid-phase associations of Cu, Mn, Zn,

Ca, Al, and SO_4 in the subsurface through the use of sequential extractions.

Colloid transport was found to be unimportant in the acidic core of the contaminant plume (Puls and others, 1990, 1991). Puls (chapter C) presents the results of column experiments using Pinal Creek aquifer material. Puls determined conditions that favor colloid-facilitated transport of inorganic contaminants include low ionic strength, a pH range in which the colloids are stable, and increased surface charges caused by adsorption of certain ions onto the colloidal surface. In these tests, colloids were transported under favorable conditions more than 21 times faster than arsenate, a reacting contaminant. Because contaminated water at Pinal Creek has a large ionic strength and contains large concentrations of SO_4, colloids probably do not play a significant role in transport at the site, even in neutralized parts of the plume.

Surface water in the basin includes runoff and ground-water discharge, which vary considerably in discharge and chemistry. Brown and Eychaner (chapter D) describe the distribution of major and trace elements in surface water in the basin. As neutralized, contaminated ground-water discharges to the perennial reach of Pinal Creek, it equilibrates with the atmospheric gases. In the stream, concentrations of carbon dioxide decrease, and concentrations of dissolved oxygen increase. At the same time, pH rises from about 7 to 8. These reactions were simulated using the geochemical model PHREEQE (Parkhurst and others, 1985).

The rise in pH along the perennial reach of Pinal Creek results in the precipitation of Mn oxide minerals on the streambed. In chapter D, Lind and Hem explore the sequential precipitation of Fe and Mn oxides on streambed sediments along the perennial reach of Pinal Creek. The black Mn oxides are composed primarily of rancieite and takanelite, and other minerals of varying stability. Although trace metals, such as Cu, Ni, Zn, and Pb, prefer Fe rather than Mn oxides, the latter are the primary trace metal scavengers because Mn oxides are more abundant than Fe oxides in the streambed.

Chapter B

Simulation of Reactions Affecting Transport of Constituents in the Acidic Plume, Pinal Creek Basin, Arizona

By Kenneth G. Stollenwerk

Abstract

Acidic water from a copper-mining area has contaminated an alluvial aquifer and stream in the Pinal Creek Basin near Globe, Arizona. The most contaminated water has a pH of 3.3 and contains more than 100 millimoles per liter of sulfate, 50 millimoles per liter of iron, 11 millimoles per liter of aluminum, and 3 millimoles per liter of copper. Reactions between alluvium and acidic ground water were first evaluated in laboratory-column experiments. A geochemical model was developed and used in the equilibrium speciation program, MINTEQA2, to simulate breakthrough curves for different constituents from the column. The geochemical model then was used to simulate the measured changes in concentration of aqueous constituents along a flow path in the aquifer.

pH was predominately controlled by reaction with carbonate minerals. Where carbonate minerals had been dissolved, sorption of hydrogen ion by iron oxides was used to simulate pH. Acidic ground water contained little to no dissolved oxygen, and most aqueous iron was present as ferrous iron. In the suboxic core of the plume, ferrous iron was oxidized by manganese oxides to ferric iron, which then precipitated as ferrihydrite. This reaction created 1 mole of manganese (II) and 2 moles of hydrogen ion for every 2 moles of ferrous iron that were oxidized. Data from the column experiments indicated that approximately half of the manganese (II) was trapped as a coprecipitate with ferrihydrite, and the remainder entered solution.

Attenuation of aqueous manganese, copper, cobalt, nickel, and zinc was a function of pH and could be quantitatively modeled with the diffuse-layer, surface-complexation model in MINTEQA2. Equilibrium constants for sorption of copper, nickel, and zinc on ferrihydrite were obtained from a compilation of published sorption constants. Copper had a logK of 0.6; nickel, a logK of -2.5; and zinc, a logK of -1.99. Equilibrium constants for cobalt and manganese were fit to the column experimental data—cobalt, logK was -2.0; and manganese, logK was -2.6. Aluminum precipitated as amorphous aluminum hydroxide at a pH greater than 4.7 and as a basic aluminum sulfate mineral at a pH of less than 4.7. Aqueous calcium and sulfate were in equilibrium with gypsum.

After the alluvium in the column had reached equilibrium with acidic ground water, uncontaminated ground water was eluted through the column to evaluate the effect of reactants on ground-water remediation. The concentrations of iron, manganese, copper, cobalt, nickel, and zinc rapidly decreased to detection limits within a few pore volumes. All of the gypsum that had precipitated in the column initially redissolved and resulted in elevated calcium and sulfate concentrations for about five pore volumes. Aluminum and pH were the two constituents that exhibited the most potential for continued adverse effects on

ground-water quality. The pH of column effluent remained below 4.5 for more than 20 pore volumes as hydrogen ion desorbed from ferrihydrite. Extended leaching at low pH resulted in dissolution of a basic aluminum sulfate mineral. The geochemical model accurately simulated breakthrough curves from the column and successfully simulated the distribution of constituents in the aquifer.

INTRODUCTION

Contamination of ground water by wastes generated from the mining and extraction of metals from ore deposits is a problem in many parts of the world. Processes that affect the mobility of these wastes are commonly evaluated with geochemical computer programs; however, the usefulness of these programs is often limited by a lack of adequate field data. Gaps in field measurements can be supplemented with data from laboratory-column experiments designed to simulate transport and chemical reactions in the aquifer.

The objective of this study was to characterize the reactions that control mobility of constituents in the plume of acidic water that has contaminated the alluvial aquifer and stream in Miami Wash and Pinal Creek. Laboratory experiments were used in conjunction with ground- and surface-water analyses to develop a geochemical model of the aquifer that simulated the measured changes in chemical composition.

DESCRIPTION OF PLUME

The most likely sources of contamination are Webster Lake, which existed from 1940 to 1988 in Webster Gulch (fig. 6) and perhaps smaller acidic ponds in the area (Envirologic Systems, Inc., 1983). In 1986, the concentration of total dissolved solids in Webster Lake was 35,000 mg/L, and pH was 2.7 (Eychaner, 1988).

Seepage of acidic water from Webster Lake through the former channel of Webster Gulch apparently enters the alluvial aquifer near the confluence of Bloody Tanks Wash and Russell Gulch (fig. 6). As the plume travels northward, aqueous constituents are attenuated by reaction with the alluvium. Aqueous concentrations also decrease because of dilution with uncontaminated water. Primary inflows of uncontaminated ground water are from Russell Gulch and Pinal Creek. The plume also is diluted by ground water flowing upward from the basin fill and by direct infiltration of surface water after precipitation. In all cases, mixing is not necessarily instantaneous, and uncontaminated water can flow parallel to the plume for hundreds of meters before complete mixing occurs.

The plume of contaminated ground water is characterized by a series of chemical fronts that are defined by the geochemistry of individual constituents. The location of the contaminant plume in 1988, as defined by pH, is represented in figure 6, a longitudinal section of the aquifer from Webster Lake to Inspiration Dam. Most acidic contamination is within the unconsolidated alluvium; however, the water chemistry of the upper part of the basin fill also has been affected. The shape of the contaminant plume is actually three dimensional, and the reaction front extends not only in the longitudinal direction of flow, but also in the vertical and transverse directions to flow.

On the basis of ground-water composition, the aquifer can be subdivided into three zones—acidic, neutralized, and uncontaminated. Water from well 202 at site 200 (fig. 1) is representative of uncontaminated ground water in the aquifer. This water contains dissolved oxygen (DO), has nearly neutral pH, and is low in dissolved solids (table 5). Ground water in Miami Wash, the most contaminated part of the aquifer, is depleted in DO and is characterized by low pH and large concentrations of dissolved metals and sulfate (SO_4). The large concentration of SO_4 in acidic ground water has a significant effect on the speciation of aqueous cations. Approximately 50 percent of the calcium (Ca), magnesium (Mg), iron (Fe), manganese (Mn), copper (Cu), cobalt (Co), nickel (Ni), and zinc (Zn) in solution is transported as a SO_4 complex, and more than 80 percent of the aluminum (Al) is complexed with SO_4 (table 6). The front of acidic water (pH less than 5) has advanced through the alluvium at a rate of 0.2 to 0.3 km/yr (Eychaner, 1991a). Neutralized ground water, defined as having pH values greater than 5, forms a three-dimensional shell of variable extent around the acidic core. Concentrations of dissolved metals are low; however, concentrations of chloride (Cl), SO_4, Ca, Mg, and Mn are significantly greater than uncontaminated ground

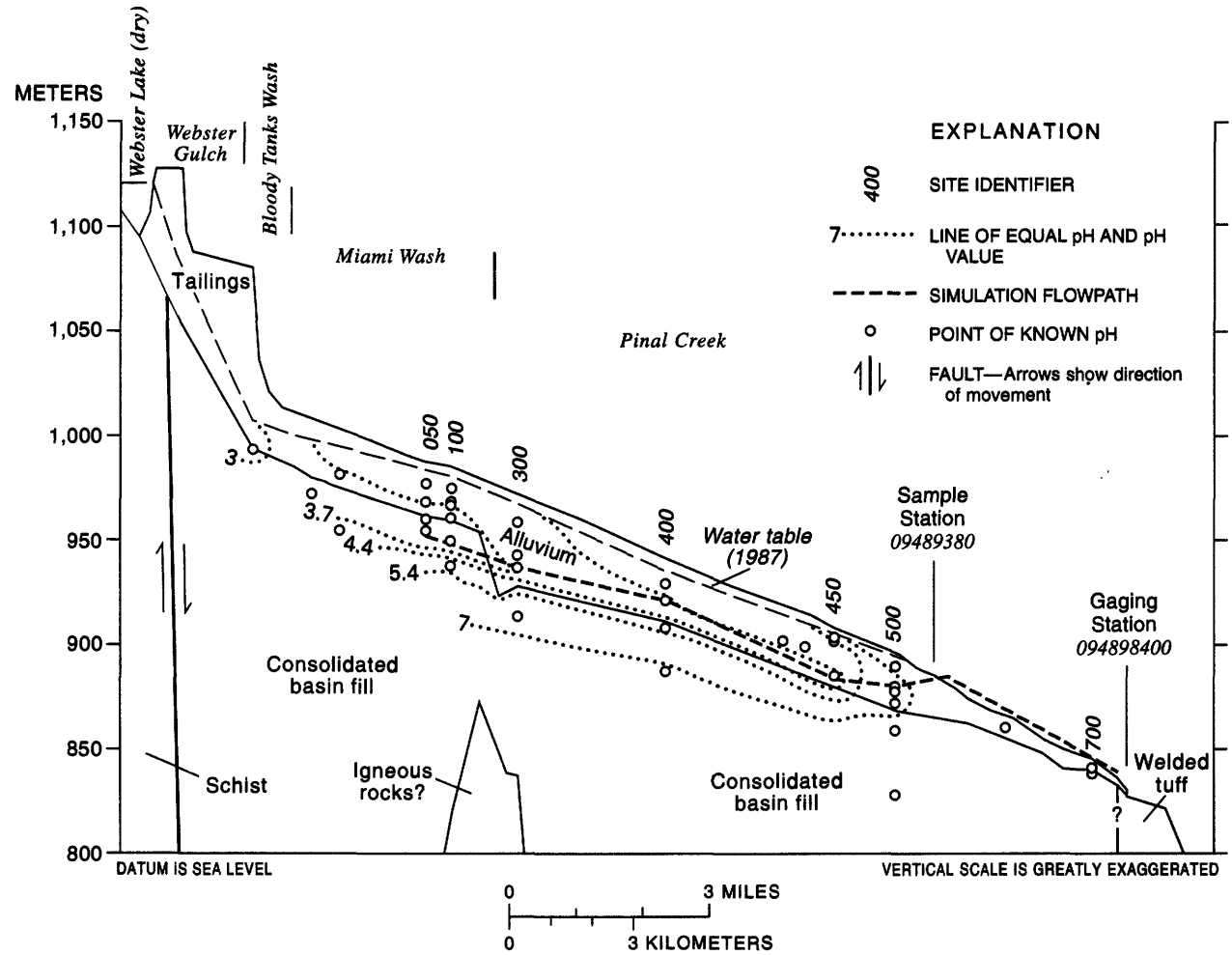

Figure 6. Distribution of pH in the aquifer. Line of section approximates the principal ground-water flow line from Webster Lake to Inspiration Dam along the channels of Webster Gulch, Bloody Tanks Wash, Miami Wash, and Pinal Creek.

water. Neutralized ground water has reached the streamflow-gaging station, Pinal Creek at Inspiration Dam, where dissolved solids have been increasing since at least 1942 (Envirologic Systems, Inc., 1983; Eychaner, 1988).

EXPERIMENTAL METHODS

Sampling and Analytical Techniques

Most ground-water samples were collected using a submersible pump. Water samples were collected only after at least three casing volumes of water had been removed and the pH, specific conductance, temperature, and dissolved-oxygen concentration had stabilized. For the analysis of dissolved constituents, both ground-water and surface-water samples were filtered through a 0.45-μm membrane filter and stored in polyethylene bottles. Preliminary experiments on sampling methodology found no significant concentration of colloids greater than 0.03 μm in size (Eychaner and Stollenwerk, 1985). Samples submitted for cation analysis were acidified with ultrapure nitric acid (HNO_3) to a pH of approximately 1.5. Samples submitted for anion analysis were unacidified. All samples were packed in ice for shipment and stored in a refrigerator until analyzed in the National Research Program (NRP) laboratory. Random replicates also were analyzed by the U.S. Geological Survey National Water-Quality Laboratory to ensure quality control. An ionic balance for each sample was computed as:

$$\frac{\text{sum cations (meq/L)} - \text{sum anions (meq/L)}}{\text{sum cations (meq/L)} + \text{sum anions (meq/L)}} \times 100 \text{ percent},$$

Table 5. Range in concentration of constituents in uncontaminated and acidic ground water and neutralized surface water, Pinal Creek, Arizona

[Constituent values are in millimoles per liter; pH, standard units; Eh, in millivolts; temperature, degrees Celsius; ionic balance, in percent]

Constituent	Uncontaminated ground water	Acidic ground water	Neutralized surface water	Constituent	Uncontaminated ground water	Acidic ground water	Neutralized surface water
	Well 202	Well 051	Pinal Creek at Inspiration Dam (09498400)		Well 202	Well 051	Pinal Creek at Inspiration Dam (09498400)
pH	7.19	3.30	7.95	Aluminum (Al)	<.004	10.5	<.004
Eh	---	430	---	Copper (Cu)	<.0003	2.4	<.0003
Temperature	17	18	25	Cobalt (Co)	<.001	.20	<.001
Dissolved oxygen (O_2)	.22	<.006	.24	Nickel (Ni)	<.002	.06	<.002
Calcium (Ca)	1.2	11.6	14.0	Zinc (Zn)	<.0005	.33	<.0005
Magnesium (Mg)	.37	15.8	5.6	Sulfate (SO_4)	.70	100	20
Sodium (Na)	.96	9.4	3.4	Chloride (Cl)	.48	9.5	2.8
Potassium (K)	.5	.2	.1	Bicarbonate (HCO_3)	2.3	0	3.3
Iron (Fe)	<.0007	52.4	<.0007	Ionic balance	-1.0	-.6	1.1
Manganese (Mn)	<.0006	1.34	.47				

Table 6. Speciation of selected constituents in ground-water and surface-water samples, Pinal Creek, Arizona

[---, no data. Speciation calculated by MINTEQA2 (Allison and others, 1991). Constituent values are in percent. Samples are taken from table 1.

Constituent	Well 202	Well 051	Pinal Creek at Inspiration Dam (09498400)	Constituent	Well 202	Well 051	Pinal Creek at Inspiration Dam (09498400)
Ca^{2+}	91	52	65	$AlSO_4^+$	---	40	---
$CaSO_4^o$	5	48	33	$Al(SO_4)_2^-$	---	44	---
Mg^{2+}	90	54	67	Cu^{2+}	---	53	---
$MgSO_4^o$	5	46	30	$CuSO_4^o$	---	47	---
Na^+	100	94	97	Co^{2+}	---	50	---
$NaSO_4^-$	0	6	3	$CoSO_4^o$	---	50	---
Fe^{2+}	--	59	---	Ni^{2+}	---	53	---
$FeSO_4^o$	--	41	---	$NiSO_4^o$	---	47	---
				Zn^{2+}	---	41	---
Mn^{2+}	--	57	68	$ZnSO_4^o$	---	41	---
$MnSO_4^o$	--	42	29	$Zn(SO_4)_2^{2-}$	---	18	---
Al^{3+}	--	16	---				

where

meq/L = milliequivalents per liter.

Any sample that did not achieve an ionic balance within ±5 percent was reanalyzed. The maximum analytical error for all analyses reported in this paper is ±10 percent at the 95-percent confidence interval.

Cations were determined with a Jarrell-Ash Atom Comp 975 inductively coupled atomic-emission spectrophotometer. Chloride was determined by the ferric thiocyanate method and SO_4 by the turbidimetric method (Fishman and Friedman, 1989). Ferrous iron [Fe(II)] and ferric iron [(Fe(III)] were measured using the bipyridine-colorimetric procedure (Skougstad and others, 1979). Separation between Fe(II) and Fe(III) could not be achieved if the concentration of either constituent was less than 3 percent of total Fe. Dissolved oxygen was measured by probe, pH by glass electrode, and Eh with a polished platinum electrode and a silver-silver chloride reference electrode that was calibrated with Zobell's solution between measurements. The carbonate (CO_3^{2-}) content of the alluvium was determined by the Chittick method (Dreimanis, 1962). Oxides of Mn and Fe were sequentially extracted from samples of alluvium. Manganese oxides were dissolved using 0.1 N hydroxylamine hydrochloride ($NH_2OH \cdot HCl$) in 0.01 N HNO_3 and shaking for 30 minutes (Chao, 1972). Amorphous iron oxides were dissolved in a solution of 0.25 N $NH_2OH \cdot HCl$ and 0.25 N HCl at 50°C for 30 minutes (Chao and Zhou, 1983). Crystalline iron oxides were dissolved in 4.0 N HCl at 90°C for 30 minutes (Ficklin and others, 1991b).

Column Experiments

Controlled, laboratory column experiments were used to identify reactions between ground water and alluvium. Plexiglas columns (80-cm-long by 5-cm-wide inside diameter) were packed with the less than 2-mm-size fraction of alluvium. Four experiments were run—two with samples of alluvium and two with samples of basin fill. Breakthrough of individual constituents varied between columns and was primarily a function of the initial carbonate content. Results are presented from one column containing alluvium and one column containing basin fill. The alluvium sample was collected from a gravel quarry in the unconsolidated alluvium just upstream from well group 200 (fig. 2). This sampling site was necessary because zones of relatively large cobbles in the aquifer prevented collection of representative core samples for use in the laboratory experiments. Several samples were collected from the exposed sections of alluvium in the quarry and composited. Petrographic examination indicated no difference in mineralogy between the composite sample and cuttings obtained from uncontaminated alluvium during drilling of the observation wells. In addition, preliminary batch experiments conducted to test the reactivity of the composite sample and cuttings toward acidic ground water indicated no difference in reactivity. The composite sample from the gravel quarry, therefore, was assumed to represent the physical and chemical state of the unconsolidated alluvium in the aquifer before contamination. The basin-fill sample was collected from an outcrop exposed along a road cut. The large carbonate content of this basin fill resulted in a substantial amount of mineral precipitation and plugging of porosity within the column. The following discussion, therefore, focuses on the column packed with alluvium. The basin-fill experiment is discussed separately at the end of the paper.

An initial baseline was established by eluting uncontaminated ground water from well 202 through the alluvium until there was no change in the concentration of dissolved constituents. Column influent was then switched to ground water collected from a well screened in the core of the acidic plume at well 050 (fig. 2; table 1). This water had been filtered into Pyrex bottles and refrigerated until used. Acidic water was pumped through the alluvium until complete breakthrough for all constituents was achieved (effluent concentration, C, equals influent concentration, C_0). This process required about nine pore volumes of acidic water. Influent was then switched back to uncontaminated ground water to evaluate the restoration of water quality to precontamination levels.

A peristaltic pump was used to control flow through the columns in an upward direction at an average velocity of 0.4 m/d. This velocity is less than the 5-mm/d estimate for the aquifer (Eychaner, 1989); however, a slower velocity in the columns was required because of the short travel distance. Effluent was filtered through in-line 0.4-μm polycarbonate membrane filters as it exited from the columns and was collected in an automatic-fraction collector. The entire

experimental apparatus was enclosed in a glove box that contained a nitrogen (N_2) atmosphere to simulate the reducing conditions in the core of the plume. The pH and concentration of anions in effluent fractions were measured daily. Samples to be analyzed for cations were acidified with ultrapure nitric acid (HNO_3) and stored in a refrigerator until analyzed.

GEOCHEMICAL MODELING

A geochemical model was developed to simulate the measured concentration of constituents in column effluent. The intent was to find a minimum set of solid phases that would explain the measured chemistry. Thermodynamic equilibrium was assumed, and reaction kinetics were not considered. This assumption worked reasonably well for most constituents. Reactions used in this model represent only one possible set of plausible reactions that could be formulated to describe this system. Other potential combinations of solid phases may work equally well.

Reactions were simulated with the geochemical computer program MINTEQA2 (Allison and others, 1991). The MINTEQA2 thermodynamic data bases were updated with chemical equilibrium constants from Nordstrom and others (1990). Equilibrium constants for Co were calculated using thermodynamic data from Naumov and others (1974). If the necessary parameters were available, activity coefficients were calculated using the modified Debye-Hückel equation; otherwise, the Davies equation was used.

Chloride was nonreactive in the column experiment; therefore, the effect of solute dispersion could be determined from the shape of the breakthrough curve for Cl (fig. 7). If there was no dispersion, Cl would breakthrough instantaneously at one pore volume. The experimental data show that dispersion in the column caused the Cl concentration to increase before one pore volume; Cl did not reach the influent concentration until about the second pore volume. The shape of the ascending limb of the breakthrough curve for constituents other than Cl was dominated by chemical reactions, and dispersion could be disregarded. Dispersion also was evident in the rinse out of constituents from the column. In fact, the shape of the descending limb of the breakthrough curve for some constituents was dominated by dispersion; therefore, all simulations of the rinse out of constituents from the column were corrected to reflect the amount of dispersion measured in the Cl data.

After the column-breakthrough curves were simulated by MINTEQA2, the geochemical model was tested on the data set from the aquifer. This test required choosing an appropriate flow path. In contrast to the generally uniform, one-dimensional flow system of the column, the plume and the flow system in the aquifer has a three-dimensional aspect. The flow path chosen (fig. 6) connects the most contaminated well in each of the six observation-well nests and two surface-water sites. Presumably, these wells are along the same hydrologic flow path. At the very least, this flow path offers a continuous progression from the most contaminated ground water at well 051 to the least contaminated surface water at the streamflow-gaging station, Pinal Creek at Inspiration Dam (09498400).

The generally constant concentration of constituents at most of these observation points for the nine sampling rounds between November 1984 and August 1987 indicates that the observation wells were not in any zones of rapidly changing chemistry. The concentration of each constituent plotted in all of the figures of field data in this paper, therefore, is an average of the nine sampling rounds. The associated error bars show the minimum and maximum concentration at each site for the averaged time period. The exception is well 452, which was not completed until 1988. Data from this site are for just two sampling periods.

In addition to simulating chemical reactions along this flow path in the aquifer, simulation of the field data also has to account for dilution of constituents in the acidic plume by ground water from other sources. Hydrologic data for the flow system in the Miami Wash-Pinal Creek area is too limited to determine the location and amount of mixing; therefore, a chemical tracer was used to calculate dilution between wells. The assumption was made that Cl was nonreactive. Therefore, the decrease in Cl concentration along the flow path was assumed to be a result of dilution by uncontaminated ground water. These assumptions appear to be reasonable in that there are no known sources of mineral Cl in the aquifer, and the column data indicated no precipitation or sorption of Cl.

Dilution of contaminated ground water along the flow path was accomplished by using the mixing option in the geochemical computer program PHREEQE (Parkhurst and others, 1980). The volume of uncontaminated water (well 202, table 5) added to the model first was calculated from the decrease in Cl

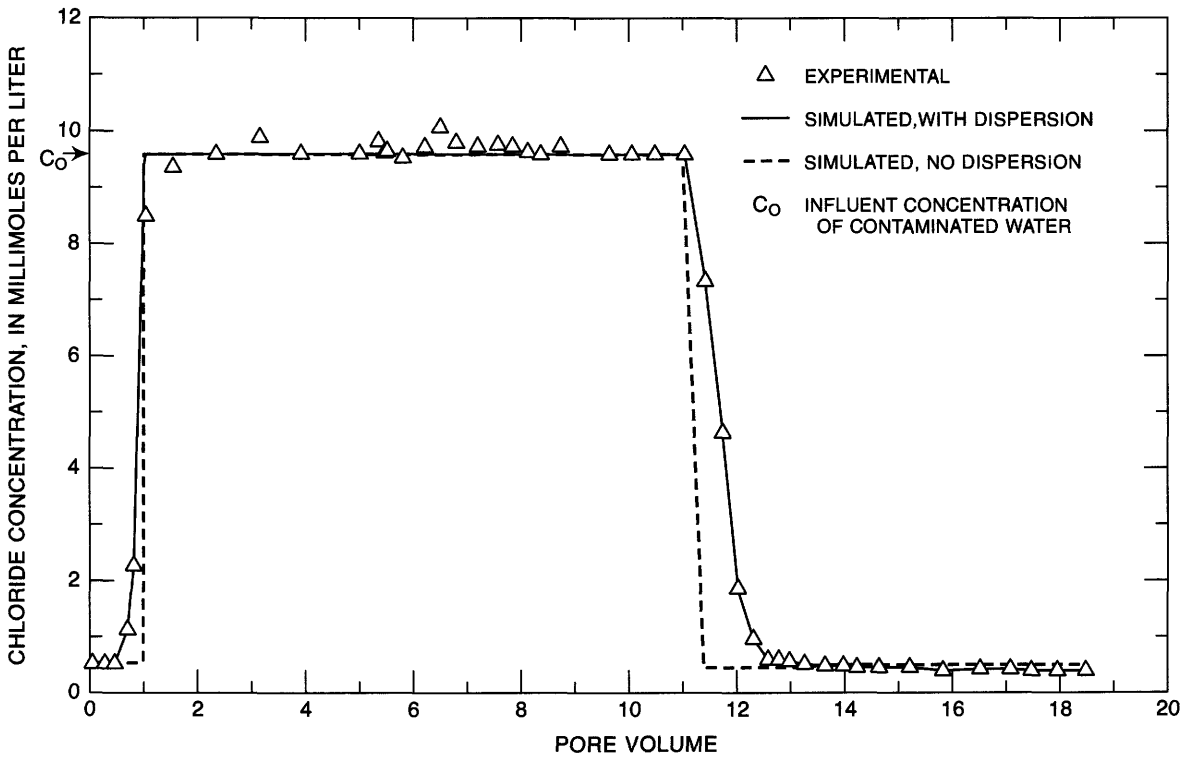

Figure 7. Experimental and simulated concentrations of chloride in column effluent.

concentration between successive sites along the flow path (fig. 7). The resultant mixed water then was used as the input solution for MINTEQA2. The data in figure 8 indicate that most dilution occurs within the first 2 km as ground water from Russell Gulch and Pinal Creek mixes with the acidic plume.

Sorption

The aqueous concentrations of hydrogen ion (H^+), Mn, Cu, Co, Ni, and Zn were controlled by pH-dependent sorption on oxide minerals. These reactions were simulated using the diffuse-layer surface-complexation model in MINTEQA2. Parameters that are required by the model include the mass of sorbent, its specific surface area, and the concentration of sorption sites. At least one sorption reaction and an equilibrium constant must be defined for each constituent. Surface charge and potential are computed by MINTEQA2. Sorption parameters for the diffuse-layer model are listed in table 7.

The alluvium contained a mixture of potential sorbents. Iron oxides were expected to dominate sorption reactions because all of the grains in core samples were visibly coated with reddish iron oxides, even in uncontaminated alluvium. In addition, large amounts of Fe(II) were oxidized to Fe(III) and precipitated from the acidic plume. Mn and Al oxides also are present in the alluvium and are potentially important sorbents; however, it was not possible to separate the effect of Mn and Al oxides from Fe oxides. Therefore, all sorption reactions were assumed to occur on ferrihydrite [$Fe(OH)_3$].

The concentration of $Fe(OH)_3$ was calculated by adding the amount of "amorphous iron oxides," determined by sequential chemical extraction of the alluvial sample, to the amount of $Fe(OH)_3$ that precipitated from solution as acidic ground water moved through the column or aquifer. Thus, the concentration of $Fe(OH)_3$ used in the simulation increased proportionally with the amount that precipitated. The surface area of 600 m^2/g and the sorption site density of 3.84 $\mu mol/m^2$ are values recommended by Dzombak and Morel (1990) and Davis and Kent (1990) for sorption on $Fe(OH)_3$.

The equilibrium constants for H^+, Cu, Ni, and Zn also were taken from Dzombak and Morel (1990; table 7, this report) and are based on an extensive compilation and interpretation of published experimental data for sorption of ions by $Fe(OH)_3$.

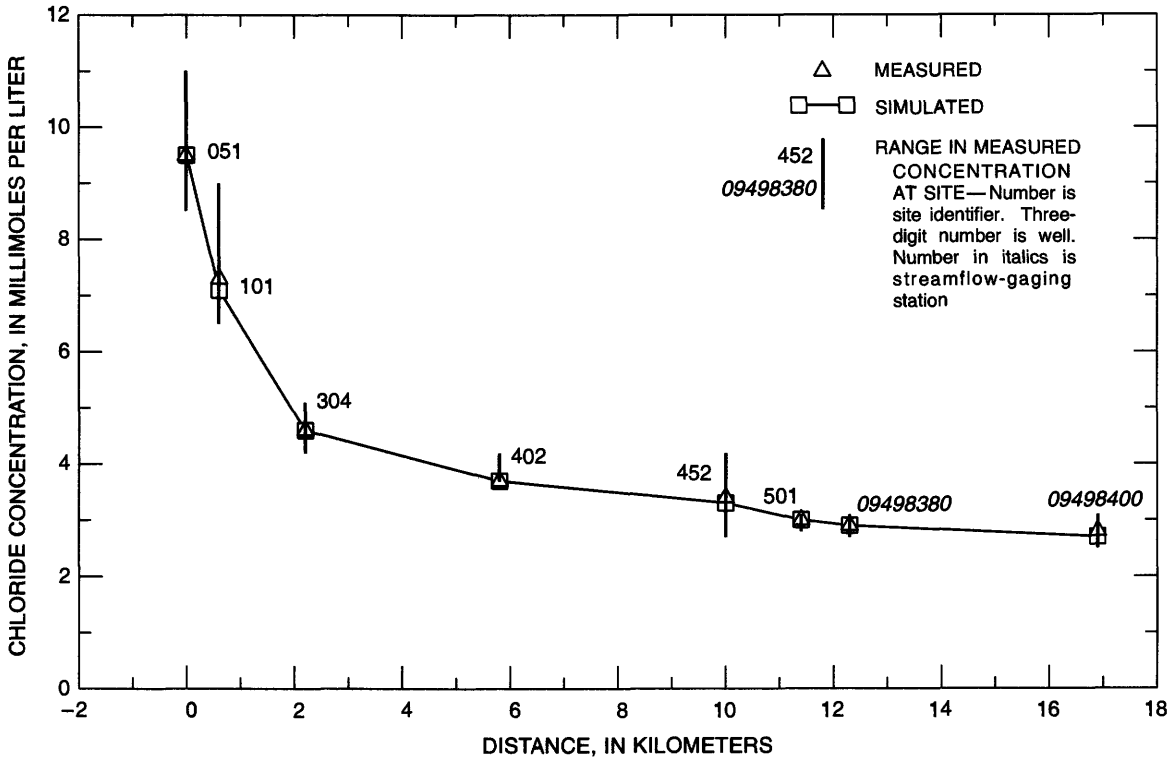

Figure 8. Measured and simulated concentrations of chloride at observation points along flow path.

Table 7. Sorption parameters for the diffuse-layer model, Pinal Creek, Arizona

[$Fe(OH)_3$ properties: Specific surface area, 600 meters squared per gram; concentration of sorption sites, 3.85 micromoles per square meter; concentration $Fe(OH)_3$, 1.4 –1.8 gram per kilogram[1]]

Reaction number	Surface-complexation reactions[2]	LogK
1	$\equiv FeOH^o + H^+ = \equiv FeOH_2^+$	[3]7.29
2	$\equiv FeOH^o = \equiv FeO^- + H^+$	[3]–8.93
3	$\equiv FeOH^o + Cu^{2+} = \equiv FeOCu^+ + H^+$	[3].6
4	$\equiv FeOH^o + Co^{2+} = \equiv FeOCo^+ + H^+$	[4]–2.0
5	$\equiv FeOH^o + Ni^{2+} = \equiv FeONi^+ + H^+$	[3]–2.5
6	$\equiv FeOH^o + Zn^{2+} = \equiv FeOZn^+ + H^+$	[3]–1.99
7	$\equiv FeOH^o + Mn^{2+} = \equiv FeOMn^+ + H^+$	[4]–2.6

[1]Sum of $Fe(OH)_3$ initially present in alluvium plus $Fe(OH)_3$ precipitated from solution.

[2]$\equiv FeOH^o$ is a surface-complexation site.

[3]LogK from literature review by Dzombak and Morel (1990).

[4]LogK by empirical fit to column data.

The published logK values for Co and Mn were modified to fit the data from the column experiments.

EXPERIMENTAL AND SIMULATED RESULTS

pH

The concentration of free and complexed H^+ in acidic ground water (well 051, table 5) accounted for only 0.7 mmol/L of the total potential acidity in this sample. Additional H^+ was produced by hydrolysis of metal ions and the exchange of cations for H^+ on oxide surfaces. The solutes that contributed most to the acidity of ground water from well 051 are summarized in table 8. These reactions have the potential to produce 114 mmol/L of H^+ and will maintain low pH values until these solutes are removed from solution.

Experimental and simulated breakthrough curves were developed for pH of effluent from the column experiment (fig. 9). Initially, CO_3 minerals in the alluvium buffered pH at approximately 8. The concentration of CO_3 in this alluvium was 0.022 mol of CO_3/kg calculated independently by the Chittick

method. A ratio of 90-percent calcite to 10-percent dolomite was used on the basis of the amount of Mg released to solution during the experiment. Both minerals were allowed to react in MINTEQA2 until depleted according to:

$$CaCO_3 + 2H^+ = Ca^{2+} + H_2O + CO_{2(g)}, \quad (1)$$

and

$$MgCa(CO_3)_2 + 4H^+ = Mg^{2+} + Ca^{2+} + 2H_2O + 2CO_{2(g)}. \quad (2)$$

A partial pressure for carbon dioxide of $10^{-2.9}$ atmospheres was used in the simulations while carbonates were present. This value was computed from the concentration of HCO_3^- measured in the effluent. The rapid pH decrease to 4.4 observed in the experimental data coincided with depletion of carbonate minerals in the simulations.

Even though all of the carbonate minerals in the alluvium were apparently depleted by the end of the second pore volume, an additional three pore volumes were required to finally decrease pH to the influent value of 3.3, which indicated additional reactions of H^+ with the alluvium. Two different types of reactions were considered. One possibility is alteration of silicate minerals such as feldspars:

$$2NaAlSi_3O_8 + 2H^+ + 9H_2O = Al_2Si_2O_5(OH)_4 + 2Na^+ + 4H_4SiO_4, \quad (3)$$

Table 8. Hydrogen-ion production potential for groundwater sample from well 051, Pinal Creek, Arizona

Solute	Process	Hydrogen, in millimoles per liter
Iron	Oxidation and precipitation	52.4
Aluminum	Precipitation	31.5
Manganese	Reduction and sorption	27.5
Cobalt	Sorption	3.0
Copper	...do	
Nickel	...do	
Zinc	...do	
Total		114.4

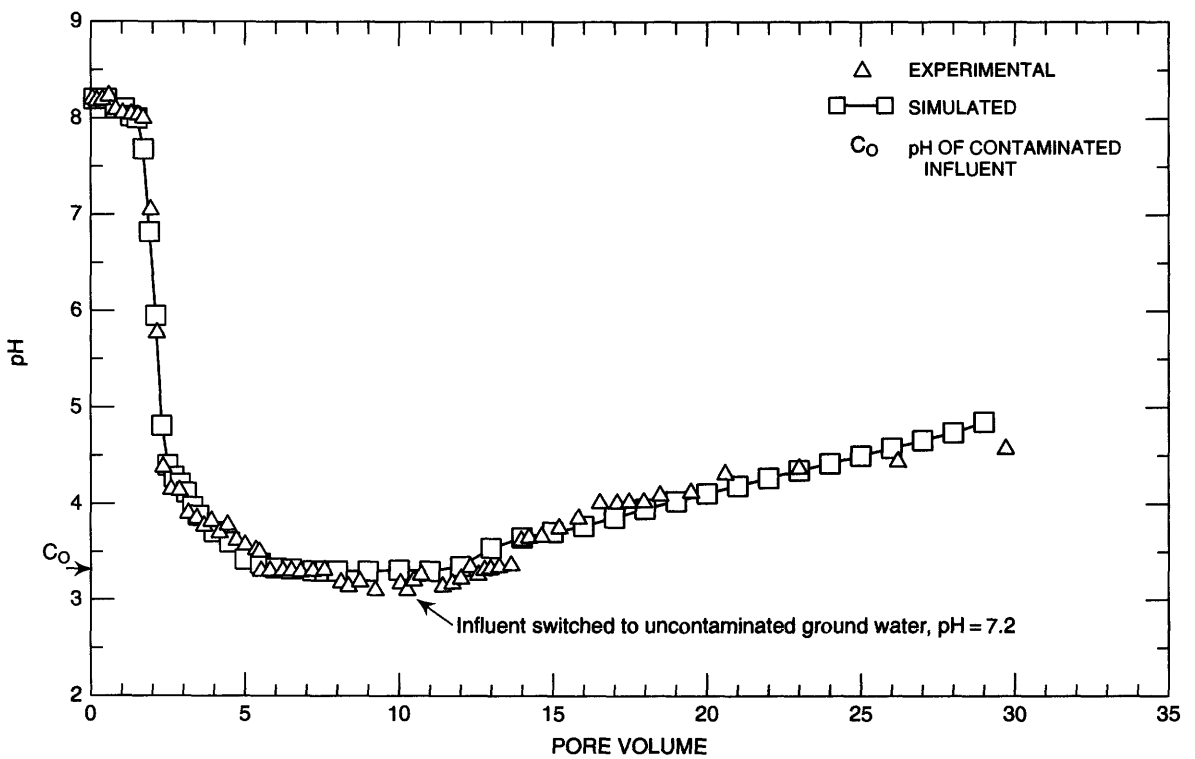

Figure 9. Experimental and simulated pH of column effluent.

where

$2NaAlSi_3O_8$ = albite and

$Al_2Si_2O_5(OH)_4$ = kaolinite.

Petrographic examination of thin sections made from alluvium collected during the drilling of observation wells did show that feldspars were partially to completely replaced by clay minerals. No difference was observed in the percent of altered grains between alluvium collected from the core of the plume and alluvium unaffected by the acidic ground water.

Some evidence exists for reactions such as equation (3) from laboratory-batch experiments. Several different samples of alluvium were mixed with deionized water and acidified with sulfuric acid (H_2SO_4) to pH values of about 3.3 (after removal of CO_3 minerals). In all samples, pH increased although the rate of increase was slow. Typically, a week or more was required to increase pH one-tenth of a unit, and the rate of increase slowed to nearly zero within a month. The data from these batch experiments indicated that only about 10 percent of the H^+ removed from solution between pore volumes 2 and 5 (fig. 9) could have been neutralized by reaction with silicate minerals within the timeframe of the column experiment; therefore, silicate alteration was omitted in these simulations.

The other reaction considered was sorption of H^+ by $Fe(OH)_3$ (equation 1, table 7). Formation of $\equiv FeOH_2^+$ is pH dependent. MINTEQA2 simulations indicated that almost all of the available oxide surfaces were saturated with H^+ at pH 3.3. Simulation of pH with the diffuse-layer model resulted in an excellent fit to the experimental data for pH values less than 4.4. Perhaps the most compelling reason to simulate low pH values with a sorption mechanism is the nature of the rinse-out data. At pore volume 10, the influent solution was changed to uncontaminated ground water (fig. 9). In the absence of any reactions with the alluvium, effluent pH should have rapidly increased to the influent value of 7.2 within a few pore volumes. Effluent pH increased gradually as indicated by the rinse-out data in figure 9. Even after 20 pore volumes of water with a pH of 7.2 had eluted through the column, pH was only 4.6. The experimental pH was simulated by allowing disassociation of the $\equiv FeOH_2^+$ surface complex:

$$\equiv FeOH_2^+ = \equiv FeOH + H^+. \quad (4)$$

As a consequence of this reaction, HCO_3^- in uncontaminated water was removed from solution by reaction with H^+. Bicarbonate was not detected in any of the effluent even though the concentration of HCO_3^- in the influent water was 2.3 mmol/L. MINTEQA2 simulations indicated that approximately 50 percent of the surface sites were still saturated with H^+ at pore volume 30. Additional simulations predicted that an additional 18 pore volumes of uncontaminated water needed to be eluted through the column to increase pH to 7.2. Considerable time may be required to restore the pH of ground water to precontaminant conditions.

The change in pH of ground water along the flow path chosen for the aquifer simulations (fig. 10) was simulated with the same reactions that were used to simulate pH in the column experiment. The acidic core of the plume, characterized by a pH of less than 4.5 extended 10 km downgradient from the starting point of the simulations. Carbonate minerals should have previously been removed from this reach of aquifer, so pH was simulated by a combination of sorption on $Fe(OH)_3$ and neutralization of H^+ by HCO_3^- in uncontaminated ground water that mixed with the plume. Reaction with HCO_3^- removed 20 percent of the total H^+ from solution along the first 10 km and the remainder was sorbed. CO_3 minerals were assumed to be present in the aquifer only if the pH of the ground water was greater than 4.5, as was the case between kilometer 10 and kilometer 12. The sharp increase in pH along this reach defined the transition zone between acidic and neutralized ground water. Actual concentration of carbonate in alluvium between these observation wells could not be determined; therefore, the actual amount of carbonate dissolved between kilometer 10 and kilometer 12 was used as a fitting component to simulate the measured pH. The ratio of calcite to dolomite in the aquifer was assumed to be the same as that used in the column experiment. pH of the two surface-water sites also was near equilibrium with CO_3 minerals.

Iron

Ferrous iron is the dominant cation in acidic ground water; its chemical reactions have a significant effect on the mobility of other solutes. In the column experiment, Fe(II) was completely removed from solution until pore volume 2; then the effluent

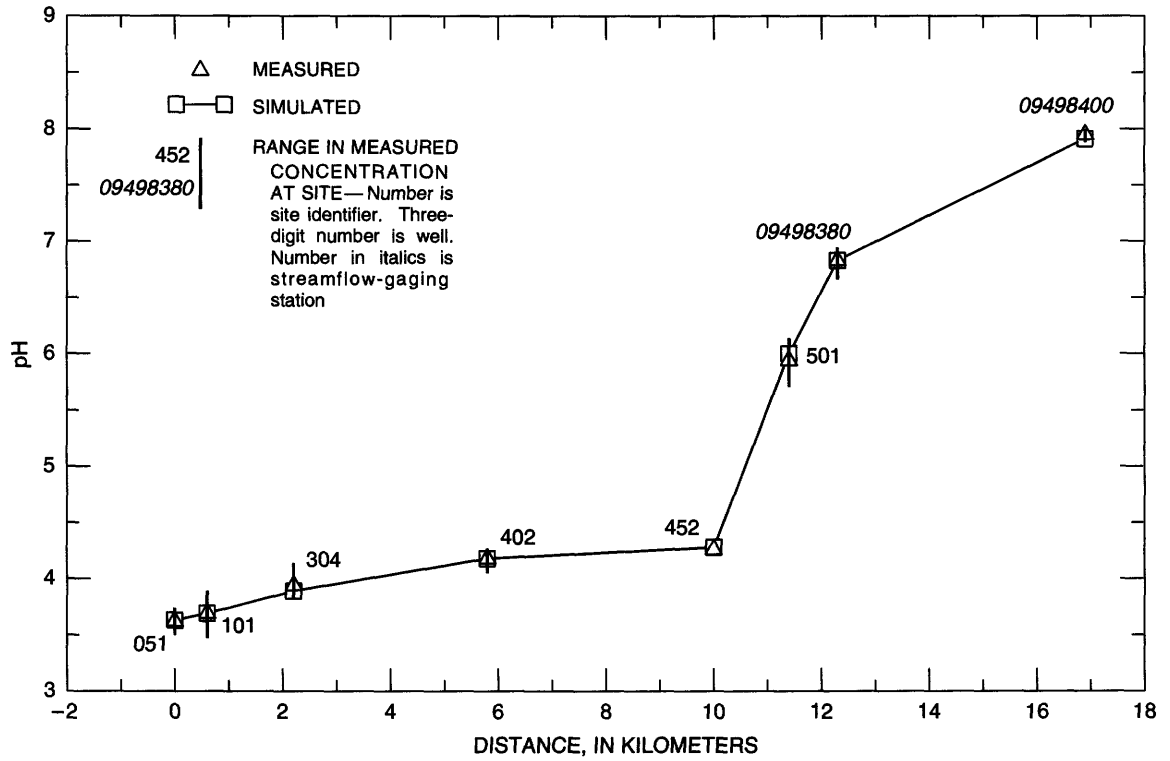

Figure 10. Measured and simulated pH of ground water and surface water at observation points along flow path.

concentration rapidly increased to the influent concentration of 55 mmol/L (fig. 11). In fact, the concentration of Fe(II) actually exceeded 55 mmol/L between pore volumes 3 and 4. Apparently, some Fe(II) may have been sorbed by the alluvium initially and was remobilized as pH decreased. Sorption of Fe(II) was not considered in the model.

Experimental and thermodynamic evidence indicate that the most plausible mechanism for attenuation of Fe was oxidation of Fe(II) to Fe(III), followed by precipitation of $Fe(OH)_3$:

$$Fe^{2+} + 3H_2O = Fe(OH)_3 + 3H^+ + e^-. \qquad (5)$$

Jarosite $[(H,Na,K)Fe_3(SO_4)_2(OH)_6]$, the only other mineral that was supersaturated with respect to Fe, could not be detected in reacted column alluvium or in cuttings from the aquifer by either X-ray diffraction or electron microprobe and was not considered in this study. Jarosite supersaturation without precipitation has been reported elsewhere (Nordstrom and others, 1979). Apparently some kinetic inhibition to precipitation does exist.

Equation (5) requires an electron acceptor. Although several potential oxidants could be considered for this system, most can be excluded. Oxidation of Fe(II) by oxygen (O_2), nitrate (NO_3^-), and nitrite (NO_2^-) would be thermodynamically favorable; however, O_2 was excluded from the column experiment, and the concentrations of NO_3^- and NO_2^- in acidic ground water were below detection. SO_4 and carbon dioxide (CO_2) were present in solution; however, oxidation of Fe(II) by these species was computed to be thermodynamically unfavorable. Likewise, independent experiments verified that the N_2 atmosphere of the glove box had no effect on the oxidation state of Fe.

The most plausible oxidants in this system are Mn oxide minerals such as birnessite (MnO_2), which generally are abundant in alluvium that has not been in contact with the acidic plume. Oxidation of Fe(II) by Mn oxides has been described by Asghar and Kanehiro (1981) who measured an increase in the amount of Mn that could be leached from soil upon addition of Fe(II). Traina and Doner (1985), Golden and others (1986), Krishnamurti and Huang (1987) have found that Fe(II) is readily oxidized by synthetic birnessite $[Mn_7O_{13}{\cdot}5H_2O]$. No attempt, however, was made to exclude atmospheric O_2 from any of these experiments, which complicates interpretation of reaction rates and

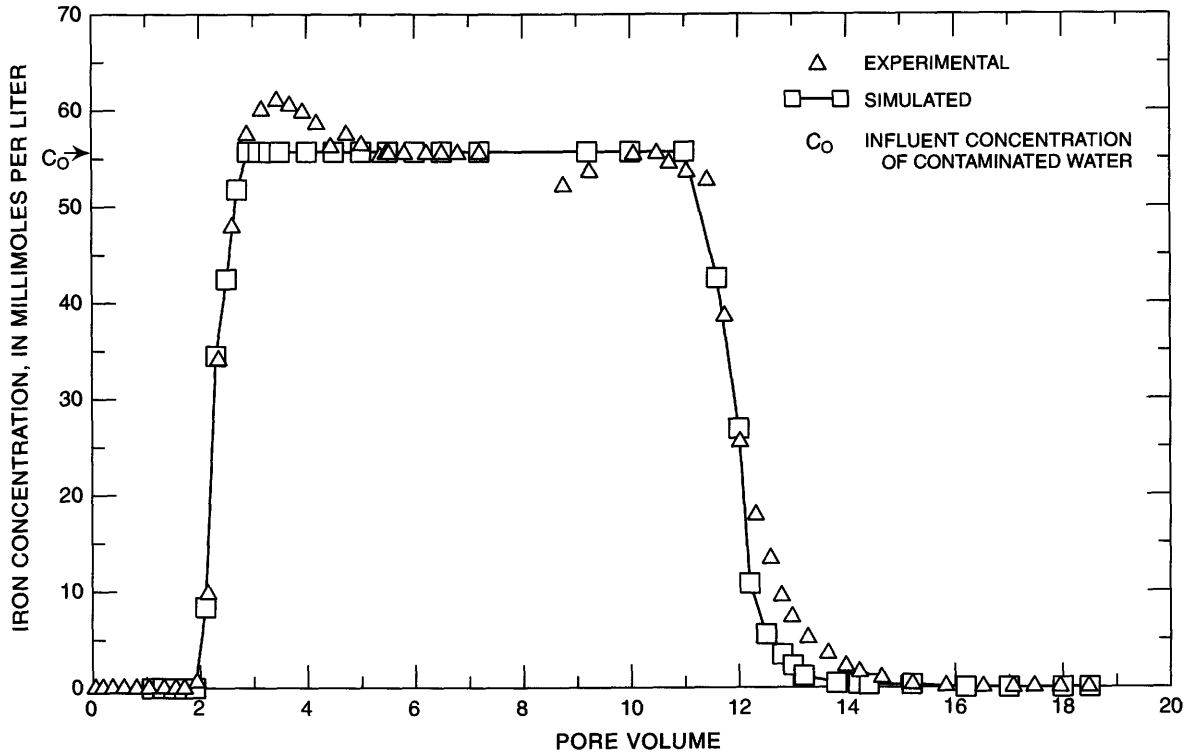

Figure 11. Experimental and simulated concentrations of total dissolved iron in column effluent.

stoichiometry. Postma (1985) conducted laboratory experiments under a N_2 atmosphere. Postma's results confirmed that synthetic birnessite oxidized Fe(II) in the absence of O_2 and yielded a ratio of 1.7 mol of Fe(II) oxidized per mole of Mn(II) produced.

MINTEQA2 simulations indicated that the following overall reaction between the acidic water and alluvium was thermodynamically feasible:

$$2Fe^{2+} MnO_2 + 4H_2O = 2Fe(OH)_3 + Mn^{2+} + 2H^{2+}. \quad (6)$$

For every 2 mol of Fe(II) oxidized, 1 mol of Mn(II) and 2 mol of H^+ should have been produced. A total of 37 mmol of Fe(II) were removed from solution in the column experiment. This amount is equivalent to 14.2 mmol Fe(II) oxidized per kilogram of alluvium. According to equation 6, at least 7.1 mmol/kg of MnO_2 should have been in the column alluvium initially to account for the measured Fe(II) oxidation. The actual concentration and oxidation state of Mn oxides in the alluvium were difficult to determine. In freshly precipitated oxides, the oxidation state of Mn generally ranges from 2.67 to about 3.00; however, these oxides are unstable under oxic conditions and tend to eventually alter to MnO_2 (Hem and Lind, 1983). Considering that the alluvium used in the column experiment had been exposed to oxic conditions for several years, Mn(IV) probably was the dominant oxidation state.

A semiquantitative estimate of the Mn oxide content of alluvium used in the column experiment was made using the sequential chemical-extraction technique. A total of 6.2±0.4 mmol/kg of Mn were measured in the Mn oxide extractable fraction of alluvium. An additional 2.4±0.3 mmol/kg of Mn was associated with amorphous $Fe(OH)_3$. If all of this Mn were available for reaction with Fe(II), then there was a total of 8.6±0.7 mmol Mn oxides per kilogram of alluvium, which is more than enough to account for the observed oxidation of Fe(II) in the column. Furthermore, sequential chemical extraction of the reacted alluvium after completion of the column experiment measured a decrease in Mn oxide content from 6.2 to 0.23 mmol/kg, which is an observation that is consistent with equation 6.

An increase in concentration of Mn in the effluent gives additional evidence for equation 6. Effluent Mn concentrations indicate that a total of 3.3 mmol of Mn were solubilized per kilogram of alluvium. Although this amount is only 46 percent of the 7.1 mmol/kg predicted to dissolve, it is still substantial and could not be explained by simple dissolution of any known Mn

mineral. The concentration of Mn in the carbonate extractable fraction was small. The remaining Mn(II) that should have been formed was found to be associated with the amorphous $Fe(OH)_3$ extractable fraction; Mn associated with $Fe(OH)_3$ increased from 2.4 mmol/kg before the column experiment to 4.4 mmol/kg after leaching with acidic water. Possibly, some of the Mn(II) formed by oxidation of Fe(II) coprecipitated with $Fe(OH)_3$.

A separate batch experiment was conducted to quantify equation 6 under conditions that eliminated the possibility of Mn coprecipitation (table 9). Briefly, 100 mL of water collected from Webster Lake was mixed with 30 g of alluvium in a N_2 atmosphere. The pH of water from Webster Lake was 2.8 and was acidic enough to prevent precipitation of $Fe(OH)_3$ and coprecipitation of Mn. The large ratio of Fe(III)/Fe(II) in the initial solution—3:1—was a result of Webster Lake being open to the atmosphere, which allowed oxidation of Fe(II) by O_2. Complete oxidation of Fe(II) in Webster Lake apparently was inhibited by the low pH (Stumm and Morgan, 1981, p. 467).

In control experiment A, no change occurred in the concentration of Fe(III), Fe(II), or Mn in acidic water without the alluvium. Control experiment B was designed to measure the potential amount of Fe and Mn that could be dissolved from the alluvium at low pH by adjusting the pH of a deionized water-alluvium suspension to 2.8 with sulfuric acid. No Mn was dissolved from alluvium at this pH. Some Fe was dissolved in control experiment B, and the Fe concentration increased to 3 mmol/L. When alluvium was added to the acidic water from Webster Lake—replicates C–1 and C–2—the concentration of Fe(II) decreased from 14 mmol/L to 0 and Fe(III) increased correspondingly. Manganese increased from 1.4 mmol/L to 9.2 mmol/L. Approximately 1.8 mol of Fe(II), therefore, was oxidized per mol of Mn dissolved, which computes to an average oxidation number of 3.8 for Mn in this alluvial sample.

The initial concentration of MnO_2 used to simulate the experimental data was 7.1 mmol/kg (fig. 11). This amount was required to quantitatively oxidize the 14.2 mmol/kg of Fe(II) that was removed from solution and is similar to the concentration of Mn oxides measured by sequential extraction. Iron in the pore water of the alluvium was rinsed rapidly from the column by uncontaminated water (fig. 11). Concentrations approached detection limits within 3 pore volumes, which indicates essentially all of the Fe that precipitated initially remained in the alluvium.

The concentration of Fe along the flow path chosen to simulate changes in aquifer chemistry is plotted in figure 12. Iron concentrations decreased from 53 mmol/L at well 051 to near the limit of detection in ground water 11 km downgradient. Dissolved Fe was not detected in surface water.

Data indicate that oxidation of Fe(II) by Mn oxides takes place in the aquifer as well. Ficklin and others (1991b) used sequential chemical extraction to identify elements associated with the carbonate, MnO_2, and FeO_2 phases of alluvium collected from five split-spoon samples from drill holes in contaminated, neutralized, and uncontaminated sections of the

Table 9. Oxidation of ferrous iron by manganese oxides, Pinal Creek, Arizona

[Procedure: All experiments were conducted in 250-milliliter Pyrex bottles under a nitrogen atmosphere]

	Concentration, in millimoles per liter						Ratio of moles per ferrous iron, oxidized to moles per manganese, dissolved
	Initial			Final			
Treatment	Ferrous iron	Ferric iron	Manganese	Ferrous iron	Ferric iron	Manganese	
A[1]	14	42	1.4	14	42	1.4	0
B[2]	0	0	0	0	3	0	0
C–1[3]	14	42	1.4	0	59	9.2	1.8:1
C–2[3]	14	42	1.4	0	60	9.3	1.8:1

[1]Nitrogen control—100 milliliters (mL) of water from Webster Lake. pH, 2.8.
[2]pH control—30 grams (g) of alluvium in 100 mL of deionized water and acidified to pH 2.8 with sulfuric acid.
[3]Replicates—Each beaker contained 30 g of alluvium in 100 mL of ground water.

aquifer. Ficklin and others (1991b) data show that little MnO_2 is in the alluvium from the core of the plume at well 101 compared with the larger content of MnO_2 in neutralized and uncontaminated alluvium. This observation is consistent with the depletion of MnO_2 in the column-reacted alluvium.

Two additional mechanisms affect the concentration of Fe in the aquifer. First of all, the concentration of Fe is decreased by physical dilution with uncontaminated ground water. Secondly, DO is present in parts of the aquifer and can oxidize Fe(II) according to the following reaction:

$$10H_2O + 4Fe^{2+} + O_2 = 4Fe(OH)_3 + 8H^+. \quad (7)$$

The only oxygen of concern in these simulations is that added to the plume by mixing with uncontaminated ground water that contained about 0.25 mmol/L of DO. Some atmospheric O_2 also diffuses directly into the aquifer across the air and water interface; however, this process did not affect the chemistry of Fe along the ground-water part of the flow path in these simulations. Atmospheric O_2 rapidly reacts with Mn(II) and Fe(II) near the water table and is depleted before it can diffuse to the core of the plume. A zone of greater MnO_2 and FeO_2 content has been identified in alluvium at the water table (Ficklin and others, 1991b).

The primary solid phase controlling the solubility of Fe in the aquifer appears to be $Fe(OH)_3$. Grains of alluvium coated with thick crusts of $Fe(OH)_3$ were identified in many cuttings from the core of the plume. The redox state of most ground-water samples was close to the $Fe^{2+}/Fe(OH)_3$ boundary, although most Eh values were about 100 to 200 mV lower than equilibrium and was not surprising considering the errors that are inherent in most Eh measurements. Errors in Eh measurements are caused by mixed potentials, irreversible redox reactions, and other factors that have been discussed in great detail by Lindberg and Runnells (1984). The most accurate Eh measurements usually are obtained from solutions dominated by the Fe^{2+}/Fe^{3+} redox couple (Morris and Stumm, 1967; Nordstrom and others, 1979). Concentrations of Fe^{2+} and Fe^{3+}, however, should be at least 10^{-5} mol/L in order to provide an exchange current at the electrode-solution interface that is great enough to establish a Nernstian Eh (Stumm and Morgan, 1981). If the assumption that Fe(II) is in equilibrium with $Fe(OH)_3$ is accurate, the

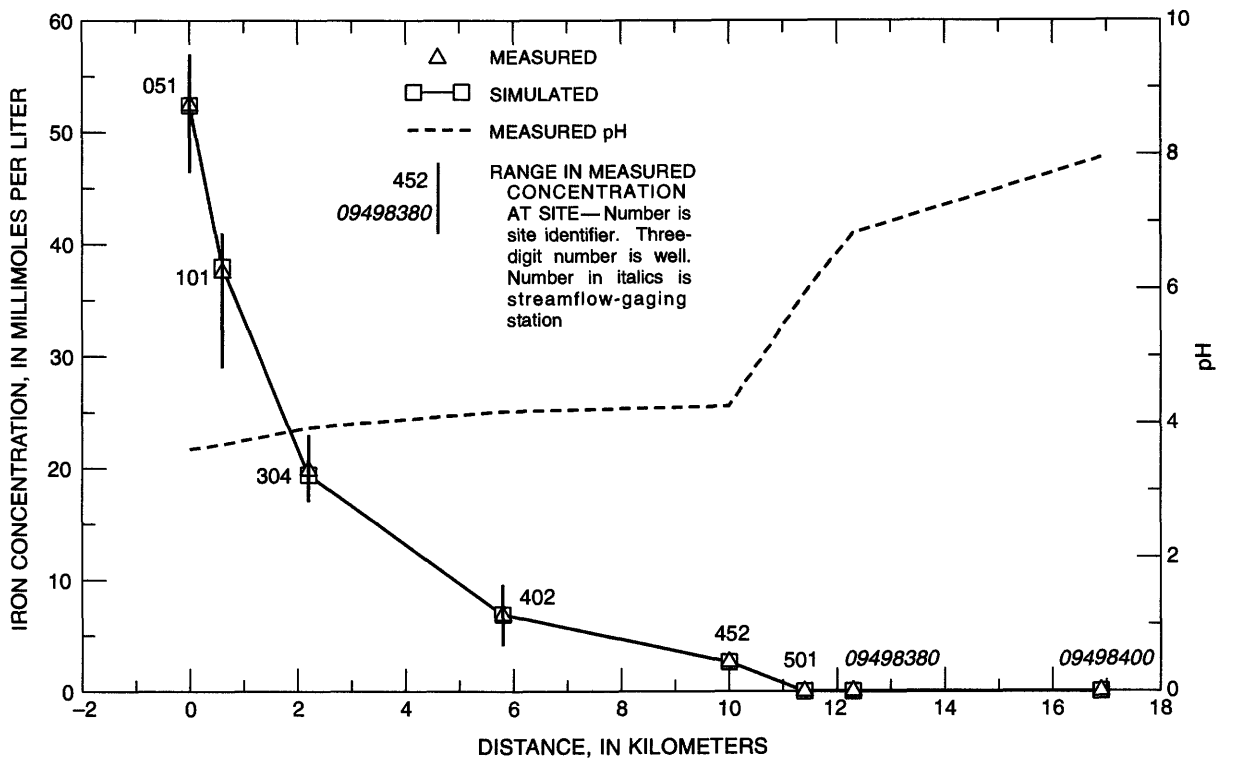

Figure 12. Measured and simulated concentrations of total dissolved iron and measured pH at observation points along flow path.

concentration of Fe^{3+} in the ground-water samples plotted in figure 8 would range from 10^{-7} to 10^{-9} mol/L, which is well below the concentration required to establish an accurate equilibrium Eh.

The concentrations of Fe along the first 2 km of the flow path (fig. 12) were simulated using only dilution and is consistent with data from Ficklin and others (1991b), which indicated a lack of Mn oxides in this reach of the aquifer. From kilometer 2 to kilometer 11, dilution was not as significant, and oxidation by MnO_2 became the primary mechanism for removing Fe(II) from solution. The actual mass of MnO_2 in alluvium along this part of the flow path was not known. Therefore, the quantity of MnO_2 added in each simulation was based on the quantity of Fe(II) that had to be oxidized to match the measured concentration of Fe(II) in the aquifer.

Manganese

Reductive dissolution of Mn oxides by Fe(II) resulted in a net release of Mn to solution in the column experiment (fig. 13). Manganese concentrations as high as 17.5 mmol/L were measured in the effluent; whereas, the influent concentration was only 1.4 mmol/L. As was discussed in the previous section, the total amount of Mn dissolved from the alluvium—3.3 mmol/kg—was substantially less than the 7.1 mmol/kg predicted to dissolve by equation 6.

Three mechanisms can be hypothesized to explain why all of the Mn(II) that should have been formed by equation 6 was not measured in effluent. The first possibility is that complete reduction of Mn(IV) to Mn(II) may have been inhibited by the formation of an $Fe(OH)_3$ coating on the Mn oxides. Stone and Morgan (1987) have suggested a two-step reaction sequence similar to the following equations.

Adsorption

$$\equiv Mn^{IV}OH + Fe^{2+} = (\equiv Mn^{IV}OFe^{II})^{+} + H^{+}. \quad (8)$$

Electron transfer

$$(\equiv Mn^{IV}OFe^{II})^{+} + H_2O = \equiv Mn^{III}OFe^{III}OH + H^{+}. \quad (9)$$

The Mn(III) in this oxide phase could be shielded from further aqueous Fe(II); therefore, the amount of Mn in solution would be less than expected from equation 6. A second possibility is that some Mn(II) formed by oxidation of Fe(II) may have been occluded from the flowing phase by coprecipitation with $Fe(OH)_3$. Some evidence exists for such a process

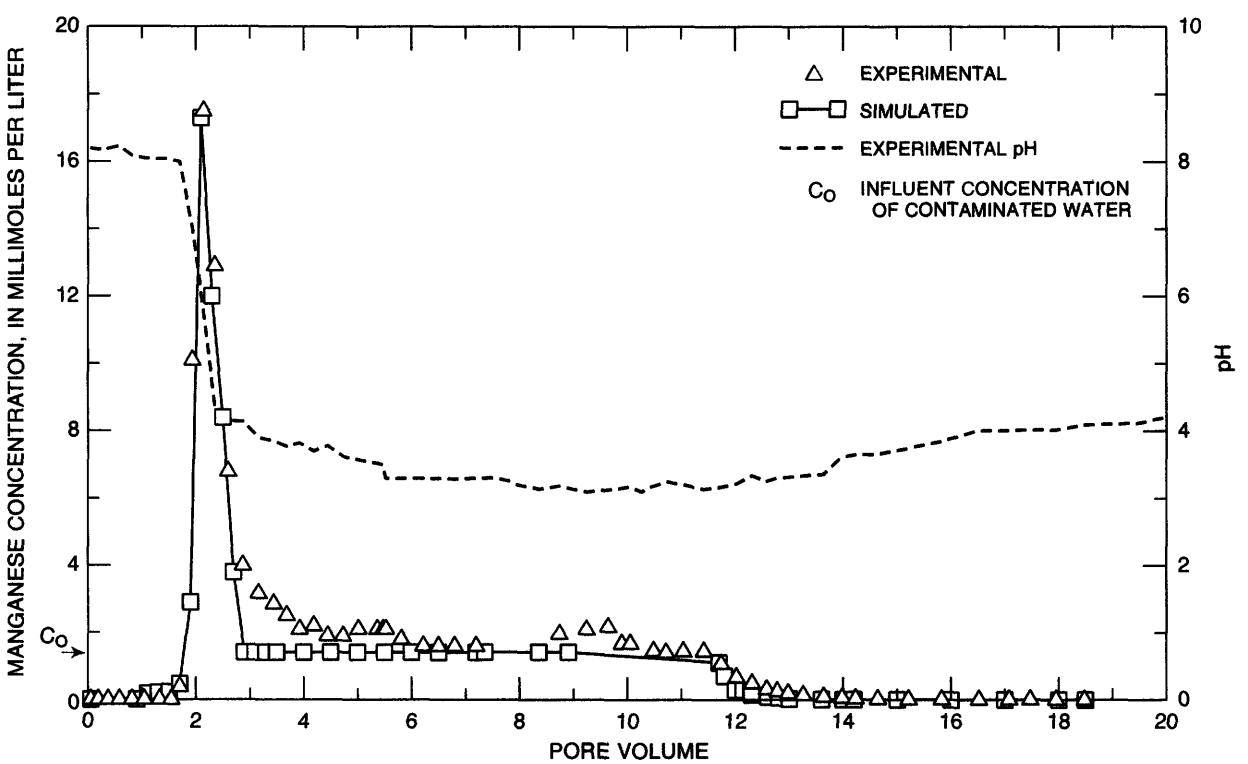

Figure 13. Experimental and simulated concentrations of manganese and experimental pH in column effluent.

from the shape of the breakthrough curve in figure 13. After the initial spike, Mn concentrations never returned to the influent concentration. This slow leaching of Mn from the alluvium is consistent with diffusion of Mn(II) trapped in $Fe(OH)_3$ to the flowing phase. Also, sequential chemical extraction of the reacted alluvium after completion of the column experiment did measure an increase in the amount of Mn associated with amorphous Fe oxides. Cornell and Giovanoli (1987) have described a Mn substituted $Fe(OH)_3$ that was precipitated in laboratory experiments. The third possibility is that Mn(II) solubility may have been controlled by a discrete mineral phase that was not listed in any of the thermodynamic data bases used in this study.

Most of the Mn that was measured in the column effluent could be simulated using the diffuse double-layer model. A logK of –2.6 (equation 7, table 7) gave the best fit to the experimental data. This value generally is close to the logK of –3.5 estimated by Dzombak and Morel (1990) for sorption of Mn on fresh amorphous $Fe(OH)_3$. The simulations correctly predicted that essentially all of the Mn in the influent as well as the Mn reduced by Fe(II) should be sorbed at pH values greater than 7.7. Sorption was modeled as an irreversible reaction to simulate coprecipitation of Mn with $Fe(OH)_3$. As pH decreased below 7.7, sorption decreased and the concentration of Mn in the effluent rapidly increased. Less than 1 percent Mn was sorbed at pH 4.4. The concentration spike of Mn between pore volumes 2 and 3 correlated with the decrease in pH and represents the Mn reduced by Fe(II) that was not sorbed. In contrast to the measured effluent concentration, the model indicated that Mn should rapidly decline to the influent concentration after depletion of the available MnO_2. No attempt was made to model the apparent diffusion-controlled leaching of Mn from alluvium between pore volumes 3 and 11.

The concentration of Mn rapidly approached the detection limit when the influent was switched to uncontaminated ground water. The uncontaminated water contained DO that would be expected to reoxidize Mn(II) in the alluvium and prevent any further leaching.

Manganese in ground water and surface water was simulated by a combination of dilution, sorption, and precipitation. The decline in Mn concentrations along the first 2 km of the flow path, which was the most acidic (pH <4) was successfully simulated by dilution alone and is consistent with the fact that the decrease in Fe(II) along this same stretch of aquifer was simulated without reduction of MnO_2 (fig. 14). Sequential chemical-extraction data indicated that Mn oxides were depleted from the most acidic part of the plume. Alluvium collected from well group 100 (1 km) contained only 0.1 mmol/kg of Mn oxides; whereas, alluvium from Russell Gulch, which is upgradient from the contaminated aquifer, contained an average of 1.5 mmol/kg of Mn (Ficklin and others, 1991b). Also, the amount of exchangeable Mn at well group 100 increased. These field results are comparable to results obtained from the column experiments where Mn oxides in reacted alluvium were only 6 percent of the unreacted concentration.

The measured increase in the concentration of Mn in ground water between 2 and 9 km could be simulated by the reductive dissolution of MnO_2. Initial computer simulations, however, predicted less than 1 percent sorption of Mn at wells 402 (pH = 4.18) and 452 (pH = 4.26); therefore, the simulated concentrations of Mn were much greater than measured concentrations. The column data indicated that about 65 percent of the Mn that was reduced by Fe(II) remained in the solid phase. The same mechanism, therefore, was assumed to have occurred in the aquifer, and aqueous Mn at wells 402 and 452 was simulated by removing 65 percent from solution as a coprecipitate after all reactions had taken place. Subsequent simulated concentrations of Mn in solution at well 402 were still too large, and at well 452, simulated concentrations of Mn were too small. The results, however, are more comparable to the field data than they would have been if no correction been applied. Although this approach can be justified on the basis of the chemistry of Mn and Fe in the column experiment, there are not enough data on the solid-phase associations of Mn or the kinetics of these reactions to quantify the process.

Simulations of aqueous Mn were more accurate along the remainder of the flow path (fig. 14). The decrease in Mn from kilometer 10 to kilometer 11.5 corresponded with an increase in pH to 5.9, and was accurately simulated by sorption using the logK determined for the column data. Ground-water discharges at the surface near kilometer 12 and becomes oxygenated. Manganese precipitates as an oxide and coats the streambed. The concentrations of Mn in surface-water samples taken at kilometer 12 and kilometer 16 were simulated by assuming equilibrium with birnessite.

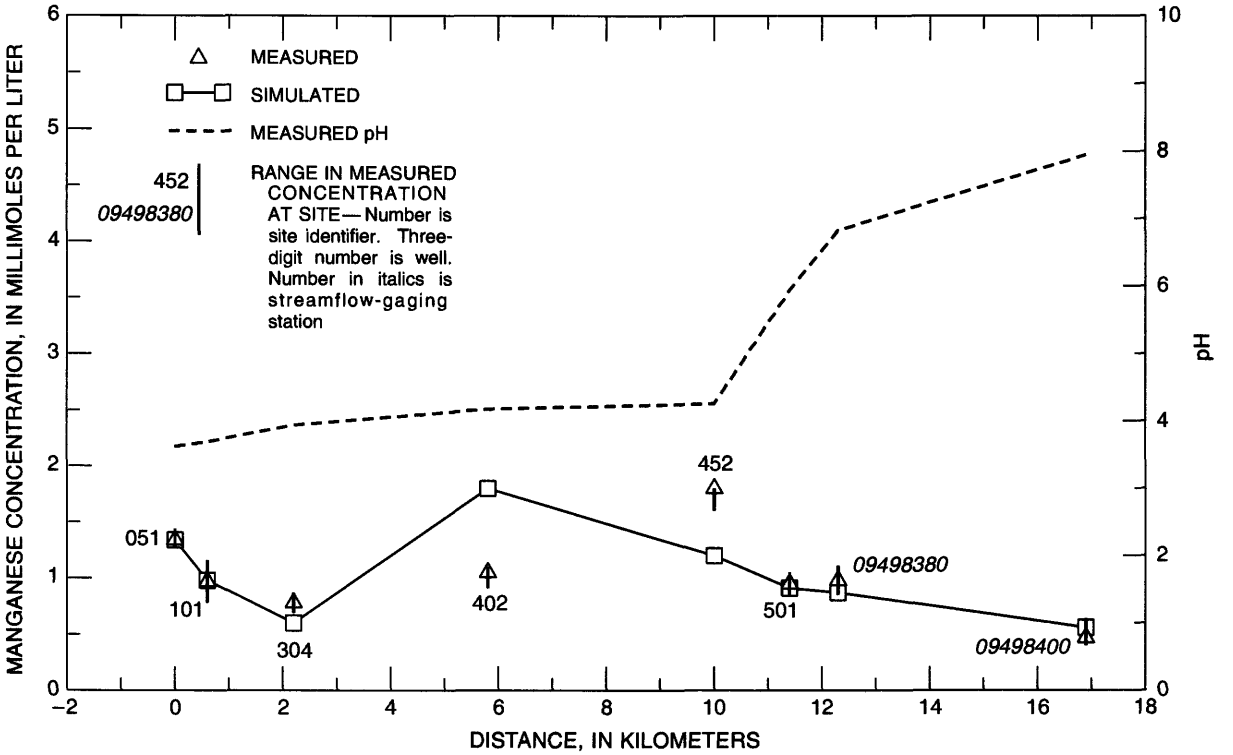

Figure 14. Measured and simulated concentrations of manganese and measured pH at observation points along flow path

Copper, Cobalt, Nickel, and Zinc

Experimental breakthrough curves for Cu, Co, Ni, and Zn were similar and are typical of the pH-dependent sorption of cations on oxide surfaces (figs. 15*A*–15*D*). Concentrations were below the limits of detection at pH greater than 7 and then rapidly increased as the pH of column effluent decreased. The spike in the concentration of Cu, Co, and Ni can be explained by desorption as the acidic front eluted through the column. Mass-balance calculations indicated that all of the Ni initially removed from solution was desorbed compared to 25 percent of the Co and only 6 percent of the Cu. Evidence indicates that the Cu retained by the alluvium was associated with Fe oxides. The amount of Cu irreversibly sorbed was 0.95 mmol/kg, which compares well with the 0.91 mmol/kg Cu that was chemically extracted from the reacted alluvium. Electromicroprobe analyses of reacted alluvium measured as much as 10 percent by weight of Cu associated with Fe oxides. The irreversibly sorbed Co also was associated with Fe oxides. A concentration spike also was measured for Zn; however, preliminary leaching experiments indicated the potential for Zn contamination at low pH from some of the components used in column construction. Only the initial part of the breakthrough curve and the rinse-out curve, therefore, are plotted for Zn.

The diffuse double-layer model was used to simulate the breakthrough curves for Cu, Co, Ni, and Zn. Equilibrium constants for sorption of Cu, Ni, and Zn (table 7) were reported by Dzombak and Morel (1990) for sorption on $Fe(OH)_3$. The equilibrium constant for Co was the value that gave the best fit to the experimental data. The pH at which the four metals were first detected in column effluent and the steep rise in concentration were accurately simulated (figs. 15*A*–15*D*). The concentration spikes were simulated by desorption. The amount of each metal that was allowed to desorb in the model was equal to the amount actually measured in the column experiment. All of the Ni was allowed to desorb; however, only 25 percent of the Co and 6 percent of the Cu was allowed to desorb. The model indicated that desorption should be almost instantaneous. Actual concentrations approached influent values more slowly and probably reflected the slower process of diffusion out of pores of stagnant water within the column. The concentration of all four metals decreased to below detection limits

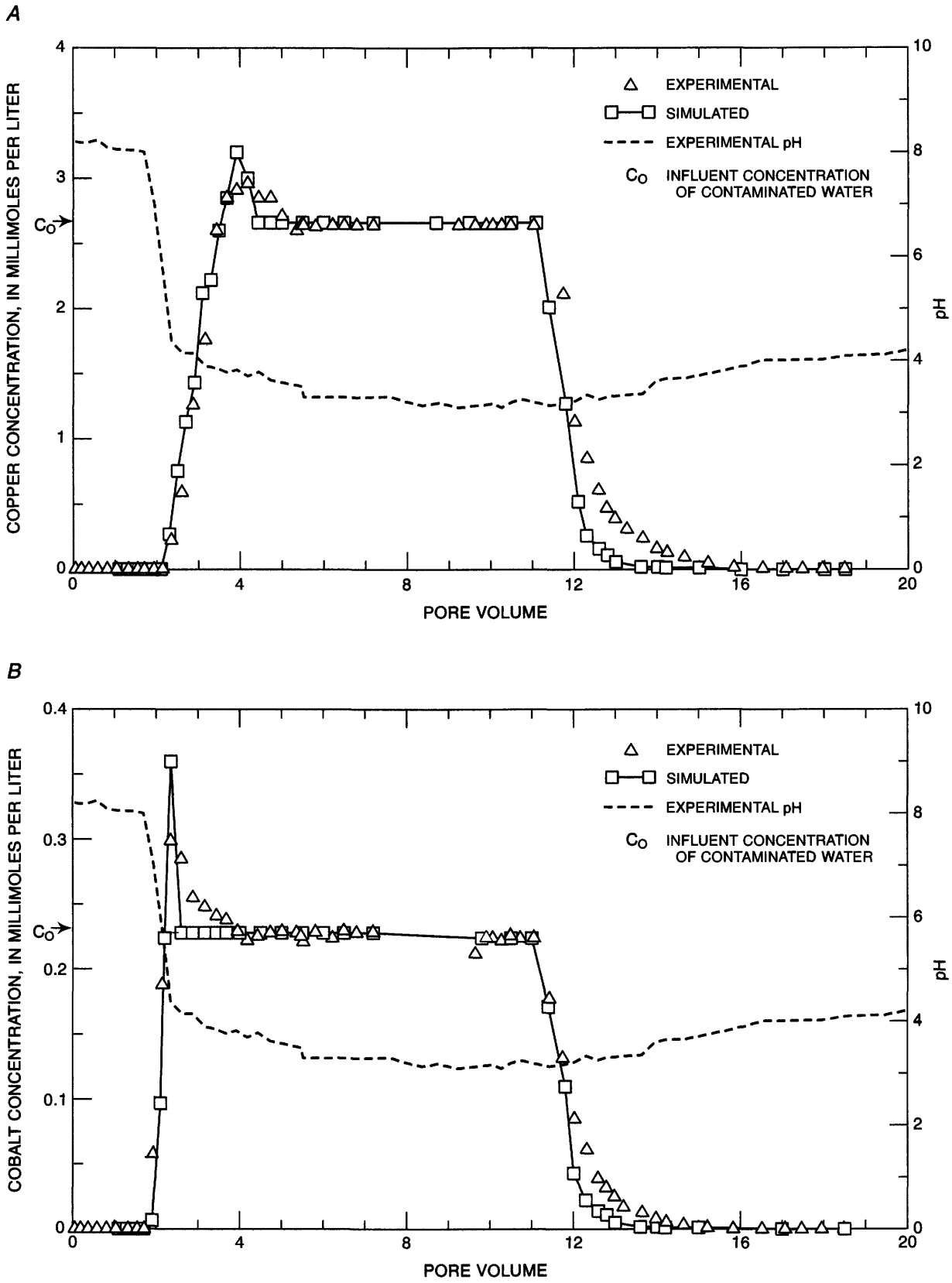

Figure 15. Experimental and simulated concentrations of constituents and experimental pH in column effluent. *A*, Copper; *B*, Cobalt; *C*, Nickel; *D*, Zinc.

C

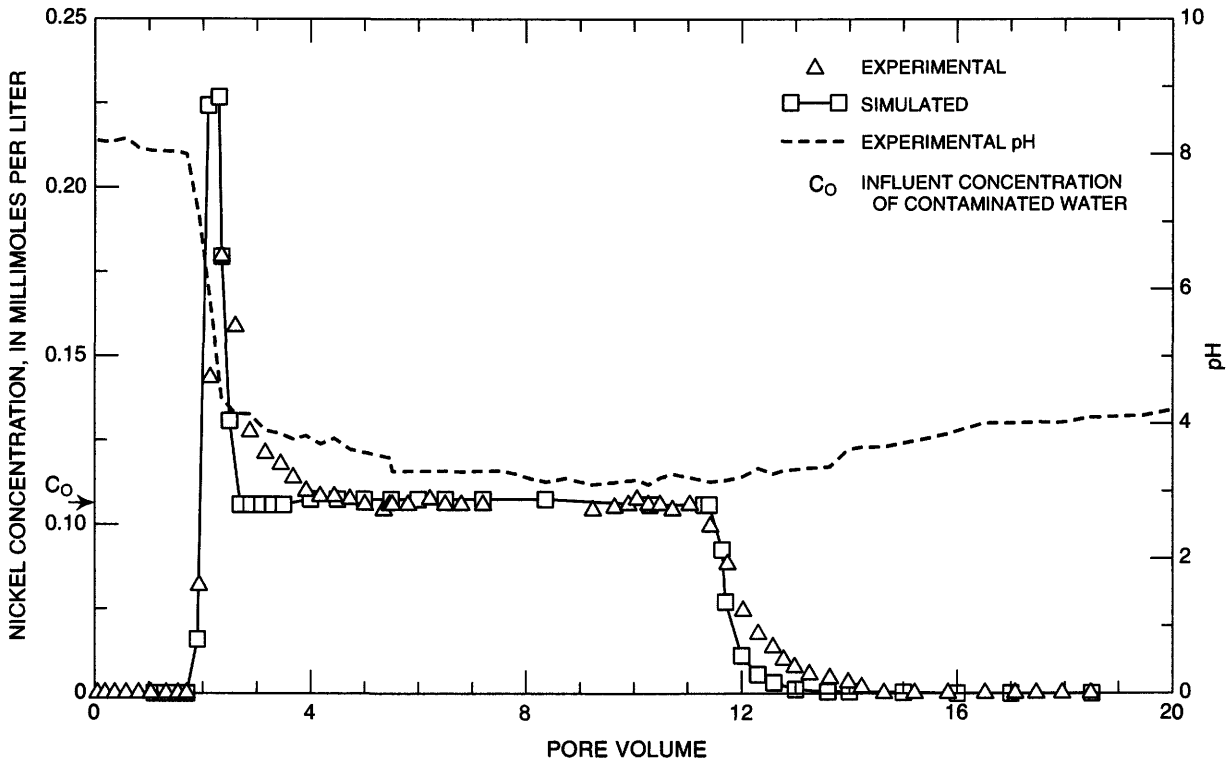

D

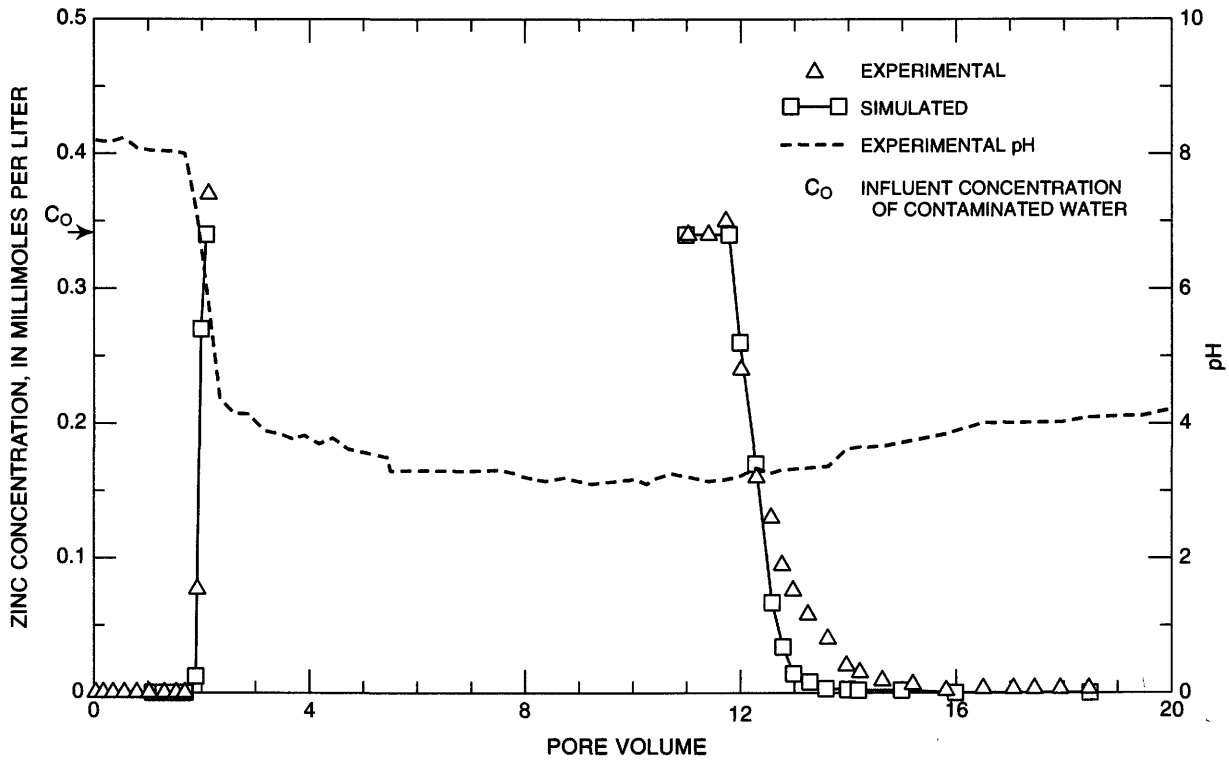

Figure 15.—Continued.

within a few pore volumes after switching back to uncontaminated ground water.

The concentrations of Cu, Co, Ni, and Zn along much of the aquifer also were a function of pH (figs. 16*A*–16*D*). The diffuse double-layer model predicted no sorption of Co, Ni, or Zn in the first 10 km because of the low pH. Concentrations along this part of the aquifer were simulated only by dilution. The decrease in concentration downgradient from kilometer 10 corresponded with the increase in pH and was simulated by sorption on $Fe(OH)_3$. Sorption of Cu was predicted throughout the entire flow path, even in the acidic core of the plume. The combination of dilution plus sorption accurately simulated Cu in ground water.

Aluminum

The concentration of Al in column effluent was a function of both pH and the concentration of SO_4 (fig. 17). Mass-balance calculations by MINTEQA2 indicated that precipitation of amorphous $Al(OH)_3$ caused the complete removal of Al from the first 2.5 pore volumes of acidic influent. As pH decreased to less than 4.7, several aluminum sulfate minerals became supersaturated, including jurbanite ($AlSO_4OH \cdot 5H_2O$), alunite [$KAl_3(SO_4)_2$], and a basic aluminum sulfate ($AlOHSO_4$). Jurbanite has been reported to form only in environments more acidic than existed in the column, and evidence exists for kinetic inhibition to precipitation of alunite at low temperatures (Nordstrom, 1982). Neither mineral, therefore, was considered to control Al solubility. The logK for $AlOHSO_4$—3.23—was closest to the experimental-ion activity product for most effluent samples. Accordingly, $AlOHSO_4$ was used to control the solubility of Al at a pH of less than 4.7. The logK, however, was changed to 2.2 to provide the most accurate fit to the experimental data. The combination of amorphous $Al(OH)_3$ and $AlOHSO_4$ yielded an excellent match of the experimental breakthrough curve. MINTEQA2 simulations also indicated that the $Al(OH)_3$ that precipitated initially should have dissolved and reprecipitated as $AlOHSO_4$ as the low pH, SO_4-rich water eluted through the column.

Aluminum in the interstitial pore water was rapidly rinsed from the column initially; however, concentrations leveled off at about 0.6 mmol/L by pore volume 14. The experimental data from pore volume 12 through 18 were modeled by allowing dissolution of $AlOHSO_4$. By pore volume 18, only 10 percent of the $AlOHSO_4$ in the column had dissolved. Thus, a significant reservoir of Al remained in the alluvium and was predicted to continually leach into solution as long as pH remained low. As pH increased, $Al(OH)_3$ regained control over Al solubility.

The combination of amorphous $Al(OH)_3$ and $AlOHSO_4$ as controls on concentrations of aqueous Al worked reasonably well in simulating Al in the aquifer (fig. 18). The simulated concentrations plot within the range of concentrations of Al measured in the aquifer with the exception of well 402 at kilometer 5.8. $AlOHSO_4$ controlled solubility in the first 10 km where pH was less than 5. Precipitation of gibbsite maintained Al below detection limits along the remainder of the flow path.

Calcium and Sulfate

The concentration of Ca and SO_4 in the acidic ground water used in the column experiment were in equilibrium with gypsum ($CaSO_4 \cdot 2H_2O$), and concentrations in the column effluent were simulated reasonably well by maintaining equilibrium with gypsum (figs. 19*A*–19*B*). As acidic water moved through the column, dissolution of calcite initially released a large amount of Ca. Although much of this Ca precipitated with SO_4, concentrations as large as 26 mmol/L were measured in the effluent. This value is more than twice the concentration in the influent solution. Sulfate concentrations were kept low initially as gypsum precipitated. As carbonates were depleted, Ca decreased and SO_4 increased until influent concentrations were reached.

Effluent from the column was apparently supersaturated with respect to gypsum, and gypsum precipitated in the collection tubes. Equilibrium with gypsum indicated that there should have been less Ca and SO_4 in solution than was actually measured between pore volumes 1 and 5. The kinetics of gypsum precipitation in this system appeared to be a function of ionic strength. As ionic strength increased, the degree of supersaturation decreased, and the simulated concentrations approached the experimental values.

Gypsum began to dissolve when uncontaminated ground water was eluted through the column. All of the gypsum initially precipitated was dissolved by pore volume 17, and concentrations of Ca and SO_4 decreased to the influent values of uncontaminated water.

Data indicates that gypsum probably precipitates in the aquifer. Most gypsum identified in cuttings from the aquifer was cryptocrystalline; however, selenate blades as much as 1 cm long have been identified in some parts of the acidic plume. Growth of such large crystals probably was related to zones rich in carbonate minerals where dissolution provided a continuous source of Ca.

Simulations by MINTEQA2 predicted gypsum precipitation at each point along the flow path except for the last one at kilometer 17 where gypsum was undersaturated (figs. 20*A*–20*B*). The concentration of Ca increased along the flow path and reflected dissolution of calcite and dolomite. Precipitation of gypsum and $AlOHSO_4$ and dilution caused concentrations of SO_4 to decrease. At Inspiration Dam, the measured concentrations of Ca and SO_4 were greater than concentrations of Ca and SO_4 in uncontaminated water in this area.

BASIN-FILL EXPERIMENT

Basin fill, which underlies the alluvium, has a much smaller hydraulic conductivity and tends to act as a barrier to downward migration of acidic water. Data, however, indicates that acidic ground water has contaminated some of the upper basin fill near the contact with alluvium (Eychaner, 1991a). The following discussion of the basin-fill column experiment describes the effect of increased carbonate content on transport of constituents in acidic ground water.

pH

The sample of basin fill packed in the column contained 0.15 mol/kg of carbonate minerals, which is almost seven times the carbonate content of the alluvium. As would be expected, the basin fill neutralized more pore volumes of acidic ground water (fig. 21). In fact, pH never decreased to less than 6 during the course of the experiment that lasted for 16 pore volumes. Initial attempts to model the column results using the same geochemical model developed for the alluvium predicted that the pH should have been buffered near 8 until all of the carbonate minerals were dissolved. At approximately pore volume 9, pH should have rapidly decreased to 3.3, which is the influent pH. The gradual decrease in pH in the experimental data indicates disequilibrium between acidic water and carbonates. Disequilibrium probably developed as carbonates became coated by precipitation of gypsum, iron, and aluminum hydroxides. Effluent became a mixture of acidic water that had not come into contact with carbonates and water that had been neutralized by the remaining coated carbonates.

By pore volume 8, the amount of precipitation had become great enough to significantly reduce the velocity of water through the column. The amount of Ca, SO_4, Fe, and Al that precipitated in the basin fill was estimated (table 10). The amount precipitated by the alluvium is listed for comparison as well as the amount of Cu, Co, and Ni that were sorbed by both sediment types. The greater carbonate content of basin fill resulted in a significant increase in attenuation of constituents.

The lack of equilibrium in this experiment made simulation of most constituents difficult. Only the pH-dependent sorption of Co, Cu, Ni, and Zn; and the pH-dependent precipitation of Al were simulated.

Iron and Manganese

Fe did not begin to break through until about pore volume 6 (fig. 22). The assumption was that oxidation by manganese oxides caused precipitation of a significant fraction of the 80 mmol/kg of Fe(II) that were removed from solution. Sorption of Fe(II) at the higher pH values, and substitution of Fe(II) in carbonate minerals, however, cannot be discounted. Mn began to break through near pore volume 4 and exhibited the same type of concentration spike observed in the alluvium. The peak concentration of Mn in the spike was 33 times the influent concentration.

Copper, Cobalt, Nickel, and Aluminum

Cu and Ni began to break through near pore volume 5, when pH values decreased to less than 7 (fig. 23). This reaction is consistent with the pH-dependent sorption observed in the alluvium-column experiment. The basin-fill data were simulated using the diffuse-layer model and the equilibrium constants for Co and Ni (table 7). The model was able to match the experimental data reasonably well.

Cu and Al were not detected in effluent from the basin fill, which is consistent with predictions by the

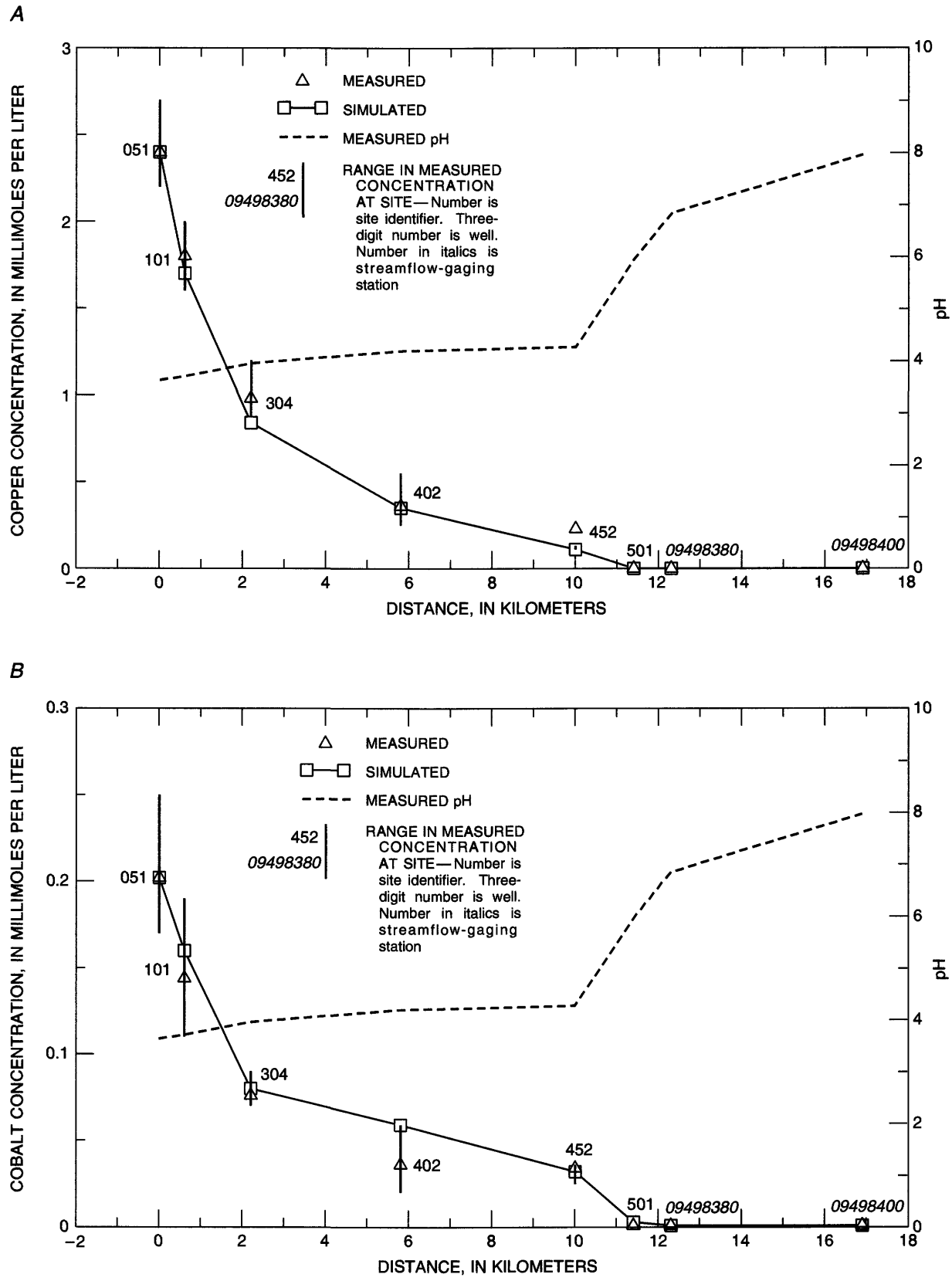

Figure 16. Measured and simulated concentrations of constituents and measured pH along flow path. *A*, Copper; *B*, Cobalt; *C*, Nickel; *D*, Zinc.

C

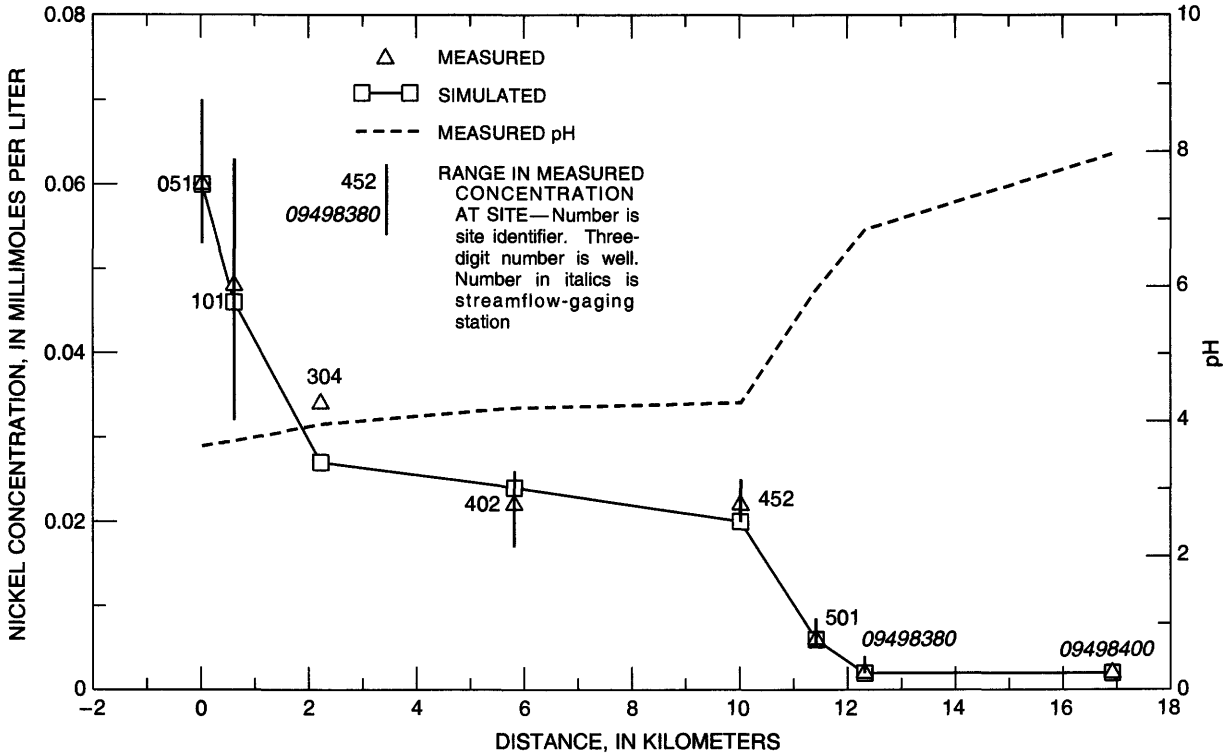

D

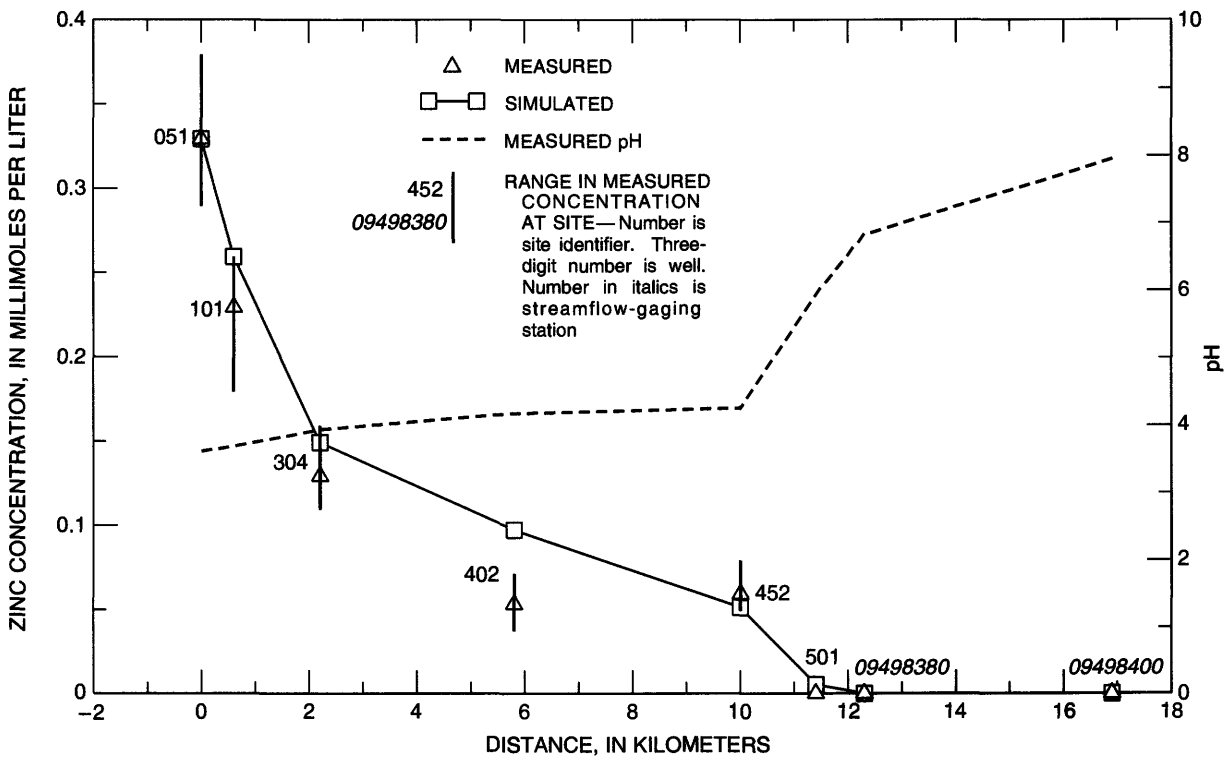

Figure 16.—Continued

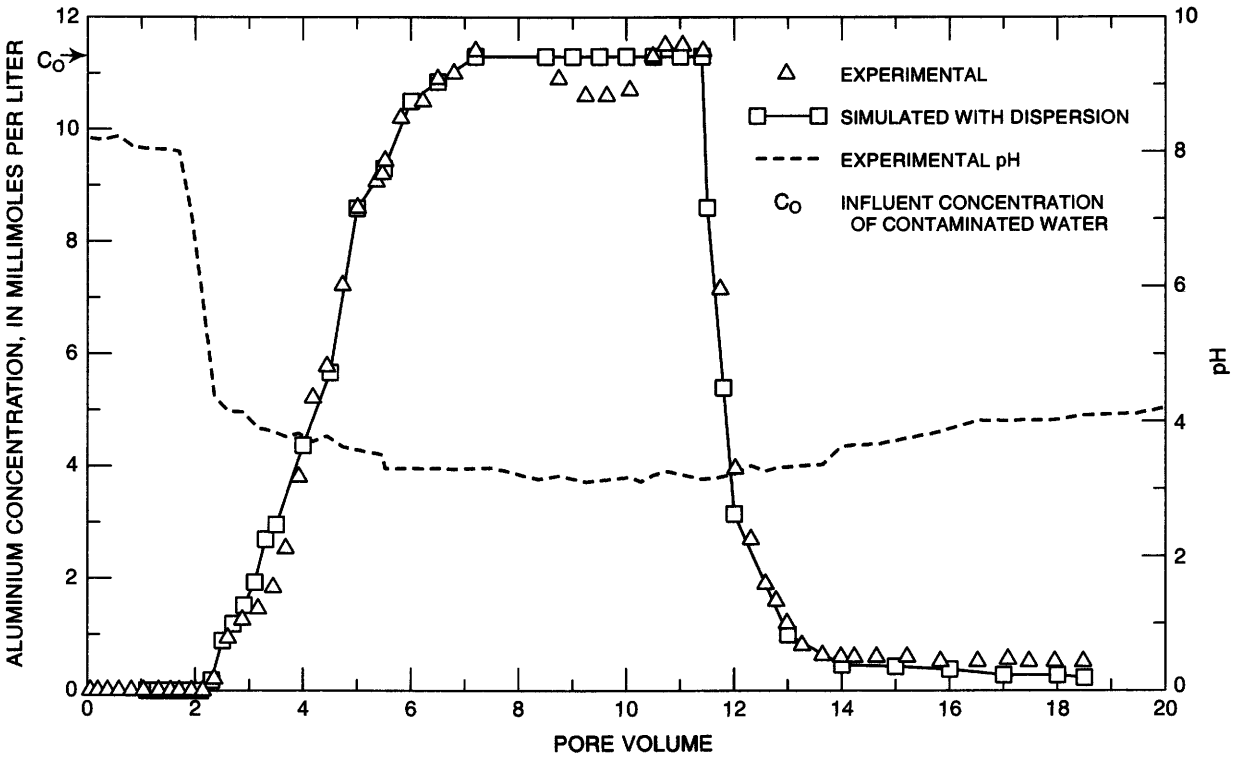

Figure 17. Experimental and simulated concentrations of aluminum and experimental pH in column effluent.

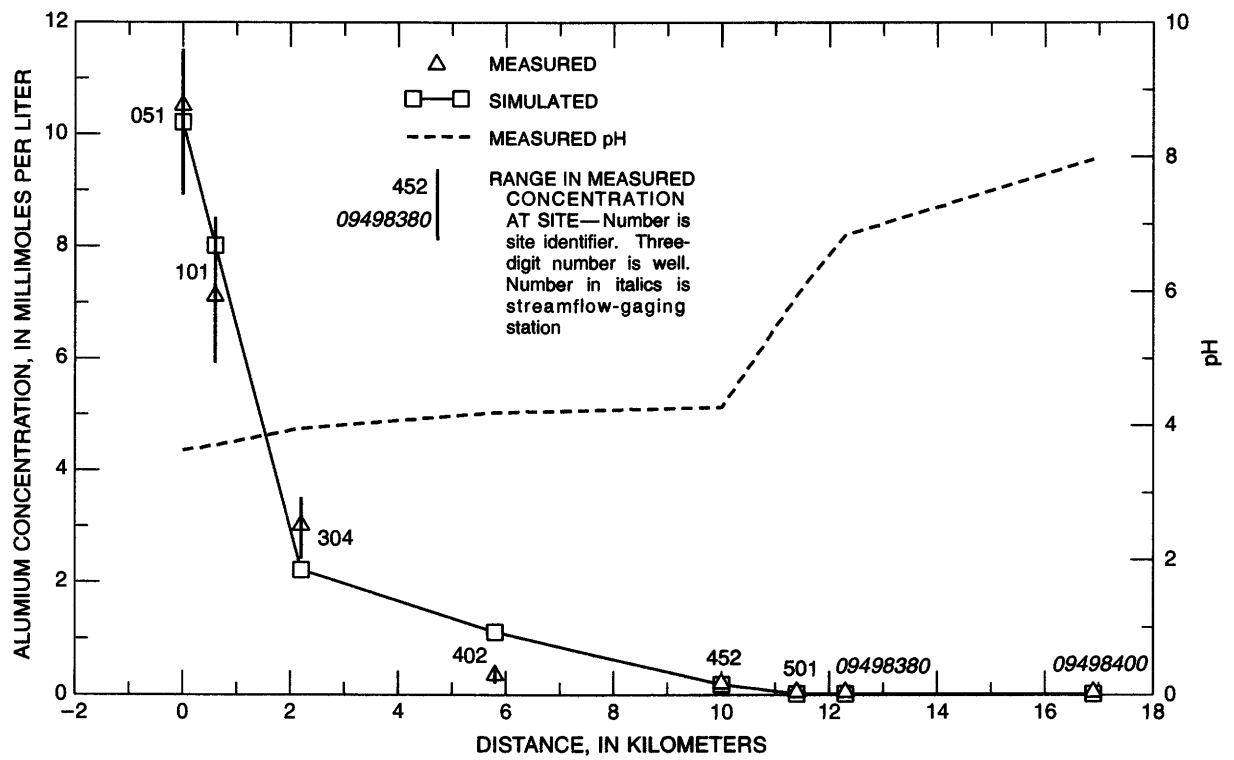

Figure 18. Measured and simulated concentrations of aluminum and measured pH at observation points along flow path.

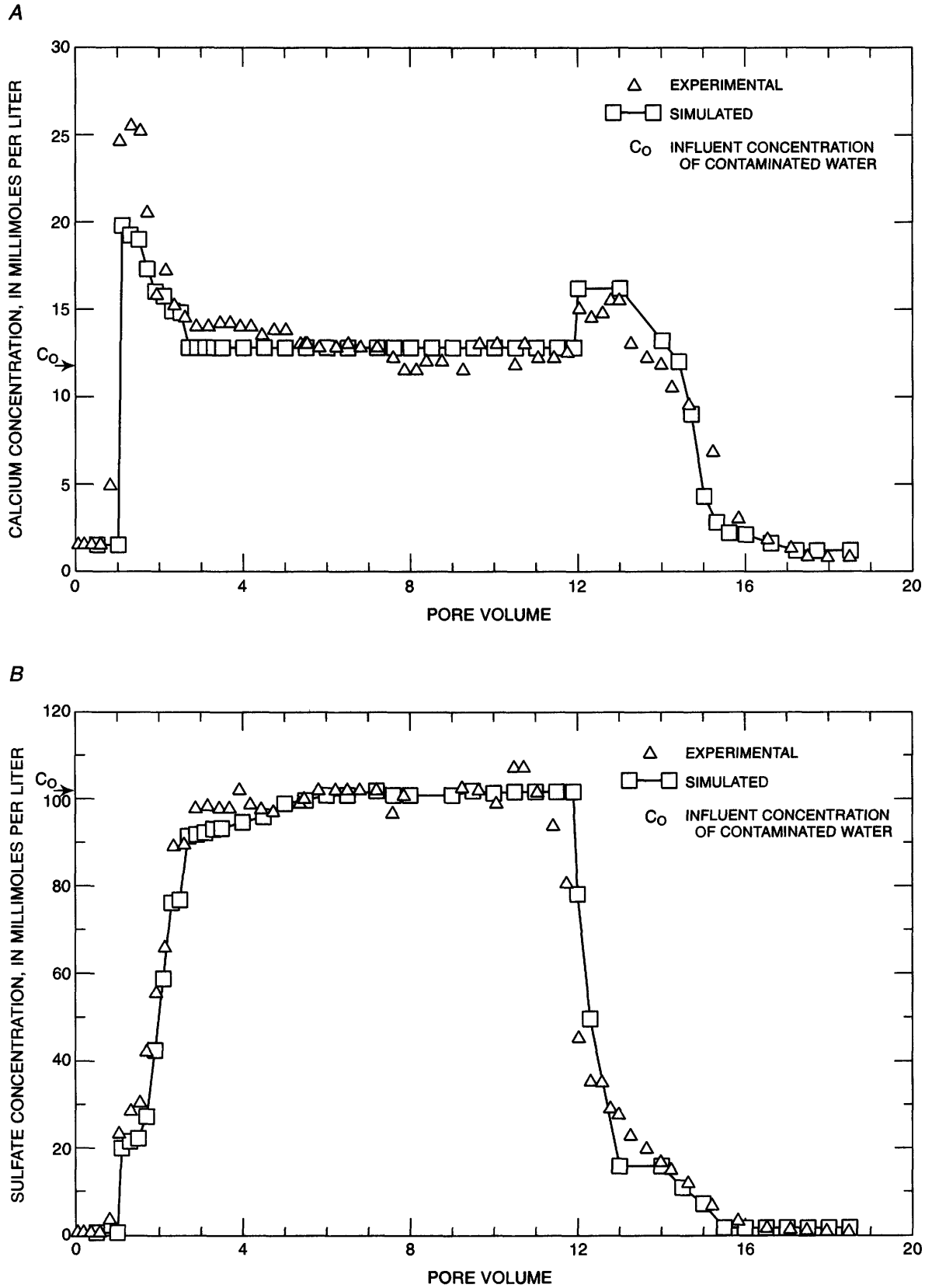

Figure 19. Experimental and simulated concentrations of constituents in column effluent. *A*, Calcium; *B*, Sulfate.

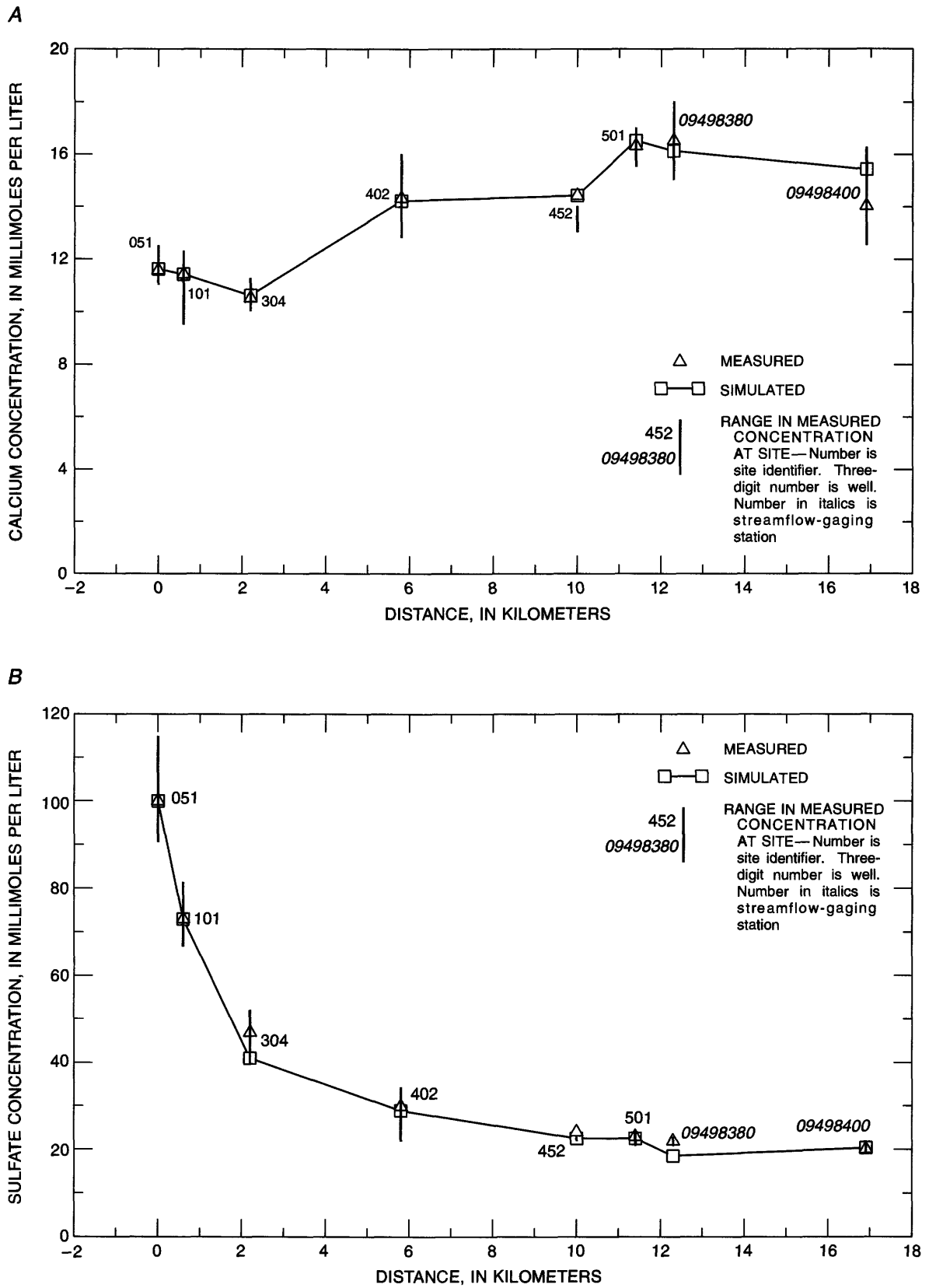

Figure 20. Measured and simulated concentrations of constituents at observation points along flow path. *A*, Calcium; *B*, Sulfate.

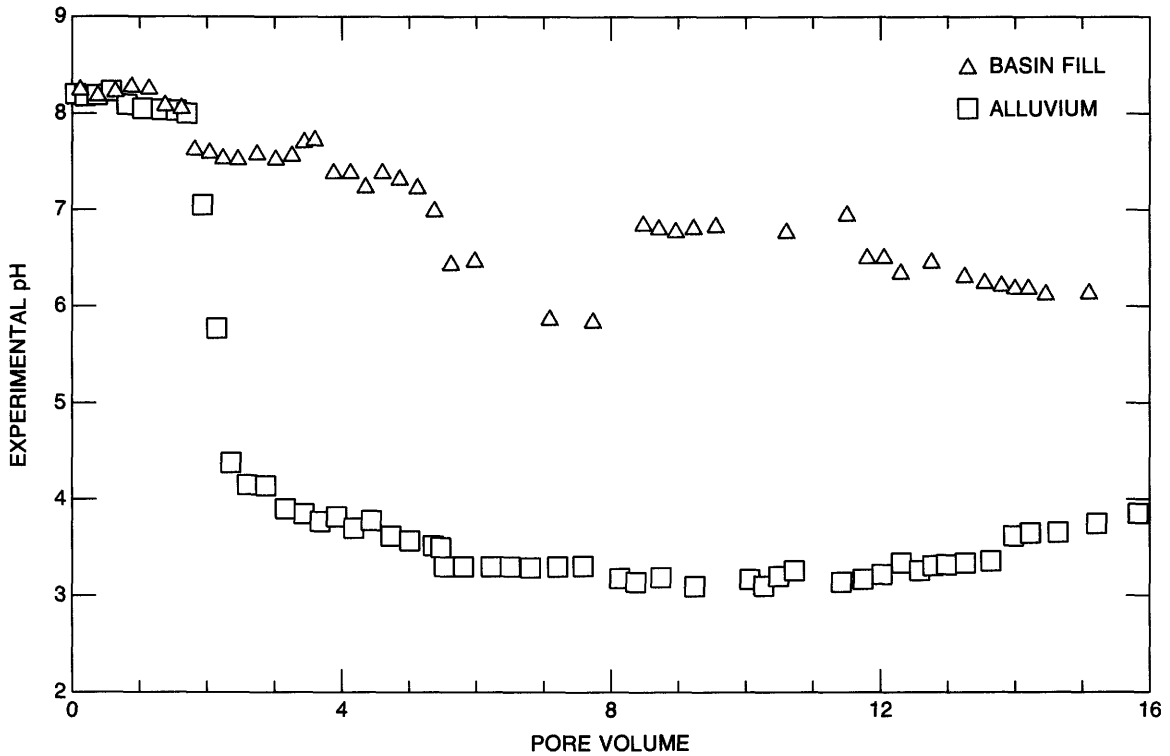

Figure 21. Experimental pH in effluent from basin-fill and alluvial columns.

Table 10. Mass of constituents removed by alluvium and basin fill, Pinal Creek, Arizona

Constituent	Alluvium	Basin fill
Millimoles per kilogram precipitated		
Calcium plus sulfate	17	104
Iron	14	80
Aluminum	8	20
Millimoles per kilogram sorbed		
Cobalt	.04	.32
Copper	.95	3.9
Nickel	.002	.14

geochemical model. The geochemical model indicated that all of the Cu should sorb at pH values greater than 6, and Al should precipitate as $Al(OH)_3$.

CONCLUSIONS

A geochemical model was developed to define the evolution of a plume of acidic ground water in an alluvial aquifer in Pinal Creek, Arizona. Reactions that controlled the concentration of selected constituents were identified by evaluating ground-water analyses in conjunction with data from laboratory experiments. The model was calibrated first by adjusting reaction hypotheses and equilibrium constants in order to match concentrations in breakthrough curves from a laboratory-column experiment. The model then was made to simulate the change in ground-water composition along a one-dimensional flow path in the aquifer. The main conclusions are as follows.

1. Cl was shown in column experiments to be non-reactive and therefore could be used to estimate the amount of dispersion in breakthrough curves from the column experiment and the amount of dilution of the acidic plume in the aquifer.
2. H^+ was neutralized primarily by reaction with carbonate minerals. These reactions generally were rapid and resulted in a steep gradient in pH over a short distance. In parts of the aquifer where carbonates were depleted and pH was less than 4.5, sorption on ferrihydrite was the dominant control on pH. Reaction with silicate minerals may have some effect on pH; however, reaction rates are probably too slow to have any significant effect on pH.
3. The concentration of Fe in the alluvial aquifer was controlled by oxidation of Fe(II) to Fe(III) and

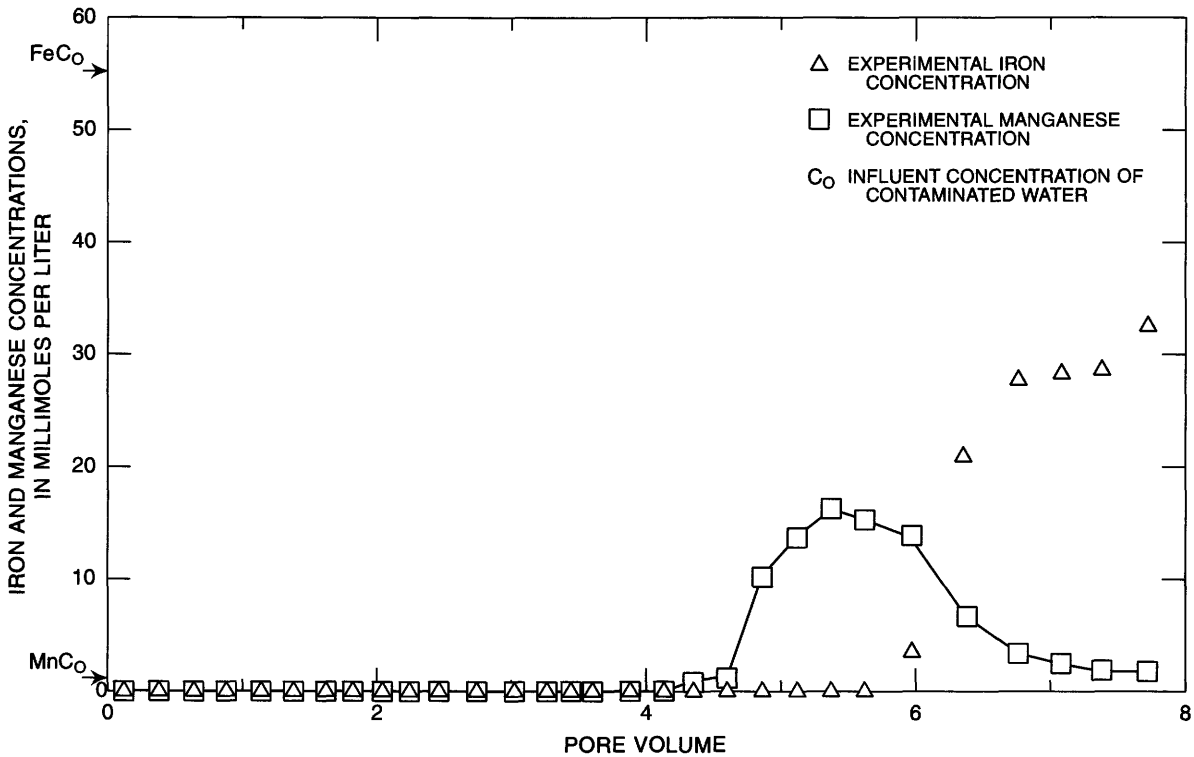

Figure 22. Experimental concentrations of iron and manganese in basin-fill column effluent.

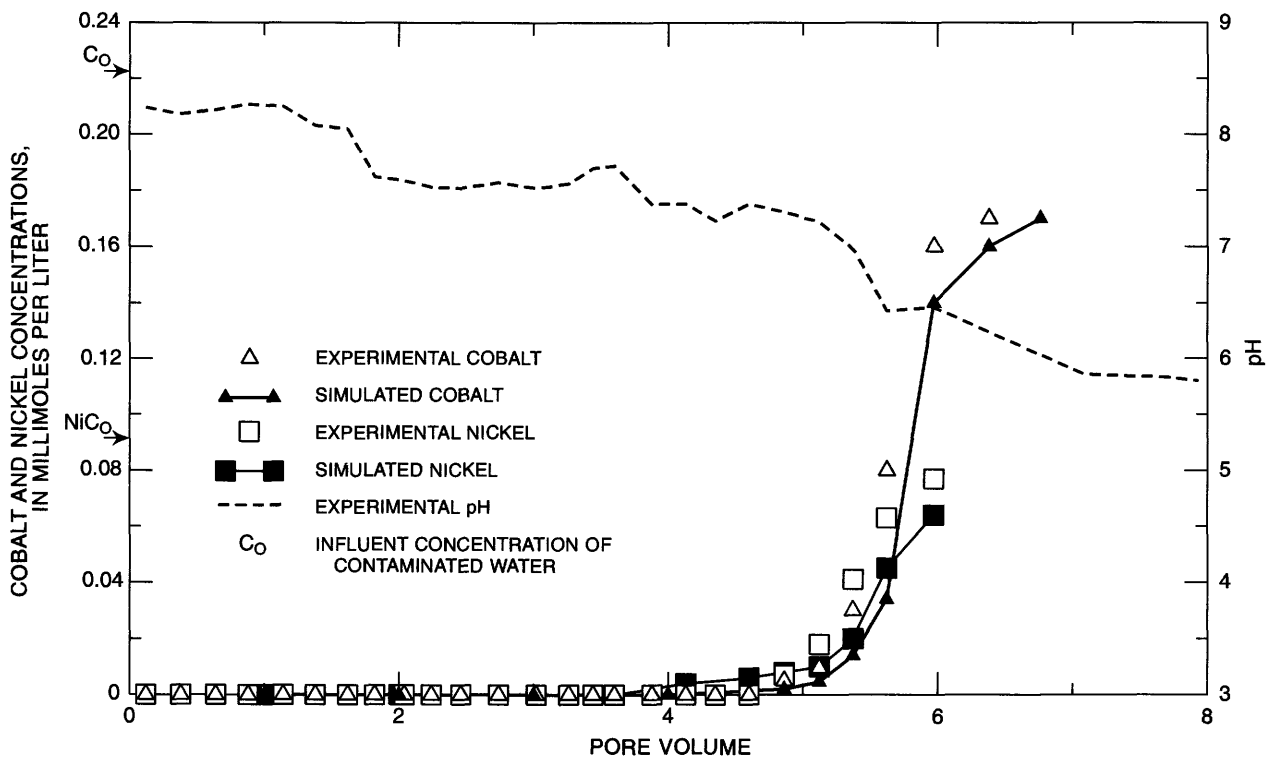

Figure 23. Experimental and simulated concentrations of cobalt and nickel and experimental pH in basin-fill column effluent.

precipitation of $Fe(OH)_3$. In the column experiment, Mn(III,IV) oxides were the only apparent oxidants. In the aquifer, Fe(II) was oxidized by using a combination of Mn oxides and DO in uncontaminated ground water that mixed with the plume.

4. Reduction of Mn by Fe(II) increased the concentration of Mn in column effluent and in ground water. Some of this Mn was sorbed by $Fe(OH)_3$ at higher pH values. Desorption occurred as pH decreased. A significant fraction of the Mn remained associated with the solid phase, either as a coprecipitate or an incompletely reduced oxide.
5. The concentration of aqueous Cu, Co, Ni, and Zn in solution were a function of pH. Sorption of these metals was simulated using the diffuse layer surface-complexation model.
6. Aluminum was controlled by precipitation of $Al(OH)_3$ at pH greater than 4.7. $AlOHSO_4$ appeared to control solubility at lower pH values.
7. Calcium and sulfate concentrations were controlled by precipitation of gypsum.
8. Attenuation of constituents in the acidic plume increases with carbonate content.

The column experiment also provided useful information about the potential fate of contaminants in the aquifer after the source of acidic water is eliminated. The pH is likely to remain low for a long time because of disassociation of the $FeOH\text{-}H^+$ complex. Aluminum also may pose a long-term threat to water quality because of slow dissolution of $AlOHSO_4$. While pH remains below 4.6, precipitation of $Al(OH)_3$ is unlikely and may result in increased Al concentrations. Dissolution of gypsum will result in larger concentrations of Ca and SO_4; however, most of the gypsum should be removed within a few pore volumes. Any Fe, Mn, Cu, Co, Ni, or Zn associated with alluvium in the acidic part of the plume generally should remain immobile, and the concentration of these constituents should rapidly return to background levels.

The reactions used in this model represent one plausible set of reactions that were able to successfully simulate breakthrough curves from the column experiment as well as the change in the composition of ground water in the aquifer. Other possible combinations of reactions may work as well. Some of the reactions could be demonstrated from analysis of the field data; whereas, other reactions only became evident through analyzing data from controlled laboratory experiments. The successful simulation of the field data emphasizes the benefit of using laboratory experiments in conjunction with field data whenever possible.

Chapter C

Assessment of Colloidal Transport in Ground Water, Pinal Creek Basin, Arizona

By Robert W. Puls[1], Robert M. Powell[2], *and* Donald A. Clark[1,3]

Abstract

Laboratory columns packed with natural aquifer material from Pinal Creek Basin, Arizona, were used to investigate the transport of inorganic colloids under saturated-flow conditions. Radiolabeled spherical colloids of various diameters of iron oxide were synthesized and introduced into the columns under varying conditions of pH, ionic strength, electrolyte composition, and colloid concentration. Column influent and effluent were evaluated by photon-correlation spectroscopy and scintillation-counting techniques. The maximum breakthrough concentration of colloids in the column effluent was 99 percent of the influent concentration under certain hydrochemical conditions. In all cases where transport was greater than 50 percent, the colloids arrived at approximately the same time or earlier than the conservative tracer, tritium. Conditions favoring colloidal transport in this system were: (1) low ionic strength, (2) pH in the range where the colloids are stable, and (3) the presence of specifically-sorbed ions that enhance colloid stability. Arsenate was used as a model-reactive contaminant to evaluate its facilitated transport on the iron oxide colloids. Sorption capacity of the colloids for arsenate determined from batch tests was 1 percent by weight. Compared with transport of dissolved arsenate in the same columns, the colloids were transported more than 21 times faster.

INTRODUCTION

Colloids are suspended stable particles that are small enough so that the surface free energy of the particle dominates the bulk free energy. In ground water, this typically includes particles with diameters between 0.01 and 2 μm. Colloidal particles can be organic, inorganic, or a combination of the two. Several mechanisms can account for colloids in ground water.

1. Dissolution of cementing agents due to changes in pH or redox conditions.
2. Mineral supersaturation resulting in the formation by nucleation and precipitation of inorganic colloids.
3. Physical disruption of the subsurface system caused by alterations in flow conditions from contaminant injection or ground-water withdrawal.
4. Release of particles due to weathering.
5. Release and transport of viruses and bacteria (as contaminants or as carriers of contaminants).

The arrival of a contaminant plume can result in the formation of colloidal particles through processes 1–3 listed above. A subsequent reduction in ionic strength due to, for example, infiltration of lower ionic strength water or recharge of water with lower ionic

[1]U.S. Environmental Protection Agency, R.S. Kerr Environmental Research Laboratory, Ada, Oklahoma.

[2]ManTech Environmental, R.S. Kerr Environmental Research Laboratory, Ada, Oklahoma.

[3]Scientists in the U.S. Environmental Protection Agency, Office of Research and Development have prepared this chapter. Review was done in accordance with the U.S. Environmental Protection Agency administrative review policy, and the report has been approved for publication.

strength can mobilize colloids, enhance their stability, and therefore increase their transportability.

Gschwend and Reynolds (1987), Robertson and others (1984), Kim and others (1984), and Ryan and Gschwend (1990) studied the mobility of colloidal particles in ground water at a number of sites. Other studies have demonstrated the facilitated transport of contaminants associated with reactive-mobile colloidal particles in both laboratory and field studies (Saltelli and others, 1984; Penrose and others, 1990; Enfield and Bengtsson, 1988; Buddemeier and Hunt, 1988). Because of diffusional and sedimentation constraints, colloidal particles ranging in size from 0.1 to 1.0 μm may be most mobile in porous media. Although Cerda (1987) and Champlin and Eichholz (1976) demonstrated that changes in the chemistry of aqueous systems may play a major role in mobilization of colloids in porous media, little additional research has been done in colloidal-transport. Solution chemistry can affect colloid stability, mobility, and reactivity because of its effect on surface-charge phenomena. Inorganic particles generally carry a charge that is either net negative or net positive depending on a number of factors. These factors include: (1) mineralogy, (2) pH, (3) ionic strength, and (4) the presence or absence of strongly adsorbing potential-determining ions. Mineral species can have a fixed surface charge (montmorillonite), a variable surface charge (iron oxides), or a combination of the two (kaolinite). In general, the immobile aquifer material will have a net negative charge because of the large amounts of silica and aluminosilicate minerals in the matrix that have a pH of low zero point charge (table 11). Solution chemistry also can affect the particle-to-particle interactions for example, attraction, which results in agglomeration and settling, or repulsion, which can keep particles in suspension.

From March 1988 through September 1990, a study was conducted to assess the significance of colloidal transport in a shallow, heterogeneous sand-and-gravel aquifer in the Pinal Creek Basin. Field investigations initially focused on the effects of ground-water sampling techniques on colloid mobilization (Puls and others, 1990). These studies indicated the importance of pumping at low flow rates to obtain accurate and representative water-quality data. Evidence was not sufficient to suggest colloid-facilitated transport of inorganic contaminants at the site probably because of the high ionic strength (0.4 mol/L) of the ground waters resulting from the acidic metal wastes. Such transport may occur in waters with lower ionic strength (<0.1 mol/L) downgradient and near the leading edge of the acidic plume at the site where pH and redox changes are significant.

Laboratory-column experiments were made to determine chemical effects on inorganic-colloidal transport through contaminated aquifer material collected from the site. Variables that were evaluated included pH, electrolyte composition, and ionic strength. Redox changes were not evaluated because of the difficulty of controlling this variable in a laboratory setting. Radio-labeled iron oxide (Fe_2O_3) was used as the model mobile reactive colloid. Arsenate was investigated as a potentially reactive and transportable contaminant.

Acknowledgments

Cynthia J. Paul of ManTech Environmental Technology, Inc., provided laboratory support

Table 11. Selected pH_{iep} data for some primary and secondary minerals

[pH_{iep}, pH where the electrokinetic potential of the particles is zero; <, less than]

Constituents	pH_{iep}	Constituents	pH_{iep}	Constituents	pH_{iep}
Quartz	1.8	Manganese dioxide	2.8	Fe_3O_4	6.5
Albite	2	Calcite	9.5	α-$Al(OH)_3$	5
Augite	2.7	α-FeOOH	4–7	γ-$Al(OH)_3$	9.3
Muscovite	4	γ-FeOOH	7.4	γ-AlOOH	<4
Biotite	1.2	α-Fe_2O_3	5–8.6	Al_2O_3 amorphous	8
Glauconite	2	$Fe(OH)_3$ amorphous	8.5		

particularly during the early stages of this study. Terry F. Rees, USGS, provided X-ray diffraction and scanning electron-microscopy analyses.

MATERIALS AND METHODS

Characterization of Colloids and Aquifer Solids

Spherical, monodisperse Fe_2O_3 colloids (0.1–0.25 μm) were prepared from solutions of ferric chloride ($FeCl_3$) and hydrochloric acid (HCl) using the method of Matijevic and Scheiner (1978). The method was modified by the addition of a spike of $_{26}Fe^{59}Cl_3$, before heating, which permitted detection of the colloids by liquid scintillation-counting techniques. The colloids were washed three times with pH 3 deionized water to remove unreacted materials from the suspensions. Colloid concentration, in milligrams per liter, was determined by filtration and residue-on-evaporation techniques. Scanning electron microscopy (SEM) and photon-correlation spectroscopy (PCS) were used to determine the particle size. PCS also was used to evaluate stability of the diluted colloidal suspensions by monitoring particle size in influent and effluent column suspensions.

The pH of zero point of charge (pH_{zpc}) is the pH at which the net surface charge of the colloid equals zero. Below this value, the surface has a net positive charge, and above the pH_{zpc}, the surface has a a net negative charge. The pH_{zpc} was determined by titrating colloid suspensions under nitrogen at different ionic strengths of sodium perchlorate ($NaClO_4$), a nonspecifically adsorbed electrolyte, with sodium hydroxide (NaOH). The pH at which electrolyte concentration has no influence on surface charge should equal the pH_{zpc}. For the Fe_2O_3 colloids, pH was estimated to range from 7.3 to 7.6. The isoelectric point (pH_{iep}) of the surface or the pH where the electrokinetic potential of the particles is zero, was determined to be 7.0 using microelectrophoresis (Puls and Powell, 1992). These two measurements should be about equal in the absence of nonspecifically sorbed species or where hydrogen (H^+) and hydroxyl (OH^-) ions are the only potential determining ions in solution.

Core material from well 107 was air-dried and sieved, and subsamples were analyzed by X-ray diffraction. Predominant mineral phases in subsamples of the material were identified by X-ray diffraction. The order of intensity of these phases were: quartz > albite >> magnesium orthoferrosilate > muscovite > samsonite > manganese oxide. Relevant aqueous geochemical constituents for well 107 are in table 12. Particle microelectrophoresis (Rank Brothers Mark II, Malvern ZetaSizer) was used to characterize the surface-charge properties of the synthesized Fe_2O_3 colloids and the fine fraction (< 2 μm) of the aquifer-matrix solids used in the column experiments.

Batch and Column Tests

Adsorption of arsenic on Fe_2O_3 colloids and aquifer solids was assessed to determine differential reactivity of the two components and in particular, the adsorption capacity of the colloids. Desorption was important, particularly from the colloids, to determine strength of adsorption or retention (reversibility). Preliminary experiments were performed to determine steady-state equilibration time and appropriate solid to

Table 12. Concentrations of major constituents and water-quality components for well 107, March 1989

[mg/L, milligrams per liter; μS/cm, microsiemens per centimeter at 25° Celsius; °C, degrees Celsius; mV, millivolts; mol/L, moles per liter; <, less than]

Cations and anions	Concentration in milligrams per liter	Water-quality components	Value
Calcium	440	pH (standard units)	3.72
Magnesium	140	Specific conductance (μS/cm)	4,310
Sodium	140	Temperature (°C)	18.5
Potassium	7.2	Dissolved oxygen (mg/L)	<.1
Sulfate	3,300	Oxidation-reduction potential (mV)	440
Chloride	33	Ionic strength (mol/L)	.13

solution ratio that would produce measurable changes in solution compositions and allow for adequate characterization of the adsorptive capacity of solids and colloids. A 24-hour equilibration period and solids-to-solution ratios of 6 grams to 30 mL for the aquifer solids and 4.5 mg to 30 mL for the Fe_2O_3 particles were used. Initial arsenate concentrations ranged from 3×10^{-6} to 7×10^{-5} molar (M) in 0.01 M $NaClO_4$. The pH range that was examined was 4 to 8, and a temperature of about 25°C was used in all experiments. Samples were shaken on a rotary shaker throughout the equilibration to insure mixing. After equilibration, samples were centrifuged at 2,560 × g for 70 minutes and filtered through a 0.2 μm Nuclepore membrane filter to prevent the inclusion of solid flocs and microparticles in the determination of aqueous concentrations of arsenate. Aqueous samples were analyzed for arsenic (As) using a Perkin-Elmer Zeeman/3030 Atomic Absorption Spectrophotometer with graphite furnace (AAGF). Adsorption was determined by the difference between initial and final arsenate concentrations. Desorption of arsenate from the Fe_2O_3 particles and the aquifer solids was accomplished by repeated replacement of arsenic with arsenate-free 0.01 M $NaClO_4$ on the centrate. The pH of the desorption solution generally was kept constant at the same pH as the adsorption solutions to evaluate only the impact of changes in arsenate concentration, however, in some cases, the pH of the desorption solution was increased to a pH value of 9 to evaluate enhanced desorption under these conditions and to compare these results with desorption using phosphate. The desorption equilibration time was 24 hours, and was based on preliminary experiments to evaluate contributions from mineral-dissolution effects.

Adjustable-length glass columns (2.5-cm diameter) were used for all column experiments. Column lengths ranged from 2.5 to 5.0 cm. Core material from well 107 (106–2,000 μm sieved fraction) was used to pack the columns. Column flow rates were comparable to estimated ground-water velocities in the alluvium. Columns were slowly (0.08 m/d) saturated from below with 0.01 M $NaClO_4$, and flushed for at least 1 week before initiation of experimental runs. Darcy velocities used in the experiments were 0.8, 1.7, and 3.4 m/d. Tritium was used as a conservative tracer to analyze column operation and to compare transport of injected colloids and dissolved arsenate. Solutions were injected until effluent concentration equaled influent concentration (C_0). PCS was used to verify the size and stability of column-influent colloidal suspensions. Comparisons of the size and stability of the colloidal material between selected influent and effluent samples also were made. The effluent fractions were collected in polypropylene test tubes over various time intervals depending on the flow rate and experiment (longer collection times for the dissolved-arsenate experiments). For the radio-labeled colloid experiments, 0.5 mL from each fraction was mixed with a Beckman CP cocktail in 7-mL polyethylene vials and placed in a (Beckman model) scintillation spectrophotometer for 20 minutes. Aqueous samples for the dissolved arsenate experiments were analyzed using an AAGF.

ASSESSMENT OF COLLOIDAL TRANSPORT

The movement of colloids and associated contaminants at Pinal Creek was assessed through the use of batch and column experiments and through sampling for colloids in acidic and neutralized contaminated ground water at the site. The role of particle size, contaminant concentrations, surface charge, and other physicochemical factors in colloid-facilitated contaminant transport were examined.

Adsorption and Desorption

Batch-test results were used to define the adsorption and desorption isotherm of a contaminant on iron oxide colloids. Data for arsenate sorption on the synthesized Fe_2O_3 colloids were fitted to a Langmuir isotherm defined by the relation:

$$S = \frac{\left(k\left(C_f\right)b\right)}{\left(1+k\left(C_f\right)\right)},$$

where

k = Langmuir solid-surface affinity term,
b = adsorption capacity,
S = concentration on the solid phase, and
C_f = steady-state solution concentration.

One advantage of the Langmuir model is the incorporation of the capacity term. The correlation coefficient for the linearized Langmuir form of the

above equation was 0.97, and the *b* value was 0.01 g/g, or 1 percent of the colloid mass is sorbed arsenate. Data for arsenate adsorption on the aquifer solids were fitted to a Freundlich isotherm. The correlation coefficient for these data was 0.94. The Freundlich isotherm is defined by the relation:

$$S = KC_f^n$$

where terms are the same as above except that *n* is an empirical coefficient related to the monolayer capacity and energy of adsorption. The latter isotherm is more typically applied to heterogeneous solid-phase systems. Little desorption of the As occurred from either the aquifer solids or the Fe_2O_3 particles (fig. 24*A*, *B*). Three successive desorptions of the synthesized Fe_2O_3 colloids with 0.005 M NaH_2PO_4 at pH 7 resulted in only about 3-percent desorption, and three successive desorptions with 0.01 M $NaClO_4$ at pH 9 resulted in 11-percent desorption. The strength of binding with the Fe_2O_3 surface is such that little desorption is expected during transport unless the geochemistry of the system changes such as an increase in pH or the presence of competing anions.

Stability and Surface Charge

Colloid stability, in terms of coagulation, was monitored using laser-light scattering with PCS. The colloid suspensions were stable in solutions containing 0.01 M NaCl, $CaCl_2$, and $NaClO_4$ and had a pH range from 3.0 to 6.5. Under these conditions, the colloids are net positively charged. At a pH range from 6.5 to 7.6, which is near the estimated pH_{zpc}, the colloids were extremely unstable. At a pH range from 7.6 to 9.7, the colloids were semistable in solutions containing 0.005 M NaCl and $NaClO_4$, which means that the kinetics of coagulation were slow (several hours). At a pH range from 9.7 to 11.0, the colloids were stable in solutions containing 0.01 M $NaClO_4$ and NaCl. Colloidal-size distributions in the influent and effluent were compared when the pH of the soil-column effluent was near the pH_{zpc}, or in the pH range of 6.5 to 7.6 where the colloids are unstable.

Liang and Morgan (1990) observed that hematite colloids bear an overall net negative charge at pH<< $pH_{zpc,\ pristine}$ in the presence of specifically sorbed anions, such as the phosphate species, which increases the stability region where the colloids are negatively charged ($pH_{zpc,\ pristine}$= ionic strength ≈0). Similarly, significant enhancement of colloid stability in solutions containing 0.01 M Na_2HAsO_4 and 0.01 M NaH_2PO_4 was observed in the present study at a pH as low as 6.9. This enhancement was not observed in solutions containing sulfate. When the pH is less than the pH_{zpc}, the particles were unstable and coagulated in calcium sulfate ($CaSO_4$) as low as 1 mmol. When pH is greater than the pH_{zpc}, semistable suspensions occurred. These findings have important implications for this study because near the source of contamination the ground water is nearly supersaturated with gypsum. Concentrations of sulfate (SO_4) range from 0.005 M to 0.1 M near the original tailings pond and about 0.03 M at well 107. These results correspond with previous investigations that demonstrated that SO_4 can broaden the pH range of particle instability (Packham, 1965; Snodgrass and others, 1984).

Electrophoretic-mobility data for the colloids and fine fraction (<2 μm) of the aquifer material (fig. 25) was documented. The pH_{iep} for the colloids in a solution containing 0.01 M $NaClO_4$ is about 6.9, comparable to the pH_{zpc} determined from titration (7.3–7.6). The pH_{iep} of the aquifer solids is less than 4. When the surfaces of the colloid and the aquifer material are similarly charged, some repulsion will occur. The magnitude of these repulsions mainly depends on the differences of the pH_{iep} of the two surfaces. Repulsion of these surfaces would not occur in the more contaminated portions of the aquifer, except where specifically sorbed species are present such as phosphate and arsenate. Because these Fe_2O_3 colloids are extremely unstable in solutions that contain large amounts of SO_4 and that have a pH of less than 7, transport would be unlikely at the site. This assumption would hold true for other colloids having a similar pH_{iep}.

Column Transport

When the colloids had a net positive surface charge opposite to the surface charge of the column matrix material, the colloids were unstable and were not transported through the columns (table 13). This positive surface charge occurred when the major anion in solution was chloride (Cl), which is a non-specifically sorbing species, and pH was less than 7. Attraction between the positively charged colloids and the predominantly negatively charged matrix surfaces accounts for this result. When these columns were

dismantled, most of the colloids were located at the column inlet. When the colloids were net negatively charged ($pH > pH_{zpc}$), transport of greater than 50 percent of the injected colloids was observed in solutions containing 0.005 M NaCl and ~0.001 M $NaClO_4$. More than 50 percent of the injected colloids were detected in the effluent. Solutions containing SO_4 transported less than 20 percent of the injected colloids through the columns, presumably because of colloidal instability. In the solutions containing phosphate and arsenate, greater than 90 percent of the injected colloids were transported through the column. In all

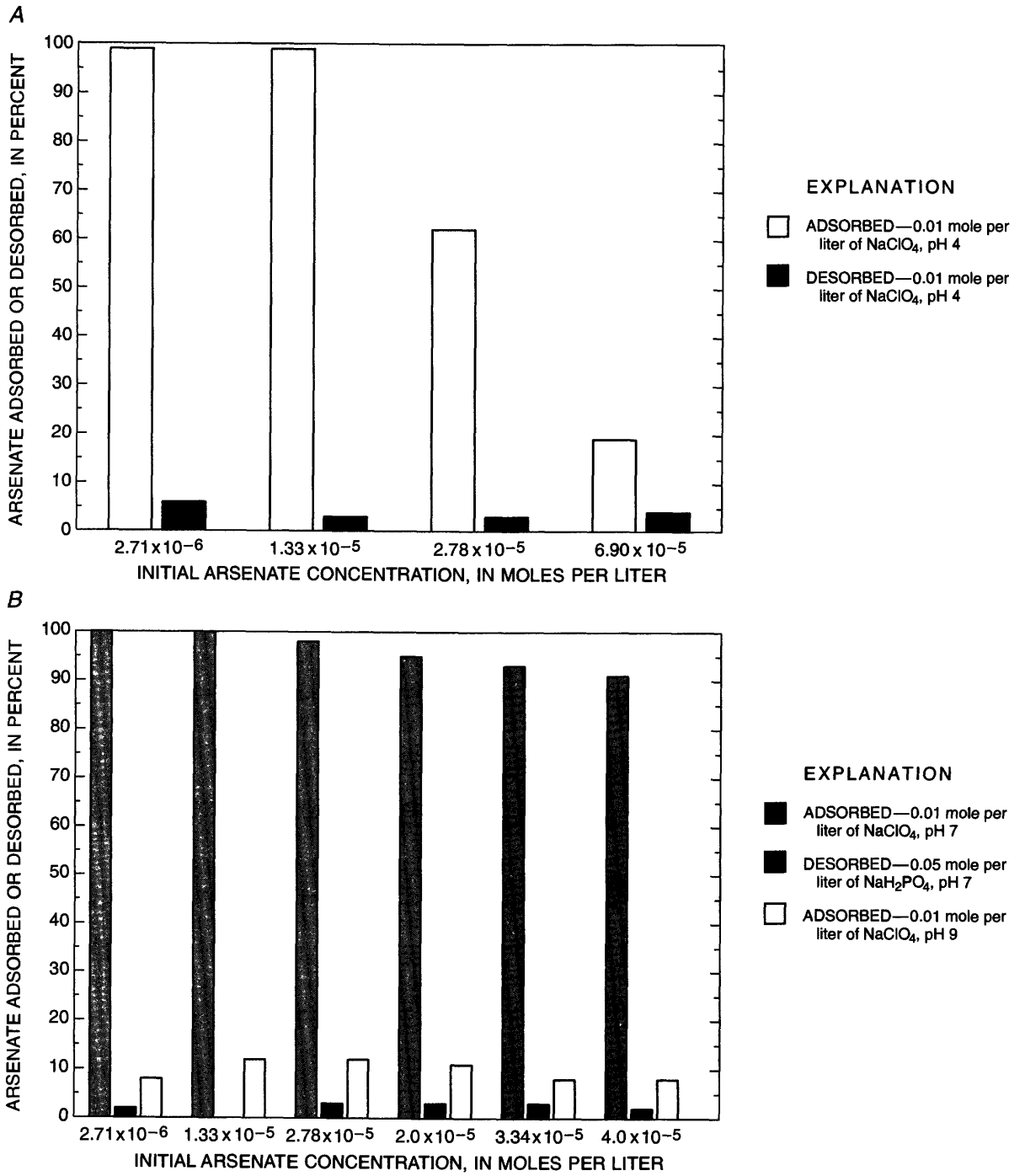

Figure 24. Adsorption and desorption of arsenate. *A*, Arsenate, in percent, from aquifer solids from well 107 (pH 4, 0.01 mole per liter of $NaClO_4$); *B*, Arsenate from synthesized iron oxide particles.

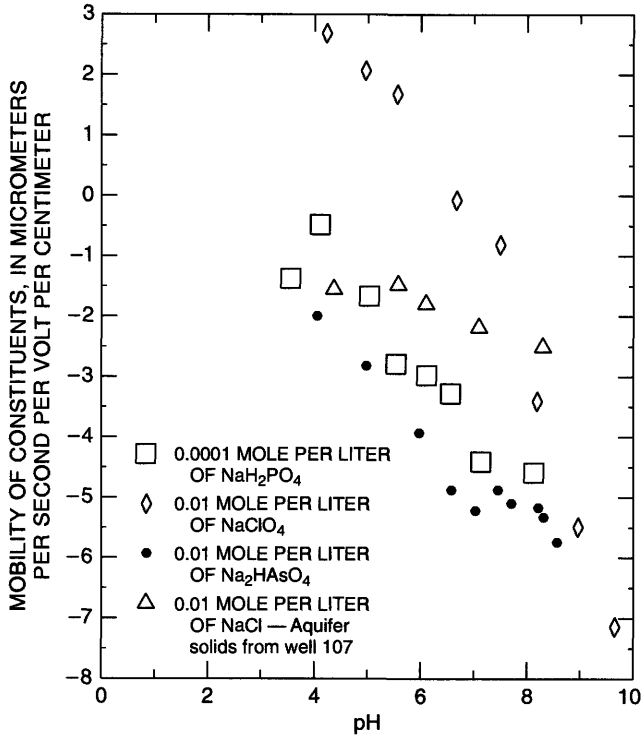

Figure 25. Electrophoretic mobility for aquifer solids and iron oxide particles from well 107.

cases, breakthrough occurred about the same time or earlier than the tritiated water (fig. 26*A–C*).

A column also was injected with dissolved arsenate to compare its retardation to the retardation of the colloids. Breakthrough curves of these solutions is shown in figure 27. The calculated retardation factor (*Rf*) for the dissolved arsenate is defined as:

$$Rf = V_w/V_s,$$

where

V_w = velocity of the water or conservative tracer (tritium), and

V_s = velocity of the solute.

Rf was calculated to be 21; therefore, the colloidal arsenate exhibited 21 times the velocity of the dissolved arsenate.

Movement of Colloids in Ground Water

For many of the wells, ground-water sampling was done using sequential filtration and laser-light scattering detection techniques for assessment of colloidal mobility (Puls and Barcelona, 1989; Puls and others, 1990; Puls and others, 1992). Data did not indicate significant colloidal-facilitated transport of contaminants at the site. In well 451 near the leading edge of the acidic waste plume, however, anomalously high turbidity was observed. In well 451, the sediments generally are fine grained, and dissolution of iron oxide cementing agents may be responsible for the high concentration of suspended particles (~20 mg/L). SEM analyses identified the particles, captured on filters, as smectite clays and Fe_2O_3. The persistence of clays and iron oxide as stable suspensions would depend on pH, ionic strength, oxidation-reduction potential and ground-water flow velocity. On the basis of the

Table 13. Colloidal transport through contaminated aquifer material

[$\%C_0$, percent initial concentration colloids; <, less than]

Size, in nano-meters	Particle concentration, in milligrams per liter	Flow rate, in meters per day	pH	Ionic strength	Anion	Maximum concentration ($\%C_0$)
200	10	3.4	3.9	0.005	Cl^-	0
125	10	1.7	8.9	.005	Cl^-	54
150	5	1.7	8.1	<.001	ClO_4^-	57
250	10	1.7	8.1	.03	SO_4^{2-}	17
150	5	1.7	8.9	.03	SO_4^{2-}	14
100	5	.8	7.6	.03	$HAsO_4^{2-}$	93
100	5	1.7	7.6	.03	HPO_4^{2-}	99

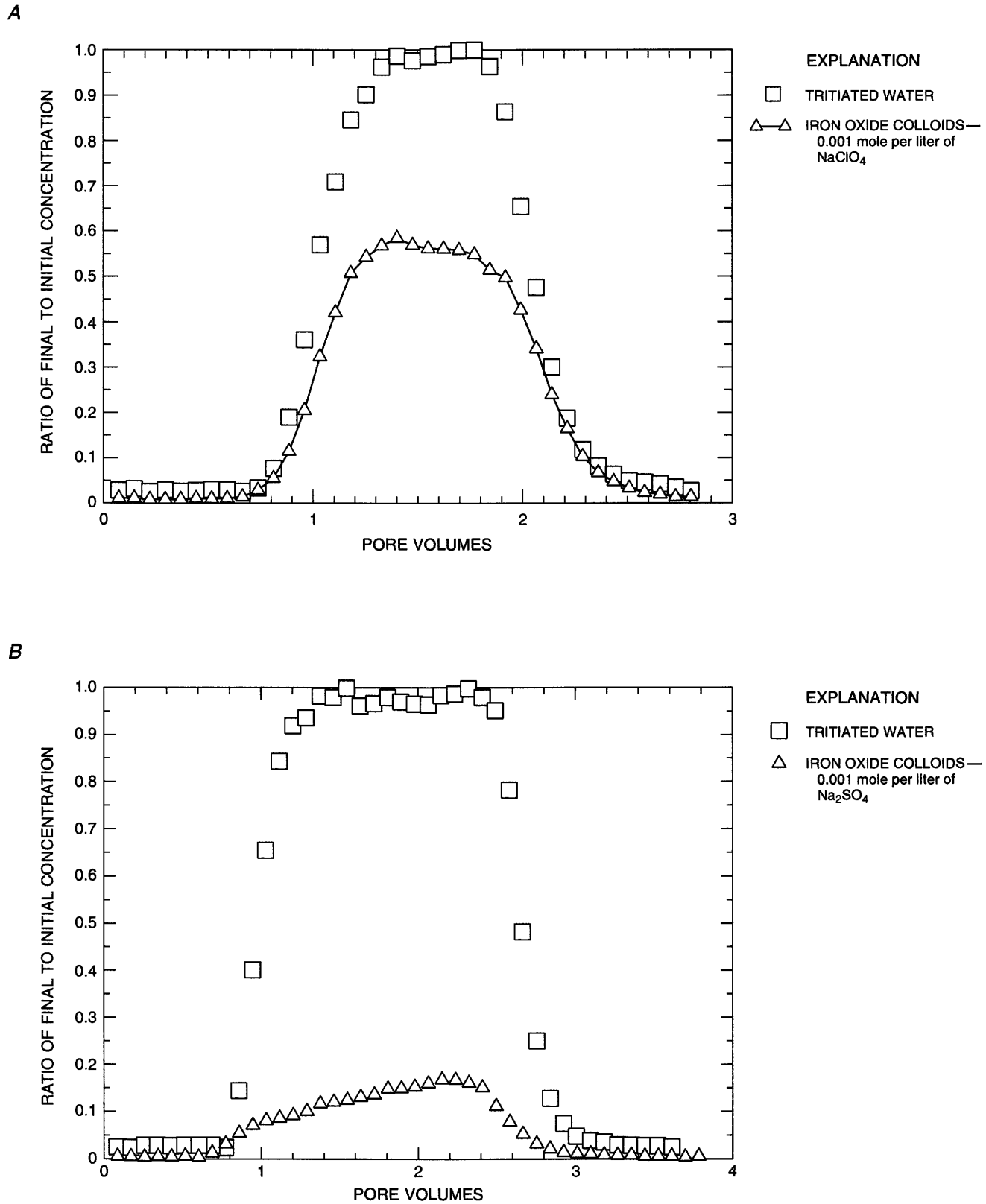

Figure 26. Column breakthrough for iron oxide particles. *A*, 0.001 mole per liter of sodium perchloride ($NaClO_4$); *B*, 0.001 mole per liter of sodium sulfate (Na_2SO_4); *C*, 0.01 mole per liter of sodium dihydrogen phosphate ($Na_2H_2PO_4$).

C

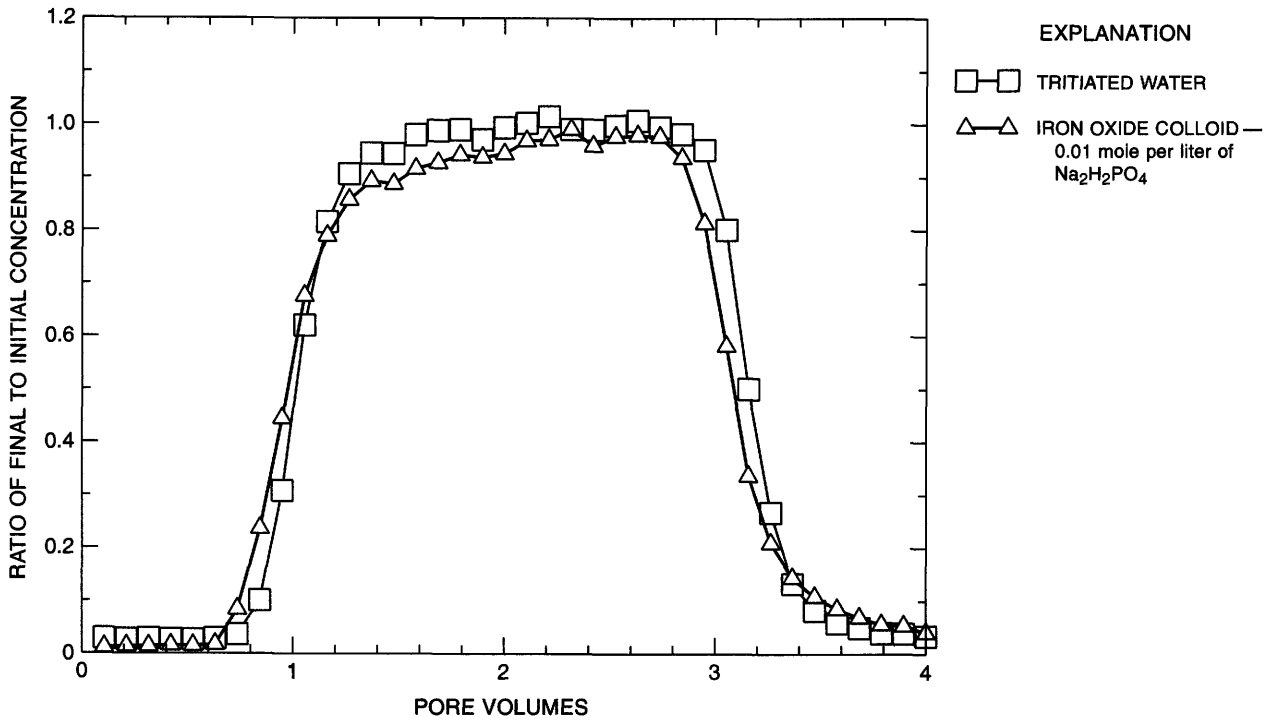

Figure 26. Continued

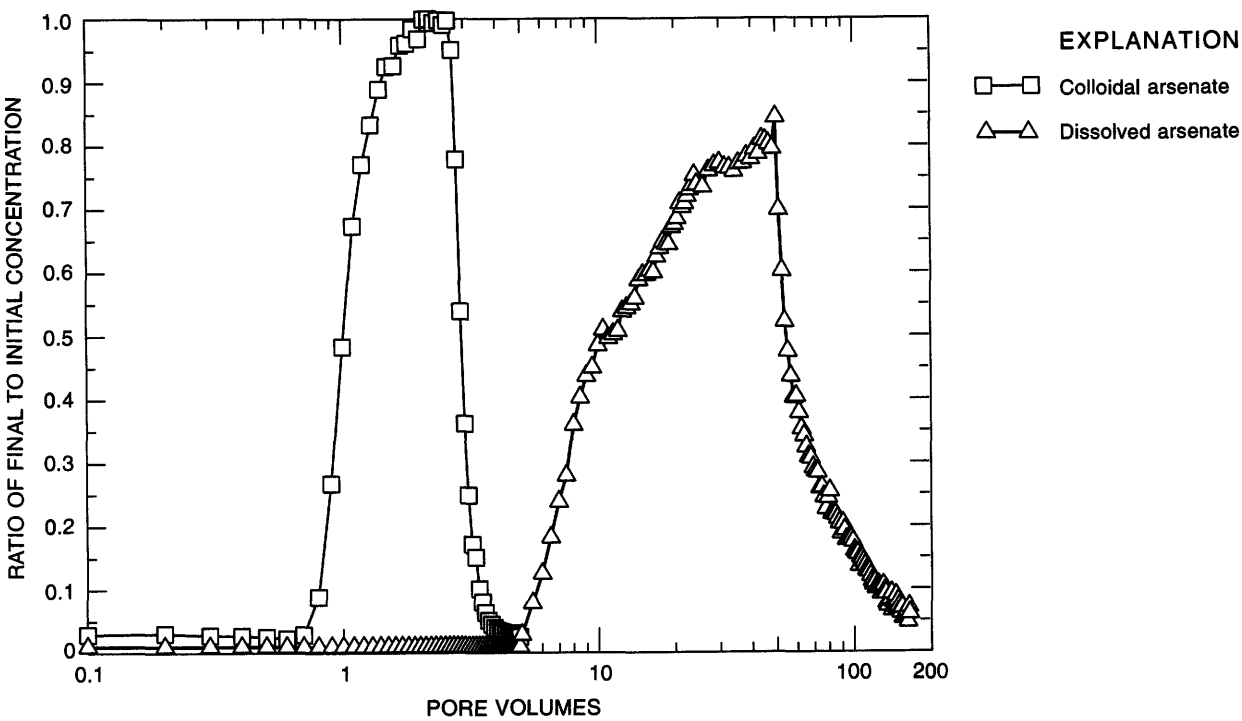

Figure 27. Column breakthrough for dissolved and colloidal arsenate transport through aquifer solids from well 107.

existing hydrochemical profile of the plume, it is expected that this condition would be transitional.

SUMMARY AND CONCLUSIONS

In this study, Fe_2O_3 colloids were capable of sorbing a significant mass of contaminant (arsenate) and were transported more than 21 times faster than dissolved arsenate under the following hydrochemical conditions: (1) low ionic-strength waters, (2) high-flow velocity, and (3) a negative net surface charge of the colloids and aquifer matrix. Solutions containing SO_4 provided the least stable colloidal suspensions and the lowest amount of colloidal transport. This condition is significant for the Pinal Creek Basin because SO_4 is the predominant anion in the ground water. This condition, together with the high ionic strength of most waters at the site, indicates that colloidal transport does not significantly facilitate transport of contaminants at the site. Monitoring of the aquifer as fresh (uncontaminated) water recharges the system may be needed to evaluate the effect that decreased ionic strength would have on colloid mobilization and stability.

Chapter D

Distribution of Chemical Constituents in Surface Water, Pinal Creek Basin, Arizona

By James G. Brown *and* James H. Eychaner

Abstract

Surface-water flow in most of Pinal Creek Basin is ephemeral and consists of storm runoff, snowmelt, and occasional, accidental spills or releases from impoundments from copper mining. Ephemeral flow in the basin can be uncontaminated runoff or can include contaminated runoff from tailings and other mine areas. From about 1941 until Webster Lake was drained in 1988, a mixture of natural runoff, acidic water from mining processes, and wastewater contained in the lake infiltrated into tributary alluvium and entered the regional aquifer.

The pH of ephemeral streamflow in Miami Wash at Highway 88 varied from 5.1 at a discharge of 0.00085 cubic meters per second to 7.7 at a discharge of 0.368 cubic meters per second. Concentrations of dissolved copper and zinc generally varied inversely with discharge.

Prior to January 1985, streamflow recharge to ground water caused ground-water levels to rise and resulted in the surface discharge of acidic ground water to the seepage ditch at Bixby Road. In March 1985, ephemeral flow in Pinal Creek included acidic ground-water discharge from the seepage ditch, surface runoff from undeveloped and mined areas, and neutralized ground-water discharge in the perennial reach. Sulfate concentration of this water was 1,400 milligrams per liter at Inspiration Dam. Concentrations of dissolved copper were 40 micrograms per liter and concentrations of dissolved iron were less than 40 micrograms per liter.

From 1985 through 1991, discharge of neutralized, contaminated ground water to Pinal Creek produced perennial flow from about 6 km above Inspiration Dam to the mouth. As ground water discharged to the stream and equilibrated with the atmosphere, pH increased between one and two units. In March 1990, pH increased downstream from 6.0 to 7.5. In response to this increase, concentrations of dissolved manganese decreased from about 90 to 15 milligrams per liter and precipitated as crust on the streambed.

Concentrations of dissolved solids at Inspiration Dam were 800 milligrams per liter in 1942 and 2,800 milligrams per liter in 1979 and gradually increased to more than 3,500 milligrams per liter by late 1988. Dissolved concentrations of most trace metals were near or below detection limits in most samples collected between 1979 and 1991. Manganese concentrations increased steadily from 0.26 to 40 milligrams per liter from 1979 through 1988 and were more variable from 1989 through 1991. Accumulations of manganese in the streambed were first observed in 1985. Streambed sediments are only a temporary sink for manganese, however, because flood discharges break up and transport the cemented sediments.

Using only analytical concentrations of ground water, a simple conservative mixing model of base-flow chemistry in the perennial reach above Inspiration Dam adequately represented sodium, chloride, and silica concentrations in surface water

but diverged from measured concentrations of dissolved gases and manganese.

Reaction paths were computed with PHREEQE to develop the simplest possible model that adequately represented measured changes in the streamflow. The model began with the same proportions of ground water as in the conservative-mixing model and simulated three additional processes: (1) degassing of carbon dioxide in amounts that decreased linearly downstream, (2) manganese oxidation and precipitation, and (3) dissolution of calcite. The amount of each reaction was calibrated to match measured pH, manganese concentration, and dissolved inorganic carbon in surface water. The model adequately represented measured streamflow chemistry by using reasonable amounts of likely reactions. The model reproduced the calcite saturation index of streamflow samples, which indicates that the specified dissolution was reasonable. Model saturation index for all manganese oxides exceeded 3 and increased as simulated flow moved downstream.

INTRODUCTION

Surface-water flow in most of Pinal Creek Basin is ephemeral, and consists of storm runoff, snowmelt, and occasional, accidental spills or releases from impoundments related to copper mining. These sources, along with sewage releases into Pinal Creek a few kilometers north of Globe (fig. 1), provide recharge to the aquifer. Ephemeral flow in the basin can be uncontaminated runoff from undeveloped areas, or can include contaminated runoff from tailings and other mining areas. North of the mouth of Horeshoe Bend Wash, the aquifer is constricted, and ground-water discharge to Pinal Creek generates perennial flow to the Salt River.

In the perennial reach, base flow consists entirely of ground-water discharge. Most of this discharge is neutralized contaminated water from a 15-km-long plume of acidic ground water in the alluvium of Miami Wash and lower Pinal Creek. Following periods of prolonged or extended rainfall, storm runoff enters the perennial reach from tributaries and from Pinal Creek upstream from the head of perennial flow. During these times, water in the stream is a mix of contaminated ground water and storm runoff, which may or may not be contaminated depending on the part of the basin from which the runoff originated. Following the cessation of direct runoff, water stored in the bank during the period of high flow returns to the creek.

The purpose of this chapter is to (1) characterize areal and temporal trends in surface-water chemistry, (2) describe surface-water chemistry during a period of recharge from snowmelt, and (3) summarize the results of a study of chemical reactions in the base flow in the perennial reach.

WEBSTER LAKE

From about 1941 until it was drained in 1988, Webster Lake (fig. 1) was used to store natural runoff, process water and wastewater generated from mining activities. During that time, lake water infiltrated the alluvium of Webster Gulch and entered the regional aquifer beneath Bloody Tanks Wash. Chemical analyses of lake water prior to 1976 are few but it is assumed, on the basis of the nature of past and present mining methods and practices, that the lake was acidic most of the time and generally contained large concentrations of dissolved metals. From 1976 to 1988, dissolved-solids concentrations ranged from 27,000 to 42,000 mg/L. In 1986, dissolved-solids concentrations varied from 30,000 mg/L at the surface to 39,000 mg/L at a depth of 21 m. From 1981 through 1988, pH from the surface to the lake bottom (21 m below the lake surface) varied from 2.4 to 2.8 (Arthur, 1987a, b; Brown, 1990). In the same period of time, concentrations of sulfate (SO_4) generally were at least 20,000 mg/L but were 13,000 on an unknown date in 1980 (U.S. Environmental Protection Agency, 1978–89). This decrease probably reflects dilution of lake water by intense and prolonged rainfall that occurred in February 1980. On February 1, 1988, the concentrations of dissolved iron (Fe) and SO_4 in lake water were 6,000 and 19,000 mg/L, respectively (table 14). Analyses done by other agencies indicate that during 1976–88 the lake contained large concentrations of SO_4, Fe, and other metals. The precise concentrations of individual species or complexes, however, are questionable because the sum of constituents of these analyses are significantly less than the measured concentrations of total dissolved solids.

Table 14. Selected chemical analysis of water, Webster Lake, Arizona

[Water filtered through 0.45-micrometer filter before analysis. Data from Brown (1990)]

Date of sample	Temperature, in degrees Celsius	Specific conductance, in microsiemens per centimeter	pH	Calcium, in milligrams per liter (Ca)	Chloride, in milligrams per liter (Cl)	Magnesium, in milligrams per liter (Mg)	Manganese, in milligrams per liter (Mn)
2-1-88	11.0	13,800	27	510	350	730	100

Sodium, in milligrams per liter (Na)	Aluminum, in micrograms per liter (Al)	Cobalt, in micrograms per liter (Co)	Copper, in micrograms per liter (Cu)	Iron, in micrograms per liter (Fe)	Sulfate, in micrograms per liter (SO_4)	Zinc, in micrograms per liter (Zn)
240	850,000	20,000	210,000	6,000,000	19,000	32,000

EPHEMERAL STREAMFLOW

Most of the streams in the basin usually are dry and flow only in response to intense or prolonged rainfall. Nevertheless, short-lived large flows can transport large quantities of contaminants out of the basin. Occasionally during such periods of precipitation, impoundments of acidic wastewater or process water at mines in the area have overflowed and discharged contaminated water to washes and streams. Some of this water exits the basin as streamflow and ultimately reaches the Salt River. The rest recharges the regional aquifer with contaminated water, although such flows also include uncontaminated runoff as a significant component.

The chemical composition of ephemeral streamflow in Miami Wash at Highway 88 (fig. 28) varied in relation to discharges that ranged from 0.00028 to 0.363 m^3/s. Alkalinity as $CaCO_3$, pH, SO_4, and dissolved-solids concentrations increased with discharge (fig. 29). The pH was 5.1 at a discharge of 0.00085 m^3/s and 7.7 at a discharge of 0.368 m^3/s. $CaCO_3$ varied from about 10 to almost 80 mg/L over the same discharge interval but the relation between discharge and concentration was variable. Concentrations of dissolved copper (Cu) and zinc (Zn) for the most part varied inversely with discharge. At a discharge of 0.00085 m^3/s, concentrations of dissolved Cu and Zn were 3,000 and 640 µg/L, respectively (fig. 29). No samples were available with which to examine the chemical composition at flows greater than 0.368 m^3/s.

On March 1, 1985, streamflow samples were collected at 11 locations (fig. 28) to determine the distribution of chemical constituents in ephemeral streamflow (Eychaner and others, 1989). These samples were collected 8 days after the last significant precipitation during a period of snowmelt. Precipitation during the previous 3 months was above normal. Because the distribution and intensity of precipitation varies from storm to storm, these data may not represent the chemical character of runoff from other events, especially those caused by severe, often localized summer thunderstorms. When these samples were collected, streamflow in Pinal Creek upstream from the mouth of Miami Wash (site 1) and in Russell Gulch south of Highway 60 (site 4) was uncontaminated. Dissolved-solids concentrations at both sites were 186 mg/L; concentrations of dissolved metals were near or below reporting limits. Sulfate concentrations at both sites were less than 40 mg/L (table 15). In contrast, water in Bloody Tanks Wash (site 3), which flows eastward through Miami at the base of large tailings piles, contained concentrations of dissolved copper, manganese (Mn), and SO_4 greater than that found in uncontaminated runoff at sites 1 and 2. Concentration of dissolved solids in Bloody Tanks Wash was more than 400 mg/L; concentrations of SO_4 and dissolved Mn were 310 and 0.35 mg/L, respectively.

Streamflow recharge to ground water prior to January 1985 caused ground-water levels to rise to within 1 m of the land surface in monitor wells of the USGS adjacent to Miami Wash (fig. 5). In low-lying areas, the ground-water table rose to the land surface, resulting in the surface discharge of acidic ground water. On March 1, flow in the seepage ditch at Bixby Road was generated entirely by local ground-water

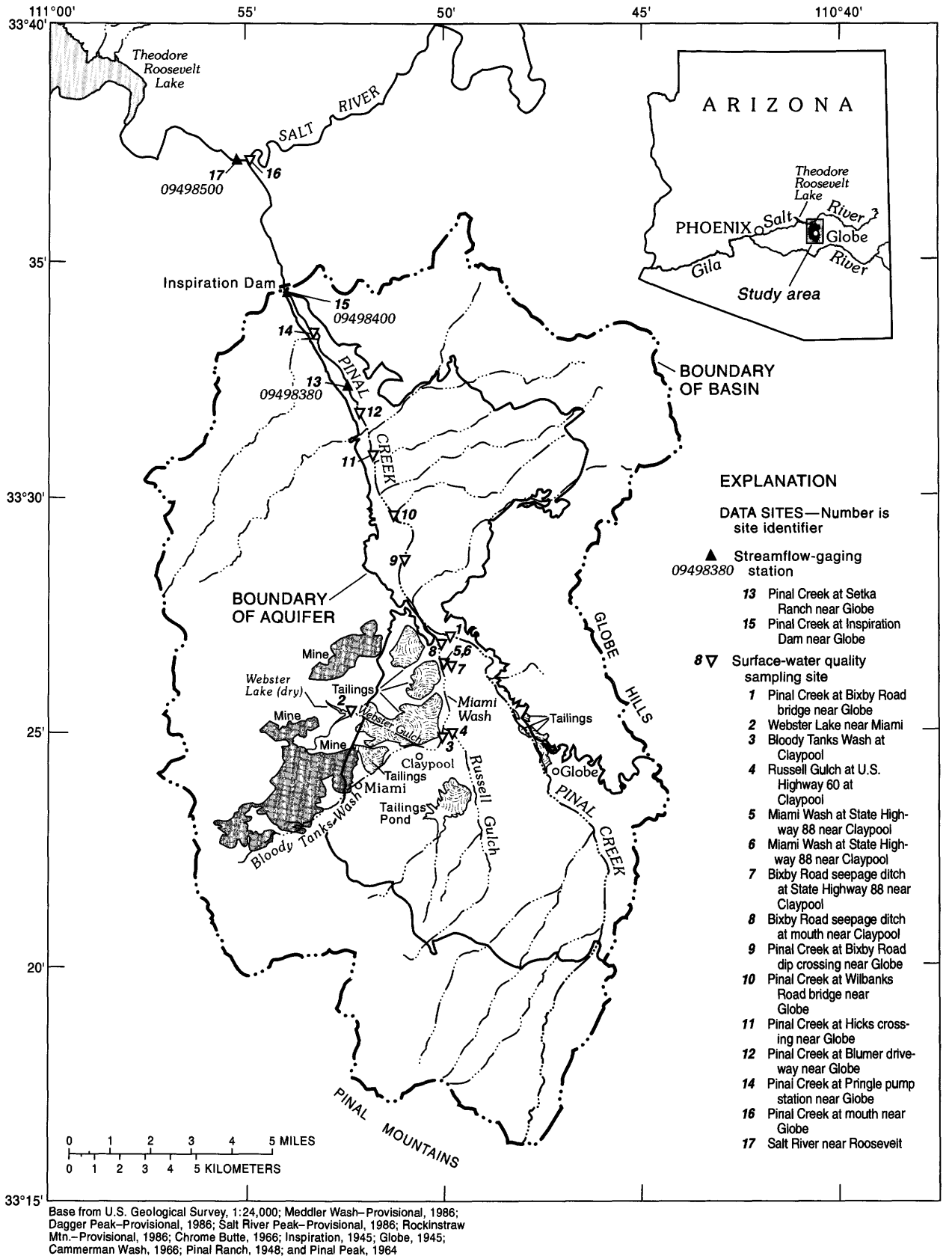

Base from U.S. Geological Survey, 1:24,000; Meddler Wash–Provisional, 1986; Dagger Peak–Provisional, 1986; Salt River Peak–Provisional, 1986; Rockinstraw Mtn.–Provisional, 1986; Chrome Butte, 1966; Inspiration, 1945; Globe, 1945; Cammerman Wash, 1966; Pinal Ranch, 1948; and Pinal Peak, 1964

Figure 28. Surface-water data-collection sites in and near Pinal Creek Basin, Arizona.

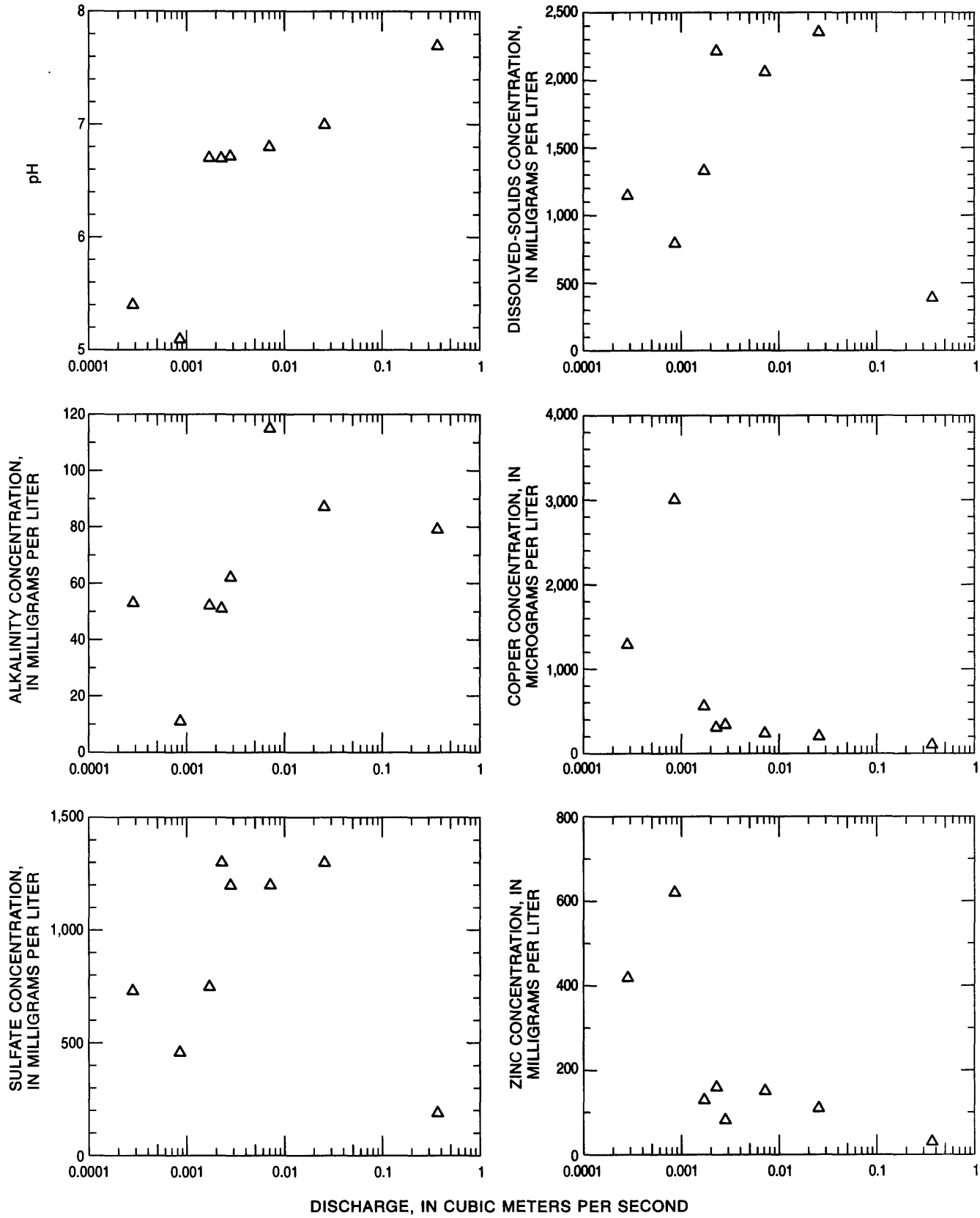

Figure 29. pH, selected dissolved chemical constituents, and discharge, Miami Wash at State Highway 88, 1984–85.

Table 15. Selected chemical analyses of streamflow, Pinal Creek Basin, Arizona, March 1, 1985

[Data from Eychaner and others (1989)]

Site number	Discharge, in cubic meters per second	pH	Alkalinity, in milligrams per liter ($CaCO_3$)	Calcium, in milligrams per liter (Ca)	Magnesium, in milligrams per liter (Mg)	Sodium, in milligrams per liter (Na)	Sulfate, in milligrams per liter (SO_4)
1	0.139	8.6	110	37	9.5	25	33
3	.224	8.2	45	45	10	20	310
4	.258	8.2	121	38	13	19	37
6	.368	7.7	79	77	17	24	240
7	.051	6.0	60	640	130	100	2,000
8	.102	5.1	4	590	140	110	2,300
9	.623	7.5	14	190	40	39	760
10	.623	6.9	63	370	72	56	950
11	.680	7.8	69	410	81	60	1,000
12	.680	7.0	77	420	84	59	1,100
15	.878	8.0	100	460	95	60	1,400

Site number	Chloride, in milligrams per liter (Cl)	Manganese, in milligrams per liter (Mn)	Copper, in micrograms per liter (Cu)	Iron, in micrograms per liter (Fe)	Nickel, in micrograms per liter (Ni)	Zinc, in micrograms per liter (Zn)
1	14	<0.03	20	60	<50	20
3	10	.35	170	20	<50	30
4	6.8	<.03	<11	50	<50	30
6	15	.63	140	<20	<50	70
7	96	26	3,300	44,000	430	1,000
8	150	35	9,700	120,000	760	1,600
9	50	7.3	80	40	100	210
10	61	14	80	20	130	260
11	63	17	40	<20	170	70
12	63	17	60	20	170	170
15	69	16	40	<20	100	80

discharge. Water in the seepage ditch (sites 7 and 8) was similar to ground water in the acid part of the plume (fig. 6) in that it contained large concentrations of metals and other contaminants. Concentrations of Mn, Fe, Cu, and Zn in the ditch (site 7) were 26 mg/L, 44,000 µg/L, 3,300 µg/L, and 1,000 µg/L, respectively (table 15). At the time of sampling, flow in the ditch near the mouth was more than 25 percent of the flow in Miami Wash.

On March 1, 1985, pH was 6.0 in the seepage ditch at Highway 88 (site 7) and 5.1 downstream at the mouth (site 8). Because ground water directly below the ditch was not sampled, the cause of the decrease cannot be determined. Because concentrations of SO_4, Fe, and other metals, however, are higher at the mouth, it is likely that the measured trends in pH and other constituents indicate that ground water that discharges to the ditch downstream from Highway 88 contained greater concentrations of metals and acidity than ground water that discharged upstream from Highway 88.

Streamflow in Pinal Creek below the mouth of Miami Wash was a mixture of water from Russell Gulch, Bloody Tanks Wash, Pinal Creek above Miami Wash, and the seepage ditch at Bixby Road. Discharge measurements of surface water at sample sites indicate that from the mouth of Miami Wash to Inspiration Dam (site 15), surface-water discharge was either steady or increased downstream. Because the most recent precipitation had occurred about 8 days before sampling, and because ground-water levels were about 1 m below the land surface in wells adjacent to the creek, the

measured surface-water gains were caused by ground-water discharge to the stream.

Concentrations of SO_4 increased downstream from 760 mg/L at sample site 9 to 1,400 mg/L at Inspiration Dam (site 15). Other major constituents increased slightly or remained about the same over the same distance (table 15), and trace constituents decreased. Concentrations of dissolved Fe and Cu decreased from 40 to <20 µg/L and from 80 to 40 µg/L, respectively. On March 1, 1985, streamflow at Pinal Creek at Inspiration Dam consisted of about two-thirds runoff and one-third perennial ground-water discharge. By August 1985, the creek had returned to base flow, and concentrations of sulfate had increased to 1,800 mg/L. The concentration trends in SO_4 and other constituents on March 1, 1985, and changes in stream chemistry at Inspiration Dam as the stream returned to base flow indicate that ground-water discharge to lower Pinal Creek was more contaminated than ephemeral surface flow that originated upstream. The higher discharge in March relative to discharge in August resulted in greater loads of contaminants being transported into the perennial reach and out of the basin even though concentrations were less in March than in August.

PERENNIAL STREAMFLOW

From 1985 through 1991, ground-water discharge to Pinal Creek produced perennial flow from about 6 km upstream from Inspiration Dam to the mouth. Because the aquifer narrows less than 1 km south of well group 500 (fig. 2) and is truncated at Inspiration Dam, most of the perennial reach above Inspiration Dam is a gaining stream. The natural system is disrupted at about 2 km upstream from Inspiration Dam, where surface-water diversions at Pringle pump station resulted in a decrease in flow from 0.20 to about 0.13 m^3/s (fig. 30).

Upstream from Inspiration Dam

At base flow, the measured surface-water chemistry upstream from Inspiration Dam is the result of (1) the chemical and advective processes that take place upgradient in the ground-water contaminant plume, (2) equilibration of discharging ground water with the atmosphere, and (3) variations in the chemistry of ground water that contributes to base flow along the perennial reach. Samples of streamflow and shallow ground water collected at 11 sites along the perennial reach in 1990 (fig. 31) revealed changes in surface-water chemistry that take place as neutralized, contaminated ground water discharges to the stream and equilibrates with the atmosphere. As the water equilibrated with the atmosphere, dissolved inorganic carbon decreased from 29 to 16 mg/L (fig. 32) through the degassing of CO_2 and pH increased from 6.0 to 7.4. In response to the increase in pH, concentrations of dissolved Mn decreased from about 90 to 15 mg/L and precipitated as crust on the streambed. The measured concentrations of other dissolved trace constituents and major ions are controlled by these processes and by the variations in chemistry of ground water that discharges to and mixes with streamflow along the entire perennial reach.

In shallow ground water adjacent to the stream, pH varied from 5.8 to 6.8 (fig. 32) and generally increased downstream. The concentration of dissolved inorganic carbon (DIC) generally varied between 40 and 60 mg/L and decreased downstream but was 30 mg/L and 14 mg/L at two locations.

Chloride (Cl), sodium (Na), and calcium (Ca) decreased slightly in streamflow and shallow ground water from the head of perennial flow to about 1.5 km upstream from Inspiration Dam (fig. 32). Ground water from less than 1.5 km upstream from Inspiration Dam contained significantly smaller concentrations of Cl and Ca than ground-water samples farther upgradient, which indicates that ground water near Inspiration Dam contained a larger percentage of uncontaminated water. Concentrations of dissolved silica (SiO_2) in surface water and ground water varied from 72 to 53 mg/L and from 66 to 34 mg/L, respectively, and generally decreased downstream.

Concentrations of Mn, cobalt (Co), nickel (Ni), cadmium (Cd), and barium (Ba) in surface water decreased downstream (fig. 32). In ground water, concentrations of Mn, Co, and Ni decreased to near detection levels about 3 km upstream from Inspiration Dam. Concentrations of Cu in surface water decreased downstream from 15 µg/L near the head of flow to less than 5 µg/L about 2 km above Inspiration Dam. Concentrations of Cu in ground water similarly decreased, except for about 2.5 km above the dam, where concentrations of dissolved Cu were almost 90 µg/L, or about nine times greater than concentrations in adjacent upgradient and downgradient samples.

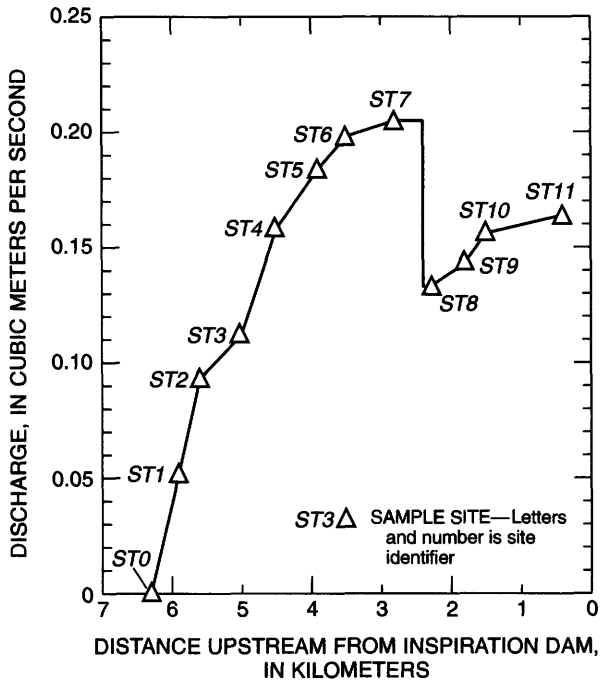

Figure 30. Discharge in the perennial reach of Pinal Creek upstream from Inspiration Dam, March 5–9, 1990 (from Faires and Eychaner, 1991).

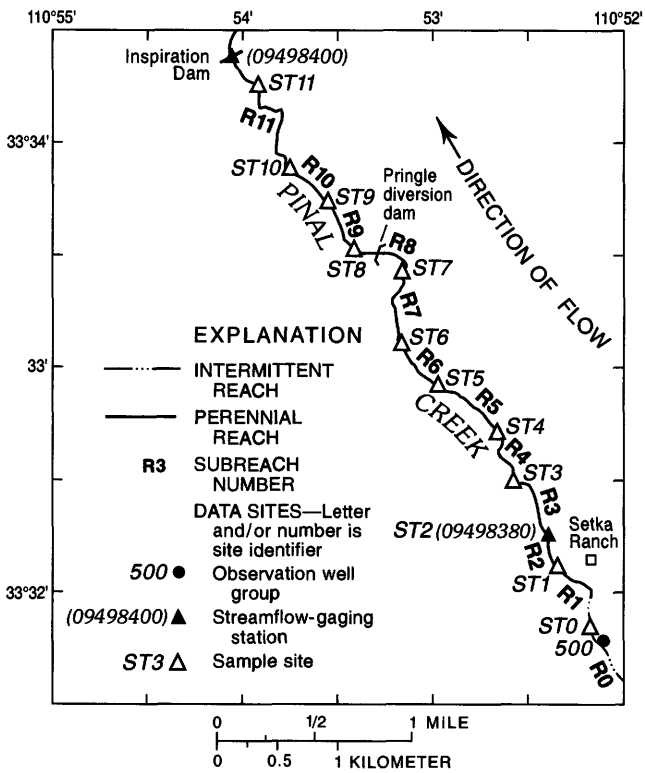

Figure 31. Locations of ground-water and surface-water sites sampled during the solute-transport study, March 1990.

Pinal Creek at Mouth

The creek channel between Inspiration Dam and the Salt River differs from the channel above Inspiration Dam. Stream alluvium is absent downstream from the dam. Ground-water flow is restricted to thin deposits of unconsolidated materials that overlie consolidated rocks, and the channel slope is twice as steep below the dam. Samples were collected at the mouth on three occasions at or near base-flow conditions on the same days that samples were collected at Inspiration Dam. Discharge on July 31, 1987, was about the same at both locations: 0.147 m^3/s at Inspiration Dam and 0.141 m^3/s at the mouth. On July 31, 1987, pH was 7.8 at Inspiration Dam and 8.4 at the mouth. Over the same interval, dissolved Mn decreased slightly from 220 to 200 mg/L, SO_4 was unchanged at 1,800 mg/L, and concentrations of dissolved Ca increased from 500 to 600 mg/L.

Salt River Below Mouth of Pinal Creek

Pinal Creek flows into the Salt River above Roosevelt Lake, which stores water for municipal, agricultural, and other uses by the metropolitan area of Phoenix. In water year 1991, the pH of the river below the mouth of Pinal Creek ranged from 8.0 to 8.5. Dissolved-solids concentrations in the river generally are inversely related to discharge because large flows include runoff that has had little time to react with either minerals or soil. In water year 1991, dissolved solids ranged from 216 mg/L at a discharge of 3,250 m^3/s to 2,030 mg/L at a discharge of 183 m^3/s. River water was a sodium chloride type within the range of discharges sampled, although Na and Cl became less dominant at greater discharges. Beginning in the mid-1980's, inflow from Pinal Creek caused a gradual increase in concentrations of Mn in the Salt River (fig. 33). Inflow from Pinal Creek had no discernible effect on concentrations of dissolved and total Cu and Ni in river water. Only flows of less than 11.3 m^3/s are shown on figure 33 because at higher flows, contaminated flow from Pinal Creek becomes a small fraction of the total flow in the Salt River.

Temporal Changes in Stream Chemistry

Prior to 1979, sampling for chemical analyses in surface water in the basin was sporadic. In Novembe

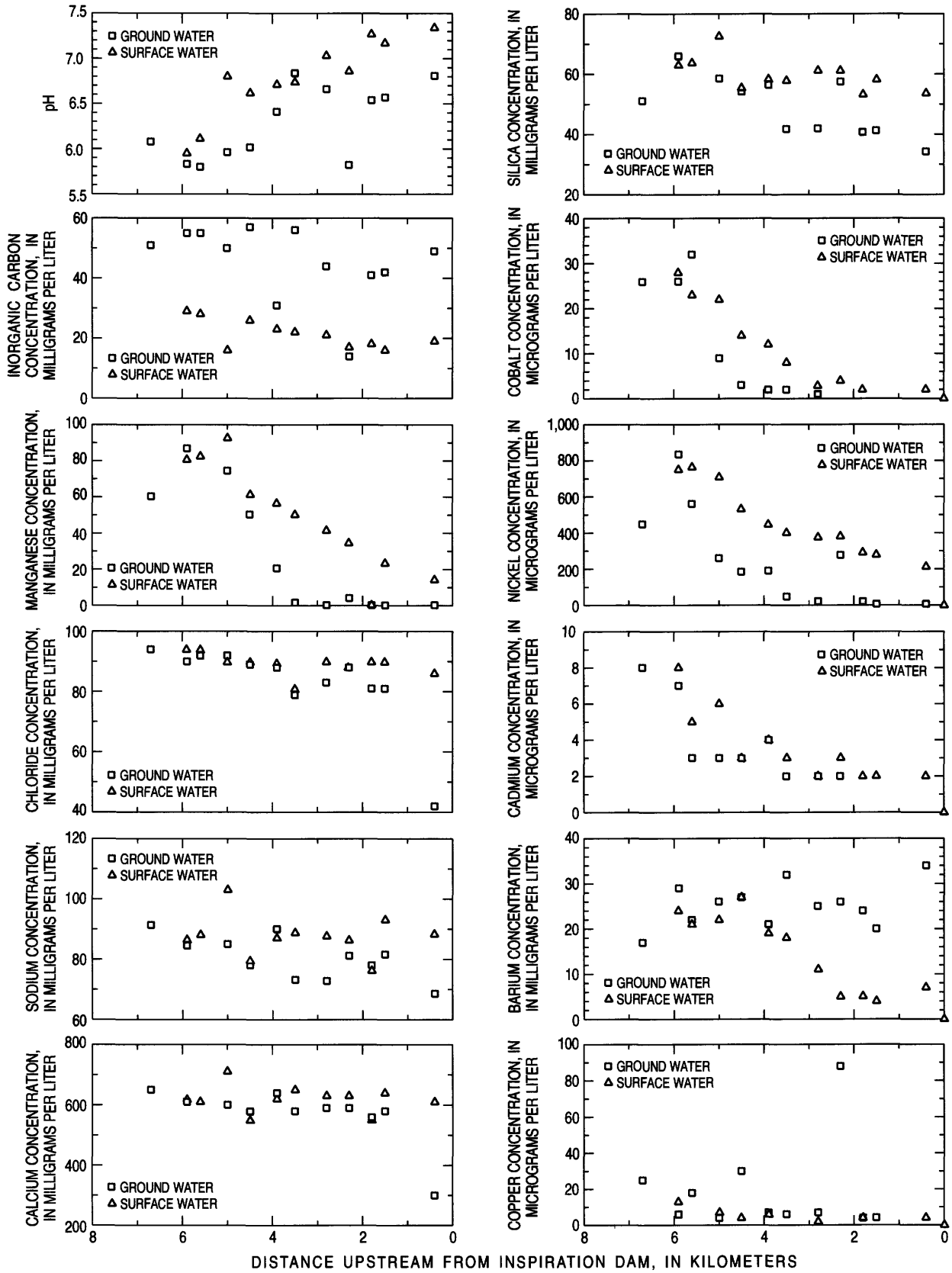

Figure 32. pH and concentrations of dissolved chemical constituents in surface water and ground water upstream from Inspiration Dam, March 1990.

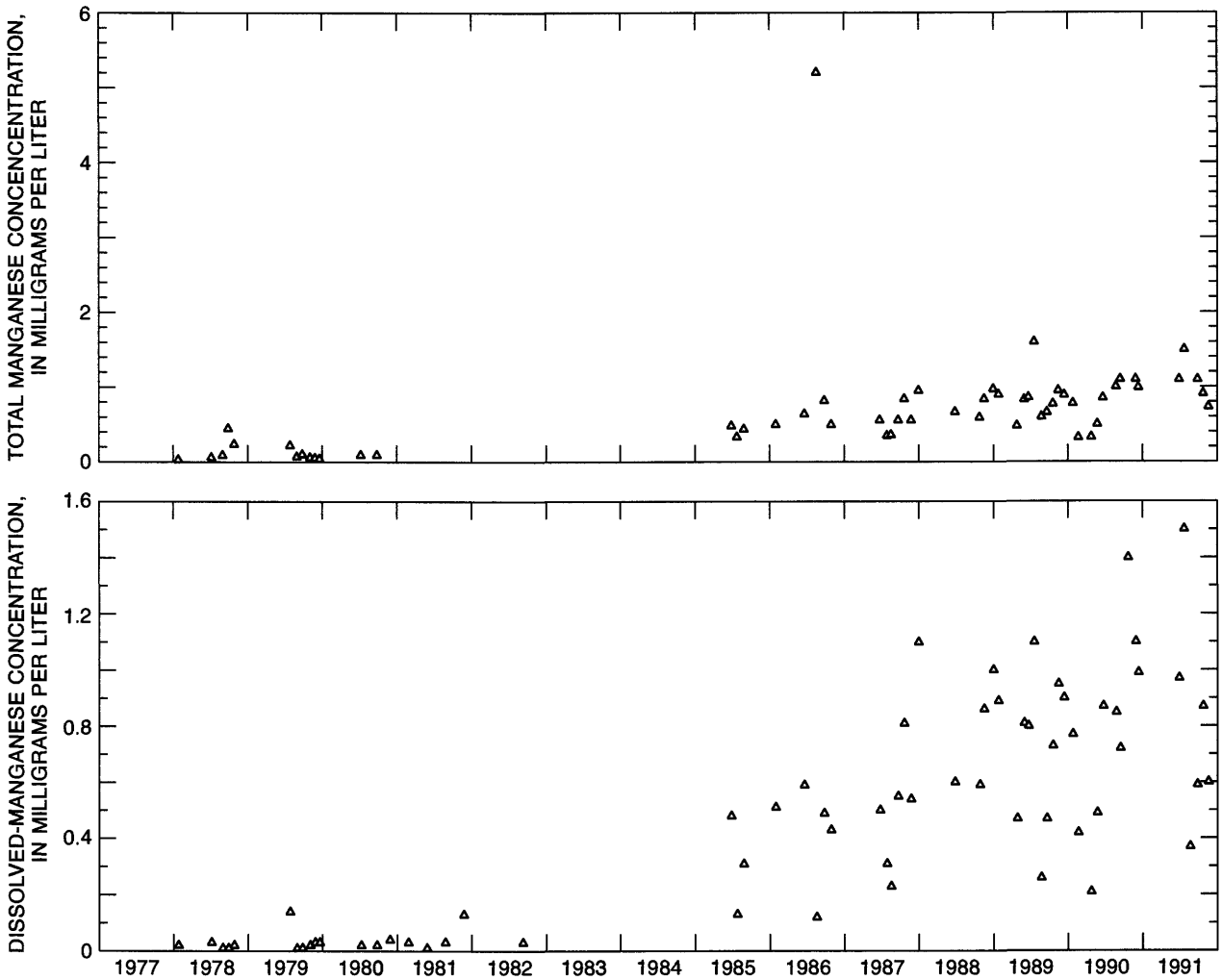

Figure 33. Total and dissolved manganese concentrations at discharges below 11.3 cubic meters per second, Salt River near Roosevelt.

1979, the USGS began periodic sampling of streamflow at Pinal Creek at Inspiration Dam. Analyses of these samples have provided a useful record of chemical trends of perennial flow that leaves the basin. The USGS began periodic sampling near the head of perennial flow (Pinal Creek at Setka Ranch, 09498380) in 1987.

Pinal Creek at Inspiration Dam

Concentrations of dissolved solids from a sample collected at Inspiration Dam in 1942 were about 800 mg/L (Envirologic Systems, Inc., 1983, p. 6), which indicated that little if any contaminants had entered the perennial reach by that year. Sometime after that, concentrations of dissolved solids in streamflow began increasing and were about 2,800 mg/L in 1979. Concentrations of dissolved solids in perennial flow gradually increased to more than 3,500 mg/L by late 1988 but decreased to about 3,400 mg/L by 1991 (fig. 4). Superimposed on this increasing long-term trend are decreases in concentrations of dissolved solids during the winters of most years. Concentrations of dissolved solids decreased during those times because winter base flow probably includes some uncontaminated recharge from winter storms that mixed with older, neutralized contaminated ground water. Samples collected during periods of runoff into the creek are characterized by smaller concentrations of dissolved solids than are measured during base flow. For example, the sample collected at the highest discharge had a dissolved-solids concentration of 1,310 mg/L, which is the smallest concentration of dissolved solids for the period of record (fig. 4).

Some major dissolved constituents in base flow in the perennial reach had similar trends. From 1979

through 1991, SO_4, which is the dominant anion, increased from about 1,700 mg/L to more than 2,000 mg/L (fig. 4). SO_4 generally was between 60 and 70 mg/L through 1984, but from 1986 through 1991 increased to nearly 100 mg/L (fig. 34). $CaCO_3$, which was usually between 100 and 200 mg/L, increased slightly from 1979 through 1984 but has decreased slightly since 1984. Concentrations of Ca, Mn, potassium (K), and Cl did not vary with time.

Dissolved concentrations of most trace metals, including arsenic (As), chromium (Cr), lead (Pb), selenium (Se), silver (Ag), mercury (Hg), and Zn were near or below detection limits in most samples collected between 1979 and 1991. Concentrations of dissolved Fe varied from less than 10 to 150 µg/L, but usually were below 100 µg/L. Concentrations of dissolved Cu varied from 4 to 37 µg/L between 1984 and 1991 (fig. 34). Neither constituent exhibited notable trends with time. Concentrations of Mn increased steadily from 0.26 to 40 mg/L from 1979 through 1988. From 1989 through 1992, the variability in dissolved Mn increased markedly (fig. 4); the largest and smallest concentrations that occurred during this period—56 and 10 mg/L Mn, respectively—were measured in consecutive months. The large variation of Mn concentration at Pinal Creek at Inspiration Dam may reflect variation in the rate of Mn precipitation along the perennial reach. Visible accumulations of Mn in the streambed were first observed in 1985. Streambed sediments provide only a temporary sink for Mn, however, because flood discharges break up and transport the cemented sediments (Judith Haschenburger, graduate student, Department of Geography, Arizona State University, written commun., 1988).

Pinal Creek at Setka Ranch

Water chemistry of Pinal Creek at Setka Ranch (fig. 35) has been monitored on a regular basis since 1987. Measured stream chemistry is a function of the chemistry of the ground water that discharges to the creek upstream from Setka Ranch and the reactions that occur as ground water surfaces to the stream. The head of perennial flow moved downstream steadily toward Setka Ranch from 1984 to 1990; from 1988 to 1990, the head of flow moved downstream about 600 m, and in November 1990, was 400 m upstream from the sampling site at Setka Ranch. Base flow varied from about 0.15 m^3/s in 1987 to 0.05 m^3/s in 1991 and was slightly higher in winter months (fig. 35).

Dissolved-solids concentrations increased from 3,600 mg/L in July 1987 to 3,900 mg/L in March 1990, and decreased to 3,500 mg/L by the end of 1991 (fig. 35). Alkalinity and pH steadily decreased over the period of record. Ca, Cl, and SO_4, though variable, exhibited no significant trends through 1989 but decreased during 1990 and 1991. Concentrations of Na increased from less than 80 to 100 from 1987 through mid-1991 but decreased to 90 mg/L in the latter part of 1991 (fig. 35).

In contrast to most of the major ions, concentrations of dissolved Ni and Mn increased steadily during the period of record. Concentrations of Ni increased from about 280 µg/L in 1987 to 880 in November 1991 (fig. 35). Mn increased from 52 mg/L in 1987 to 94 mg/L in November 1990 but decreased to 85 mg/L by the end of 1991. Dissolved and total concentrations of Fe and Cu increased and became more variable with time. The average concentration of dissolved Fe was 18 µg/L in 1987–89 and 33 µg/L in 1990–91. The average concentration of dissolved Cu was 49 µg/L in 1987–89 and 75 µg/L in 1990–91. The solubility of Fe, Cu, Mn, Ni, and other metals is a function, in part, of pH. The observed trends of increasing dissolved concentrations of metals with lower pH is characteristic of pH-dependent solubilities.

The observed trends in chemistry in Pinal Creek at Setka Ranch from 1987 through 1991 are similar to those measured in ground water about 500 m upstream from the head of perennial flow. The pH of water from well 503, perforated 24 m below land surface, decreased from 6.2 to 5.6 from 1986 through 1991 (fig. 36). Over the same period, alkalinity decreased from 100 to 55 mg/L. Conversely, concentrations of dissolved Mn increased from 46 to 116 mg/L and concentrations of dissolved Ni increased from 400 to about 1,000 µg/L, but the concentration was less than 100 µg/L in one sample in 1987. Concentrations of Cu and Fe generally were below detection limits, which varied from 50 to 100 µg/L. Given the measured similarities in chemical trends between surface water and ground water at the two sites, further increases in acidity, Ni, or other contaminants in water samples from well 503 will probably precede increases in concentrations of contaminants in surface flow in the perennial reach.

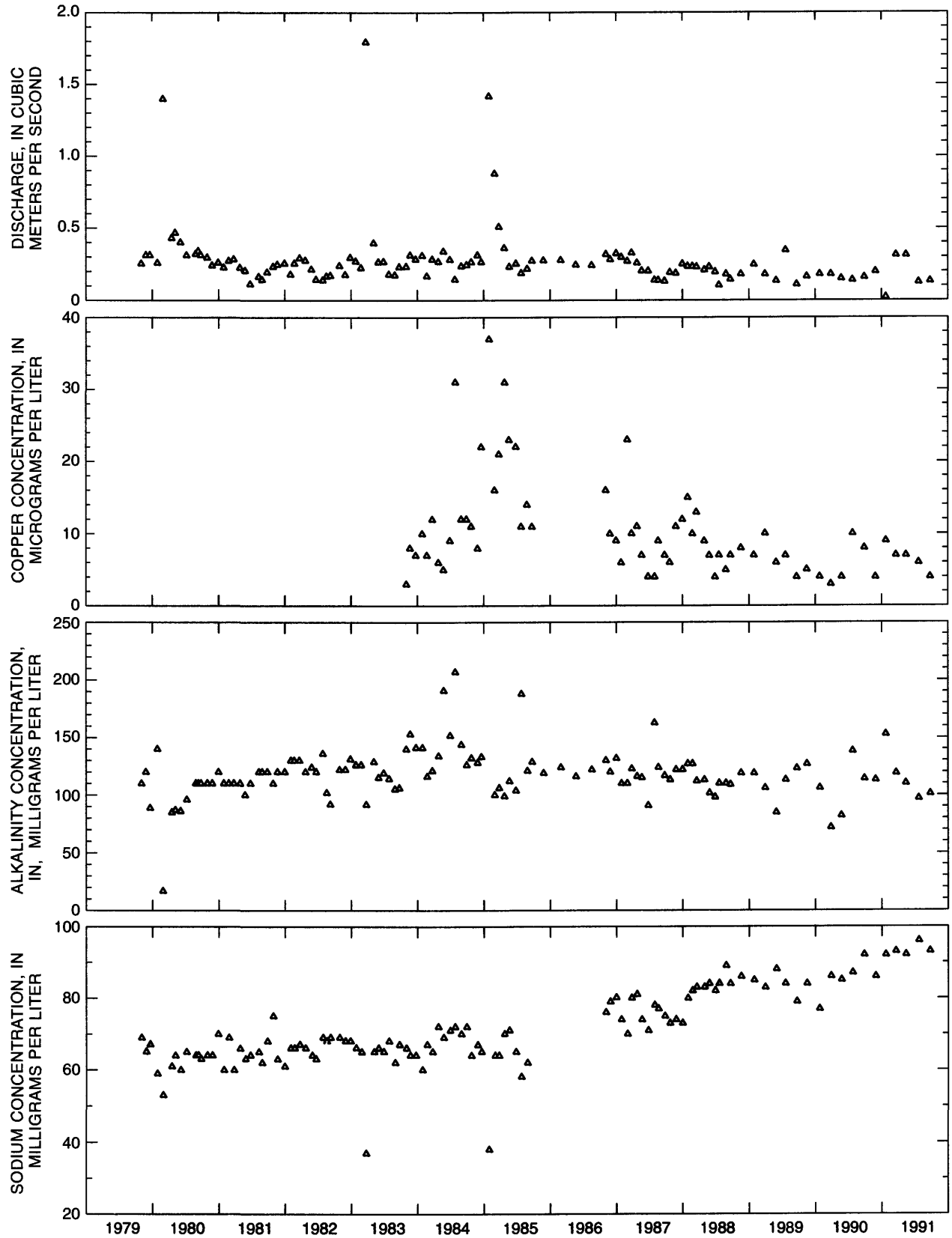

Figure 34. Discharge and concentrations of dissolved copper, alkalinity, and sodium, Pinal Creek at Inspiration Dam.

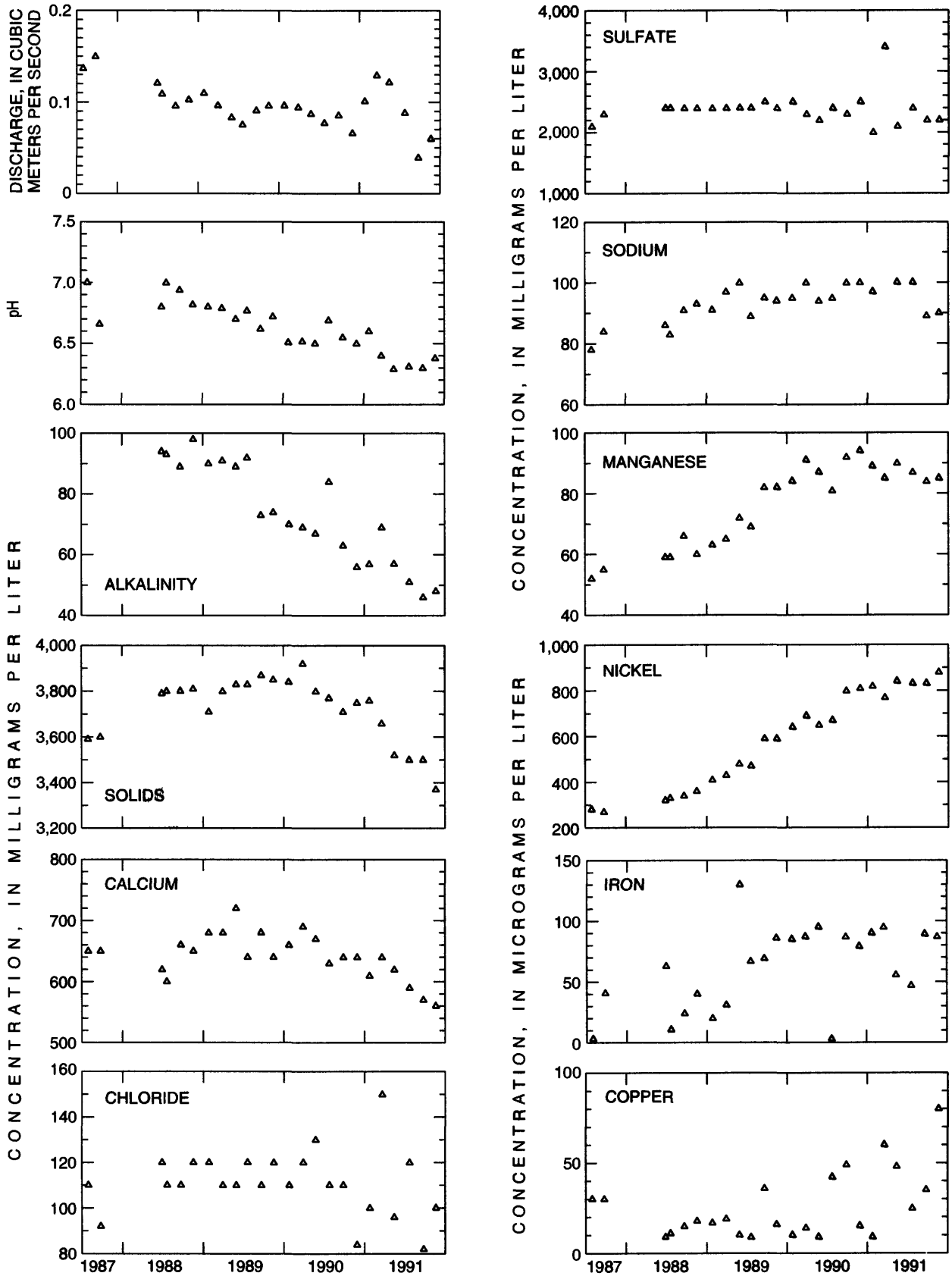

Figure 35. Discharge, pH, and dissolved chemical constituents, Pinal Creek at Setka Ranch.

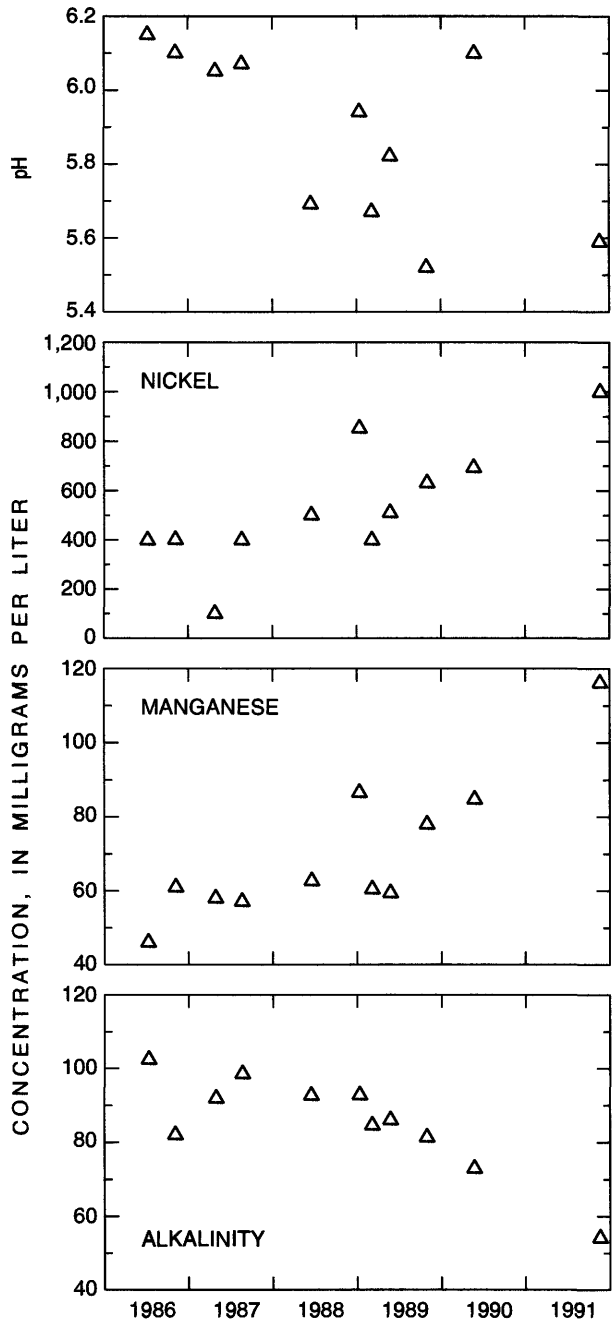

Figure 36. pH and concentrations of dissolved nickel, manganese, and alkalinity in water from well 503.

Simulation of Contaminant Transport

During March 6–8, 1990, surface water and ground-water samples were collected at 11 sites in the perennial reach of Pinal Creek (fig. 31) to evaluate the interactions among pH, Mn precipitation, and gas exchange with the atmosphere as well as other processes. An additional ground-water sample was collected a small distance upgradient from the head of perennial surface flow. Six additional streamflow samples were collected at 5 sites from 6 hours before to 27 hours after the major sampling.

Methods

Sites were selected at intervals of 250 to 1,160 m to examine the expected variations of discharge and chemistry; the exact points were selected in the field on the basis of channel characteristics and accessibility (fig. 31). Sites ST2 and ST11 were at previous periodic sampling sites—Pinal Creek at Setka Ranch and Pinal Creek at Inspiration Dam, respectively (Eychaner, 1991b).

Surface-water samples were collected with a peristaltic pump connected to a nylon sediment-sample nozzle fixed near the center of streamflow. Ground-water samples were collected with the peristaltic pump connected to an adjacent 1.9-cm-diameter stainless-steel well casing. Wells had stainless-steel wire-wound 30-cm-long screens that had 0.02-cm-wide openings. Each well was driven by hand to about 1.5 m below the water table and was developed by pumping for 10 to 20 minutes. Sample water was pumped without atmospheric contact through a cell in which pH, temperature, dissolved oxygen (DO), specific conductance, and platinum (Pt) electrode potential were measured. Samples that required filtration before analysis were pumped through a 0.45-μm filter. Other samples were pumped directly to bottles. Reusable equipment was rinsed thoroughly with stream water between uses and a final rinse with commercial deionized water. Streamflow discharges were measured by the current-meter method.

Streamflow temperature, DO concentration, pH, and specific conductance were recorded every 30 minutes at sites ST2, ST7, ST8, and ST11. Atmospheric pressure, temperature, relative humidity, and wind speed were recorded continuously at ST7 and measured at each site during sample collection.

The geochemical computer program PHREEQE (Parkhurst and others, 1985) was used to compute elemental speciation in solutions, saturation indices with respect to selected minerals, and results of mass transfers between minerals and solutions. The saturation index used in this report is

$$SI = \log (IAP/K)$$

where

IAP = ion-activity product, and
K = equilibrium constant for the solubility product associated with a given reaction between a solid phase and solute species.

When SI is less than 1, the system is undersaturated with respect to the mineral under consideration; and when SI equals 0, the system is at equilibrium with the mineral. An SI greater than 1 indicates supersaturation.

Conservative Mixing Model

Discharge in the study reach was steady throughout the sampling period. Analysis of 17 discharge measurements and 77 gage-height observations indicated that discharge varied less than 10 percent at any one site. The last previous increase in discharge caused by precipitation had been about 7 weeks earlier. Analytical concentrations of all nonvolatile constituents varied less than 10 percent at each site during the sampling period, which began 6 hours before and ended 27 hours after the concurrent sampling of surface water and ground water. The system, therefore, was considered chemically at steady state.

Discharge measurements indicated that about 40 percent of the discharge from the aquifer to the stream occurred in the first 0.6 km of streamflow (fig. 30). Temperature and DO varied diurnally in the streamflow. The diurnal range of temperature was greater downstream, although the diurnal range of DO did not vary (fig. 37). Average temperature decreased downstream by about 0.4°C/km but remained 4.5°C above average air temperature after 5 km. Average DO was 5.6 mg/L after the initial 0.7 km of flow and increased downstream by about 0.5 (mg/L)/km. Abundant algae in the creek contributed to DO variations. Diurnal variations of pH and specific conductance were small, and streamflow ionic strength was about 0.06 mol/L.

Conservative mixing was modeled as a cumulative mass balance:

$$C_{S2} = [C_{S1}Q_{S1} + 0.5\,(C_{G1} + C_{G2})\,(Q_{S2} - Q_{S1})\,]/Q_{S2}, \quad (10)$$

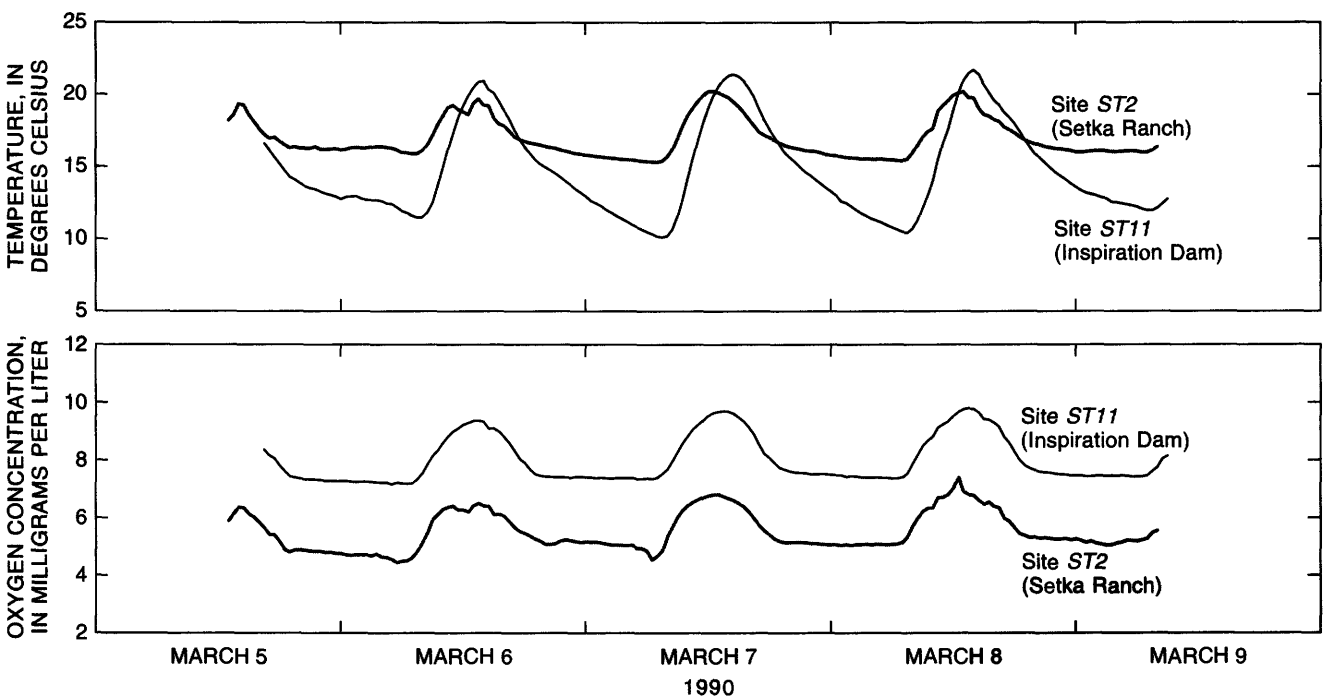

Figure 37. Diurnal variation of temperature and concentration of dissolved oxygen, Pinal Creek (modified from Eychaner, 1991b).

where

C_{S2} = constituent concentration in streamflow at the downstream end of a subreach,

C_{S1} = constituent concentration in streamflow at the upstream end of a subreach,

Q_{S1} = discharge of streamflow at the upstream end of a subreach,

Q_{S2} = discharge of streamflow at the downstream end of a subreach,

C_{G1} = discharge of ground water at the upstream end of a subreach, and

C_{G2} = constituent concentration in ground water at the downstream end of a subreach.

Constituent concentrations in streamflow just below the Pringle diversion (site 8) were calculated using the estimated natural flow at site 8. To estimate this flow, ground-water inflow between sites 7 and 8 was first estimated by averaging measured ground-water inflows between sites 6 and 7 and between sites 8 and 9. The natural flow then was computed by adding this estimated ground-water inflow to the measured streamflow at site 7. The measured discharge at site 8 (fig. 30) was used to calculate constituent concentrations at site 9.

Using ground-water analytical concentrations only, this simple model adequately represented most constituents in streamflow (fig. 38), including constituents that were expected to react but varied only slightly in the reach, such as Na and SiO_2. The mixing model diverged from measured concentrations, however, for dissolved gases and Mn (fig. 39). DIC in the model was about 2.5 times greater than measured, and DO was less than 10 percent of measured concentrations. Simulated Mn was close to measured concentrations at the beginning of the reach but was three times higher 5 km downstream.

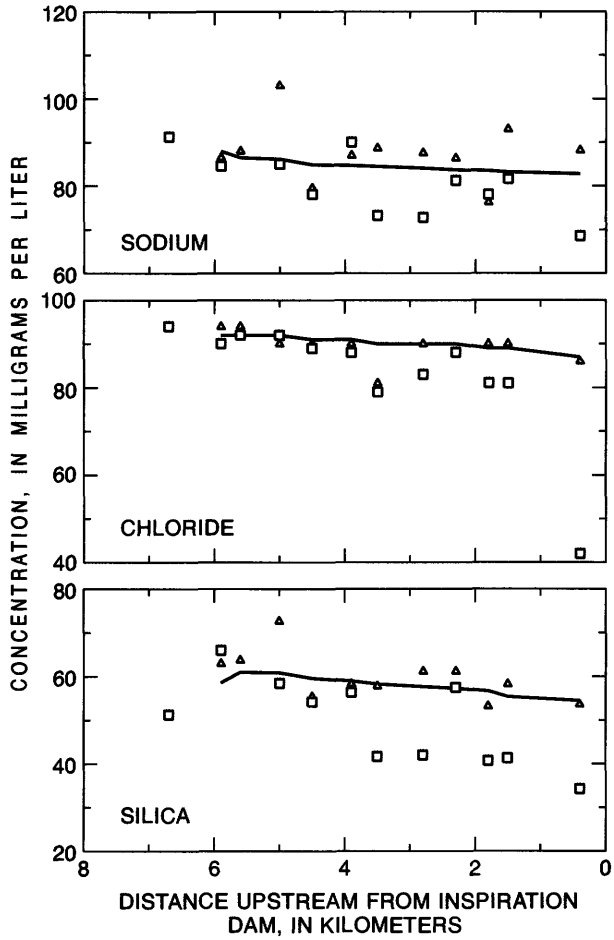

Figure 38. Measured and simulated concentrations of dissolved sodium, chloride, and silica in surface water and ground water upstream from Inspiration Dam (modified from Eychaner, 1991b).

Reaction-Path Model

Partial pressure of carbon dioxide (pCO_2) in streamflow samples decreased from $10^{-1.4}$ to $10^{-2.7}$ atmospheres, and the SI for calcite increased from −1.6 to 0.2 through the study reach. Average SI for all sites was 0.04 for gypsum and −0.22 for amorphous silica, and no trend was evident. Using Pt electrode potential to estimate the oxidation potential (Eh) of streamflow, SI generally was less than −2 for Mn oxides, although Mn oxides form in the reach. SI was about 1 for rhodochrosite. Mn in fine-grained crusts of unknown age in Pinal Creek streambed can be represented as $(Mn[II]_{0.85}Ca_{0.15})Mn[IV]_4O_9 \cdot 3H_20$ although several minerals were present (Lind, 1991, p. 488); thermodynamic data for this form are not available.

Reaction paths were computed with PHREEQE to develop the simplest possible model that adequately represents measured changes in streamflow chemistry. The model began with the same proportions of ground water as in the conservative-mixing model, and three additional processes were simulated. Reaction amounts

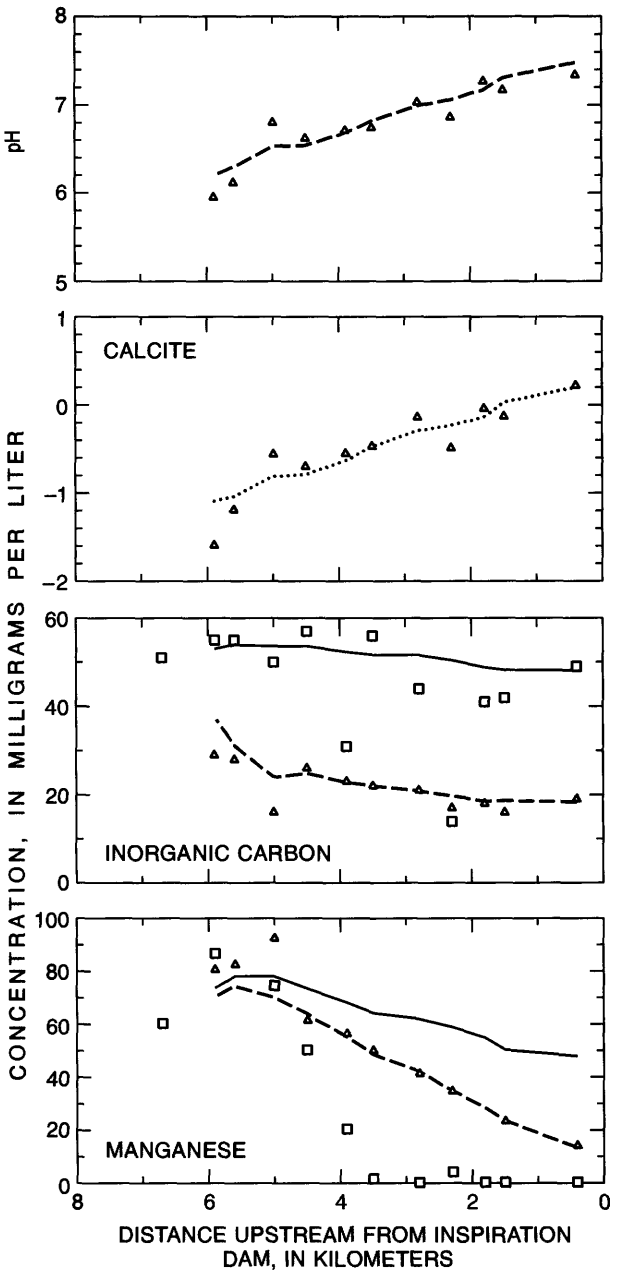

Figure 39. Measured and simulated pH and concentrations of dissolved chemical constituents in surface water and ground water upstream from Inspiration Dam (modified from Eychaner, 1991b).

given in this section are based on 1 kg of solution and are stated in terms of distance, because travel time through the reach is uncertain. Simulation results are described in terms of subreaches between adjacent sample sites.

First, net degassing of 5,360 μmol of CO_2 was specified in amounts that decreased linearly from subreach 1 (fig. D4) to subreach 6 and continued, at a smaller rate of decrease, to subreach 11. The average rate was 900 μmol/km. Second, Mn precipitation as

$$4.85Mn^{2+} + 0.15Ca^{2+} + 9H_2O = \quad (11)$$

$$(Mn_{0.85}H^{+}_{0.15})\,Mn_4O_{9(s)} + 18H^{+} + 8e^{-}.$$

was specified at 300 μmol/km for the mineral. Oxidation of Mn[II] to Mn[IV] was balanced by oxygen reduction, which can be represented by

$$O_2 + 4H^{+} + 4e^{-} = 2H_2O.$$

Dissolved oxygen was specified at 600 μmol/km to balance reaction (2). The complete redox reaction for Mn oxidation is

$$4.85Mn + 0.15Ca^{2+} + 2O_2 + 5H_2O = \quad (12)$$

$$(Mn_{0.85}Ca_{0.15})\,Mn_4O_{9(s)} + 10H^{+}.$$

The dissolution of calcite,

$$CaCO_{3\,(s)} + 2H^{+} = Ca^{2+}H_2CO_3, \quad (13)$$

was specified at 135 μmol/km to consume protons produced by reaction 3. An equal amount of CO_2 degassing maintained the net downstream decrease in DIC. The amount of each reaction was calibrated to match measured pH, Mn, and DIC concentrations in streamflow.

The reaction-path model adequately represented measured stream-water chemistry by using reasonable amounts of likely reactions (fig. D12). The model reproduced the calcite SI of streamflow samples, which indicates the specified dissolution was reasonable. Simulated concentrations of Ca varied less than 3 percent through the reach; the differences from measured concentrations were too small to require

additional reactions. Average model SI was 0.04 for gypsum and –0.23 for amorphous silica.

Simulated SI for all Mn oxides exceeded 3 and increased downstream. SI for hausmanite (Mn_3O_4) exceeded 9 for subreaches 10 and 11. The large difference between the modeled SI values and those computed from samples was primarily the result of using simulated Eh rather than Pt electrode potential. The logarithmic ion-activity product for reaction 2, for example, is more sensitive to pH and Eh than to Mn activity.

The reaction-path model represents the changes along the perennial reach of Pinal Creek, but no attempt was made to represent details in each subreach. A different combination of reactions or amounts could improve the results, particularly in the four upstream subreaches (fig. 39) where the proportion of ground-water inflow is greatest and pH and dissolved-gas concentrations change most rapidly. Ion-exchange reactions might be significant.

For the entire reach, reactions involving gypsum and amorphous silica are likely but probably are of minor importance. Information on the spatial distribution of CO_2 degassing rates could improve the specification of CO_2 degassing as a function of pCO_2 and subreach length. Finally, diurnal variations in reaction rates caused by temperature, illumination, DO, or biological activity could be considered.

SUMMARY

Surface-water flow in most of Pinal Creek Basin is ephemeral, and consists of storm runoff, snowmelt, and occasional, accidental spills or releases from impoundments related to copper mining. Ephemeral flow in the basin can be mostly uncontaminated runoff from undeveloped areas, or may be a combination of the uncontaminated runoff and runoff from tailings and other mine areas that contain variable amounts of contaminants. From about 1941 until it was drained in 1988, Webster Lake was used to store natural runoff and process water and wastewater generated from mining activities. From 1981 through 1988, pH from the surface to the bottom (a depth of as much as 21 m) varied from 2.4 to 2.8 and contained large concentrations of sulfate and metals.

The chemical composition of ephemeral streamflow in Miami Wash at Highway 88 varied in discharges from 0.00028 to 0.363 m^3/s. The pH was 5.1 at a discharge of 0.00085 m^3/s and 7.7 at a discharge of 0.368 m^3/s. Concentrations of dissolved Cu and Zn generally varied inversely with discharge. On March 1, 1985, runoff in Bloody Tanks Wash (site 3), which flows eastward through Miami at the base of large tailings piles, contained concentrations of dissolved Cu, Mn, and SO_4 greater than concentrations found in uncontaminated runoff at sites 1 and 2.

Streamflow recharge to ground water prior to January 1985 caused ground-water levels to rise, resulting in the surface discharge of acidic ground water to Bixby Road seepage ditch. Water in the seepage ditch (sites 7 and 8) in March 1985 was similar to that in the acidic part of the subsurface contaminant plume. Concentrations of Mn, Fe, Cu, and Zn in the ditch were 26, 44, 3.3, and 1.0 mg/L, respectively. Streamflow and chemistry in Pinal Creek below the mouth of Miami Wash were mixtures of water from Russell Gulch, Bloody Tanks Wash, Pinal Creek above Miami Wash, and Bixby Road seepage ditch. Concentrations of SO_4 increased downstream from 760 mg/L at sample site 9 to 1,400 mg/L at Inspiration Dam (site 15). Other major constituents increased slightly or remained about the same over the same distance, and trace constituents decreased. Concentrations of dissolved Fe and Cu decreased from 40 to <20 µg/L and 80 to 40 mg/L, respectively.

From 1985 through 1991, discharge of neutralized, contaminated ground water to Pinal Creek produced perennial flow from about 6 km above Inspiration Dam to the mouth. As ground water discharges to the stream and equilibrates with the atmosphere, pH increases one to two units. In March 1990, pH increased downstream from 6.0 to 7.5. In response to this increase, dissolved Mn concentrations decreased from about 90 to 15 mg/L and precipitated as crust on the streambed.

Dissolved-solids concentrations at Inspiration Dam were 800 mg/L in 1942 and 2,800 mg/L in 1979. Dissolved-solids concentrations gradually increased to more than 3,500 mg/L by late 1988 and decreased to about 3,400 mg/L by 1991. Most concentrations of dissolved trace metals were near or below detection limits in most samples collected between 1979 and 1991. Mn concentrations increased steadily from 0.26 to 40 mg/L from 1979 through 1988 and were more variable from 1989 through 1991. Visible accumulations of Mn in the streambed were first observed in 1985. Streambed sediments provide only a temporary sink for Mn, however, because flood discharges break up and transport the cemented sediments.

Using only ground-water analytical concentrations, a simple conservative-mixing model of base-flow chemistry in the perennial reach above Inspiration Dam adequately represented concentrations of SO_4, Cl, and SiO_2 in surface water but diverged from measured concentrations for dissolved gases and Mn. Reaction paths were computed with PHREEQE to develop the simplest possible model that adequately represents measured changes in the streamflow. The model began with the same proportions of ground water as in the conservative-mixing model, and three additional processes were simulated: (1) degassing of CO_2 in amounts that decreased linearly downstream, (2) Mn oxidation and precipitation, and (3) dissolution of calcite. The amount of each reaction was calibrated to match measured streamflow pH, Mn, and DIC. The model adequately represented measured streamflow by using reasonable amounts of likely reactions. Reproduction by the model of the calcite SI of streamflow samples indicates that the specified dissolution was reasonable. Simulated SI for all Mn oxides exceeded 3 and increased downstream.

Chapter E

Manganese and Iron Oxide Deposits and Trace-Metal Associations in Stream Sediments, Pinal Creek Basin, Arizona

By Carol J. Lind *and* John D. Hem

Abstract

Ground water and surface water of Pinal Creek, Arizona, have been affected by metal-mining and refining wastes. The high acidity of the metal-rich ground water is gradually reduced as the water passes through and reacts with solid-phase minerals in the alluvium. As the acidified iron- and manganese-rich ground water loses carbon dioxide, takes up atmospheric oxygen, and increases in pH value, iron and manganese oxides precipitate sequentially near the land surface and in the streamflow. The manganese oxides especially are concentrated in the alluvium at levels where the water table has fluctuated and in the downstream creek bed where the pH of streamflow approaches neutrality. The precipitation sequence of iron and then manganese agrees with the downstream increase of the manganese-to-iron molar ratios in the stream sediments and with the known relation of pH values to iron oxide and manganese oxide precipitation rates.

Manganese oxides precipitate as coatings on sediments and as fine particulates attached to stream sediments that consist of magnetite, hematite, and silicate minerals. The manganese oxide content becomes more significant as sediment particle size decreases and constitutes as much as 70 percent of some sediments in Pinal Creek that are less than 63 micrometers in diameter. The part of these black stream deposits that consists of manganese-oxide rich, nonmagnetic particles less than 63 micrometers in diameter is composed primarily of carbonates containing varying ratios of calcium, manganese, and magnesium; several manganese oxides (primarily 7-Å phyllomanganates, such as rancieite and takanelite); amorphous iron oxides; and silicates. As manganese precipitation and oxidation progresses, these particulates and coated sediments are cemented together into black crusts.

The distributions of manganese, iron, and trace metals in the extractable phases of stream deposits are related to major components of these phases and to various coprecipitation effects, especially within microdomains. Some of the many possible constituents of these microdomains are as follows.

1. Manganese oxides (hausmannite, groutite, manganite, sodium birnessite, rancieite, takanelite, and other forms of manganese oxides).
2. Mixed trace metal-manganese oxides such as hetaerolite, cadmium manganese oxide, and copper manganese oxide.
3. Other coprecipitates such as otavite, tenorite, and nickel hydroxide.
4. Mixed manganese minerals such as nickel asbolane (manganese oxide layers regularly alternating with nickel hydroxide layers).
5. Iron-manganese oxides such as manganese-goethite, jacobsite, and other variations.
6. Carbonates such as calcite, rhodochrosite, carbonates containing various calcium-to-

manganese ratios, and a solid resembling the calcium-rich kutnahorite crystal form.

7. Ferrihydrite (semiamorphous Fe^{3+} hydroxide hydrate).
8. Iron-trace metal oxides.
9. Gypsum.

In the sediments tested, a much higher trace-metal concentration occurred in the iron and manganese oxide extractants than in the carbonate extractants and much higher ratios of trace metal to manganese oxide and trace metal to iron oxide in the sediments that were less than 20 micrometers than in the coatings of the magnetic particles. Trace metals were present in higher proportions mole per mole in amorphous iron oxides than in manganese oxides; however, in the sediments containing primarily manganese oxides, the total amount of trace metals in the manganese oxides was greater than in the amorphous iron oxides.

In the amorphous iron oxide extractants, mole ratio comparisons indicated that there was a strong copper to iron affinity and that nickel and zinc were related to manganese. Copper was the most concentrated trace metal in the bottom sediments at Setka Ranch and in sediment that settled behind a boulder at Inspiration Dam. Concentrations of nickel were higher than concentrations of the other trace metals in the bottom sediments at Inspiration Dam. In these sediments, nickel concentrations decreased slightly as the crusts formed and aged. Nickel was more concentrated in the manganese oxide phase than in the other extracted phases.

INTRODUCTION

Widely studied manganese (Mn) and iron (Fe) oxide-redox reactions have been described in the literature in terms of the controls these oxides exert on trace-metal concentrations in soils and water (Jenne, 1968); their participation in surface chemical processes in ground-water systems (Hem, 1978); the Mn-zinc (Zn), Mn-copper (Cu), Mn-nickel (Ni), and Mn-cadmium (Cd) coprecipitation mechanisms and products (Hem and others, 1987; Hem and others, 1989; and Hem and Lind, 1991); and Mn oxide precipitation and trace-metal concentration by adsorption, cation exchange, and coprecipitation (Lind and others, 1987).

Over the last 100 years, metal-mining wastes have greatly altered the pH and increased the metal content of Pinal Creek, Arizona. By March 1985, the pH of the ground water at well 101, which is a site downstream from the major tailings piles, was 3.47, and the pH of the surface water at site 11, which is near the beginning of perennial flow, was 7.00. Samples from sites 1, 2, and 3, on Pinal Creek tributaries upstream from contaminated ground-water inflow, had pH's of 8.60, 8.18, and 8.18, respectively (Eychaner and others, 1989; fig. 3, chapter A, this report). In September 1992, the surface-water flow at site 12, at Setka Ranch, about 1.2 km downstream from site 11, had a pH of 6.15. As the contaminated ground water nears the land surface, it loses carbon dioxide (CO_2), absorbs oxygen (O_2), and increases in pH. Iron oxides precipitate first, and then Mn oxides precipitate in surface water of near-neutral pH.

Studies of the compositions of alluvial sediments within the contaminated ground-water flow path in Pinal Creek and in Mn-oxide streambed deposits in the downstream reach of perennial flow have determined the following.

1. Where acid neutralization is incomplete, sorption controls Cu, Ni, and cobalt (Co) distribution in the subsurface alluvium. Amorphous $Fe(OH)_3$ is the principal sorbent (Stollenwerk, 1990, 1991).
2. In the alluvium at a level where the water table had fluctuated a few years earlier, trace-metal coprecipitation by the Mn oxides is indicated by high concentrations of extracted trace metals and Mn oxides. Compared with the alluvium just above or below this level, these extracted trace-metal and Mn concentrations in the alluvium were about 15 to 27, 2.4 to 8.0, 1.3 to 2.2, and 2.2 to 4.2 times greater for Mn, Cu, Zn, and Ni, respectively (calculated from Ficklin and others, 1991).
3. Trace-metal contents of selected cemented manganese crusts in the streambed sediment can be as high as 40,000 μg/g for Mn, 900 μg/g for Fe, 620 μg/g for Cu, and 190 μg/g for Zn (Eychaner and others, 1989).

This report describes the Mn- and Fe-oxides precipitating in the perennial reach of Pinal Creek and the trace-metal relationships to some extractable phases of newly formed Mn-rich sediments.

METHODS

Field sampling, field observations, and chemical extraction of stream sediments were used to characterize the Mn oxides and Fe oxides in Pinal Creek. In conjunction with laboratory titrations and precipitations, this information was used to determine the conditions under which different mineral species precipitate in the streambed of Pinal Creek.

Precipitation Procedure

Mn oxides were precipitated from two samples of ground water and from one sample of surface water. The ground-water samples, 503–1 and 503–2, were collected in June 1988 from well 503, which is near the beginning of perennial surface flow. The surface-water sample, PC1, was collected in January 1989 at streamflow-gaging station, 09498380, Pinal Creek at Setka Ranch near Globe, Arizona, which is about 1.2 km downstream from well 503 (fig. 1, chapter A, this report).

During the titrations, CO_3-free air was flushed through an aliquot of the Mn-bearing ground water or surface water in a stirred, closed reaction vessel. The temperature was controlled by partial immersion of the vessel in a thermostated water bath. The pH of the aliquot was adjusted to a desired value by addition of 0.047 molar (M) NaOH solution using an autoburet as a pH-stat. As the desired pH was maintained, more sample water was added at a slow, constant rate of 0.5 mL/min using another autoburet. During the titrations, the pH in the solution was maintained between 9.00 and 8.50.

The titration of ground-water sample 503–1 was intended to test the effect of supplying O_2 to ground water. In ground water and surface water of Pinal Creek, dissolved CO_2 species included substantial proportions of undissociated dissolved CO_2. To evaluate the possible effect of the CO_2 species, the pH of surface-water sample, PC1, was first lowered to pH 4.93 by adding dilute hydrochloric acid (HCl); ground-water sample, 501–2, and the acidified surface-water sample, PC1, then were pretreated by flushing with CO_2-free air before titration.

The experiments were run for 5 to 7 hours daily for a week or more. After the experimental titrations were completed, the solutions and accompanying solids were aged for several months. During aging, contact with the atmosphere and room temperature were maintained. Samples of solution and solids were taken for analysis during the titrations and the aging periods (table 16).

Mineralogical Determination of Laboratory Precipitates

The mineralogies of the laboratory-produced precipitates were deciphered from the X-ray diffraction (XRD) and electron-diffraction analyses, Mn oxidation numbers, and analyses of sample solutions and oxalate sulfuric-acid solutions remaining from the oxidation-number determinations. The Mn oxidation numbers of the precipitates were determined by the oxalate sulfuric-acid method (Hem, 1980, p. 55). The solutions were analyzed by atomic-adsorption spectrometry (AAS; Hem and Lind, 1994).

Table 16. Composition of laboratory precipitates in ground-water and surface-water samples, Pinal Creek Basin, Arizona

Sample	Time since start of titration	Manganese oxidation number	Mineral species
503–1	5 hours	2.46	No data.
	83 days	2.65	$(Ca,Mn,Mg)CO_3$ resembling kutnahorite ($Ca_{0.74}(Mn,Mg)_{0.26}CO_3$); gypsum; and possibly hausmannite.
503–2	7 hours	2.43	No data.
	112 days	3.62	(Mn,Ca) oxides (such as todorokite or takanelite).
PC1	12 hours	2.82	Silicate (such as clinoenstatite), hausmannite, and manganite.
	39 hours	2.69	Probably hausmannite.
	132 days	2.99	Manganite.

Collection and Preparation of Stream Sediments

Manganese-rich sediments that were in contact with streamflow were obtained near well 503, at Setka Ranch, at the Pringle diversion (about 4.1 km downstream from well 503), and at streamflow-gaging station, 09498400, Pinal Creek at Inspiration Dam, near Globe, Arizona (about 6.3 km downstream from well 503; fig. 1, chapter A, this report). The sediments (noncemented particles and cemented crusts) were separated according to size and then into magnetic and nonmagnetic fractions (table 17). The sediments collected near well 503 (503 samples) and at the Pringle diversion (PD samples) were separated into coarse and fine sizes by panning and settling; other sediments were separated by wet sieving. During the separations, distilled, demineralized water was used for the 503 samples and the PD samples. Composited water that simulated water from Pinal Creek was used for the samples from Inspiration Dam (ID samples) that were collected in 1990. Water from the respective sampling sites was used for the samples from Setka Ranch and Inspiration Dam and was collected in 1991–92 (SR, B, and LT–NC–SS samples). Precautions were taken to avoid trace-metal contamination during preparation and examination of the samples collected in 1991–92. The oxides and carbonates of Mn and Fe have a greater density than do the silicates; thus, segregation of these minerals from the silicates by settling was attempted for some of the <38-μm particles in crusts collected in 1990 at Inspiration Dam. Conclusions, however, were not drawn concerning the differences in these segregated fractions (table 17).

Determination of the Chemical Composition of Stream Sediments

The sediments were extracted with several different media, and the resulting extractants were analyzed for cation content. Because an extraction method does not necessarily represent a precise delineation of one phase from another, a specific extraction may have removed more phases than the one indicated by its name.

Molar ratio of major cation to Mn in selected portions of the ID samples were determined by extraction with hot 12 M HCl. The surface content of the large, nonmagnetic particles (ID–CC–NM–250S) was determined by heating in HCl for only 5 minutes. The total contents of the other samples were determined by heating in HCl for several hours. These other samples included large particles (samples ID–CC–M–250T and ID–CC–NM–250T) and smaller, easily suspended particles that had been attached to sample ID–CC–NM–250T surfaces (samples ID–CC–NM–150SP and ID–CC–NM–10SP).

Samples ID–CC–NM–63, ID–CC–NM–45, ID–CC–NM–>10H, and ID–CC–NM–38L were examined to determine the cation distribution in the phases extracted. The exchangeable cations were extracted with an NH_4 acetate/acetic acid buffer. The carbonates along with the exchangeable cations were extracted with a Na acetate/acetic acid buffer. The reducible oxides, carbonates, and exchangeable cations all were extracted with ascorbic acid in a Na acetate/acetic acid buffer (table 18). A different sample aliquot was used for each extraction (Lind and Hem, 1993).

Aliquots of the nonmagnetic fractions (<20 μm) and of the magnetic fractions (150–250 μm) of stream sediments collected in 1991–92 (SR, B, and LT–NC–SS samples) were sequentially extracted (table 18). The aliquots were extracted with 1 M $MgCl_2$ at a pH of 7.00 to determine the exchangeable cations. Then these aliquots were extracted with 1 M Na acetate brought to pH 5.0 with acetic acid to determine the carbonates. Next these aliquots were extracted with 0.1 M NH_2OH•HCl in 0.01 M HNO_3 at pH 2 to determine the Mn oxides. And finally, these aliquots were extracted with 0.25 M NH_2OH.HCl in 0.25 M HCl to determine the amorphous Fe oxides (Chao, 1972; Tessier and others, 1979; Chao and Zhou, 1983; and Lind and Anderson, 1992). Sample B–A–NC was excluded from the sequential extractions.

The oxidation numbers of stream sediments were determined by the oxalate sulfuric-acid method (Hem, 1980, p. 55). Solutions remaining from the oxidation-number determinations and the supernatants from various extractions of the ID sample series were analyzed by AAS. The supernatants from the sequential extractions of the SR, B, and LT–NC–SS samples were analyzed by inductively coupled argon plasma.

CHEMISTRY OF STREAM SEDIMENTS

Sequential and nonsequential chemical extractions of sediments provided information on the major cation, trace-element composition, and mineralogy of stream

Table 17. Description and composition of selected stream sediments, Pinal Creek Basin, Arizona

[---, no data; >, greater than; <, less than. Sample LT–NC–SS was light tan and had settled behind a boulder. All other samples were black streambed sediment. Concentrations and molar ratios are from oxalate-solution analysis]

Sample identifier	Date of sample	Age of manganese crust	Sediment type	Range, in micrometers, or description of sediments	Magnetic property	Manganese oxidation number	Manganese, in percent	Iron to manganese molar ratio	Mineral type
Near Well 503									
503–CC–1F	08–87	---	Well cemented.....	Finely divided	No	3.60	---	---	---
503–CF–2F	08–87	---	.....do	.....do.....	No	3.55	---	---	---
503–CC–3M	09–88	---	.....do	Coarse	Yes	---	---	---	Quartz, magnetite, hematite
503–CC–3F	09–88	---	.....do	Finely divided	No	3.59	---	0.094	Quartz, magnetite, Na birnessite
Setka Ranch (1.2 km downstream from Well 503)									
SR–B–LCM	11–91	<4 months	Loosely cemented	63–250	Yes	---	---	---	Quartz, magnetite, mica/illite, (Mn,Ca,Mg)CO_3, hematite, (rancieite, jacobsite, and (or) kutnahorite)-?
SR–B–LC–250	11–91	....do.....	.....do	63–250	No	---	---	---	Quartz, mica/illite, plagioclase, (Mn,Ca)CO_3-?, (rancieite, jacobsite, and (or) kutnahorite)
SR–B–LC	11–91	...do.....	.....do	8–20	No	3.69	20.1	---	Quartz, Na birnessite, mica/illite, plagioclase, rancieite, takanelite
SR–B–CC	11–91	...do.....	Well cemented.....	8–20	No	3.68	32.1	---	Quartz, Na birnessite-?, rancieite, plagioclase, takanelite, K feldspar
Pringle diversion (4.1 km downstream from Well 503)									
PD–CO–R	09–88	---	Coating on rocks.....	---	No	3.28	---	.111	Quartz, mica, (manganite, Na birnessite, hausmannite, illite/chlorite)(?)
PD–CO–P	09–88	---	Coating on pebbles ...	---	No	3.39	---	.048	Do.
PD–CC–M	09–88	---	Well cemented.....	Coarse	Yes	---	---	---	Quartz, magnetite
PD–CC–F	09–88	---	.....do	Finely divided	No	3.59	---	.018	Quartz, Na birnessite
Inspiration Dam (6.3 km downstream from Well 503)									
ID–CC–M–250T	06–90	>1 year	Well cemented.....	150–250	Yes	---	---	---	Magnetite and ---?
ID–CC–NM–250T	06–90	....do.....	.....do	....do.....	No	---	---	---	Quartz>plagioclase; some mica.
ID–CC–NM–250S	06–90	....do.....	.....do	Surface of 150–250.	No	---	---	---	---
ID–CC–NM–150SP	06–90	...do.....	.....do	10–150 attached to surface of 150–250.	No	---	---	---	Quartz>plagioclase; some mica
ID–CC–NM–10SP	06–90	...do.....	.....do	0.1–10 attached to surface of 150–250.	No	3.64	31.4	.03	Quartz, mica, plagioclase, (Ca,Mg,Mn)CO_3, rancieite, takanelite

Table 17. Description and composition of selected stream sediments, Pinal Creek Basin, Arizona—Continued

Sample identifier	Date of sample	Age of manganese crust	Sediment type	Range, in micrometers, or description of sediments	Magnetic property	Manganese oxidation number	Manganese, in percent	Iron to manganese molar ratio	Mineral type
Inspiration Dam (6.3 km downstream from Well 503)—Continued									
ID–CC–NM–75	06–90	>1 year	Well cemented.....	63–75	No	3.68	34.8	0.017	Quartz, mica, plagioclase, Ca,Mg,Mn(CO_3), rancieite, takanelite
ID–CC–NM–63	06–90	...do.....	.....do.....	45–63	No	3.65	40.6	.010	Do.
ID–CC–NM–45	06–90	...do.....	.....do.....	38–45	No	3.64	23.8	.014	Do.
ID–CC–NM–8	06–90	...do.....	.....do.....	0.1–38	No	3.63	39.8	.017	Do.
ID–CC–NM–38H	06–90	....do.....	.....do.....	0.1–38 Settled rapidly	No	3.68	41.8	.016	---
ID–CC–NM–38L	06–90	...do.....	.....do.....	0.1–38 Settled slowly	No	3.66	39.4	.0086	---
ID–CC–NM–>10H	06–90	...do.....	.....do.....	10–38 Settled rapidly	No	3.62	---	.0079	Quartz, mica, plagioclase, Ca,Mg,Mn(CO_3) rancieite, takanelite
ID–CC–NM–<10H	06–90	...do.....	.....do.....	0.1–10 Settled rapidly	No	3.69	43.4	.01	
B–NC–BSM	07–91	Before crust	Noncemented	63–250	Yes	---	---	---	Magnetite, hematite, (Mn,Ca,Mg)CO_3
B–NC–BS	07–91	...do.....	.....do.....	<20	No	3.63	34.5	---	Quartz, clay, (Ca,Mn,Mg)CO_3, rancieite, takanelite, spinel resembling hausmannite, jacobsite-?, ferrihydrite-?
B–NC–CCM	11–91	<4 months	Well cemented.....	63–250	Yes	---	---	---	Magnetite, hematite, (Ca,Mn,Mg)CO_3
B–N–CC	11–91	...do.....	.....do.....	<20	No	3.71	26.0	---	Quartz, clay, (Ca,Mn,Mg)CO_3, rancieite, takanelite, spinel resembling hausmannite, jacobsite-?, ferrihydrite-?
B–A–NC	01–92	<6 months	Noncemented, not part of crust.	<20	No	3.61	23.3	---	---
B–A–CCM	01–92	...do.....	Well cemented.....	63–250	Yes	---	---	---	Magnetite, hematite, (Mn,Ca,Mg)CO_3
B–A–CC	01–92	...do.....	.....do.....	<20	No	3.65	27.4	---	Quartz, clay, (Ca,Mn,Mg)CO_3, rancieite, takanelite, spinel resembling hausmannite, jacobsite-?, ferrihydrite-?
LT–NC–SS	01–92	...do.....	Noncemented, not part of crust.	<20	No	3.56	8.2	---	Quartz, clay, (Ca,Mn,Mg)CO_3, rancieite, takanelite, spinel resembling hausmannite, jacobsite-?, ferrihydrite-?, goethite-?

Table 18. Comparison of molar ratios of major cations to manganese and to iron in some extractants of selected sediment samples from Inspiration Dam

[---, iron concentrations are below detection; therefore, ratios are not shown]

Sample identifier	Range of particle size, in micrometers	Molar ratios				
		Iron to manganese	Calcium to iron	Calcium to manganese	Magnesium to iron	Magnesium to manganese
Ammonium acetate extraction (exchangeable cations)						
ID–CC–NM–63	45–63	0.018	157	2.89	22	0.406
ID–CC–NM–45	38–45	.012	241	2.87	37	.446
ID–CC–NM–>10H	10–38 Settled rapidly	.0071	302	2.15	44	.316
ID–CC–NM–38L	0.1–38 Settled slowly	.0057	435	2.49	60	.305
Sodium acetate extraction (exchangeable plus carbonate cations)						
ID–CC–NM–63	45–63	---	---	8.53	---	1.26
ID–CC–NM–45	38–45	---	---	7.65	---	1.13
ID–CC–NM–>10H	10–38 Settled rapidly	---	---	3.14	---	.45
ID–CC–NM–38L	0.1–38 Settled slowly	---	---	6.43	---	.86
Hydrochloric acid extraction (total sample)						
ID–CC–M–250T	150–250	9.43	.034	.32	.012	.19
ID–CC–NM–250T	150–250	1.54	.24	.36	.49	.22
ID–CC–NM–250S	Surface of 150–250	.08	3.5	.26	1.0	.079
ID–CC–NM–150SP	10–150 Attached to surface of 150–250	.02	12	.22	1.7	.030
ID–CC–NM–10SP	0.1–10 Attached to surface of 150–250	.03	6.1	.16	1.4	.037

sediments. Particles from each of the size fractions were present in the ID samples from crust collected in 1990 at Inspiration Dam. The 63–250-μm sediments comprised 82–97 weight percent of the <250-μm particles in sediments and crusts collected in 1991–92 at Inspiration Dam. The 63–250-μm particles together with the <20-μm particles comprised 96–100 weight percent of these samples. Particle-size distribution in the crusts collected in 1991 at Setka Ranch was not measured but appeared to be similar to particle-size distribution of the material collected in 1991–92 from Inspiration Dam.

A considerable amount of strongly magnetic material was found in all sediment samples. The magnetic material was especially concentrated in fractions that were 63–250 μm in size and was not obvious in fractions that were <20 μm in size. In the ID samples, the Mn oxide precipitates were primarily coatings or fine particulates loosely attached to the surface of the 150- to 250-μm sediments.

The contents of the different extractants for each sample are illustrated in terms of major cations and total trace metals in Figures 40*A* and 40*C* and in terms of individual trace metals in figures 40*B* and 40*D*. The correspondence of a specific trace metal to the major cations in an extract can be observed by vertical comparison of figures 40*A* and 40*B*. The Mn concentration in the Mn oxides was so predominant that log units were used in figure 40*A* and 40*C* so that differences between the major cation concentrations

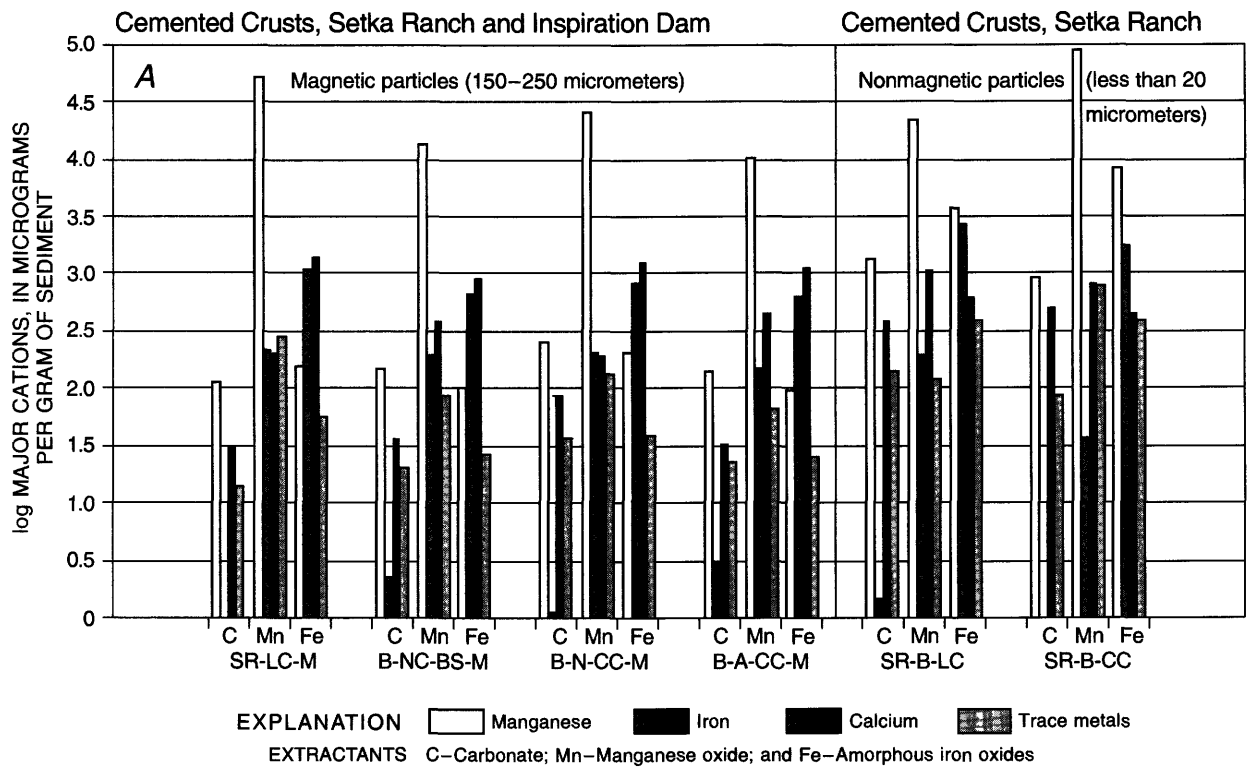

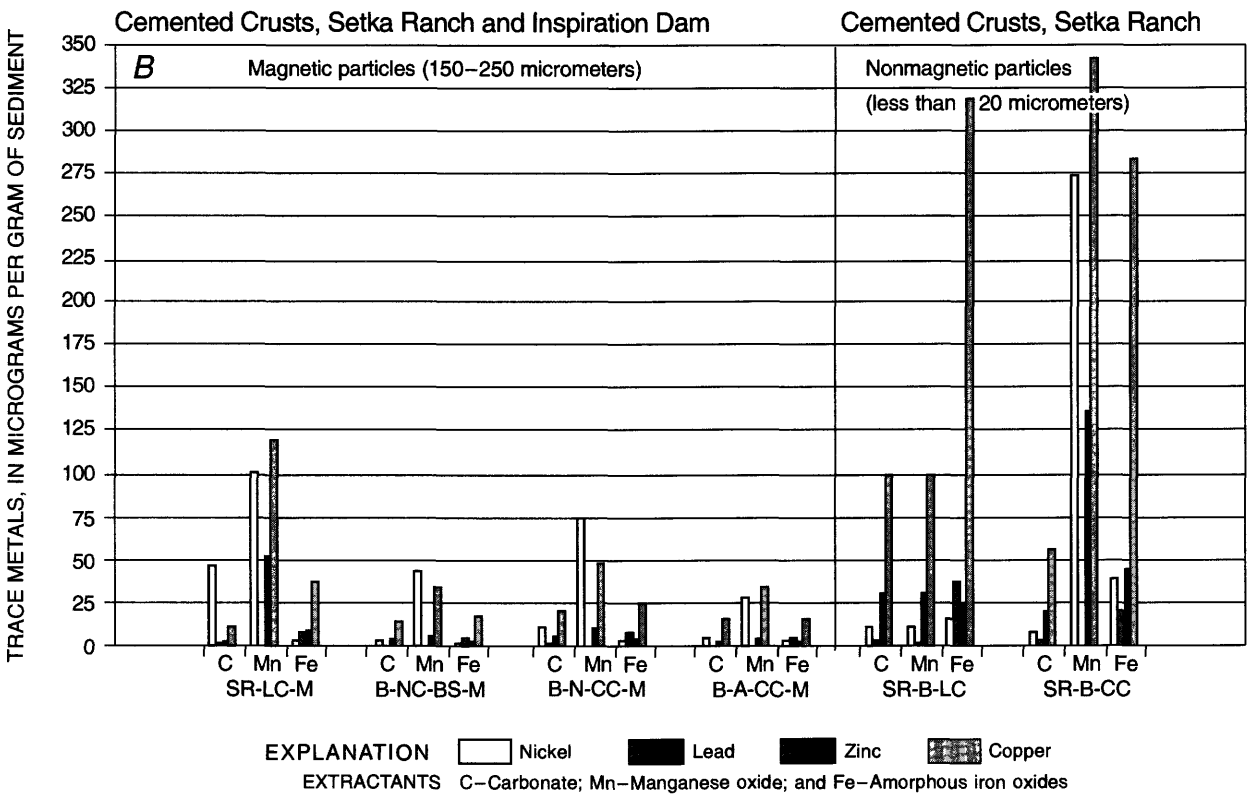

Figure 40. Results of sequential extractions of selected sediments. *A* and *C* indicate the major cation contents of the extractants in log units, and *B* and *D* indicate the trace-metal contents of the extractants in linear units.

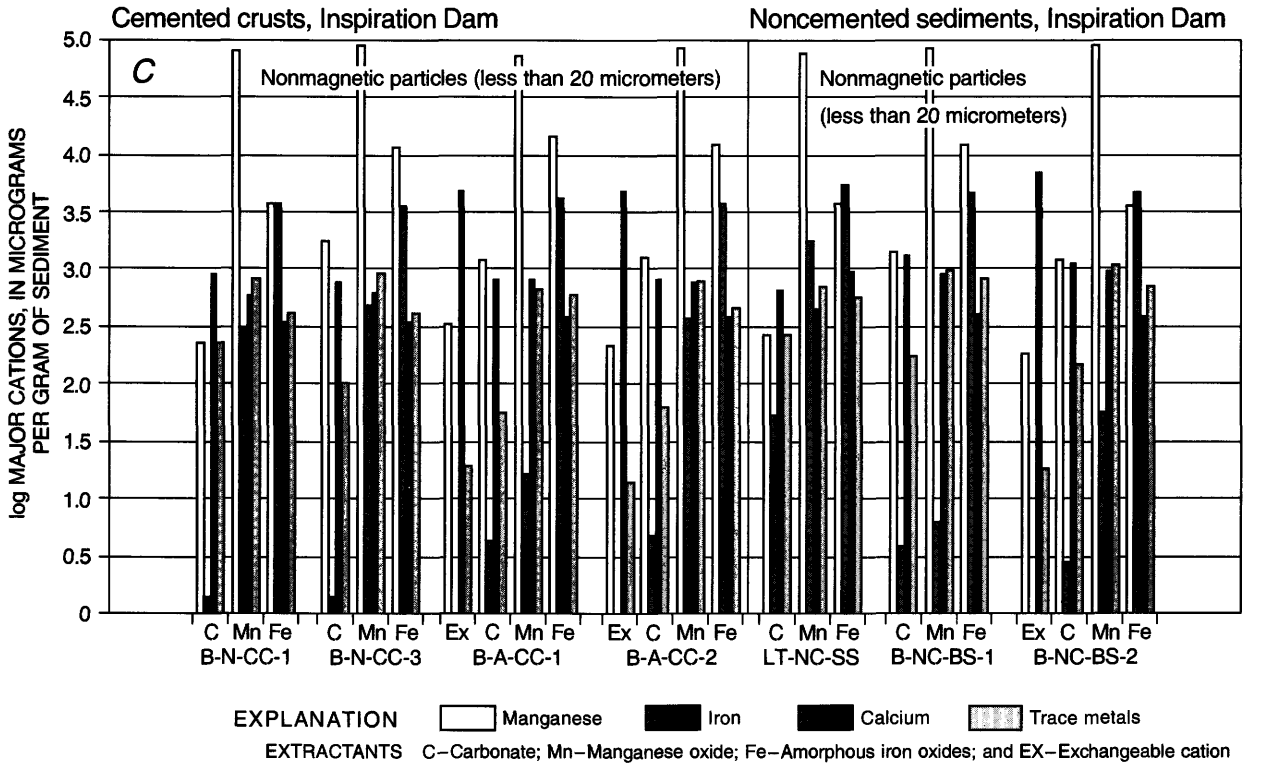

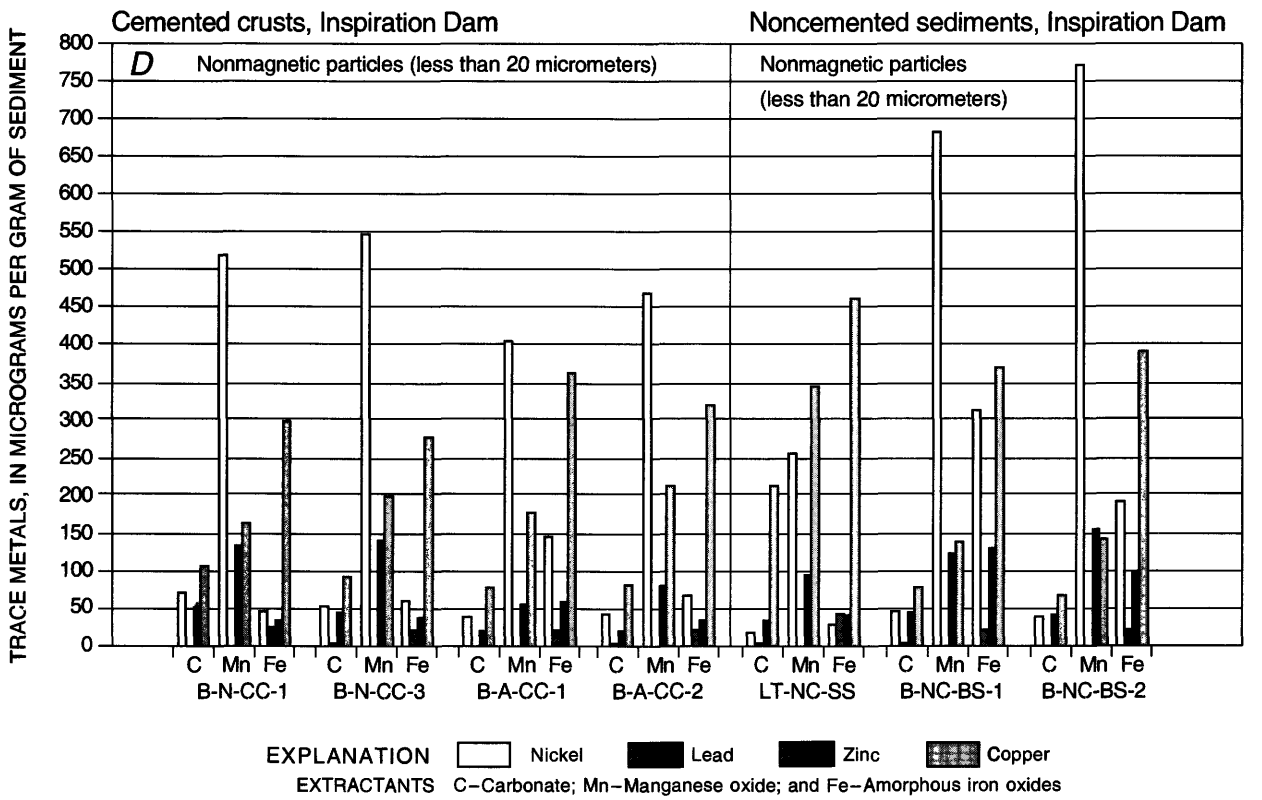

Figure 40.—Continued.

could be illustrated. In figures 40*B* and 40*D*, the trace-metal concentrations are plotted on a linear scale. In this chapter, the term "trace metals" only applies to Cu, Ni, Pb, and Zn and not to Mn or Fe.

Major Cation Distribution in Stream Sediments

In the <63-μm samples from Inspiration Dam, the molar concentrations of the exchangeable cations decreased in the following order: Ca, Mn, Mg, Na, K, Ni, Cu, Zn, and Fe. In these samples, exchangeable Ca was two to three times that of Mn; however, Mg was only 0.3 to 0.4 times that of Mn (mole/mole). In the carbonate-plus-exchangeable-cation extractant of these samples, Fe was below detection, and the molar ratios of Ca to Mn averaged near 6 although the molar ratio Mg to Mn averaged slightly less than 1. Mn, however, was about 10 times more concentrated than Ca in the extractant that removed all three phases (reducible oxides, carbonates, and exchangeable cations). In this extractant, the ascorbic-acid extractant, the molar ratio of Ca to Mn, Mg to Mn, and Fe to Mn did not vary much with sediment size and were 0.10–0.11, 0.01–0.02, and 0.05–0.07, respectively (table 18).

A brief summary of the major cation distribution in the SR, B, and LT–NC–SS samples is as follows:

1. In the exchangeable extractants, Ca was the major cation in the nonmagnetic B samples and sample LT–NC–SS (all <20 μm). Ca was 10 times more concentrated than Mn, which was the next most concentrated cation.
2. In the carbonate extractants, Mn and Ca were the primary cations in the nonmagnetic samples (<20 μm). Mn was the dominant carbonate cation in the magnetic samples (150–250 μm) and in several nonmagnetic <20-μm samples. The carbonate Fe content was 10 or more times greater in sample LT–NC–SS than in both magnetic and nonmagnetic B samples.
3. In all Mn-oxide extractants, Mn was the primary cation.
4. In the amorphous Fe-oxide extractants, Fe and Mn were the major cations in the nonmagnetic samples that were <20 μm in size. Ca content was slightly greater than that of Fe in the amorphous Fe-oxide extractants of the magnetic samples (150–250 μm; figs. 40*A* and 40*C*).

Trace-Metal Distribution in Stream Sediments

The trace-metal contents of the Mn-oxide and amorphous Fe-oxide extractants of the nonmagnetic samples (SR–B–CC, B, and LT–NC–SS samples; <20 μm) were much greater than the contents of the carbonate extractants. The trace-metal content of the amorphous Fe-oxide extractant of the loosely cemented crust from Setka Ranch (SR–B–LC) was greater than that of the Mn oxide and carbonate extractants. In the Mn oxides, molar ratios of total trace metal to Mn were from 1.4 to 2.0 times greater in the nonmagnetic samples (<20 μm) than in the magnetic samples (150–250 μm). In the amorphous Fe oxides molar ratios of total trace metal to Fe were from 2.7 to 4.8 times greater in the nonmagnetic samples (<20 μm) than in the magnetic samples (150–250 μm).

Cu was the major trace metal in most extractants. Cu was the predominant trace metal in the carbonate extractants of all the samples except in magnetic sample SR–B–LCM in which Ni was the predominant trace metal. Cu was the major trace-metal cation in the Mn oxide extractants of the nonmagnetic and magnetic SR samples from the Setka Ranch site, which is about 1.2 km downstream from well 503 and in the nonmagnetic sample (LT–NC–SS) from Inspiration Dam, which is 6.3 km downstream from well 503 but not in the nonmagnetic B samples from Inspiration Dam. Cu was the most concentrated of the trace metals in the amorphous Fe-oxide extractants of all the magnetic and nonmagnetic samples from both sites.

In the Mn oxide extractant of the B samples, concentrations of Ni were higher than concentrations of other trace metals and were higher than concentrations of Ni in the other extractants. Concentrations of Ni decreased slightly as the crusts developed and aged. Ni content of the Mn oxide extractant of the B samples (the black, noncemented sediments and black, cemented crusts) was greater than that of sample LT–NC–SS (light-tan noncemented sediment; figs. 40*B* and 40*D*).

Mineralogy of Stream Sediments

All unaltered stream-sediment samples were examined by XRD. Some ID–CC–NM samples also were examined by XRD after the Na acetate-acetic acid extractions and (or) after the ascorbic-acid extractions. These XRD results were correlated with other data

such as Mn-oxidation numbers to determine the mineralogy of the sediment samples (table 17).

Nonmagnetic ID samples (<63 μm) contained mostly a takanelite-rancieite mixture, (Ca,Mn) 7-Å phyllomanganates. These samples also contained about 20 percent $(Ca,Mn,Mg)CO_3$, 5 percent Fe (calculated as FeOOH), 2- to 4-percent exchangeable cations, and trace amounts of several silicates. In addition to the minerals identified in the ID samples, XRD reflections for the SR, LT–NC–SS, and B samples indicated less oxidized Mn minerals and other Fe oxides. XRD reflections of the SR samples suggested the 7 Å-phyllomanganate, Na-birnessite. The magnetic samples contained magnetite and hematite, and XRD indicated jacobsite in the coatings of the magnetic SR samples. For the magnetic samples, the dominance of the magnetite peak heights and the similarity of the magnetite peak locations to those of jacobsite and hausmannite hindered definite XRD identification of minor amounts of these latter spinels.

MANGANESE- AND IRON-OXIDE DEPOSITION IN STREAM SEDIMENTS

Mn oxides found in the stream sediments along the perennial reach of Pinal Creek occur as black, noncemented and cemented crusts, and as coatings on pebbles. Much of the amorphous Fe oxide (1,000 to 5,000 μg/g of sediment) probably is present as coatings on the alluvial material. Amorphous Fe oxide suspended in the ground water, however, can become a constituent of the ground-water outflow (Lind and Hem, 1993).

Manganese-Oxidation Processes

A reaction pathway for Mn deposition can be described as follows:

1. Where Mn oxide crusts are observed, surface water can have a pH of 8.2 but generally is less than 8.0. At these pH values, the Mn oxidation rate is slow in abiotic, laboratory solutions and has no particulate surface present. In the presence of natural surfaces, however, the precipitation rate is enhanced. Diem and Stumm (1984) found that, for Mn^{2+} in surface structures or bound to hydrous oxides, oxidation by O_2 requires a much smaller activation energy than direct oxidation by O_2. The Mn^{2+} could be in the surface structures of $Mn(OH)_2$ and $MnCO_3$ or in surface complexes where Mn^{2+} is bound to hydrous oxides such as Fe^{2+}, Mn^{2+}, or Mn^{4+}. Equation 14 illustrates the (surface-hydroxyl group) - Mn^{2+} - pH - O_2 control of Mn^{2+} oxidation rate in the presence of γ-FeOOH.

$$\frac{-d(Mn^{2+})}{dt} = \frac{k(\infty FeOH)\,(Mn^{2+})\,apO_2}{(H^+)^2}, \quad (14)$$

where

Mn^{2+} = activity of Mn^{2+};
k = constant;
∞FeOH = concentration of surface-hydroxyl groups, in moles per gram of oxide;
a = concentration of oxide, in grams per liter;
pO_2 = partial pressure of oxygen, in atmospheres;
t = time; and
H^+ = activity of H^+ (Davies, 1986).

2. Hem and Lind (1983) found that hausmannite (Mn_3O_4) was the primary precipitate at 25°C in aerated, 0.01 M solutions of $MnCl_2$, $Mn(NO_3)_2$, $MnSO_4$, or $Mn(ClO_4)_2$. Thus, hausmannite is probably the initial Mn oxidation product to expect in the SO_4-rich water of Pinal Creek.

$$3Mn^{2+} + \tfrac{1}{2}O_2 + 3H_2O \rightarrow Mn_3O_4 + 6H^+. \quad (15)$$

3. Once formed, hausmannite could proceed through disproportionation cycles and produce more highly oxidized Mn oxides and Mn^{2+}. The released Mn^{2+} could recycle to form more Mn oxide.

$$Mn_3O_4 + 2H^+ \rightarrow 2MnOOH + Mn^{2+}, \text{ and} \quad (16)$$

$$2MnOOH + 2H^+ \rightarrow MnO_2 + 2H_2O + Mn^{2+}. \quad (17)$$

Molar Ratios of Major Cations

The Fe-to-Mn molar ratios of the crusts collected in June 1988 decreased by more than a factor of 5 in the 4.2-km segment of the stream from near well 503 (sample 503–CC–3F) downstream to the Pringle

diversion (sample PD–CC–F). These ratios suggest a sequence of precipitation of Fe oxide at more acidic pH values and then of precipitation of Mn oxide downstream at near-neutral pH values (table 17).

The molar-ratio data for Fe to Mn indicate that Mn is precipitating on Fe-rich surfaces and that, as the crusts form, the Mn-oxide precipitates become more significant than the substrate Fe, especially in the fine particles. For example, as the Mn oxides transformed from coatings (sample PD–CO–R and sample PD–CO–P) to fine particulates in the crust (PD–CC–F), the molar ratio of Fe to Mn decreased by a magnitude of 6 and 3, respectively (table 17). The molar ratio of Fe to Mn in the ID samples decreased in the order: magnetic (150–250 μm), nonmagnetic (150–250 μm), surfaces of these nonmagnetic particles, smaller particles attached to these surfaces (table 18). The molar ratio of Fe to Mn in the nonmagnetic ID samples (<75 μm) was even lower (table 17). This ratio in the exchangeable-cation extractant of these ID samples decreased with particle size (table 18).

The degree of oxidation of the Mn oxides may relate to the Fe-to-Mn molar ratios. This relation is illustrated by the fact that these molar ratios decreased inversely with the value of the Mn-oxidation number in the order PD–CO–R, PD–CO–P, PD–CC–F, and the <75-μm ID samples. Also, the molar ratios of Fe to Mn in the Mn-oxide, carbonate, and amorphous Fe-oxide extractants of the sample LT–NC–SS were higher than in the nonmagnetic B samples, and the Mn-oxidation number of sample LT–NC–SS was lower than that of the nonmagnetic B samples (all <20 μm; table 17; figs. 40*A* and 40*C*).

In the hot-HCl extractants of the ID samples, the molar ratios of Ca to Fe in the <150-μm particles were greater by a factor of 400 over those in the 150–250 particles. Molar ratios of Ca to Mn were between 0.36 and 0.16 in all the HCl extractants. The similarity of the molar ratios of Ca to Mn indicates a relation of Mn to Ca. (Mn,Ca) carbonates and the (Mn,Ca) oxides could have such a relation. Molar ratios of Mg to Mn varied more than molar ratios of Ca to Mn and were higher in the large particles. The hot-HCl extraction probably released Mg not only from exchange sites, carbonates, Mn oxides, and Fe oxides but also from silicates such as biotite, which is a mica. Molar ratios of Ca to Mn and Mg to Mn decreased slightly with particle size and were much higher than in the HCl extraction of the total samples in the exchangeable-cation and the exchangeable-plus-carbonate-cation extractants of the nonmagnetic ID samples (<75 μm; table 18).

Manganese Content

In the SR samples, the Mn content may have contributed to the degree of cementation. This is shown by the Mn content of 20 percent for loosely cemented crust (sample SR–B–LC) and 32 percent for well-cemented crust from (sample SR–B–CC) about a centimeter away. In the B samples, collected about 5.1 km downstream from the collection site of the SR samples, a decrease of Mn content was observed as the crusts developed. Mn content did not noticeably change after the crusts formed. Mn content was 35 percent before crust formation in sample B–NC–BS (noncemented material collected in July 1991) compared with the 26–27 percent Mn in samples B–N–CC and B–A–CC (cemented crusts collected in November 1991 and in January 1992). Higher Mn content of the black sediment before crust formation compared with the Mn content during crustal development may have been a result of dilution. In other words, the ratio of the settling rate of non-Mn fine particulates to the rate of Mn accumulation may have been greater during the time of crust development than before crust development. This higher settling rate also could account for the fact that the noncemented samples collected in January 1992 had a low Mn content of 23 percent in sample B–A–NC and 8 percent in sample LT–NC–SS (table 17).

Mineralogy of Manganese Oxides

For the material coating the rocks and pebbles, the Mn-oxidation numbers (3.28 and 3.39) and XRD indicate a mixture of Mn oxides (table 17). In the nine <75-μm ID samples, the average Mn-oxidation number was 3.65±0.04. When the Mn-oxidation numbers were corrected for Mn^{2+} in the carbonate and exchangeable extractants, the average Mn-oxidation number was 3.78±0.04. The XRD patterns of the carbonate-free samples indicated a rancieite and takanelite mixture. These 7-Å phyllomanganates are discussed extensively in Lind and Hem (1993). Some calculated Mn-oxidation numbers for 7-Å phyllomanganates are listed in table 19.

The Mn-oxidation numbers of the <20-μm nonmagnetic sediments increased during the

transformation from low Mn, settling sediments (sample LT–NM–SS); to Mn-coated, noncemented streambed particles (samples B–NC–BS and B–A–NC); and finally to Mn crusts (samples B–N–CC and B–A–CC). The oxidation numbers of the crusts from the SR samples and the B samples averaged 3.68±0.03 (table 17).

In addition to the identified minerals in the crusts, indications of other Mn oxides in the particles (<20 μm) of the SR samples, such as Na-birnessite, hausmannite, groutite, and manganite, further illustrate the mixture of minerals in the crusts and suggest that more than one Mn reaction, redox, and (or) disproportionation is occurring simultaneously.

Possible Mn-oxide and Fe-oxide coexistence and interaction during the initial crust formation may be indicated by a spinel resembling hausmannite and possibly jacobsite and ferrihydrite in the nonmagnetic B-sample series and in sample LT–NC–SS. The term "ferrihydrite" applies to a Fe^{3+} hydroxide hydrate that comprises a range of poorly ordered compounds containing 15–25 percent water (Cornell and others, 1989). The presence of goethite in sample LT–NC–SS and possibly of hausmannite and jacobsite in sample SR–B–LC adds to this evidence.

Correlation of Laboratory Manganese Precipitates With Manganese Precipitates in the Alluvium and the Streambed

Near the water table, a loss of dissolved CO_2 causes the pH of the ground water to increase; however, the low O_2 content of the ground water may restrict the rate of Mn oxidation and allow coprecipitation of carbonates such as $(Ca^{2+}Mn^{2+}Mg^{2+})CO_3$ and Mn oxide.

In the laboratory, a solid resembling a Ca-rich kutnahorite crystal form described by Gabrielson and Sundius (1966) was precipitated from sample 503–1 (table 16). The Ca-to-Mg molar ratio of carbonate in an alluvial sample also was similar to this Ca-rich kutnahorite. This alluvial carbonate contained minor amounts of Mn and Fe. The formula for the kutnahorite of Gabrielson and Sundius (1966) indicates that the relative proportions of Mn and Mg can vary. Fe has been measured as a minor component of kutnahorite (Tsusue, 1967). The alluvial sample was collected 6 months after the collection of sample 503 from a well site about 10 m from well 503 at a level about 2 m higher than the screened interval of well 503. The formula for Ca-rich kutnahorite is not greatly different from the composition calculated for the carbonate

Table 19. Calculated manganese oxidation numbers of 7-Å phyllomanganate minerals, Pinal Creek Basin, Arizona

[Values are based on general formula and chemical compositions]

Mineral name	Reference	Manganese oxidation number	General formula
	Earlier definitions		
Takanelite	Nambu and Tanida (1971)	[1]3.65	$(Mn^{2+},Ca)Mn^{4+}{}_4O_9 \cdot H_2O$
Rancieite	Fleischer and Richmond (1943)[2]	[3]4.00	$(Ca, Mn)Mn_4O_9 \cdot H_2O$
	Recent definitions		
Takanelite	Frondel and others (1960)	3.55	[4]$R_{2x}Mn_{1-x}O_2 \cdot nH_3O$
Takanelite	Kim (1991)	3.71	Do.
Rancieite	Richmond and others (1969)	3.90	Do.
Na-birnessite	Jones and Milne (1956)	3.85	Do.
Na-birnessite	Jones and Milne (1956)	3.92	[5]$R'_{2x}Mn^{4+}{}_{1-x}O_2.nH_2O$

[1]Minimum value.
[2]Kim (1990) considered this an impure rancieite containing todorokite and braunite.
[3]Maximum value.
[4]Kim (1990). (R = $M^{2+}$and other cations of 2+ charge).
[5]Kim (1990) concluded a better representation of this mineral probably would be (R' = Mn^{3+} and other cations of 1+ and 2+ charge).

in sample ID–CC–NM–63. In the smaller-sized ID samples, the Ca and Mn content was higher than in ID–CC–NM–63 (table 20).

The XRD pattern for the laboratory precipitate 503–1 correlated well with the Ca-rich kutnahorite, although XRD analysis alone is not sufficient for absolute identification of kutnahorite (Mucci, 1991). The XRD patterns for the ID samples contained many peaks that suggested that kutnahorite was present; however, the usually prominent 100-intensity peak for this mineral was not obvious. The carbonate from the core material was not examined by XRD.

Regardless of whether they are precipitating out of ground water or surface water or are forming by alteration of existing carbonate solids, mixed (Ca, Mn, Mg) carbonates probably contribute to the reactions that occur during the Mn oxide deposition.

Gypsum also was precipitated from sample 503–1. Ca content of gypsum, however, was not a significant component of the Ca content of the carbonate extractant of the alluvial material. In this material, 81 percent of the total extracted sulfate was contained in the carbonate extractant. If all this sulfate were in the form of gypsum, the Ca involved would constitute only about 1 percent of the total Ca in the carbonate extractant.

The precipitation sequence from sample 503–2 probably resembles fairly well the conditions in downstream reaches of Pinal Creek, the conditions under which naturally occurring noncemented streambed oxides are formed. The oxidation number of Mn (3.0) of the precipitate present at the end of the titration suggests that a trivalent Mn oxide predominated. With aging, the Mn oxide disproportionated in the Ca-rich solution to form (Mn,Ca) oxides such as todorokite (Frondel and others, 1960; and Lawrence and others, 1968) and (or) the related species takanelite (Nambu and Tanida, 1971).

As the concentration of dissolved HCO_3 and other CO_2 species decrease and dissolved O_2 increases, the Mn-oxidation rate increases and carbonates no longer precipitate in significant amounts. The CO_2 and HCO_3 content of sample PC1 was decreased before titration began. The Mn-oxidation sequence for precipitation from PC1 was similar to that found in previous laboratory experiments using simpler solutions that contained a Na salt for ionic-strength control and either Mn alone or Mn and one other metal ion as the reacting metal ions. The Mn oxidation sequence in sample PC1 during the titration and aging could lead to the formation of the Mn oxides, hausmannite, manganite, and Na-birnessite (a 7Å-phyllomanganate) that were found in the black coatings and crusts from the Pringle diversion (tables 1, 2).

CRUST FORMATION

The following is a summary of a lengthy discussion of literature findings and data from Pinal Creek (Lind and Hem, 1993) as well as additional observations.

1. Before and during crust formation, Fe- and Mn-rich sediments including Ca- and (or) Mn-rich carbonates, magnetic material (mostly magnetite), amorphous Fe oxides, and silicate minerals may have been washed down from surrounding soils or by turbulence from upstream areas or may already have been in the streambed. These sediments can become incorporated in the developing cemented crusts.

Table 20. Comparison of carbonate compositions, Pinal Creek Basin, Arizona

Sample identifier	Composition	Source
Ca-rich kutnahorite	$Ca_{0.74}(Mn,Mg)_{0.26}CO_3$	Gabrielson and Sundius (1966).
Pinal Creek alluvium	$Ca_{0.73}(Mn,Mg)_{0.27}CO_3$	Calculated from carbonate extractant content in Ficklin and others (1991).
ID–CC–NM–63	$Ca_{0.79}Mn_{0.09}Mg_{0.12}CO_3$	Lind and Hem (1993).
ID–CC–NM–5	$Ca_{0.83\text{-}0.84}(Mn_{0.11\text{-}0.15},Mg_{0.01\text{-}0.05})CO_3$	Do.
ID–CC–NM–38L	Do	Do.
ID–CC–NM–>10H	Do.	Do.

2. Considering saturation indices, calcite ($CaCO_3$) and rhodochrosite ($MnCO_3$) may precipitate from the streamflow in the reach between Setka Ranch and Inspiration Dam.
3. Besides precipitating as $MnCO_3$, dissolved Mn could substitute for Ca in calcite and (or) react with calcite and coprecipitate as $Ca_{(1-x)}Mn^{2+}{}_xCO_3$ resulting in Mn-rich carbonates in the streambed.
4. At the particle surfaces, Mn^{2+} in the surface structure or as surface complexes could oxidize directly as in equation 15 and disproportionate to give more highly oxidized Mn oxides as in equations 16 and 17.
5. Amorphous Fe oxide could deposit on the carbonate phases that contain Mn, and as the Fe-oxide crystal mass develops, the increased pH at the Fe oxide-mixed carbonate interface would tend to increase the Mn^{2+}-oxidation rates.
6. Hausmannite (Mn_3O_4) has some magnetic property and would be attracted to the magnetite in the sediment. Hausmannite would continue to oxidize and thus contribute to the coatings of the magnetic particles.
7. Sediment-degradation products probably are the sources of fine-grained silicate minerals in the <63-μm fraction of the black crusts.
8. Carbonate minerals could act as a cementing mechanism in the black cemented crusts by coating silicate grains. Eychaner (1991c) found that this was the general case for the alluvial material beneath the intermittent reach of the creek. Mn-oxide coatings and the magnetic properties of minerals present also could contribute to the crustal cementation.
9. Trace metals transported in the streamflow can interact with the complex mixture of Fe oxides, Mn oxides, carbonates, and silicates in the black cemented crusts.

TRACE-METAL ASSOCIATIONS

Many factors control trace-metal concentrations and molar-ratio variations of individual trace metals to Mn and to Fe in the extracted phases of the sediments. Some of these controls are trace-metal concentrations, pH and Eh values of the streamflow, Mn-oxide and amorphous Fe-oxide precipitation rates, sedimentation rate, and sediment composition. The following summary concerning metals in the B, LT–NC–SS, and SR samples include observations presented in Lind and Anderson (1992).

1. Besides the high Mn concentration, the fact that Ni was the only other measurable metal in the exchangeable-cation extractant agrees with the fact that Ni has a greater affinity for ion-exchange resins than Cu and Zn (Peters and others, 1974).
2. In the carbonate extractants, Cu was the most concentrated trace metal. Concentrations of Ni and Zn were much higher than concentrations of Fe, Pb, and Cd in all samples except sample LT–NC–SS in which Fe was second to Cu in concentration.
3. Comparison of the trace metal to Mn ratio (μmol/mol) in the Mn-oxide extractants with the trace metal to Fe ratio (μmol/mol) in the amorphous Fe-oxide extractants indicates that Cu, Ni, Zn, and Pb have a greater affinity for Fe than for Mn.
4. Mn oxides are the predominant extractable phase, and for all samples except one, the Mn-oxide extractants contained more grams of total trace metals per gram of sediment than did the amorphous Fe-oxide extractant. In the amorphous Fe oxides of sample SR–B–LC, the Cu concentration was much greater than the total trace-metal concentration in the Mn oxides.
5. The molar ratio of Mn to Fe in the Mn-oxide and amorphous Fe-oxide extractants varied between aliquots of the same samples. This variation indicates that microdomains of differing cation content and extractability are present. These microdomains may contain one or more of hydroxides and oxides of Mn, Fe, and trace metals as well as various combinations of these constituents (Hem, 1980; Hem and Lind, 1983, 1991; Hem and others, 1987, 1989; and Manceau, 1989; table 21, chapter E, this report). Manceau (1989) noted that hydroxide precipitation at solid-solution surfaces is widely recognized and that there is a growing awareness that cations are largely unmixed on a microscopic scale in sediments.
6. Ferrihydrite in the Mn-rich setting of Pinal Creek may convert to Mn goethite and jacobsite. Cornell and Giovanoli (1987) found that ferrihydrite converted to Mn-goethite and (or) jacobsite (a Mn-Fe spinel) in a $MnNO_3$ solution closed to the atmosphere at a pH range of 8 to

14 and at a temperature of 70°C. XRD suggested ferrihydrite and jacobsite in nonmagnetic B samples and sample LT–NC–SS (all <20 μm) and suggested goethite in sample LT–NC–SS. The pH's of the streamflow with which these samples were associated were 7.92, 7.54, and 8.01; and the temperatures were 30, 16, and 18°C, respectively.

7. Ni and Cu concentrations were higher than Zn and Pb concentrations in extractants of the magnetic samples. Ni was the most concentrated metal in the Mn-oxide extractant of the nonmagnetic B samples (<20 μm). In the amorphous Fe-oxide extractants of different aliquots of the same sample of nonmagnetic sediments (<20 μm), molar ratios of Ni to Fe and Zn to Fe (μmol/mol) varied with fluctuations in Mn to Fe (mol/mol). Perhaps Ni becomes incorporated into Mn oxide by initially concentrating on the oxide as an exchangeable cation or by oxidation of mixed carbonates that contain Ni. The correlation of Zn and Ni concentration with the Mn concentration may be explained by the formation of a spinel structure containing Zn and by coprecipitation of Ni hydroxide with Mn-Fe oxides as in the mixed minerals described above in observation 5.
8. The importance of the Cu-Fe relation in the <20-μm, nonmagnetic sediments is illustrated by the facts that in all the amorphous Fe-oxide extractants, the molar ratios of Cu to Fe was greater than that of the other molar ratios of trace metal to Fe, and that Cu concentration related directly to Fe concentration.
9. In the carbonate extractants of sample LT–NC–SS, the molar ratios of Cu to Ca, Cu to Mn, Fe to Ca, and Fe to Mn were higher than in the carbonate extractants of the B samples. Upstream in the well-cemented crust (sample SR–B–CC) and about 5.1 km downstream in the material settling out behind a boulder (sample LT–NC–SS), Cu is concentrated in both the Mn oxides and the amorphous Fe oxides and was more concentrated in these extractants than the other trace metals. Cu concentrations in the amorphous Fe-oxide extractant were greater than in the other extractants both upstream in the loosely-cemented crust (sample SR–B–LC) and in all downstream samples. These facts indicate that although Cu is concentrated in the upstream reach in both the Mn oxides and amorphous Fe oxides of the well-cemented crust, Cu is concentrated in primarily the amorphous Fe oxides of the loosely cemented crust and is transported downstream in Fe-rich carbonates and amorphous Fe oxides.
10. The relations of Cu to Fe may be attributed to the greater percentage of highest energy-binding sites in goethite than in δ-MnO_2 (Catts and Langmuir, 1986) and to the many possible Fe-Cu oxides resulting from redox reactions of Fe^{2+} and Fe^{3+} with Cu^{+} and Cu^{2+}. XRD suggested goethite was present in sample LT–NC–SS.

Amorphous Fe oxide has been shown to be the principal sorbent that controls the distribution of Cu, Ni, and Co in the alluvium underlying the intermittent reach of Pinal Creek (Stollenwerk, 1990, 1991). Amorphous Fe oxide, if suspended in the ground water,

Table 21. Some potential constituents of microdomains of manganese deposits

Spinels	(Oxy)hydroxides	Other oxides
Hausmannite (Mn_3O_4)	Manganite (γMnOOH)	Pyrolusite (MnO_2)
Jacobsite ($mnFe_2O_4$)	Groutite (αMnOOH)	Hematite (Fe_2O_3)
Hetaerolite ($ZnMn_2O_4$)	Goethite (αFeOOH)	Cadmium manganese oxide ($Cd_2Mn_3O_8$)
Magnetite (Fe_3O_4)		Copper manganese oxide ($Cu_2Mn_3O_8$)
		Tenorite (CuO)
7-Å phyllomanganates	**Carbonates**	**Other mineral forms**
Na birnessite	Carbonates with varying ratios of	Ferrihydrite
Rancieite	Ca, Mn, and Mg such as kutnahorite	$Ni(OH)_2$
Takanelite	Otavite ($CdCO_3$)	Mixed minerals such as Ni asbolane (interlayers of MnO_2 and $Ni(OH)_2$)

would continue to transport these trace metals when the ground water becomes part of the surface flow. Fe and Mn oxides in suspended sediments or in coatings of mobile streambed sediments are transport media for trace metals in the perennial reach of Pinal Creek.

Trace metals, especially Cu, have a preference for amorphous Fe oxide over Mn oxides. Mn oxides, however, make a significant contribution to the distribution of trace metals, especially Ni. Mn coatings and crusts concentrate and immobilize the trace metals in the stream bottom and stream banks.

Mn deposits consist primarily of particles <63 μm in diameter. When crusts are broken up by turbulence due to increased streamflow or when the cementing material (carbonates-?) is removed by chemical action, these fine-grained Mn-oxide particulates and associated trace metals are readily transported downstream. As of 1990, intermittent sediment transport was a major vehicle for trace-metal conveyance out of the Pinal Creek Basin (Eychaner, 1991c). Eychaner (1991c) states that "A median annual flood of 35 km^3/second could transport 10 to 50 megagrams of Mn in a single day."

SUMMARY AND CONCLUSIONS

Amorphous Fe oxides have been shown to be a major factor in trace-metal distribution in ground water and surface water of Pinal Creek Basin. Mn-rich strata in the alluvium beneath the intermittent reach of Pinal Creek and Mn-rich sediment in the stream bottom along the perennial reach of the creek have been shown to concentrate and immobilize trace metals from the metal-rich surface water.

A carbonate resembling the mineral kutnahorite may be present in the Pinal Creek alluvium and streambed sediments. Increasing the pH of a ground-water sample in the laboratory precipitated hausmannite and a $Ca(Mn,Mg)CO_3$ that resembled kutnahorite. The carbonate fraction of alluvial material from a nearby well site had a Ca/(Mn,Mg) ratio similar to kutnahorite. The alluvial material was obtained from a depth that was slightly higher than the depth of the source of the ground-water sample. The composition of the $Ca(Mn,Mg)CO_3$ from particles (45–63 μm) in the streambed crusts sampled in 1990 at Inspiration Dam also did not differ significantly from that of kutnahorite.

Increasing the pH of oxygenated, low CO_2 surface water initially precipitated Mn oxide as hausmannite, which subsequently altered to manganite. This precipitation sequence was found in laboratory solutions containing only a single salt (for ionic-strength control) and Mn or Mn and one other metal (as the reacting metal ions). These oxides can further oxidize to a 7 Å-phyllomanganate. The Mn oxides reported in the coatings of rocks and pebbles in contact with the streamflow at the Pringle diversion represent a mixture of all three oxides. Black stream sediments are composed of Mn oxides, (Ca,Mn) carbonates, amorphous Fe oxides, silicates, and a notable fraction of magnetic material (primarily magnetite with some hematite). Size distribution and relative amounts of each type of mineral in the less than 250-μm fraction of the sediments varies with the sediment sample. Magnetic material is most concentrated in the larger particles, and the Mn oxides are concentrated in the <63-μm particles. Mn oxides can comprise as much as 70 percent or more of these smaller particles.

Molar ratio of Fe to Mn was high in the large particles of the sediments and low in the coatings of the large particles. Molar ratio decreased with particle size and decreased as the sediments changed from coatings and loose sediments to cemented crusts. Molar ratio of Fe to Mn in the Mn oxides decreased as the Mn-oxidation number increased.

Development of more highly oxidized Mn species is shown by an increase in the Mn oxidation number as the sediments change from settling sediment to loose stream-bottom material and then to cemented crusts. Mn-oxide composition of the black, Mn-rich sediments varies with the degree of oxidation. In the crusts, the composition is mostly 7-Å phyllomanganates, such as Na birnessite or more likely a rancieite-takanelite mixture. A Mn oxidation number as high as 3.78 has been measured for these 7-Å phyllomanganates.

Mn oxides may form by a complex reaction system that includes incorporation of Mn in carbonates by precipitation, substitution of Mn^{2+} for Ca in calcite, and Mn coprecipitation with Ca. Whether part of the surface structure or present as a surface complex bound to hydrous oxides, Mn^{2+} at particulate surfaces initially oxidizes primarily to hausmannite and then disproportionates to form more oxidized species at temperatures near 25°C. Where Fe oxides are precipitating on carbonate surfaces, the oxidation rate would be increased if the Mn-Fe interaction occurred at the higher pH interface between Fe-oxide and carbonate particles.

Comparison of molar ratios of trace metals to Fe and Mn to Fe for duplicate samples suggested microdomains of differing composition. Microdomains are consistent with literature findings and with previous laboratory results describing some possible components of these microdomains. The microdomains may be mixtures of the Mn oxides, such as hausmannite, manganite, and 7-Å phyllomanganates (Na birnessite, rancieite, and takanelite). Mixed trace metal and Mn oxides, such as hetaerolite, jacobsite, cadmium manganese oxide ($Cd_2Mn_3O_8$), and copper manganese oxide ($Cu_2Mn_3O_8$) also are included. Coprecipitates, such as otavite ($CdCo_3$), tenorite (CuO), and nickel hydroxides as well as mixed minerals, such as Ni-asbolane are other possible microdomain constituents.

A much higher trace-metal concentration existed in the Fe- and Mn-oxide extractants than in the carbonate extractants. Even though there is a trace-metal affinity for Fe, the Mn-oxide extractant contained the highest concentration of trace metals per weight of sediment and probably was because the Mn oxides were the main constituents of the black sediments.

Molar ratios of trace metal to Mn oxide and trace metal to Fe oxide were much higher in the <20-μm sediments than in the 150–250-μm magnetic particles. Extraction data indicate that Ni may be incorporated into Mn oxide by initially concentrating on the oxide as an exchangeable cation or by oxidation of mixed carbonates that contain Mn and Ni. The correlation of Zn and Ni concentration with the Mn concentration may be explained by the formation of a spinel structure containing Zn and by coprecipitation of Ni hydroxide with Mn oxides to form the mixed minerals described above. The Ni content of the sediments decreased in concentration as the crusts formed and aged. Ni is retained and transported downstream in the Mn-oxide portion of the sediments and crusts. Although Cu is concentrated in the upstream reach in both the Mn oxides and amorphous Fe oxides of well-cemented crust, Cu is concentrated in the amorphous Fe oxides of the loosely-cemented crust and is transported downstream in Fe-rich carbonates and amorphous Fe oxides. Extraction data suggest a Cu affinity to Fe that may be attributed to the greater percentage of highest energy of binding sites in goethite compared with δ-MnO_2 and to the many possible Fe-Cu oxides resulting from Fe-Cu redox reactions.

SELECTED REFERENCES

Aggett, J., and O'Brian, G.A., 1985, Detailed model for the mobility of arsenic in lacustrine sediments based on measurements in Lake Ohakuri: Environmental Science and Technology, v. 19, no. 3, p. 231–238.

Allison, J.D., Brown, D.S., and Novo-Gradic, K.J., 1991, MINTEQA2/PRODEFA2, a geochemical assessment model for environmental systems—Version 3.0 user's manual: Athens, Georgia, U.S. Environmental Protection Agency Report EPA/600/3–91/021, 106 p.

Anderson, T.W., Freethey, G.W., and Tucci, Patrick, 1992, Geohydrology and water resources of alluvial basins in south-central Arizona and parts of adjacent States: U.S. Geological Survey Professional Paper 1406–B, 67 p.

Arizona Bureau of Mines, 1969, Geology and mineral resources of Arizona: Arizona Bureau of Mines Bulletin 180, 467 p. [reprinted 1989]

Arthur, G.V., 1986, NPDES compliance monitoring report, Inspiration operations, NPDES Permit Number AZ0020508, May 1, 1986: U.S. Environmental Protection Agency, Water Management Division, Region 9, v.p.

———1987a, NPDES sampling, documentation, and results report, Inspiration operations, Identification Number AZD008398521, January 7, 1987: U.S. Environmental Protection Agency, Water Management Division, Region 9, v.p.

———1987b, NPDES compliance monitoring report, Inspiration operations, NPDES Permit Number AZ0020508, April 17, 1987: U.S. Environmental Protection Agency, Water Management Division, Region 9, v.p.

Asghar, M., and Kanehiro, Y., 1981, The fate of applied iron and manganese in an oxisol and a ultisol from Hawaii: Soil Science, v. 131, no. 1, p. 53–55.

Beckett, P.G., 1917, The water problem at the Old Dominion Mine: American Institute of Mining Engineers, Transactions, v. 55, p. 35–66.

Biswas, A.K., and Davenport, W.G., 1980, Extractive metallurgy of copper, 2d ed.: Oxford, England, Pergamon Press, 438 p.

Brown, J.G., 1990, Chemical, geologic, and hydrologic data from the study of acidic contamination in the Miami Wash-Pinal Creek area, Arizona, water years 1988–89: U.S. Geological Survey Open-File Report 90–395, 75 p.

Buddemeier, R.W., and Hunt, J.R., 1988, Transport of colloidal contaminants in ground water—Radionuclide migration at the Nevada test site: Applied Geochemistry, v. 3, no. 5, p. 535–548.

Burch, H.K., 1916, Mine and mill plant of the Inspiration Consolidated Copper Company: American Institute of Mining Engineers, Transactions, v. 55, p. 707–740.

Burgin, L.B., 1986, The mineral industry of Arizona, *in* Area Reports—Domestic: U.S. Bureau of Mines Minerals Yearbook 1984, v. II, p. 65–85.

Catts, J.G., and Langmuir, D., 1986, Adsorption of Cu, Pb, and Zn by δ-MnO_2—Applicability of the site binding-surface complexation model: Applied Geochemistry, v. 1, p. 255–264.

Central Arizona Association of Governments, 1983, Past and current major mining operations in the Globe-Miami area: Florence, Arizona, Central Arizona Association of Governments Report METF–2, 106 p.

Cerda, C.M., 1987, Mobilization of kaolinite fines in porous media: Colloids and Surfaces, v. 27, p. 219–241.

Champlin, J.B.F., and Eichholz, G.G., 1976, Fixation and remobilization of trace contaminants in simulated subsurface aquifers: Health Physics, v. 30, p. 215–219.

Chao, T.T., 1972, Selective dissolution of manganese oxides from soils and sediments with acidified hydroxylamine-HCl: Soil Science Society of America Proceedings, v. 36, p. 764–768.

Chao, T.T., and Zhou, Liyi, 1983, Extraction techniques for selective dissolution of amorphous iron oxides from soils and sediments: Soil Science Society of America Journal, v. 47, p. 225–232.

Cooper Aerial Survey Co., 1989, Pinal Creek project topographic maps: Claypool, Arizona, Cyprus Miami Mining Corporation, 17 sheets, scale 1:4,800.

Cornell, R.M., and Giovanoli, Rudolf, 1987, Effect of manganese on the transformation of ferrihydrite into goethite and jacobsite in alkaline media: Clays and Clay Minerals, v. 35, p. 11–20.

Cornell, R.M., Giovanoli, Rudolf, and Schindler, Walter, 1989, Review of the hydrolysis of iron (III) and the crystallization of amorphous iron (III) hydroxide hydrate: Journal of Chemical Technology and Biotechnology, v. 46, p. 115–134.

Daily Silver Belt, 1912, Pipe line from Burch to Miami: Globe, Arizona, Daily Silver Belt, v. 6, no. 294, September 8, 1912, p. 5.

Davies, Simon, 1986, Mn(II) oxidation in the presence of lepidocrocite—The influence of other ions, *in* Davis, James, and Hayes, Kim, eds., Geochemical Processes at Mineral Surfaces: Washington, D.C., American Chemical Society Symposium Series 323, p. 491.

Davis, J.A., and Kent D.B., 1990, Surface complexation modeling in aqueous geochemistry, *in* Hochella, M.F., Jr., and White, A.F., eds., Mineral-Water Interface Geochemistry: Mineralogical Society of America, Reviews in Mineralogy, v. 23, chap. 5, p. 177–260.

Diem, Dieter, and Stumm, Werner, 1984, Is dissolved Mn^{2+} being oxidized by O_2 in absence of Mn-bacteria or surface catalysts?: Geochimica et Cosmochimica Acta, v. 48, p. 1571–1773.

Dreimanis, A., 1962, Quantitative gasometric determination of calcite and dolomite by using Chittick apparatus: Journal of Sedimentary Petrology, v. 32, no. 3, p. 520–529.

Dzombak, D.A., and Morel, F.M.M., 1990, Surface complexation modeling: New York, John Wiley and Sons, 393 p.

Earl, T.A., 1973, A hydrogeologic study of an unstable open-pit slope, Miami, Gila County, Arizona: Tucson, University of Arizona, unpublished doctoral thesis, 154 p.

Enfield, C.G., and Bengtsson, G., 1988, Macromolecular transport of hydrophobic contaminants in aqueous environments: Groundwater, v. 26, no. 1, p. 64–76.

Envirologic Systems, Inc., 1983, Mining activities and water-quality report: Florence, Arizona, Central Arizona Association of Governments Report METF–7, 137 p.

Eychaner, J.H., 1988, Evolution of acidic ground-water contamination in a copper-mining area in Arizona, *in* Ouazar, D., Brebbia, C.A., and Stout, G.E., eds., Water Quality, Planning, and Management: New York, Springer–Verlag, v. 6, Computer Methods and Water Resources, First International Conference, Morocco, 1988, Proceedings, p. 291–302.

———1989, Movement of inorganic contaminants in acidic water near Globe, Arizona, *in* Mallard, G.E., and Ragone, S.E., eds., U.S. Geological Survey Toxic Substances Hydrology Program—Proceedings of the Technical Meeting, Phoenix, Arizona, September 26–30, 1988: U.S. Geological Survey Water-Resources Investigations Report 88–4220, p. 567–575.

———1991a, Inorganic contaminants in acidic water near Globe, Arizona, *in* Survival in the Desert: Water Quality and Quantity Issues into the 21st Century: Arizona Hydrological Society, Proceedings of the Third Annual Symposium, Casa Grande, Arizona, September 20–22, 1990, p. 242–252.

———1991b, Solute transport in perennial streamflow at Pinal Creek, Arizona, *in* Mallard, G.E., and Aronson, D.A., eds., U.S. Geological Survey Toxic Substances Hydrology Program—Proceedings of the Technical Meeting, Monterey, California, March 11–15, 1991: U.S. Geological Survey Water-Resources Investigations Report 91–4034, p. 481–485.

———1991c, The Globe, Arizona, research site—Contaminants related to copper mining in a hydrologically integrated environment, *in* Mallard, G.E., and Aronson, D.A., eds., U.S. Geological Survey Toxic Substances Hydrology Program—Proceedings of the Technical Meeting, Monterey, California, March 11–15, 1991: U.S. Geological Survey Water-Resources Investigations Report 91–4034, p. 439–447.

Eychaner, J.H., and Stollenwerk, K.G., 1985, Neutralization of acidic ground water near Globe, Arizona, *in* Schmidt, K.D., ed., Proceedings of Symposium on Groundwater Contamination and Reclamation: Bethesda, Maryland, American Water Resources Association, Tucson, Arizona, August 14–15, 1985, p. 141–148.

———1987, Acidic ground-water contamination from copper mining near Globe, Arizona—I. Overview, *in* Franks, B.J., ed., U.S. Geological Survey Program on Toxic Waste—Ground-Water Contamination—Proceedings of the Third Technical Meeting, Pensacola, Florida, March 23–27, 1987: U.S. Geological Survey Open-File Report 87–109, p. D–13 to D–18.

Eychaner, J.E., Rehmann, M.E., and Brown, J.G., 1989, Chemical, geologic, and hydrologic data from the study of acidic contamination in the Miami Wash-Pinal Creek area, Arizona, water years 1984–87: U.S. Geological Survey Open-File Report 89–410, 105 p.

Faires, L.M., and Eychaner, J.H., 1991, Trace-element trends at Pinal Creek, Arizona, *in* Mallard, G.E., and Aronson, D.A., eds., U.S. Geological Survey Toxic Substances Hydrology Program—Proceedings of the Technical Meeting, Monterey, California, March 11–15, 1991: U.S. Geological Survey Water-Resources Investigations Report 91–4034, p. 461–465.

Farnham, L.L., Stewart, L.A., and DeLong, C.W., 1961, Manganese deposits of eastern Arizona: U.S. Bureau of Mines Information Circular 7990, 178 p.

Ficklin, W.H., Love, A.H., and Briggs, P.K., 1991a, Analytical results for total and partial metal extractions in aquifer material, Pinal Creek, Globe, Arizona: U.S. Geological Survey Open-File Report 91–111, 33 p.

Ficklin, W.H., Love, A.H., and Papp, C.S.E., 1991b, Solid-phase variations in an aquifer as the aqueous solution changes, Globe, Arizona, *in* Mallard, G.E., and Aronson, D.A., eds., U.S. Geological Survey Toxic Substances Hydrology Program—Proceedings of the Technical Meeting, Monterey, California, March 11–15, 1991: U.S. Geological Survey Water-Resources Investigations Report 91–4034, p. 475–480.

Fishman, M.V., and Friedman, L.C., eds., 1989, Methods for determination of inorganic substances in water and fluvial sediments: U.S. Geological Survey Techniques of Water-Resources Investigations book 5, chap. A1, 545 p.

Fleischer, M., and Richmond, W.E., 1943, The manganese oxide minerals—A preliminary report: Economic Geology, v. 38, no. 4, p. 269–286.

Freethey, G.W., Pool, D.R., Anderson, T.W., and Tucci, Patrick, 1986, Description and generalized distribution of aquifer materials in the alluvial basins of Arizona and adjacent parts of California and New Mexico: U.S. Geological Survey Hydrologic Investigations Atlas HA–663, 4 sheets.

Frondel, Clifford, Marvin, U.B., and Ito, J., 1960, New data on birnessite and hollandite: American Mineralogist, v. 45, no. 7 and 8, p. 871–875.

Gabrielson, O., and Sundius, N., 1966, Ca-rich kutnahorite from Långban, Sweden: Arkiv for Mineralogi och Geologi, v. 4, no. 6, p. 287–289.

Gilbert, G.K., 1875, Report on the geology of portions of New Mexico and Arizona: U.S. Geographical and Geological Surveys West 100th Meridian Report, v. 3, p. 525–544.

Gilkey, M.M., and Beckman, R.T., 1963, Water requirements and uses in Arizona mineral industries: U.S. Bureau of Mines Information Circular 8162, 97 p.

Golden, D.C., Dixon, J.B., and Chen, C.C., 1986, Ion exchange, thermal transformations, and oxidizing properties of birnessite: Clays and Clay Minerals, v. 34, no. 5, p. 511–520.

Greeley, M.N., and Kissinger, L.E., 1990, The mineral industry of Arizona: U.S. Bureau of Mines Minerals Yearbook 1988, p. 69–81.

Gschwend, P.M., and Reynolds, M.D., 1987, Monodisperse ferrous phosphate colloids in an anoxic groundwater plume: Journal of Contaminant Hydrology, v. 1, no. 3, p. 309–327.

Guy, H.P., and Norman, V.W., 1970, Field methods for measurement of fluvial sediment: U.S. Geological Survey Techniques of Water-Resources Investigations book 3, chap. C2, 59 p.

Hardwick, W.R., 1963, Mining methods and costs, Inspiration Consolidated Copper Co. open-pit mine, Gila County, Arizona: U.S. Bureau of Mines Information Circular 8154, 64 p.

Hazen, G.E., and Turner, S.F., 1946, Geology and ground-water resources of the upper Pinal Creek area, Arizona: U.S. Geological Survey unnumbered open-file report, 55 p.

Heindl, L.A., 1958, Cenozoic alluvial deposits of the Upper Gila River area, New Mexico and Arizona: Tucson, University of Arizona, doctoral dissertation, 249 p.

Hem, J.D., 1978, Surface chemical processes in ground-water systems, *in* Paquet, H., and Tardy, Y., eds., Proceedings of the Second International Symposium on Water-Rock Interaction: Strasbourg, France, Université Louis Pasteur Centre National de la Recherche Scientifique Institute de Géologie, v. IV, p. 76–85.

———1980, Redox coprecipitation mechanisms of manganese oxide, *in* Kavanaugh, M.C. and Leckie, J.O. eds., Particulates in Water: Washington, D.C., American Chemical Society, Advances in Chemistry Series 189, p. 45–72.

Hem, J.D., and Lind, C.J., 1983, Nonequilibrium models for predicting forms of precipitated manganese oxides: Geochimica et Cosmochimica Acta, v. 47, no. 11, p. 2037–2046.

———1991, Coprecipitation mechanisms and products in manganese oxidation in the presence of cadmium: Geochimica et Cosmochimica Acta, v. 55, no. 9, p. 2435–2451.

———1994, Chemistry of manganese precipitation in Pinal Creek, Arizona, U.S.A.—A laboratory study: Geochimica et Cosmochimica Acta, v. 58, p. 1601–1613.

Hem, J.D., Roberson, C.E., and Lind, C.J., 1987, Synthesis and stability of hetaerolite, $ZnMn_2O_4$, at 25°C: Geochimica et Cosmochimica Acta, v. 51, no. 6, p. 1539–1547.

Hem, J.D., Lind, C.J., and Roberson, C.E., 1989, Coprecipitation and redox reactions of manganese oxides with copper and nickel: Geochimica et Cosmochimica Acta, v. 53, no. 11, p. 2811–2822.

Honeyman, P.D.I., 1954, The "new look" at Inspiration: Mining Congress Journal, September 1954, v. 40, no. 9, p. 30–32, 72.

Hydro Geo Chem, Inc., 1989, Investigation of acid water contamination along Miami Wash and Pinal Creek, Gila County, Arizona: Claypool, Arizona, Cyprus Miami Mining Corporation, 140 p.

Jenne, E.A., 1968, Controls on Mn, Fe, Co, Ni, Cu, and Zn concentrations in soils and water—The significant role of hydrous Mn and Fe oxides, *in* Gould, R.F., ed., Trace Inorganics in Water: Washington, D.C., American Chemical Society, Advances in Chemistry Series 73, p. 337–387.

Jones, L.H.P., and Milne, A.A., 1956, Birnessite, a new manganese oxide mineral from Aberdeenshire, Scotland: Mineralogy Magazine, v. 31, p. 283–385.

Kim, S.J., 1990, Crystal chemistry of hexagonal 7 Å-phyllomanganate minerals: Journal of the Mineralogical Society of Korea, v. 3, p. 34–43.

———1991, New characterization of takanelite: American Mineralogist, v. 76, p. 1426–1430.

Kim, J.I., Buckau, G, Baumgartner, F., Moon, H.C., and Lux, D., 1984, Colloid generation and actinide migration in Gorleben groundwaters, *in* McVay, G.L., ed., Scientific Basis for Nuclear Waste Management: New York, Elsevier Publishing Company, v. 7, p. 31–40.

Kiven, C.W., and Ivey, J.B., 1981, Geology of the Pinal and Pinto Creek drainage basins, Gila, Pinal, and Maricopa Counties, Arizona: Florence, Arizona, Central Arizona Association of Governments Report METF–4, 64 p.

Krisnamurti, G.S.R., and Huang, P.M., 1987, The catalytic role of birnessite in the transformation of iron: Canadian Journal of Soil Science, v. 67, no. 3, p. 533–543.

Larson, L.P., and Henkes, W.C., 1970, The mineral industry of Arizona, *in* Area Reports—Domestic: U.S. Bureau of Mines Minerals Yearbook 1968, v. III, p. 89–111.

Lawrence, L.J., Bayliss, P., and Tonkin, P., 1968, An occurrence of todorokite in the deuteric stage of a basalt: Mineralogical Magazine, v. 36, p. 757–760.

Lind, C.J., and Anderson, L.D., 1992, Trace metal scavenging by precipitating Mn and Fe oxides, *in* Kharaka, Y.K., and Maest, A.S., eds., Proceedings of the 7th International Water-Rock Interaction-WRI–7, Park City, Utah: Rotterdam, Balkema Publishers, v. 1, p. 397–402.

Lind, C.J., and Hem, J.D., 1993, Manganese minerals and associated fine particulates in the streambed of Pinal Creek, Arizona—A mining-related acid drainage problem: Applied Geochemistry, v. 8, no. 1, p. 67–68.

Lind, C.J., Hem, J.D., and Roberson, C.E., 1987, Reaction products of manganese-bearing waters, *in* Averett, R.C., and McKnight, D.M., eds., Chemical Quality of Water and the Hydrologic Cycle: Chelsea, Michigan, Lewis Publishers, Inc., p. 271–301.

Liang, L., and Morgan, J.J., 1990, Chemical aspects of iron oxide coagulation in water—Laboratory Studies and Implications for Natural Systems: Aquatic Sciences, v. 52, no. 1, p. 32–55.

Lindberg, R.D., and Runnels, D.D., 1984, Ground water redox reactions—An analysis of equilibrium state applied to Eh measurements and geochemical modeling: Science, v. 225, no. 4665, p. 925–927.

Longsworth, S.A., and Taylor, A.M., 1992, Hydrologic data from the study of acidic contamination in the Miami Wash-Pinal Creek area, Arizona, water years 1990–91: U.S. Geological Survey Open-File Report 92–468, 59 p.

Manceau, A., 1989, Synthetic 10-Å and 7-Å phyllomanganates: Their structures as determined by EXAFS—Discussion: American Mineralogist, v. 74, no. 11, p. 1386–1389.

Matijevic, E., and Scheiner, P., 1978, Ferric hydrous oxide solutions—Part III, Preparation of uniform particles by hydrolysis of Fe(III)-chloride, -nitrate, and -perchlorate solutions: Journal of Colloid and Interface Science, v. 63, no. 3, p. 509–524.

Morris, J.C., and Stumm, Werner, 1967, Redox equilibria and measurements of potentials in the aquatic environment, *in* Stumm, Werner, ed., Equilibrium Concepts in Natural Water Systems: Washington, D.C., American Chemical Society, Advances in Chemistry Series 67, p. 270–285.

Mucci, A., 1991, The solubility and free energy of formation of natural ķutnahorite: Canadian Mineralogist, v. 29, no. 1, p. 113–121.

Nambu, M., and Tanida K., 1971, New mineral takanelite: Journal of the Japanese Association of Mineralogy, Petrology, and Economic Geology, v. 45, p. 48–56.

National Atmospheric Deposition Program, 1990, NADP/NTN annual data summary of precipitation chemistry in the United States—1989: Fort Collins, Colorado State University, Natural Resource Ecology Laboratory, 482 p.

Naumov, G.B., Ryzhenko, B.N., and Khodakovsky, I.L., 1974, Handbook of thermodynamic data: U.S. Department of Commerce, NTIS Report PB–266/722, 328 p.

Neaville, C.C., 1991, Hydrogeology and simulation of ground-water and surface-water flow in Pinal Creek basin, Gila County, Arizona: Tucson, University of Arizona master's thesis, 149 p.

Neaville, C.C., and Brown, J.G., 1994, Hydrogeology and hydrologic system of Pinal Creek basin, Gila County, Arizona: U.S. Geological Survey Water-Resources Investigations Report 93–4212, 33 p.

Nordstrom, D.K., 1982, The effect of sulfate on aluminum concentrations in natural waters—Some stability relations in the system Al_2O_3-SO_3-H_2O at 298°K: Geochimica et Cosmochimica Acta, v. 46, no. 4, p. 681–692.

Nordstrom, D.K., Jenne, E.A., and Ball, J.W., 1979, Redox equilibria of iron in acid mine waters, *in* Jenne, E.A., ed., Chemical Modeling in Aqueous Systems: Washington, D.C., American Chemical Society Symposium Series 93, p. 51–79.

Nordstrom, D.K., Plummer, L.N., Langmuir, D., Busenberg, E., May, H.M., Jones, B.F., and Parkhurst, D.L., 1990, Revised chemical equilibrium data for major water-mineral reactions and their limitations, *in* Melchior, D.C., and Bassett, R.L., eds., Aqueous System II: Washington, D.C., American Chemical Society Symposium series 416, p. 398–413.

Packham, R.F., 1965, Some studies of the coagulation of dispersed clays with hydrolyzing salts: Journal of Colloidal Science, v. 20, no. 1, p. 81–92.

Parkhurst, D.L., Thorstenson, D.C., and Plummer, L.N., 1980, PHREEQE—A computer program for geochemical calculations, revised edition: U.S. Geological Survey Water-Resources Investigations Report 80–96, 193 p.

Penrose, W.R., Polzer, W.L., Essington, E.H., Nelson, D.M., and Orlandi, K.A., 1990, Mobility of plutonium and americium through a shallow aquifer in a semiarid region: Environmental Science and Technology, v. 24, no. 2, p. 228–233.

Peters, D.G., Hayes, J.M., and Hieftje, G.M., 1974, Chemical separations and measurements—Theory and practice of analytical chemistry: Philadelphia, Pennsylvania, Saunders Publishers, p. 583.

Peterson, N.P., 1962, Geology and ore deposits of the Globe-Miami district, Arizona: U.S. Geological Survey Professional Paper 342, 151 p.

Pool, D.R., and Eychaner, J.H., 1995, Measurements of aquifer-storage change and specific yield using gravity surveys: Ground Water, v. 33, no. 3, p. 425–432.

Postma, D., 1985, Concentration of Mn and separation from Fe in sediments—I. Kinetics and stoichiometry of the reaction between birnessite and dissolved Fe(II) at 10°C: Geochimica et Cosmochimica Acta, v. 49, no. 4, p. 1023–1033.

Puls, R.W., and Barcelona, M.J., 1989, Filtration of ground water samples for metals analyses: Hazardous Waste and Hazardous Materials, v. 6, no. 4, p. 385–393.

Puls, R.W., and Powell, R.M., 1992, Transport of inorganic colloids through natural aquifer material—Implications for Contaminant Transport: Environmental Science and Technology, v. 26, no. 3, p. 614–621.

Puls, R.W., Eychaner, J.H., and Powell, R.M., 1990, Colloidal-facilitated transport of inorganic contaminants in ground water—Part 1. Sampling considerations: Ada, Oklahoma, U.S. Environmental Protection Agency, Robert S. Kerr Environmental Research Laboratory, Environmental Research Brief EPA/600/M/90/023, 12 p.

Puls, R.W., Powell, R.M., and Rees, T.F., 1991, Stability and transport of inorganic colloids through contaminated aquifer material, *in* Mallard, G.E., and Aronson, D.A., eds., U.S. Geological Survey Toxic Substances Hydrology Program—Proceedings of the Technical Meeting, Monterey, California, March 11–15, 1991: U.S. Geological Survey Water–Resources Investigations Report 91–4034, p. 507–510.

Puls, R.W., Clark, D.A., Bledsoe, B., Powell, R.M., and Paul, C.J., 1992, Metals in ground water—sampling artifacts and reproducibility: Hazardous Waste and Hazardous Materials, v. 9, no. 2, p. 149–162.

Ransome, F.L., 1903, Geology of the Globe copper district, Arizona: U.S. Geological Survey Professional Paper 12, 168 p.

———1919, The copper deposits of Ray and Miami, Arizona: U.S. Geological Survey Professional Paper 115, 192 p.

Richmond, W.E., Fleischer, M., and Morse, M.D., 1969, Studies on manganese oxide minerals—IX, Rancieite: Bulletin de la Societe Francaise de Mineralogie et de Cristallographie, v. 92, no. 2, p. 191–195.

Robertson, F.N., 1991, Geochemistry of ground water in alluvial basins of Arizona and adjacent parts of Nevada, New Mexico, and California: U.S. Geological Survey Professional Paper 1406–C, 90 p.

Robertson, W.D., Barker, J.F., LeBeau, Y, and Marcous, S., 1984, Contamination of an unconfined sand aquifer by Waste Pulp Liquor—A case study: Ground Water, v. 22, no. 2, p. 191–197.

Rouse, J.V., 1981, Geohydrology of the Globe-Miami, Arizona, area: Florence, Arizona, Central Arizona Association of Governments, Mineral Extraction Task Force Report METF–5, 103 p.

———1983, Water quality report for the Globe-Miami area, Arizona: Florence, Arizona, Central Arizona Association of Governments, Mineral Extraction Task Force Report METF–6, 2 volumes, 448 p.

Ryan, J.N., and Gschwend, P.M., 1990, Colloid mobilization in two Atlantic Coastal Plain aquifers—Field studies: American Geophysical Union, Water Resources Research, v. 26, no. 2, p. 307–322.

Saltelli, A., Avogadro, A, and Bidoglio, G., 1984, Americium filtration in glauconitic sand columns: Nuclear Technology, v. 67, p. 245–254.

Sellers, W.D., Hill, R.H., and Sanderson-Rae, Margaret, eds., 1985, Arizona climate—The first hundred years: Tucson, Arizona, University of Arizona Press, 80 p.

Sheffer, H.W., and Evans, L.G., 1968, Copper leaching practices in the western United States: U.S. Bureau of Mines Information Circular 8341, 57 p.

Skougstad, M.W., Fishman, M.J., Friedman, L.C., Erdmann, D.E., and Duncan, S.S., eds., 1979, Methods for determination of inorganic substances in water and fluvial sediments: U.S. Geological Survey Techniques of Water-Resources Investigations, book 5, chap. A1, 626 p.

Snodgrass, W.J., Clark, M.M., and O'Melia, C.R. 1984, Particle formation and growth in dilute aluminum (III) solutions—Characterization of particle size at a pH of 5.5: American Geophysical Union, Water Resources Research, v. 18, no. 4, p. 479–488.

Stollenwerk, K.G., 1988, Neutralization of acidic ground water in eastern Arizona, *in* Ragone, S.E., ed., U.S. Geological Survey Program on Toxic Waste—Ground-Water Contamination: Proceedings of the second technical meeting, Cape Cod, Massachusetts, October 21–25, 1985: U.S. Geological Survey Open-File Report 86–481, p. E–7 to E–8.

_____ 1990, Simulation of the sorption of Co, Cu, Ni, and Zn with a two-site, diffuse layer sorption model: EOS Transactions, American Geophysical Union, v. 71, no. 17, p. 519.

_____ 1991, Simulation of copper, cobalt, and nickel sorption in an alluvial aquifer near Globe, Arizona, *in* Mallard, G.E., and Aronson, D.A., eds., U.S. Geological Survey Toxic Substances Hydrology Program—Proceedings of the Technical Meeting, Monterey, California, March 11–15, 1991: U.S. Geological Survey Water-Resources Investigations Report 91–4034, p. 502–506.

Stone, A.J., and Morgan, J.J., 1987, Reductive dissolution of metal oxides, *in* Stumm, Werner, ed., Aquatic Surface Chemistry: New York, John Wiley and Sons, chap. 9, p. 221–254.

Stumm, Werner, and Morgan, J.J., eds., 1981 Aquatic Chemistry, 2nd ed.: New York, John Wiley and Sons, 780 p.

Timmers, Jake, 1986, Response to finding of violation and order IX–FY86–78: Inspiration Consolidated Copper Company letter to U.S. Environmental Protection Agency, Water Management Division, August 27, 1986, 44 p.

Tessier, A., Campbell, P.G.C., and Bisson, M., 1979, Sequential extraction procedure for the speciation of particulate trace metals: Analytical Chemistry, v. 51, no. 7, p. 844–851.

Titley, S.R., and Hicks, C.L., eds., 1966, Geology of the porphyry copper deposits, southwestern North America: Tucson, University of Arizona Press, 287 p.

Traina, S.J., and Doner, H.E., 1985, Copper-manganese(II) exchange on a chemically reduced birnessite: Soil Science Society of America Journal, v. 49, no. 2, p. 307–313.

Tsusue, Akio, 1967, Magnesium kutnahorite from Ryujima mine, Japan: American Mineralogist, v. 52, nos. 11 and 12, p. 1751–61.

U.S. Bureau of the Census, 1991, Summary population and housing characteristics—Arizona: U.S. Department of Commerce, Bureau of the Census 1990 Census of Population and Housing Report CPH–1–4, 5 p.

U.S. Environmental Protection Agency, 1978–89, Correspondence file for NPDES permit AZ0020508, Inspiration operations: San Francisco, U.S. Environmental Protection Agency, Water Management Division, Region 9, v.p.

———1986, Finding of violation and order: U.S. Environmental Protection Agency, Water Management Division, Docket No. IX–FY86–78, v.p.

University of Arizona, 1965, Normal annual precipitation—Normal May-September precipitation—1931–60, State of Arizona: Tucson, University of Arizona map, scale 1:500,000.

Van Arsdale, G.D., 1926, Leaching mixed copper ores with ferric sulfate, Inspiration Copper Company: American Institute of Mining and Metallurgical Engineers Transactions, v. 73, p. 58–74.

Wood, W.W., 1976, Guidelines for collection and field analysis of ground-water samples for selected unstable constituents: U.S. Geological Survey Techniques of Water-Resources Investigations, book 2, chap. D2, 24 p.

SELECTED SERIES OF U.S. GEOLOGICAL SURVEY PUBLICATIONS

Periodicals

Earthquakes & Volcanoes (issued bimonthly).
Preliminary Determination of Epicenters (issued monthly).

Technical Books and Reports

Professional Papers are mainly comprehensive scientific reports of wide and lasting interest and importance to professional scientists and engineers. Included are reports on the results of resource studies and of topographic, hydrologic, and geologic investigations. They also include collections of related papers addressing different aspects of a single scientific topic.

Bulletins contain significant data and interpretations that are of lasting scientific interest but are generally more limited in scope or geographic coverage than Professional Papers. They include the results of resource studies and of geologic and topographic investigations, as well as collections of short papers related to a specific topic.

Water-Supply Papers are comprehensive reports that present significant interpretive results of hydrologic investigations of wide interest to professional geologists, hydrologists, and engineers. The series covers investigations in all phases of hydrology, including hydrogeology, availability of water, quality of water, and use of water.

Circulars present administrative information or important scientific information of wide popular interest in a format designed for distribution at no cost to the public. Information is usually of short-term interest.

Water-Resources Investigations Reports are papers of an interpretive nature made available to the public outside the formal USGS publications series. Copies are reproduced on request unlike formal USGS publications, and they are also available for public inspection at depositories indicated in USGS catalogs.

Open-File Reports include unpublished manuscript reports, maps, and other material that are made available for public consultation at depositories. They are a nonpermanent form of publication that may be cited in other publications as sources of information.

Maps

Geologic Quadrangle Maps are multicolor geologic maps on topographic bases in 7.5- or 15-minute quadrangle formats (scales mainly 1:24,000 or 1:62,500) showing bedrock, surficial, or engineering geology. Maps generally include brief texts; some maps include structure and columnar sections only.

Geophysical Investigations Maps are on topographic or planimetric bases at various scales; they show results of surveys using geophysical techniques, such as gravity, magnetic, seismic, or radioactivity, which reflect subsurface structures that are of economic or geologic significance. Many maps include correlations with the geology.

Miscellaneous Investigations Series Maps are on planimetric or topographic bases of regular and irregular areas at various scales; they present a wide variety of format and subject matter. The series also includes 7.5-minute quadrangle photogeologic maps on planimetric bases that show geology as interpreted from aerial photographs. Series also includes maps of Mars and the Moon.

Coal Investigations Maps are geologic maps on topographic or planimetric bases at various scales showing bedrock or surficial geology, stratigraphy, and structural relations in certain coal-resource areas.

Oil and Gas Investigations Charts show stratigraphic information for certain oil and gas fields and other areas having petroleum potential.

Miscellaneous Field Studies Maps are multicolor or black-and-white maps on topographic or planimetric bases for quadrangle or irregular areas at various scales. Pre-1971 maps show bedrock geology in relation to specific mining or mineral-deposit problems; post-1971 maps are primarily black-and-white maps on various subjects such as environmental studies or wilderness mineral investigations.

Hydrologic Investigations Atlases are multicolored or black-and-white maps on topographic or planimetric bases presenting a wide range of geohydrologic data of both regular and irregular areas; principal scale is 1:24,000, and regional studies are at 1:250,000 scale or smaller.

Catalogs

Permanent catalogs, as well as some others, giving comprehensive listings of U.S. Geological Survey publications are available under the conditions indicated below from the U.S. Geological Survey, Information Services, Box 25286, Federal Center, Denver, CO 80225. (See latest Price and Availability List.)

"Publications of the Geological Survey, 1879–1961" may be purchased by mail and over the counter in paperback book form and as a set of microfiche.

"Publications of the Geological Survey, 1962–1970" may be purchased by mail and over the counter in paperback book form and as a set of microfiche.

"Publications of the U.S. Geological Survey, 1971–1981" may be purchased by mail and over the counter in paperback book form (two volumes, publications listing and index) and as a set of microfiche.

Supplements for 1982, 1983, 1984, 1985, 1986, and for subsequent years since the last permanent catalog may be purchased by mail and over the counter in paperback book form.

State catalogs, "List of U.S. Geological Survey Geologic and Water-Supply Reports and Maps For (State)," may be purchased by mail and over the counter in paperback booklet form only.

"Price and Availability List of U.S. Geological Survey Publications," issued annually, is available free of charge in paperback booklet form only.

Selected copies of a monthly catalog "New Publications of the U.S. Geological Survey" are available free of charge by mail or may be obtained over the counter in paperback booklet form only. Those wishing a free subscription to the monthly catalog "New Publications of the U.S. Geological Survey" should write to the U.S. Geological Survey, 582 National Center, Reston, VA 22092.

Note—Prices of Government publications listed in older catalogs, announcements, and publications may be incorrect. Therefore, the prices charged may differ from the prices in catalogs, announcements, and publications.